DEPOSITIONAL DYNAMICS IN A MIXED CARBONATE–SILICICLASTIC SYSTEM, TRILOBITE FAUNA, BIOSTRATIGRAPHY AND BIOFACIES: MIDDLE–UPPER CAMBRIAN ABRIGO FORMATION, SOUTHEASTERN ARIZONA

A Thesis Submitted to the College of

Graduate Studies and Research

in Partial Fulfillment of the Requirements

for the Degree of Doctor of Philosophy

in the Department of Geological Sciences,

University of Saskatchewan,

Saskatoon

By

MARCELINA ŁABAJ

PERMISSION TO USE

In presenting this thesis in partial fulfillment of the requirements for a Postgraduate degree from the University of Saskatchewan, I agree that the Libraries of this University may make it freely available for inspection. I further agree that permission for copying of this thesis in any manner, in whole or in part, for scholarly purposes may be granted by the professor or professors who supervised my thesis work or, in their absence, by the Head of the Department of Geological Sciences or the Dean of the College of Graduate Studies and Research, in which my thesis work was done. It is understood that any copying or publication or use of this thesis or parts thereof for financial gain shall not be allowed without my written permission. It is also understood that due recognition shall be given to me and to the University of Saskatchewan in any scholarly use which may be made of any material in my thesis.

Requests for permission to copy or to make other uses of materials in this thesis in whole or part should be addressed to:

Head of the Department of Geological Sciences
University of Saskatchewan
114 Science Place
Saskatoon, Saskatchewan, S7N 5E2
CANADA

ABSTRACT

The mixed carbonate–siliciclastic Abrigo Formation of middle and late Cambrian age, which crops out in southeastern Arizona, was deposited during the Sauk transgression in the craton interior, landward of the passive margin of Laurentia. The Abrigo Formation consists of ten basic rock types: claystone, siltstone, sandstone, lime mudstone, wackestone, bioclastic grainstone, packstone, oolitic packstone, oncolitic packstone, and intraclastic conglomerate. These comprise fifteen lithofacies, which are grouped into eight facies associations. They represent an array of shallow-marine environments that were dominated by wave and storm activity. The interpreted paleoenvironments include lower offshore, upper offshore, offshore transition, and lower, middle and upper shoreface. One hundred eighty-two collections, yielding 940 trilobite remains have been found in the Abrigo Formation. They represent 69 species and 42 genera. Eight of the species are new. The fossil age ranges from early Marjuman to late Steptoean. Eight trilobite biofacies are defined from the generic relative abundance data: *Ehmaniella, Olenoides–Bolaspidella, Blairella, Eldoradia, Modocia–Paracedaria, Cedaria, Coosella–Coosina,* and *Camaraspis*. Trilobites collected and identified in this study are assigned to five biostratigraphic zones: *Bolaspidella*, *Cedaria*, *Crepicephalus*, *Aphelaspis*, and *Elvinia* zones. In addition, two subzones had been defined. *Cedaria eurycheilos* Subzone recognized in the upper part of *Cedaria* Zone and *Coosella helena* Subzone recognized in the upper part of *Crepicephalus* Zone. The stratigraphic succession was divided into six distinct phases associated with large-scale relative sea-level fluctuations. An initial flooding over the Bolsa Quartzite forming the transgressive systems tract was terminated by maximum flooding, and a subsequent highstand systems tract developed during *Bolaspidella* Biozone time. The second sequence starts with another transgressive systems tract, and is overlain by a final highstand systems tract during the

Cedaria and *Crepicephalus* biozones. The uppermost part of the second sequence represents a falling stage systems tract that developed during *Aphelaspis* Biozone time. The presence of *Elvinia* Biozone trilobites near the base of the highest sandstone unit suggests that delivery and deposition of these sands took place during the lowstand that followed the protracted and widespread Sauk II–Sauk III hiatus. Sedimentary dynamics were controlled by storm-induced wave action and offshore flows. There are two carbonate factories that operated simultaneously in this Cambrian inner shelf region. Dominance of carbonate versus siliciclastic strata in the offshore transition setting is interpreted to reflect periods when siliciclastic input was depleted, such that increasing accommodation and reduction of clay and possibly nutrients promoted carbonate production. Clay and silt bypassed the nearshore carbonate-depositing zone. Siliciclastic sediment input and dispersal were not only restricted to the falls in sea level, but appear to have dominated the transgressive systems tract and late phase of the highstand. Thus, carbonate sedimentation does not dominate the entire highstand systems tract as is commonly held but, rather, only during the late phase of the transgressive and early highstand phase. The comparison of this Cambrian model with younger mixed carbonate-siliciclastic units will help reveal the subtleties of the carbonate factory and how it operated in response to biotic evolution.

ACKNOWLEDGEMENTS

First I would like to express my gratitude to my graduate supervisor, Brian Pratt for the opportunity to pursue this project and his guidance throughout my Ph.D. degree. I am truly grateful to Gabriela Mángano and Luis Buatois for their insightful advice, eye-opening conversations on several aspects of my Ph.D., and their enthusiastic support. I would like to thank Stephen Urquhart and Jim Merriam for their feedbacks. I am immensely thankful to Fred Sundberg for introducing me to the field localities. Financial support was provided by Natural Sciences and Engineering Research Council of Canada Discovery Grants awarded to Brian R. Pratt and two-term scholarship was provided by the Department of Geological Sciences. I owe special thanks to Shelly Fisher, Chantelle Edwards, and Evan Nordquist for field assistance and local ranchers from my field area for their hospitality. I would like to thank to Blaine Novakovski for the preparation of thin sections, Chantal Strachan-Crossman for being super helpful with all the administrative work. I would like to thank graduate students from the Department of Geological Sciences for their friendship, discussions and encouragement.

Finally I would like to thank all my friends for their support and patience throughout my time at the University of Saskatchewan and for always being there for me: Izabela Szelest, Robert Skomro, Ola Skomro, Aliaksei Boika, Solange Angulo, Sándor Süle, Gosia and Tomek Korbas, Magda Bromek, Belen Garcia, Aneta Radziwon-Balicka and Maciek Balicki, Asia Pszonka, Kasia Rudnicka, Ola Wojtas, Łukasz Bęben, Piotr Kukialka and Adrian Doroszko.

Last, but not least I want to thank my family for their constant encouragement and unconditional support. To my parents Zofia and Andrzej Łabajowie, my brother Filip Łabaj and my sister-in-law Aga Łabaj. There are not enough words to describe how grateful I am to them and how important they are to me.

TABLE OF CONTENTS

PERMISSION TO USE i

ABSTRACT ii

ACKNOWLEDGEMENTS iv

TABLE OF CONTENTS v

LIST OF TABLES xv

LIST OF FIGURES xv

1. INTRODUCTION 1

1.1. OVERVIEW 1

1.2. RESEARCH OBJECTIVES 8

1.3. THESIS OUTLINE 9

1.4. REFERENCES 10

2. DEPOSITIONAL DYNAMICS IN A MIXED CARBONATE–SILICICLASTIC SYSTEM: MIDDLE–UPPER CAMBRIAN ABRIGO FORMATION, SOUTHEASTERN ARIZONA 13

2.1. ABSTRACT: 13

2.2. INTRODUCTION 15

2.3. GEOLOGICAL SETTING AND STRATIGRAPHY 17

2.4. METHODS 21

2.5. FACIES 23

2.5.1 *Facies M_n: Nodular Lime Mudstone* 26

2.5.2 *Facies R_i: Intraclastic Rudstone* 27

2.5.3. *Facies C_l: Laminated Claystone* 29

2.5.4. *Facies M_l: Laminated Lime Mudstone* 29

2.5.5. *Facies Slt: Lenticular Siltstone* 30

2.5.6. *Facies S: Small-Scale Hummocky Cross-Stratified Sandstone* 32

2.5.7. *Facies G: Gutter Casts* 34

2.5.8. *Facies C_i: Intraclastic Conglomerate* 35

2.5.9. *Facies S_{HCS}: Hummocky Cross-Stratified Sandstone* 38

2.5.10. *Facies MW: Lime Mudstone and Wackestone* 40

2.5.11. *Facies St: Stromatolite* 41

2.5.12. *Facies GP: Bioclastic Grainstone and Packstone* 42

2.5.13. *Facies P_o: Oolitic–Oncolitic Packstone* 43

2.5.14. *Facies S_{AHCS}: Amalgamated Hummocky Cross-Stratified Sandstone* 47

2.5.15. *Facies S_{TCS}: Trough Cross-Stratified Sandstone* 48

2.6. FACIES ASSOCIATIONS (FA) 53

2.6.1. *Facies Association 1* 53

2.6.2. *Facies Association 2* 53

2.6.3. *Facies Association 3* 54

2.6.4. *Facies Association 4* 55

2.6.5. *Facies Association 5* 55

2.6.6. *Facies Association 6* 56

2.6.7. *Facies Association 7* 56

2.6.8. *Facies Association 8* 57

2.7. SEDIMENTARY ENVIRONMENT 57

2.7.1. *Depositional Model* 58

2.8. STRATIGRAPHIC EVOLUTION 63

2.8.1. *Sequence Stratigraphic Model* 63

2.8.2. *Inter-regional Comparison* 66

2.8.3. *Carbonate Versus Siliciclastic Sedimentation* 68

2.9. CONCLUSIONS 72

2.10. ACKNOWLEDGMENTS 74

2.11. REFERENCES 74

3. MARJUMAN AND STEPTOEAN (MIDDLE AND UPPER CAMBRIAN) TRILOBITES OF THE ABRIGO FORMATION, SOUTHEASTERN ARIZONA. 92

3.1. ABSTRACT 92

3.2. INTRODUCTION 93

3.3. STUDY AREA 94

3.4. SEDIMENTARY ENVIRONMENT 95

3.5. BIOSTRATIGRAPHY 96

3.5.1. Marjumian Stage 97

3.5.1.1. *Bolaspidella* Zone 97

3.5.1.2. *Cedaria* Zone 99

3.5.1.3. *Crepicephalus* Zone 100

3.5.2. Steptoean Stage 104

3.5.2.1. *Aphelaspis* Zone 104

3.5.2.2. *Elvinia* Zone 106

3. 6. TRILOBITE BIOFACIES 109

3.6.1. *Lower Marjuman. Ehmaniella, Olenoides–Bolaspidella,* and *Blairella* biofacies 109

3.6.2. *Upper Marjuman. Eldoradia, Modocia–Paracedaria, Cedaria,* and *Coosella–Coosina* 114
3.6.3. *Upper Steptoean. Camaraspis* 116
3.7 SYSTEMATIC PALEONTOLOGY 118
Phylum ARTHROPODA Latreille, 1829 118
Class UNCERTAIN 118
Order AGNOSTIDA Salter, 1864 118
Family AGNOSTIDAE M'Coy, 1849 118
Subfamily AGNOSTINAE M'Coy, 1849 118
Genus *Homagnostus* Howell, 1935 118
Homagnostus sp. 118
Subfamily KORMAGNOSTINAE Pratt, 1992 119
Genus *Kormagnostus* Resser, 1938 119
Kormagnostus seclusus (Walcott, 1884) 119
Subfamily Pseudagnostinae Whitehouse, 1936 120
Genus *Pseudagnostus* Jaekel, 1909 120
Pseudagnostus cf. *P. communis* (Hall and Whitfield, 1877) 121
Class TRILOBITA Walch, 1771 121
Order CORYNEXOCHIDA Kobayashi, 1935, ... 121
Family DORYPYGIDAE Kobayashi, 1935 122
Genus *Olenoides* Meek, 1877 122
Olenoides nevadensis (Meek, 1870) 122
Order PTYCHOPARIIDA Swinnerton, 1915 123

Suborder PTYCHOPARIINA Richter, 1933 123
Family ALOKISTOCARIDAE Resser, 1939 123
Genus *Ehmaniella* Resser, 1937 123
Ehmaniella sp. 123
Genus *Blairella* Rasetti, 1965 124
Blairella crassimarginata Rasetti, 1965b 124
Blairella n. sp. 125
Genus *Alokistocare* Lorenz, 1906 126
Alokistocare americanum (Walcott, 1916a) 126
Superfamily OLENACEA Burmeister, 1843 127
Family ELVINIIDAE Kobayashi, 1935 127
Subfamily ELVINIINAE Kobayashi, 1935 127
Genus *Elvinia* Walcott, 1924 127
Elvinia cf. *E. roemeri* (Shumard, 1861) 128
Genus *Irvingella* Ulrich and Resser *in* Walcott, 1924 128
Irvingella sp. 129
Genus *Dunderbergia* Walcott, 1924 129
Dunderbergia cf. *D. nitida* (Hall and Whitfield, 1877) 129
Dunderbergia? cf. *D. anyta* (Hall and Whitfield, 1877) 130
Subfamily DOKIMOCEPHALINAE Kobayashi, 1935 131
Genus *Sulcocephalus* Wilson, 1948 131
Sulcocephalus sp. 131
Genus *Kindbladia* Frederickson, 1949 132

Kindbladia wichitaensis (Resser, 1942)..... 132
Genus *Dellea* Wilson, 1949 133
Dellea rasilis Westrop, 1986 133
Dellea suada (Walcott, 1890) 134
Genus *Iddingsia* Walcott, 1924 134
Iddingsia cf. *I. anatina* Resser, 1942 135
Family PTEROCEPHALIIDAE Kobayashi, 1935.....136
Subfamily APHELASPIDINAE Palmer, 1960.....136
Genus. *Aphelaspis* Resser, 1935.....136
Aphelaspis walcotti Resser, 1938.....136
Aphelaspis buttsi (Kobayashi, 1936).....137
Subfamily PTEROCEPHALIINAE Kobayashi, 1935.....138
Genus *Pterocephalia* Roemer, 1849.....139
Pterocephalia sanctisabae Roemer, 1849.....139
Genus *Camaraspis* Ulrich and Resser, 1924.....140
Camaraspis convexa (Whitfield, 1878).....140
Camaraspis n. sp.....141
Superfamily ILLAENURACEA Vogdes, 1890.....142
Family ILLAENURIDAE Vogdes, 1890.....142
Genus *Illaenurus* Hall, 1863.....143
Illaenurus sp.....143
Superfamily SOLENOPLEURACEA, Angelin, 1854.....143
Family SOLENOPLEURIDAE Angelin, 1854.....143

Genus *Solenopleurella* Poulsen, 1927 143

Solenopleurella quadrata Rasetti, 1963..... 145

Superfamily UNCERTAIN 145

Family. MARJUMIIDAE Kobayashi, 1935 145

Genus *Marjumia* Walcott, 1916..... 145

Marjumia cf. *M. transversa* (Palmer, 1968).....145

Marjumia cf. *M. typa* Walcott, 1916b.....146

Genus *Modocia* Walcott, 1924.....147

Modocia centralis (Whitfield 1877).....147

Modocia oweni (Meek and Hayden, 1861).....148

Modocia dubia (Resser, 1938a).....149

Modocia cf. *M. crassimarginata* Rasetti, 1965.....150

Modocia n. sp.....150

Family TRICREPICEPHALIDAE Palmer, 1954b 151

Genus *Meteoraspis* Resser, 1935 151

Meteoraspis sp. 152

Genus *Tricrepicephalus* Kobayashi, 1935 152

Tricrepicephalus coria (Walcott, 1916a)..... 153

Tricrepicephalus texanus (Shumard, 1861) 154

Family CREPICEPHALIDAE Kobayashi, 1935 154

Genus *Crepicephalus* Owen, 1852 155

Crepicephalus exutus Resser, 1938a 155

Crepicephalus sp. 156

Crepicephalus n. sp. 157

Crepicephalus cf. *C. iowensis* (Owen, 1852) 158

Genus *Coosella* Lochman, 1936 158

Coosella helena Lochman, 1938b 159

Coosella andreas (Walcott, 1916b) 160

Genus *Coosia* Walcott, 1911 160

Coosia n. sp. 161

Genus *Coosina* Rasetti, 1956 162

Coosina ariston (Walcott, 1916b) 162

Family ASAPHISCIDAE Raymond, 1924 164

Subfamily KINGSTONIINAE Kobayashi, 1933 164

Genus *Kingstonia* Walcott, 1924 164

Kingstonia spicata Lochman, 1940 164

Kingstonia scrinium (Raymond, 1937) 165

Kingstonia sp. 166

Genus *Bynumia* Walcott, 1924 167

Bynumia eumus Walcott, 1924 167

Genus *Brachyaspidion* Miller, 1936b 168

Brachyaspidion rynchina Miller, 1936b 168

Family CHEILOCEPHALIDAE Shaw, 1956 170

Genus *Cheilocephalus* Berkey, 1898 170

Cheilocephalus brachyops Palmer, 1965 170

Family LONCHOCEPHALIDAE Hupé, 1955 171

Genus *Glaphyraspis* Resser, 1937 171

Glaphyraspis parva (Walcott, 1899) 172

Family NORWOODIIDAE Walcott,1916.....172

Genus *Hardyoides* Kobayashi, 1938.....173

Hardyoides cf. *H. tenerus* (Walcott, 1916a).....173

Genus *Xenocheilos* Wilson, 1949.....174

Xenocheilos cf. *X. spineum* Wilson, 1951.....174

Family MENOMONIIDAE Walcott, 1916 175

Genus *Bolaspidella* Resser, 1937 175

Bolaspidella n. sp. 176

Bolaspidella? sp. 177

Family BOLASPIDIDAE Howell, 1959.....178

Genus *Eldoradia* Resser, 1935.....178

Eldoradia linnarssoni (Walcott, 1884).....179

Eldoradia prospectensis (Walcott, 1884).....180

Family CEDARIIDAE Raymond, 1937..... 180

Genus *Cedaria* Walcott, 1924 180

Cedaria eurycheilos Palmer, 1954..... 181

Cedaria? sp. 181

Genus *Cedarina* Lochman, 1940a 182

Cedarina cf. C. obtusans Duncan *in* Lochman and Duncan, 1944 182

Cedarina? sp. 183

Subfamily RAYMONDININAE Clark, 1924 183

Genus *Paracedaria* Duncan *in* Lochman and Duncan, 1944 184

Paracedaria viriosa Lochman and Hu, 1962..... 184

Paracedaria n.sp. 185

Family LLANOASPIDIDAE Lochman in Lochman and Duncan, 1944 186

Subfamily LLANOASPIDINAE Lochman in Lochman and Duncan, 1944 . 186

Genus *Llanoaspis* Lochman, 1938a..... 186

Llanoaspis modesta Lochman, 1938a..... 187

Llanoaspis undulata Lochman, 1938a..... 188

Llanoaspis peculiaris (Resser, 1938a)..... 189

Llanoaspis cf. *L. convexifrons* Rasetti, 1961 190

Llanoaspis n. sp..... 191

Family PHYLACTERIDAE Ludvigsen and Westrop *in* Ludvigsen et al.,1989.192

Genus *Cliffia* Wilson, 1951.....192

Cliffia lataegenae (Wilson, 1949).....192

Family UNCERTAIN 193

Genus *Arapahoia* Miller, 1936 193

Arapahoia butleri (Stoyanow, 1936) 194

3.8 PLATES..... 196

3.9. REFERENCES 240

4. SUMMARY..... 255

LIST OF TABLES

Table 2.1. Lithofacies and facies associations of the Abrigo Formation. 51

Table 3.1. Faunal zones recognized in the Abrigo Formation from several fossil collections. . 239

LIST OF FIGURES

Figure 1.1. Global subdivisions of Cambrian time as recognized by the International Subcommission on Cambrian Stratigraphy 2

Figure 1.2. Correlation chart of Cambrian strata in southern Arizona and southwestern New Mexico.....6

Figure 2.1. Regional map showing the distributions of inner detrital, carbonate, and outer detrital belts in Laurentia during the Cambrian to Early Ordovician 14

Figure 2.2. Chronostratigraphic and Sauk Sequence subdivisions for northern Arizona(Grand Canyon), south-central and southeastern Arizona, southern New Mexico..... 20

Figure 2.3. Study area in southeastern Arizona with location of outcrops and simplified geological map 22

Figure 2.4. Outcrops of Abrigo Formation 23

Figure 2.5. Three composite stratigraphic sections of the Abrigo Formation showing facies successions, depositional environments, biostratigraphy, and sequence stratigraphy. 25

Figure 2.6. Facies association 1. 28

Figure 2.7. Facies association 2. 32

Figure 2.8. Facies association 2. 33

Figure 2.9. Facies association 3. 37

Figure 2.10. Facies association 4. 39

Figure 2.11. Facies association 5 41

Figure 2.12. Facies association 6. 45

Figure 2.13. Thin section photomicrographs of facies association 6. 47

Figure 2.14. Facies association 7. 48

Figure 2.15. Facies association 8. 50

Figure 2.16. Idealized bathymetric profile showing the main depositional settings recognized in the Abrigo Formation 58

Figure 2.17. Diagram illustrating idealized stratigraphic sections displaying facies associations and their distribution with respect to the bathymetric profile 59

Figure 2.18. Facies model for the mixed carbonate–siliciclastic system showing the main depositional settings recognized in Abrigo Formation. 61

Figure 2.19. Generalized SSE–NNW-oriented stratigraphic cross-section across the inner detrital belt in southeastern Arizona, showing distribution of facies associations, trilobite biostratigraphy, and sequence stratigraphy 64

Figure 3.1. Stratigraphic section of French Joe Canyon and species range chart with biostratigraphic units 98

Figure 3.2. Stratigraphic section of Ajax Hill and species range chart with biostratigraphic units 102

Figure 3.3. Stratigraphic section of Johnny Lyon Hills and species range chart with biostratigraphic units 103

Figure 3.4. Stratigraphic section of Rattlesnake Ridge and species range chart with biostratigraphic units 105

Figure 3.5. Correlation of Ajax Hill, French Joe Canyon, Johnny Lyon Hills, and Rattlesnake Ridge sections, Abrigo Formation 108

Figure 3.6. Abundance of lower Marjuman trilobite genera in the *Bolaspidella* Zone 111

Figure 3.7. Abundance of upper Marjuman trilobite genera..... 113

Figure 3.8. Distribution of trilobite genera in three collections from *Coosella* - *Coosina* Biofacies developed in *Crepicephalus* Zone, *Coosella helena* Subzone of the Upper Marjuman 115

Figure 3.9. Distribution of trilobite genera in the collection from *Camaraspis* Biofacies developed in *Elvinia* Zone of the upper Steptoean 116

Figure 3.10. Generalized SSE–NNW-oriented stratigraphic cross-section across the inner detrital belt in southeastern Arizona, showing distribution of facies associations, sequence stratigraphy, trilobite biostratigraphy, and biofacies 117

CHAPTER 1

INTRODUCTION

1.1. OVERVIEW

The Cambrian is an exciting period of time in Earth's history, when the continents split and drifted apart, and complex animal life originated and began to diversify. The burst of metazoan evolution was marked by the appearance of the first animals, which developed the ability of creating shells and skeletons. Most animal body plans were already established in the Cambrian including almost all phyla and more than 50% of all recorded classes. This turning point for life on Earth is called the 'Cambrian Explosion'. The abrupt appearance of animals raises many questions, but most researchers agree that the motor of the Cambrian explosion was largely ecological (Conway Morris, 2000). In the Cambrian, substantial changes in ocean chemistry and circulation occurred, which resulted in the rise of macroscopic predation, effective filter-feeding on the seafloor and in the pelagic zone, and the appearance of infaunal burrowers (Seilacher 1999; Conway Morris, 2000; Droser and Li, 2000). The body-fossil record (Conway Morris, 2000) as well as the trace-fossil record (Mángano and Buatois, 2014) from the Cambrian Period is a necessary tool for deciphering animal evolution. A consequence of this event is the rise of new sedimentary particles on the seafloor, such as shells and skeletons and their breakdown products called bioclasts, fecal and pseudofecal pellets, new sources of lime mud, and a variety of newly evolved microbial carbonate precipitates. During the subsequent more than half a billion years the actors on this stage changed with the continuing evolution of life, but the basic Phanerozoic story in the seas and oceans was established during the Cambrian Explosion.

A particularly interesting group of animals, which dominated the Cambrian fauna in terms of abundance and diversity, is the trilobites. These arthropods first appeared in the middle part of the early Cambrian, and quickly diversified into many families and genera exhibiting an enormous variety of morphological complexity based on the fundamental tri-lobed arthropod plan. Abundance and variety of trilobites in a wide range of Cambrian sediments provide unsurpassed value as biozonal fossils. Trilobites play the key role in Cambrian biostratigraphy starting with the beginning of Series 2 (Fig. 1.1). The current understanding of the distribution of continents during Cambrian time is based on the paleobiogeography of trilobites (Torsvik and Cocks 2013).

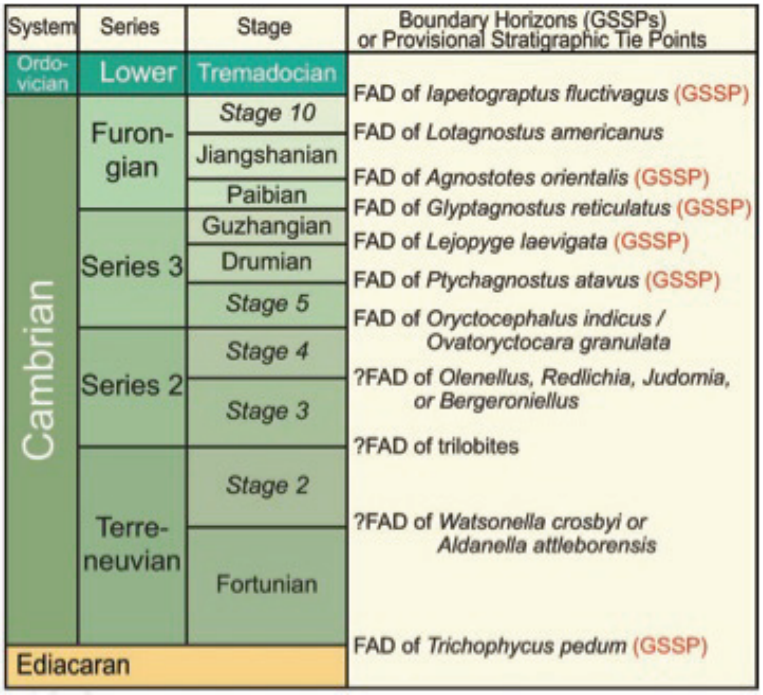

Figure 1.1. Global subdivisions of Cambrian time as recognized by the International Subcommission on Cambrian Stratigraphy of the International Commission on Stratigraphy (http://www.palaeontology.geo.uu.se/ISCS). The boundaries between all stages above the Terreneuvian are based on first occurrences of trilobites.

Paradoxically, despite trilobites being the most common fossils known from Cambrian strata, their ecology remains poorly resolved. The variety of soft- and hard-part morphology suggests that the range of ecologic diversity was substantial. Cambrian trilobites indicate a broad variety of feeding habits ranging from suspension and deposit feeding to predator-scavenger activity (Hughes, 2001). Early Cambrian trilobites were almost entirely inhabitants of continental shelves and shallow inland seas termed epeiric or epicontinental seas. There is no record of deeper water sites with trilobites at the early time in their history. By middle Cambrian time, however, the whole inshore to deep-water settings were occupied by trilobites (Robison, 1972). It is the appreciation and correlation of fossil occurrence in all parts of the globe where Cambrian rocks are found is how the Cambrian Explosion is pieced together and its sedimentary and environmental context understood.

A portion of the Cambrian Explosion phenomenon is recorded within the middle and upper Cambrian strata of southeastern Arizona. These rocks represent the early phase of the Sauk Sequence which is the first of the great Phanerozoic transgressions over Laurentia which is the name for the North American continent during the Cambrian and Ordovician. In mid-Cambrian time marginal carbonate platforms protected a vast epeiric sea, which was so broad that no modern analogues can serve to directly aid a reconstruction of how it behaved oceanographically, sedimentologically and biologically. All environments of deposition in its interior were characterized by relatively shallow water depths and were represented by mixed carbonate and siliciclastic facies. These deposits are either buried in the subsurface or, where exposed on the surface, largely recessive and visible only in scattered locations, such as in southern Arizona (Gilluly, 1956), at the bottom of the Grand Canyon (McKee, 1945), here and there in the Upper Mississippi Valley (Runkel et al., 2008), and around Cenozoic igneous uplifts

in central Montana (Lochman and Duncan, 1944). In early middle Cambrian time the shallow sea started to enter the southeastern region of Arizona and eventually it covered the metamorphic, igneous and sedimentary rocks of the Precambrian basement. The continued Sauk transgression advanced eastward up to the position of the present-day border with New Mexico (Kelley and Silver, 1952; Sabins, 1957; Hayes, 1978). During the late Cambrian the position of the shoreline fluctuated and extended even farther eastwards during Early Ordovician time (Sabins, 1957). The southeastern region of Arizona was for the first time subjected to erosion during emergence in Middle Ordovician time (Hayes, 1978). More extensive erosion of Cambrian strata took place during Early and Middle Devonian time, when the entire region was tilted southeastwards. Consequently, Middle and Late Devonian seas left their deposits on middle Cambrian rocks. Cambrain and Devonian strata have been affected by many other tectonic and erosional events in post-Devonian time.

The basal formation of the Paleozoic sequence in southeastern Arizona is the Bolsa Quartzite of presumed middle Cambrian age (Sabins, 1957). The Bolsa Quartzite was described and named by Ransome (1904) with its stratotype section in the Mule Mountains. It consists of resistant beds of reddish brown to white sandstone, with feldspar grains and conglomerates in the lower part. Planar and trough cross-laminations are abundant. Many vertical trace fossils are present, such as, *Skolithos* and *Diplocraterion* representing *Skolithos* ichnofacies. The thickness ranges from 130 m to 300 m (Bryant, 1968). The contact with the overlying Abrigo Formation is conformable, but generally rather sharp. This theme is reproduced almost everywhere across Laurentia as the shallow seas reworked the regolith and sands perched on the land surface.

The Abrigo Formation, on which my study is focused, consists of a succession of interbedded siliciclastic and carbonate facies (Gilluly, 1956; Epis and Gilbert, 1957; Cooper and

Silver, 1964; Krieger, 1968; Bryant, 1968), and records deposition in the inner detrital belt. It is characterized by a heterogeneous assemblage of limestone, dolomite, sandstone, siltstone and shale, and is typically thin- to medium-bedded.

The stratotype of the Abrigo Formation is in the same place as that of the Bolsa Quartzite and was also named by Ransome (1904). It is of middle and late Cambrian age (Stoyanow, 1936; Palmer *in* Gilluly, 1956; Palmer *in* Cooper and Silver, 1964; Hayes and Landis, 1965) and, where completely developed, ranges from 200 m to 270 m thick (Bryant, 1968). The Abrigo is a comparatively recessive formation, which forms topographic saddles between the resistant Bolsa Quartzite and the overlying Martin Formation which is Devonian in age. Stoyanow (1936) proposed a number of new formation names (Pima Sandstone, Cochise Formation, Copper Queen Limestone, Rincon Limestone, Southern Belle Quartzite and Peppersauce Canyon Sandstone) which were subsequently considered as members of the Abrigo Formation (Fig. 1.2). Instead, other authors prefered a simpler approach and subdivided the Abrigo Formation into three or four members (Epis and Gilbert, 1957; Krieger, 1961, 1968; Cooper and Silver, 1964; Hayes and Landis, 1965). The most recent subdivision was proposed by Hayes (1975, 1978), who described four units: lower member, middle member, upper sandy member and Copper Queen Member. This subdivision of the Abrigo Formation is comparable to the one proposed by Cooper and Silver (1964). None of these subdivisions was found particularly useful in this study owing to the dramatic lateral facies changes.

Fig.1.2. Correlation chart of Cambrian strata in southern Arizona and southwestern New Mexico (based on Hayes, 1978).

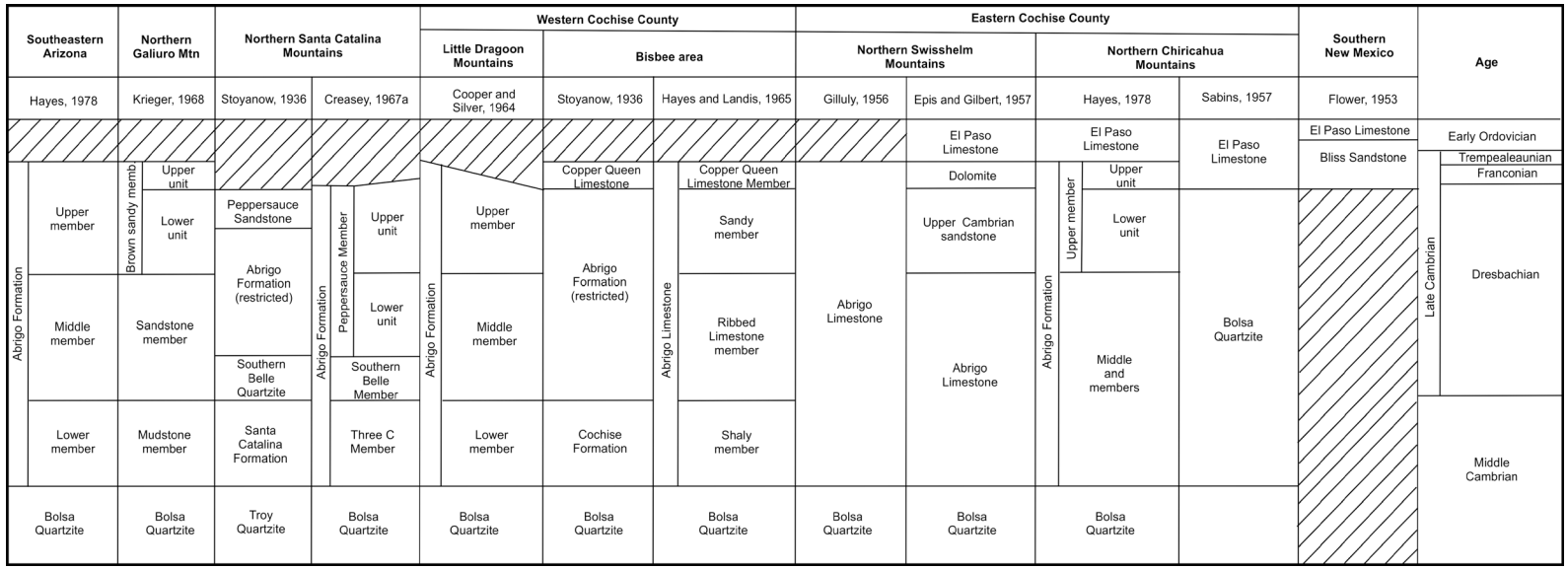

Sedimentary processes recorded in mixed carbonate–siliciclastic settings are relatively poorly understood with respect to modern facies interpretation and how the sediment-producing 'carbonate factory' must have operated in the nearshore continental interior close to sources of siliciclastic input. Moreover, in the larger perspective, it is not clear how the carbonate factory behaved over geological time via changing paleogeography and evolving sources of carbonate sediment. A better understanding of the sedimentary processes and their dynamics that prevailed during the deposition, as well as the geometry and distribution of the facies, are the key to understand how those systems worked.

In the context of the sea that covered more than half of Laurentia, the sedimentary facies distribution shows a concentric three-fold pattern. The 'outer detrital belt' which comprises the deeper water deposits developed on the continental slope, the 'middle carbonate belt' comprising a relatively narrow rim around the margin where limestones were deposited, and the 'inner detrital belt' in the continental interior (Palmer, 1960). The Abrigo Formation offers an opportunity to explore sedimentation in the inner detrital belt in a subequatorial location in what was then western Laurentia. As the unit has been studied only in a reconnaissance manner (e.g., Gilluly 1956; Hayes 1975), consequently the paleoenvironmental attributes have been only broadly outlined. Thus, several long and continuous sedimentary successions turn out to be well exposed in southeastern Arizona and these provide a unique opportunity to trace the sedimentologic and paleoecologic evolution of the continental interior of western Laurentia.

The aim of this thesis is two-fold. First, it is to present the first detailed high-resolution facies analysis and a reconstruction of the spatial distribution of the various facies across the region. The concepts of sequence stratigraphy provide an important and, here, newly applied model for the interpretation of the depositional environments. I use it to link the somewhat

disparate disciplines of sedimentology and paleoecology. It provides a framework to elucidate the major events in the middle and late Cambrian evolution of this area and enable a comparison between Abrigo Formation and other inner detrital belt examples across Laurentia. The principal controls for mixed carbonate–siliciclastic depositional systems and the interplay between siliciclastic sediment input and carbonate productivity in this region during the Cambrian are explored for the first time. This can only be achieved once there is sufficient temporal resolution provided by fossils—a trilobite-based biostratigraphy.

Thus, the second purpose of this thesis is to document the trilobite fauna in the Abrigo Formation and its stratigraphic distribution. Previously, study of the trilobite fauna was also done in a reconnaissance fashion. Samples were collected by field geologists and identified mostly just to the genus level by A. R. Palmer of the U.S. Geological Survey (Gilluly, 1956; Cooper and Silver, 1964; also Taylor *in* Hayes, 1975). This study documents the occurrence through the Marjuman and Steptoean interval (Guzhangian–Paibian) of many previously named species, but a number of new species are also described. A biostratigraphic zonal scheme is erected that should be broadly applicable to the inner detrital belt of Laurentia. These zones are integrated with the pattern of trilobite biofacies characterized for the shallow-marine, storm-dominated environment, and combined with a detailed lithofacies analysis of the Abrigo Formation, aid in the evaluation of the overall ecologic controls on faunal distribution. This study provides a comparison of biozones and biofacies with collections from other areas across Laurentia.

1.2. RESEARCH OBJECTIVES

The middle and upper Cambrian Abrigo Formation of southeastern Arizona is a mixed carbonate–siliciclastic unit, and thus it offers an opportunity to explore sedimentation in the

nearshore environment. The unit has been studied only in a reconnaissance manner (e.g., Gilluly 1956; Hayes 1975), and consequently the paleoenvironmental and biostratigraphic contexts have been only broadly outlined. The aim of this research was to: (1) present the first detailed high-resolution facies analysis and a reconstruction of the spatial distribution of the various facies across the region, (2) place the succession in a sequence-stratigraphic framework that allows changes in relative sea level to be tracked; (3) present the interplay between siliciclastic sediment input and carbonate productivity; (4) prepare a taxonomic study of the trilobite fauna; (5) create a biostratigraphic zonation; and (6) develop biofacies to help to understand animal-sediment relationships.

The overall objectives of this research were to integrate trilobite taxonomy, biostratigraphy, paleoecology and sedimentological analysis in order to provide a better understanding of sedimentary facies and depositional dynamics of inner and mid-shelf environments and the animal-sediment interplay.

1.3. THESIS OUTLINE

This is a paper-based thesis. Thus each of the two major chapters corresponds to a manuscript submitted or prepared for a peer-reviewed publication venue. The thesis is organized into four chapters. Chapter 1 provides an introduction to the thesis, including the overview of the thesis, the main thesis objectives and the thesis organization. Chapter 2 focuses on lithostratigraphic aspects, including a general description and interpretation of lithofacies for the whole Abrigo Formation unit. It describes depositional model and investigates the sequence stratigraphic aspect. It also provides insights into the siliciclastic versus carbonate sedimentation. It compares this system with the time equivalent units elsewhere in Laurentia. This manuscript has been

submitted for publication in the international *Journal of Sedimentary Research*. In Chapter 3, the trilobite fauna study of the Abrigo Formation is addressed. The study is focused on trilobite taxonomy, biostratigraphy and biofacies analysis. This manuscript will be submitted as a stand-alone, book-length monograph to *Paleontographica Canadiana*. Chapter 4 discusses the relationship of individual chapters to the entirety of the thesis and provides a summary of the major conclusions obtained.

1.4. REFERENCES

Bryant, D.L., 1968, Diagnostic characteristics of the Paleozoic formations of southeastern Arizona: Arizona Geological Society, Southern Arizona Guidebook III, p. 33–47.

Cooper, J.R., and Silver, L.T., 1964, Geology and ore deposits of the Dragoon quadrangle, Cochise County, Arizona: U.S. Geological Survey Professional Paper 416, 196 p.

Conway Morris, S., 2000. The Cambrian "explosion": Slow-fuse or megatonnage?: Proceedings of the National Academy of Sciences v. 97, p. 4426-4429.

Droser, M.L., and Li, X., 2000. The Cambrian radiation and the diversification of sedimentary fabrics: In: Zhuravlev, A.Y. & Riding, R. (Eds.), The Ecology of the Cambrian Radiation. Columbia University Press, New York. p. 137-169.

Epis, R.C., and Gilbert, C.M., 1957, Early Paleozoic strata in southeastern Arizona: American Association of Petroleum Geologists Bulletin. v. 41, p. 2223–2242.

Gilluly, J., 1956, General geology of central Cochise County, Arizona: U. S. Geological Survey Professional Paper 281, 169 p.

Hayes, P.T., 1975, Cambrian and Ordovician rocks of southeastern Arizona and New Mexico and westernmost Texas: U. S. Geological Survey Professional Paper 873, 98p.

Hayes, P.T., 1978, Cambrian and Ordovician rocks of southeastern Arizona and southwestern New Mexico: New Mexico Geological Society Guidebook, 29th Field Conference Land of Cochise. p. 165-173.

Hayes, P.T., and Landis, E.R., 1965, Paleozoic stratigraphy of the southern part of the Mule Mountains, Arizona: U.S. Geological Survey Bulletin 1201–F, 43 p.

Hughes, N.C. 2001, Ecologic evolution of Cambrian trilobites: In: A.Y. Zhuravlev and R. Riding (Ed.), The ecology of the Cambrian radiation. Columbia University Press, New York. p. 371-403.

Kelley, V. C. and Silver C., 1952. Geology of the Caballo Mountains: University of New Mexico Publications in Geology, v.4, 286 p.

Krieger, M.H., 1961, Troy Quartzite (younger Precambrian) and Bolsa and Abrigo formations (Cambrian), northern Galiuro Mountains, southeastern Arizona: U.S. Geological Survey Professional Paper 424–C, p. 160–164.

Krieger, M.H., 1968, Stratigraphic relations of the Troy Quartzite (younger Precambrian) and the Cambrian formations in southeastern Arizona: Arizona Geological Society, Southern Arizona, Guidebook III, p. 23–42.

Lochman, C. and Duncan, D. 1944. Early Upper Cambrian faunas of central Montana. Geological Society of America Special Papers, 54, 181 pp.

Mángano, M.G., Buatois, L.A., 2014, Decoupling of body-plan diversification and ecological structuring during the Ediacaran–Cambrian transition: evolutionary and geobiological feedbacks. Proceedings of the Royal Society, 281: 20140038.

McKee, E.D., and Resser, C.E., 1945, Cambrian history of the Grand Canyon region: Carnegie Institution of Washington Publication 563, p. 3-168.

Palmer, A.R., 1960, Some aspects of the early Upper Cambrian stratigraphy of White Pine County, Nevada and vicinity, *in* Boettcher, J.W., and Sloan, W.W., eds., Guidebook to the Geology of East Central Nevada, Intermountain Association of Petroleum Geologists, 11th Annual Field Conference, p. 53–58.

Ransome, F.L., 1904, Geology and ore deposits of the Bisbee quadrangle, Arizona: U.S. Geological Survey Professional Paper 21, 168 p.

Robison, R.A. 1972, Mode of life of agnostid trilobites. 24th International Geological Congress, Montreal, Canada, Section 7 p. 33-40.

Runkel, A.C., Miller, J.F., McKay, R.M., Palmer, A.R., and Taylor, J.F., 2008, The record of time in cratonic interior strata: does exceptionally slow subsidence necessarily result in exceptionally poor stratigraphic completeness?, *in* Pratt, B.R., and Holmden, C., eds., Dynamics of Epeiric Seas: Geological Association of Canada, Special Paper 48, p. 341–362.

Sabins, F.F., Jr., 1957. Stratigraphic relations in the Chiricahua and Dos Cabezas Mountains, Arizona: American Association of Petroleum Geologists Bulletin. v. 41, no.3, p. 466- 510.

Seilacher, A., 1999. Biomat-related lifestyles in the Precambrian: Palaios 14, p. 86-93.

Stoyanow, A.A., 1936, Correlation of Arizona Paleozoic formations: Geological Society of America Bulletin, v. 47, p. 459–540.

Torsvik, T.H., and Cocks, L.R.M., 2013, New global paleogeographical reconstructions for the early Palaeozoic and their generation, *in* Harper, D.A.T., and Servais, T., eds., Early Palaeozoic Biogeography and Palaeogeography: Geological Society of London , Memoirs, 38, p. 5–24.

CHAPTER 2

DEPOSITIONAL DYNAMICS IN A MIXED CARBONATE–SILICICLASTIC SYSTEM: MIDDLE–UPPER CAMBRIAN ABRIGO FORMATION, SOUTHEASTERN ARIZONA

Marcelina A. Łabaj and Brian R. Pratt. Depositional dynamics in a mixed carbonate–siliciclastic system: middle–upper Cambrian Abrigo Formation, southeastern Arizona: submitted to a Journal of Sedimentary Research.

2.1. ABSTRACT: The mixed carbonate–siliciclastic Abrigo Formation of middle and late Cambrian age, which crops out in southeastern Arizona, was deposited during the Sauk transgression in the craton interior landward of the passive margin of Laurentia. It overlies shallow-marine sandstone of the Bolsa Quartzite, which mantled the Precambrian land surface. The Abrigo Formation consists of ten distinct rock types: claystone, siltstone, sandstone, lime mudstone, wackestone, bioclastic grainstone, packstone, oolitic packstone, oncolitic packstone, and intraclastic conglomerate. These comprise fifteen lithofacies, which are grouped into eight facies associations. They represent an array of shallow-marine environments that were dominated by wave and storm activity. There is no evidence of patch reef development, strong tidal action, or restricted conditions of elevated salinity. The interpreted paleoenvironments include lower offshore, upper offshore, offshore transition, and lower, middle and upper shoreface. These persisted through time, but they migrated laterally as a function of relative sea level changes along with siliciclastic sediment input and its effect on carbonate deposition. Stratigraphic trends and correlation across 170 km of the study area suggest that these lithofacies were deposited in six temporally distinct phases. (1) Deposition of Abrigo Formation started with

transgressive lower offshore carbonates overlying shallow-marine, high-energy sandstones of the Bolsa Quartzite. (2) This was followed in *Bolaspidella* Biozone time by accumulation of highstand deposits, recorded initially by mixed siliciclastic and carbonate sedimentation in the offshore setting, and then carbonate-dominated deposition in an offshore-transition setting. (3) Subsequent flooding in early *Cedaria* Biozone time resulted in a landward shift of facies, reduction of siliciclastic input, and dominance of clay and lime mud sedimentation under somewhat deeper water conditions. This phase led to deposition of the transgressive systems tract. (4) Progressive shallowing and aggradation during the next highstand phase in late *Cedaria* and early *Crepicephalus* biozone time was accompanied by a further decrease in siliciclastic input and a switch to pure carbonate deposition in a mainly offshore-transition setting. This was followed, in late *Crepicephalus* Biozone time by renewed coarse siliciclastic input and progradation of the sandy shoreface which terminated the highstand systems tract. (5) Subsequent progradation of proximal shoreface sand in *Aphelaspis* Biozone time characterized the falling stage systems tract. (6) Presence of *Elvinia* Biozone trilobites near the base of the succeeding lowstand shoreface sandstone reveals that the widely recognized Sauk II–Sauk III hiatus is recorded in southeastern Arizona. In general, the mixed carbonate–siliciclastic depositional environment of the Abrigo Formation shows that fine-grained siliciclastic facies dominate the transgressive systems tract. By contrast, carbonate sedimentation predominated mostly during the early phase of the highstand. The upper part of the highstand systems tract records progradation of the sandy shoreface. Nevertheless, the ratio between siliciclastic versus carbonate sediment in various bathymetric zones differs from previously described inner detrital belt examples of Cambrian age. In the Abrigo Formation, some bioclastic grainstone in shoreface deposits contains sand, indicating that the two were deposited together until sand

overwhelmingly predominated. However, carbonate production and siliciclastic mud sedimentation were for the most part mutually exclusive, suggesting that the shallow-water carbonate factory during the middle and late Cambrian was vulnerable to poisoning from clay or nutrient input. Consequently, carbonate sedimentation in the offshore transition, located between sand-dominated shoreface and mixed carbonate–siliciclastic offshore facies, reflects the bypassing by siliciclastic mud.

2.2. INTRODUCTION

Half a billion years ago the broad epeiric sea that progressively covered most of Laurentia created a generalized three-fold depositional pattern: outer detrital belt, middle carbonate belt, and inner detrital belt (Palmer 1960) (Fig. 2.1). Seaward lay the outer detrital belt, where allochthonous fine-grained sediment was deposited in deeper water on the outer ramp and slope. This region is recorded by shale and lime mudstone.

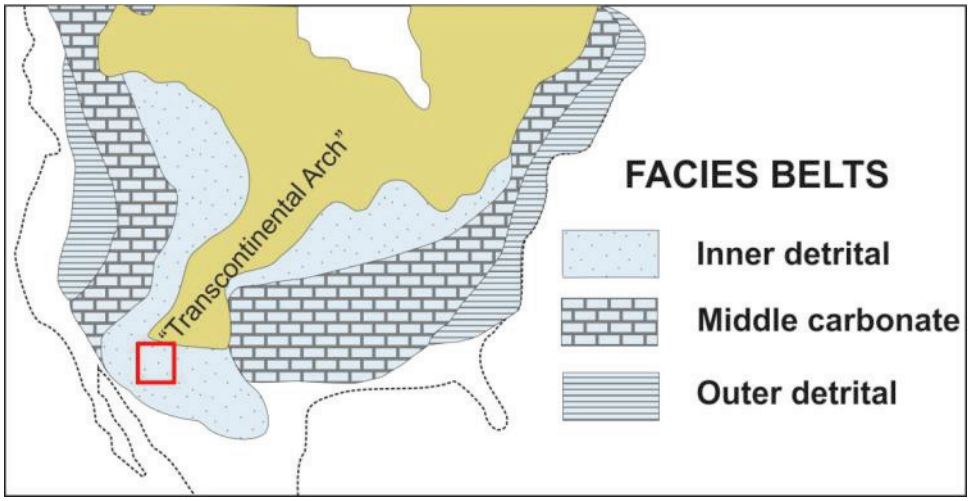

Fig. 2.1.—Regional map showing the distributions of inner detrital, carbonate, and outer detrital belts in Laurentia during the Cambrian to Early Ordovician (after Palmer 1960). Southeastern Arizona marked by red rectangle.

Shallow-marine environments of the early Paleozoic middle carbonate belt have been studied extensively in a wide variety of locations (e.g., Demicco 1985; Pratt and James 1986; Osleger and Read 1991; Osleger and Montañez 1996; Aitken 1997; Glumac and Walker 2000; Salad Hersi et al. 2002). Many of these deposits appear cyclical, in the way fluctuating relative bathymetry is expressed stratigraphically by characteristic carbonate facies. Larger scale packages of carbonate- versus siliciclastic-dominated units have been referred to as 'grand cycles' (Aitken 1976; Chow and James 1987; Cowan and James, 1993).

Recently, the broad, intracratonic inner detrital belt has been revealed, in the Upper Mississippi Valley region at least, to be a complex and variably mixed carbonate–siliciclastic depositional system recording a range of shoreface and offshore settings (Runkel et al. 2008; Runkel et al. 2012, Eoff 2014a, b). Nonetheless, this setting is relatively poorly understood with respect to fine-scale facies relationships and how the 'carbonate factory' must have operated in the nearshore continental interior close to sources of siliciclastic input (Myrow et al. 2012). Moreover, in the larger perspective, it is not clear how the carbonate factory behaved over geological time via changing paleogeography and evolving sources of carbonate sediment.

The middle and upper Cambrian Abrigo Formation of southeastern Arizona is a mixed carbonate–siliciclastic unit, and thus it offers an opportunity to explore sedimentation in the inner detrital belt in a subequatorial location in what was western Laurentia (Torsvik and Cocks 2013). The unit has been studied only in a reconnaissance manner (e.g., Gilluly 1956; Hayes 1975), and consequently the paleoenvironmental and biostratigraphic contexts have been only broadly outlined. The aim of this paper is to present the first detailed high-resolution facies analysis and a reconstruction of the spatial distribution of the various facies across the region. Placing the succession in a sequence-stratigraphic scheme allows changes in the depositional history of the

basin to be tracked, and insight into the interplay between siliciclastic sediment input and carbonate productivity in this region during the Cambrian.

2.3. GEOLOGICAL SETTING AND STRATIGRAPHY

Late Neoproterozoic and lower Cambrian sandstone units sporadically exposed around North America, record deposition above a major unconformity on the rifted margin of Laurentia (e.g., Desjardins et al. 2012) that developed in response to the breakup of the supercontinent Rodinia (e.g., Li et al. 2008). Eustatic sea level rise flooded first the margins of Laurentia and subsequently resulted in a broad intracratonic sea on either side of the Transcontinental Arch (e.g., Glumac and Walker 2000; Runkel et al. 2008). Although this major structural high has been active at various stages throughout the Phanerozoic (e.g., Sloss 1963; Carlson 1999), its extent and configuration are still uncertain, and it may not have exerted a significant influence on sedimentation patterns (Runkel et al. 1998; Myrow et al. 2003).

In southeastern Arizona the basement underlying the unconformity includes a variety of Paleoproterozoic–Mesoproterozoic granites, diorites, and metasedimentary and meta-igneous rocks (Amato et al. 2008). The unconformity had a generally low relief, amounting to not more than a few tens of meters (Hayes 1975). The continued Sauk transgression during middle Cambrian time resulted in shoreline fluctuation and movement eastwards as far as the position of the present-day border with New Mexico (Kelley and Silver 1952; Sabins 1957; Hayes 1978). Offshore, a mixed carbonate–siliciclastic shelf was established. During the late Cambrian and Early Ordovician the position of the shoreline shifted even farther eastwards (Sabins 1957). The primary source for the Cambrian sandstone in the region was middle Cambrian granite in the Florida Mountains of southwestern New Mexico (Amato and Mack 2012).

Paleozoic sedimentation in the region began during the middle Cambrian with the accumulation of the coarse-grained Bolsa Quartzite. Its thickness ranges from 130 m to 300 m (Bryant 1968). It consists of resistant beds of brown-weathering sandstone with abundant tabular and trough cross-lamination. Bioturbation, primarily in the form of burrows belonging to *Skolithos* and *Diplocraterion*, is common. This formation represents the subtidal zone of a tidally influenced shallow-marine siliciclastic environment (Hayes 1978) similar to many other early and middle Cambrian transgressive sandstone units that mantled the outer parts of Laurentia (e.g., Desjardins et al. 2012).

The contact with the overlying Abrigo Formation is conformable but sharp. In southern Arizona this unit is a succession of typically thin- to medium-bedded siliciclastic and carbonate facies comprising a heterogeneous assemblage of limestone, dolomite, sandstone, siltstone and shale (Gilluly 1956; Epis and Gilbert 1957; Cooper and Silver 1964; Krieger 1968; Bryant 1968). It weathers recessively and forms topographic saddles between the resistant Bolsa Quartzite and limestone and dolostone of the unconformably overlying Martin Formation of Late Devonian age. Where completely exposed, the Abrigo Formation ranges from 200 m to 270 m thick (Bryant 1968). In northern Sonora, ~100 km south of the study area, the Abrigo Formation is about 175 m thick and consists mostly of thin-bedded, bioturbated oolitic limestone, with intraclastic conglomerate and sandstone comprising the uppermost part (Page et al. 2010).

Ransome (1904) first named the Abrigo Formation with its type section in the Mule Mountains. The stratigraphic nomenclature in southeastern Arizona, however, is complicated by the variety of names proposed for coeval strata. Stoyanow (1936) proposed a number of formations (Pima Sandstone, Cochise Formation, Copper Queen Limestone, Rincon Limestone, Southern Belle Quartzite, and Peppersauce Canyon Sandstone), which were later considered as

informal members of the Abrigo Formation. Alternatively, it has been subdivided into three or four members (Epis and Gilbert 1957; Krieger 1961, 1968; Cooper and Silver 1964; Hayes and Landis 1965). The most recent subdivision of Hayes (1975, 1978) includes four units: lower member, middle member, upper sandy member, and Copper Queen Member, with the last restricted to the south of our study area. This subdivision is comparable to the one previously employed by Cooper and Silver (1964). None of these subdivisions was found particularly useful in this study owing to the dramatic lateral facies changes.

The Abrigo Formation yields an abundant and diverse trilobite fauna indicative of the latest middle Cambrian (= late series 3, Guzhangian stage) to the early late Cambrian (= middle Furongian series, Jiangshanian stage). This corresponds to the Marjuman, Steptoean, and early Sunwaptan stages of Laurentia (Taylor et al. 2012) (Fig. 2.2).

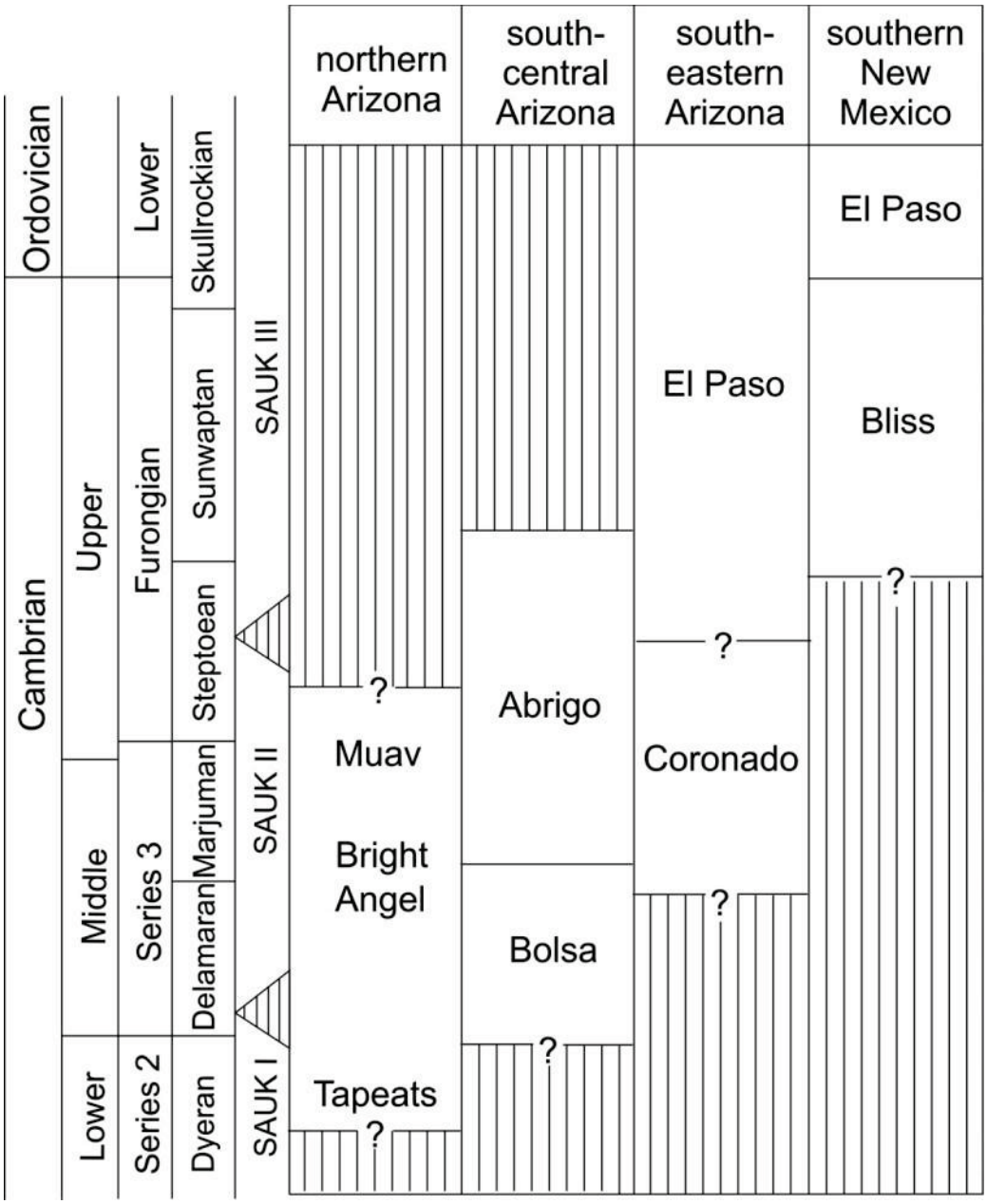

Fig. 2.2.—Chronostratigraphic and Sauk Sequence subdivisions are those reviewed in Taylor et al. (2012). Nomenclature for each area is based on the following: northern Arizona(Grand Canyon) (Poole et al. 1992); south-central and southeastern Arizona (Hayes 1975; Cooper and Silver 1964); southern New Mexico (Sabins 1957; Mack 2004).

The regional biostratigraphic framework is based on trilobites belonging to the traditional *Bolaspidella*, *Cedaria*, *Crepicephalus*, *Aphelaspis*, *Elvinia*, and probably *Ptychaspis* biozones (Stoyanow 1936; Palmer *in* Gilluly 1956, *in* Cooper and Silver 1964; Hayes and Landis 1965; Hayes, 1975). Based on our collections, the *Aphelaspis* Biozone, marking the base of the Laurentian Steptoean stage and the international Paibian stage of the lower Furongian series lies at +238 m at Ajax Hill and +138 m at Johnny Lyon Hills. Trilobites belonging to the uppermost Steptoean *Elvinia* Biozone were collected at +251.5 m at Ajax Hill, and between +202 m and +208 m at Rattlesnake Ridge. *Aphelaspis* Biozone and *Elvinia* Biozone trilobites also occur in the nearby Little Dragoon Mountains (Fig. 2.3A) (Palmer *in* Cooper and Silver 1964). Biozonal indicators of the middle Steptoean stage are absent, however. Thus, the Sauk II–Sauk III hiatus, which is widely recognized in the interior of Laurentia (Palmer 1981; Runkel et al. 1998; Saltzman et al. 2004; Morgan 2012), is recorded within the uppermost sandstone interval.

2.4. METHODS

This study is based on five stratigraphic sections in southeastern Arizona totalling 1066 m that were logged in a bed-by-bed detail (Figs. 2.3A–F, 2.4A–D). Trilobite collections were made concurrently. A number of other, previously described sections (Gilluly 1956; Hayes and Landis 1965; Hayes 1975; Krieger 1961; Hayes 1978), were field-checked.

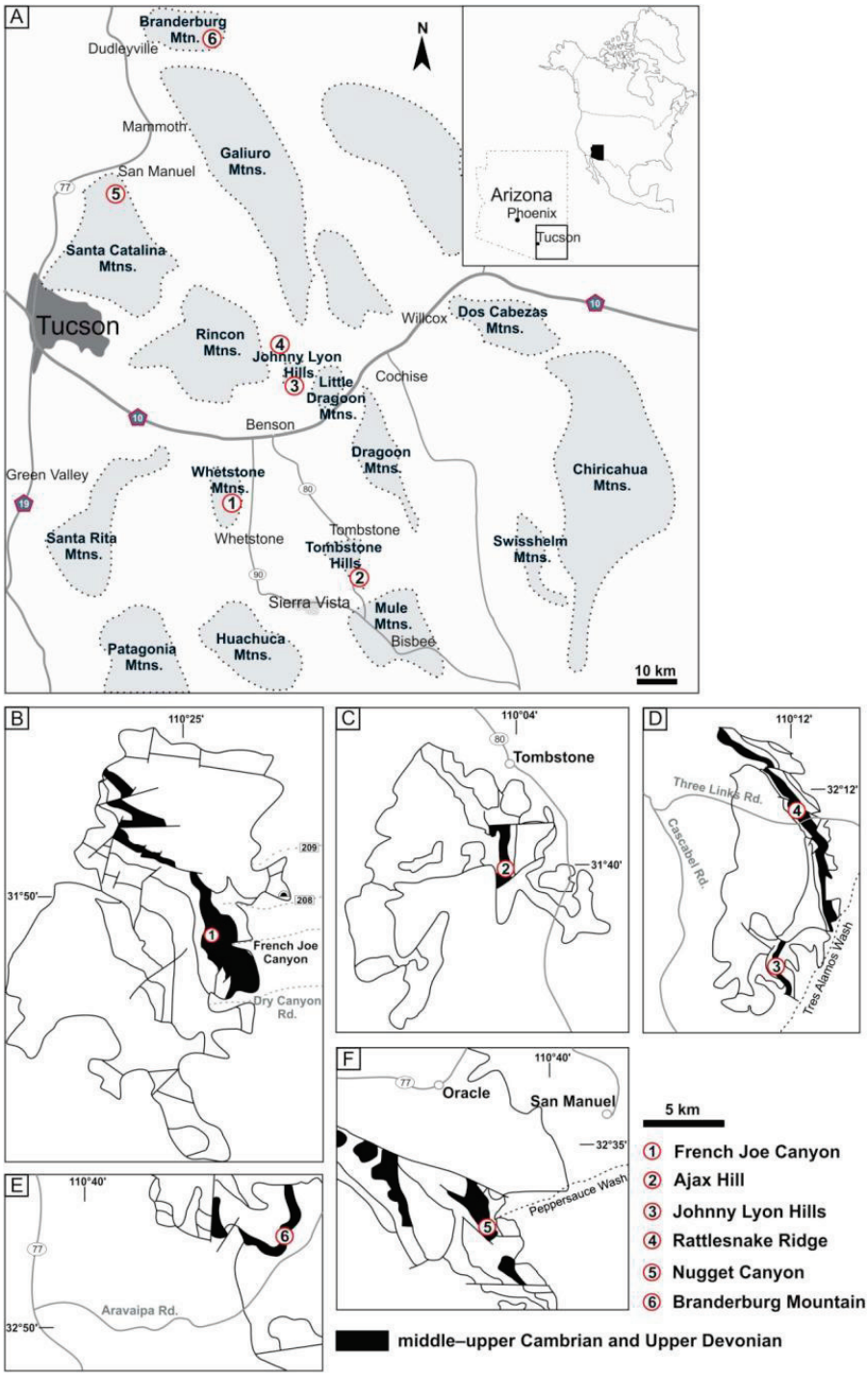

Fig. 2.3.—Study area in southeastern Arizona with locations of outcrops and simplified geological map. **A)** Map showing the main mountain ranges and the location of the studied outcrops (1–6). **B)** French Joe Canyon in Whetstone Mountains. **C)** Ajax Hill in Tombstone Hills. **D)** Johnny Lyon Hills and Rattlesnake Ridge. **E)** Brandenburg Mountain. **F)** Northern part of Santa Catalina Mountains with Nugget Canyon.

In addition to observations made at the hand-lens level, some two dozen rock samples were slabbed and polished, and 30 thin sections were prepared.

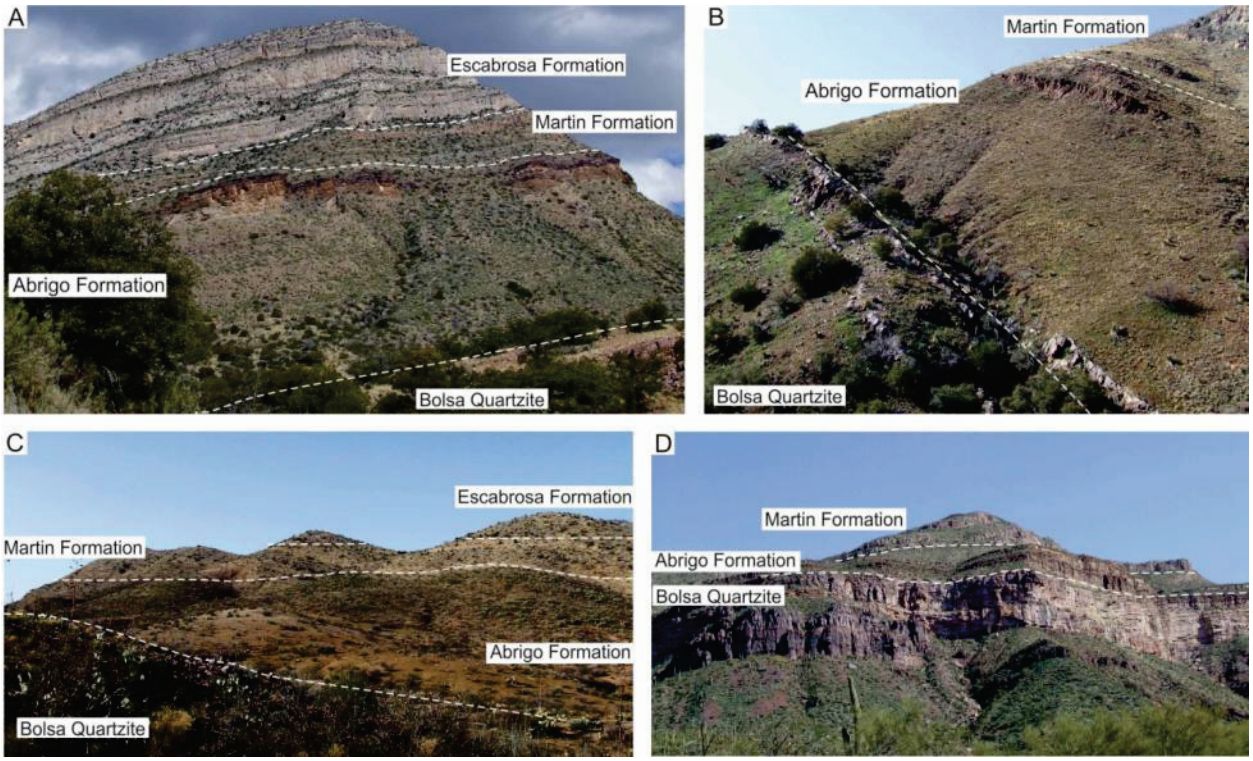

Fig. 2.4.—Outcrops of Abrigo Formation. **A)** Southeastern side of The Cape peak above French Joe Canyon in Whetstone Mountains (Fig. 2.3B). **B)** Nugget Canyon in northern Santa Catalina Mountains (Fig. 2.3F). **C)** Southwestern side of Rattlesnake Ridge (Fig. 2.3D). **D)** Southern side of Brandenburg Mountain (Fig. 2.3E).

2.5. FACIES

The Abrigo Formation consists of fifteen mixed siliciclastic and carbonate facies (Fig. 2.5) that were grouped into eight genetically related facies associations that represent deposition in six distinct, laterally intergradational marine environments (Table 1). These facies are described in order from the most distal to the most nearshore deposits.

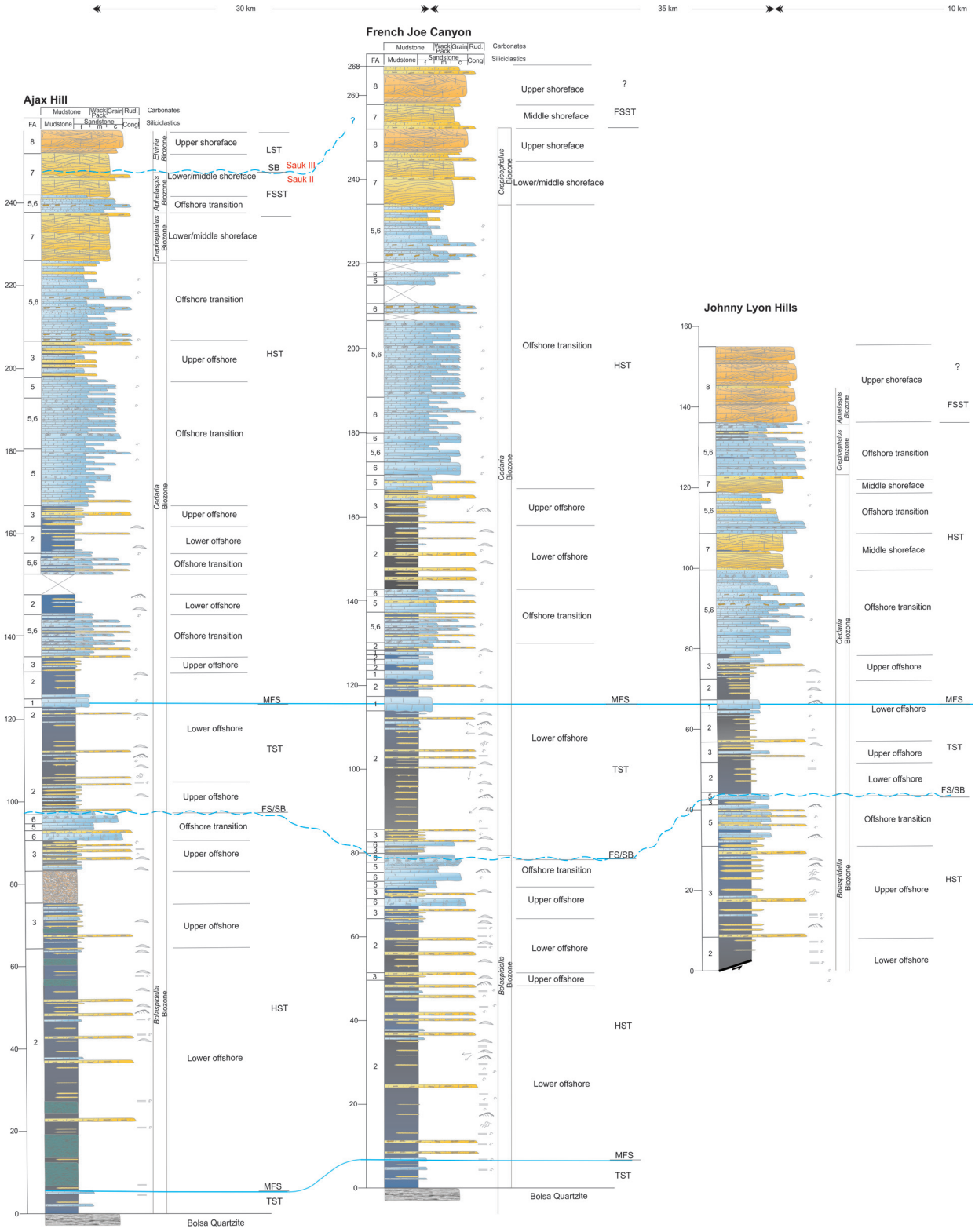
30 km
35 km
10 km
Ajax Hill
French Joe Canyon
Johnny Lyon Hills
Mudstone
Wack Pack
Grain
Rud.
Carbonates
FA
Mudstone
Sandstone
m
c
Cong
Siliciclastics
Upper shoreface
Lower/middle shoreface
Offshore transition
Upper offshore
Lower offshore
Middle shoreface
LST
SB
Sauk III
Sauk II
FSST
HST
TST
MFS
FS/SB
?
Divinia Biozone
Aphelaspis Biozone
Crepicephalus Biozone
Cedaria Biozone
Bolaspidella Biozone
Bolsa Quartzite

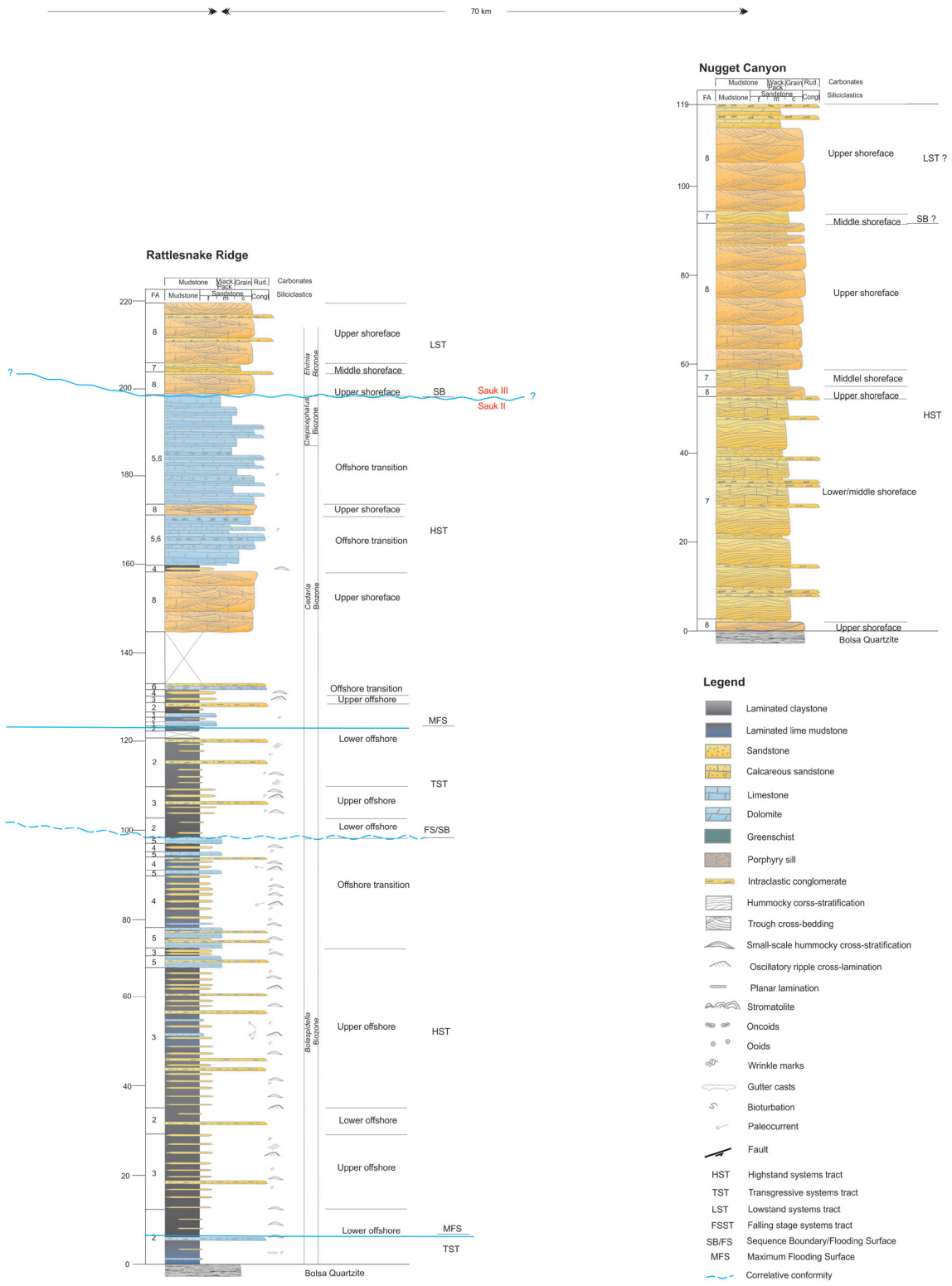

Fig. 2.5.—Five composite stratigraphic sections of the Abrigo Formation showing facies successions, depositional environments, biostratigraphy, and sequence stratigraphy. Stratigraphic top in each case is the unconformity below the Devonian Martin Formation.

2.5.1. *Facies M_n: Nodular Lime Mudstone*

Description.–Nodular lime mudstone is thin-bedded (1–3 cm thick) with intercalated argillaceous, silty lime mudstone laminae (Fig. 2.6A and B). Bedding ranges from tabular to gently wavy and laterally continuous, to lumpy due to roughly equant nodules. Oscillation ripples are sporadically present in thicker silty laminae (Fig. 2.6C and F). Macrofossils are absent, but bioturbation is common, and two ichnospecies, *Planolites montanus* and *Planolites* isp., are abundant (Fig. 2.6D and E). The former is characterized by small curved burrows rarely exceeding 5 mm in length and 2 mm in diameter, while the latter is larger and straight to gently curved. Dolomitization is located preferentially in the argillaceous laminae and locally in the burrows.

Interpretation.–The lime mud and subordinate silt were deposited from suspension fall-out under uniform, low energy conditions. The source for the lime mud was either in the overlying water column or via plumes from a nearby carbonate-producing area, or both. Oscillation ripples suggest reworking of silt layers by occasional relatively weak, distal storm waves. The abundant ichnofauna of horizontal burrows, likely from worms, suggests that sufficient organic matter was present in the sediment, at least initially, to support a bioturbating infauna. On the other hand, the absence of benthic fossils and the low diversity of trace fossils suggest unfavorable ecological factors, possibly related to the muddy substrate or nutrient availability. Environmental stress in similar facies has been interpreted to be due to, for example, dysoxic conditions (e.g., Hips 1998; Mata and Bottjer 2011). This possibility appears unlikely here, especially given the evidence in associated facies for synsedimentary cementation of lime mud and intraclast formation by current scour, pointing to a generally well mixed water column.

This is a common facies in Cambrian platform successions, often representing the deepest subtidal component of peritidal cycles (e.g., Osleger and Read 1991; Chow and James 1992; Adams and Grotzinger 1996; Osleger and Montañez 1996; Aitken 1997; Glumac and Walker 2000; Pratt and Bordonaro 2007; Chen et al., 2011). It is also present in younger deposits (e.g., Peterhänsel and Pratt 2008). It is closely similar to 'ribbon' limestone and limestone–marl or limestone–clay alternations deposited in lower energy settings, but the origin of its particular fabric is still not clear. One hypothesis argues for cyclic environmental changes (e.g., Einsele and Ricken 1991), while another proposes a purely diagenetic origin (e.g., Munnecke and Samtleben 1996). Diagenetic redistribution of calcium carbonate and differential compaction likely took place, enhancing the rhythmicity and nodularity as determined for similar facies elsewhere (Westphal et al. 2008).

2.5.2. *Facies R_i: Intraclastic Rudstone*

Description.–This facies is composed of thin (1–2 cm thick) lenses of intraclastic rudstone consisting of tabular, rounded, homogenous, lime mudstone pebbles 1–2 cm across. This facies occurs in shallow troughs between ripple crests on the top surfaces of facies M_n (Fig. 2.6C and D).

Interpretation.–This facies was deposited within the reach of storms that scoured and reworked early cemented lime mud leaving lenses of pebble-sized intraclasts in the troughs of oscillatory ripples. The lithology of the pebbles suggests that facies M_n was the source of intraclasts, and therefore facies R_i is interpreted as having been formed in the same depositional environment as facies M_n.

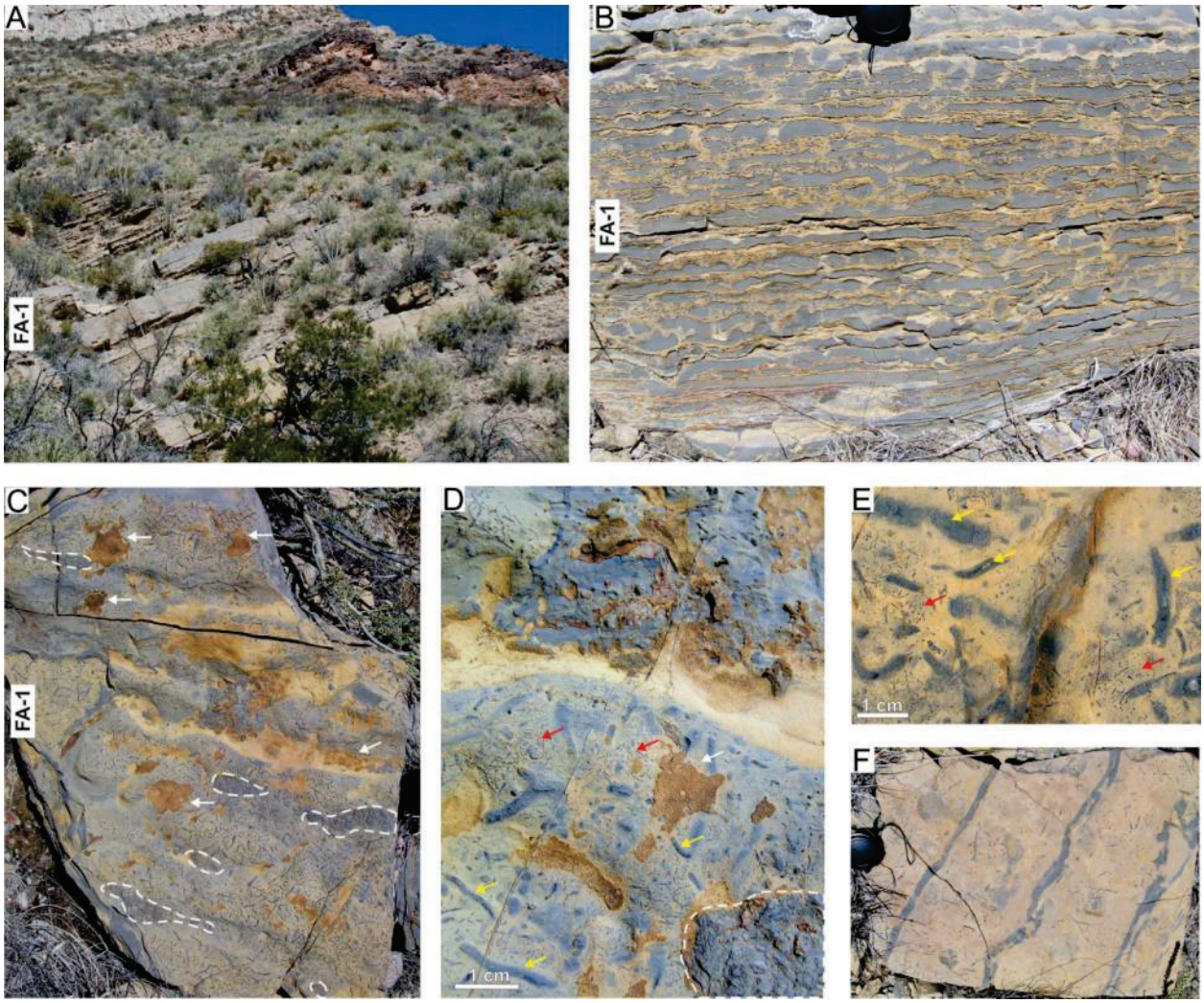

Fig. 2.6.—Facies association 1. **A)** Facies association 1 forming resistant beds in French Joe Canyon. **B)** Thin-bedded nodular lime mudstone (M_n). Primary bedding observable mainly in the lower part of the bed set, whereas the upper part is more bioturbated and hence rich in nodules. **C)** Wave ripples on the bedding plane of nodular lime mudstone. White arrows point out silty patches preserved in the ripple troughs. Intraclastic rudstone lenses (R_i) preserved in the ripple troughs are circled by dashed line. **D)** Detail of Figure 2.5C showing silty patches (white arrows), intraclastic rudstone lens (R_i), *Planolites* isp.(yellow arrows), and *P. montanus* (red arrows). **E)** *Planolites* isp. (yellow arrows) and *P. montanus* (red arrows). **F)** Wave ripples. Lens cap in B, C and F is 5 cm across.

2.5.3. *Facies C_l: Laminated Claystone*

Description.–This facies consists of olive-gray, parallel-laminated claystone (Figs. 2.7A–C; also Figs. 8A, 9A, 10A and D, and 14A). Laminae typically average 5mm thick. Silt-rich intervals are present locally.

Interpretation.–This facies was deposited from suspension fall-out of clay in a low-energy environment. The clay was derived from the adjacent land surface, possibly transported by wind or as sediment plumes produced by drainage after storm surges, or fluvial discharge and then moved offshore as dilute clouds or plumes of suspended sediment (Osleger and Read 1991). Recent studies of marine shelf-sediment dispersal show that wave-enhanced sediment gravity flows of fluid mud have the potential to move fine-grained sediment far offshore (e.g., Macquaker et al. 2010; Plint 2014; Kämpf and Myrow 2014).

2.5.4. *Facies M_l: Laminated Lime Mudstone*

Description.–This facies consists of dark to light-gray, parallel-laminated lime mudstone (Fig. 2.8A–C and E). Laminae are less than 5 mm thick. Silt-rich laminae are locally intercalated, and sparse trilobite sclerites are present.

Interpretation.–Facies M_l is interpreted as deposited in an offshore environment under low-energy conditions, with the input of lime mud derived from the water column. The darker color of mudstone and sparseness of fossils suggest that the mud was deposited under dysaerobic conditions (Osleger and Read 1991). Deposition of laminated mudstone may have taken place between major storms. Another possibility is that this facies represents settling of mud from a

dilute suspension that formed as a result of storm wave action that was sufficiently intense to disrupt a bottom-hugging fluid mud layer and dispersed the sediment upward into the water column (cf. Fan et al. 2004). It seems possible that a combination of a 'soupground' substrate—water-saturated, clay-rich sediment (Goldring, 1995)—frequent storm emplacement of fluid mud, low nutrient availability, and reduced oxygenation collectively inhibited the development of benthic populations (e.g., Macquaker and Gawthorpe 1993; Plint 2014).

2.5.5. *Facies Slt: Lenticular Siltstone*

Description.–This facies is composed of siltstone lenses that range from 5 to 20 cm across, displaying sharp erosive bases (Figs. 2.7A and B; also Figs. 8A–E) and internal laminae 0.3 to 1.0 cm thick. Wave ripple cross-lamination and symmetrical ripples on bedding surfaces are locally present

Interpretation.–The sharp basal surface overlain by wave-rippled silt implies that wind-induced turbulence, likely during storms, was responsible for introduction of silt carried in from onshore sources, and scouring and winnowing of the sea floor (Plint 2014).

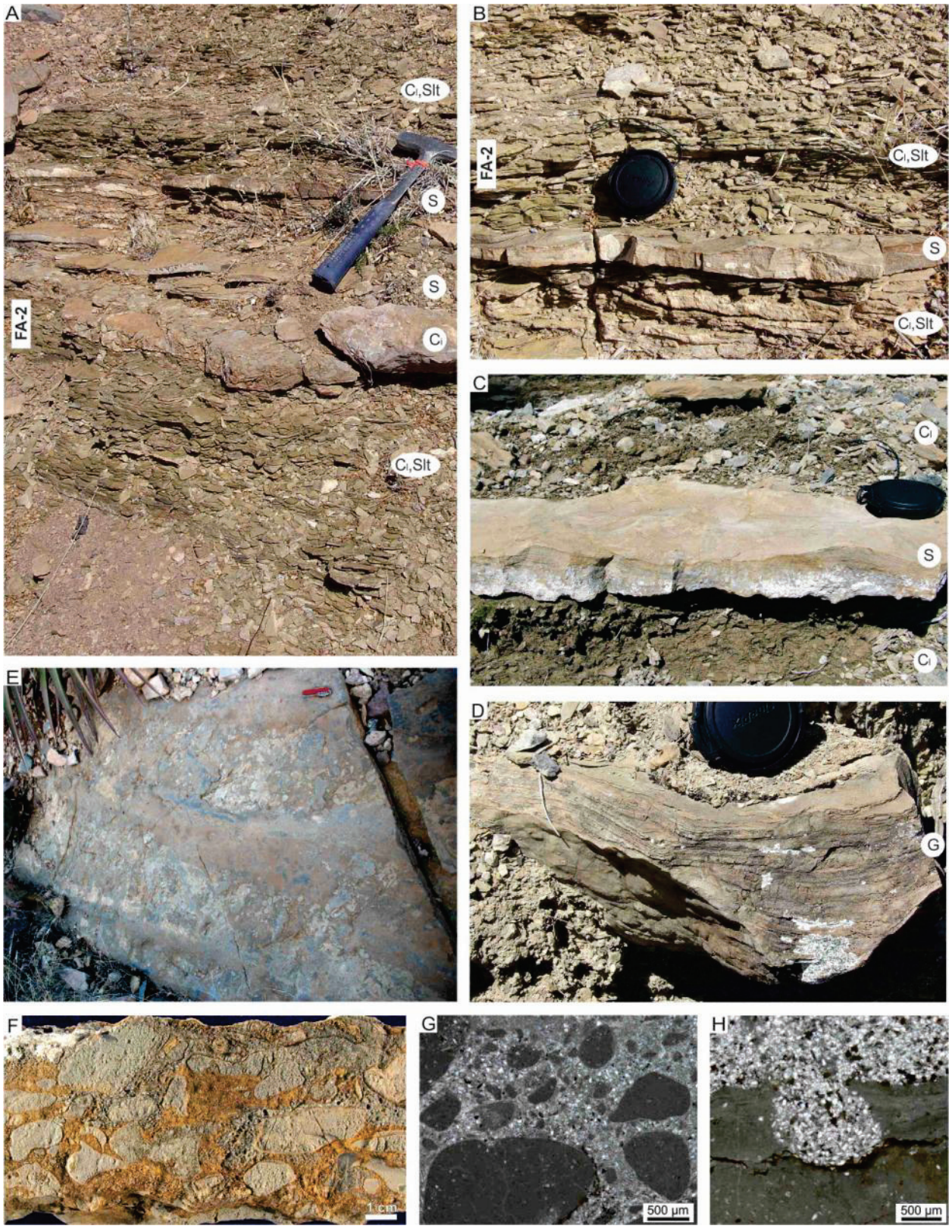
A
Cl,Slt
S
S
FA-2
Cl
Cl,Slt
B
FA-2
Cl,Slt
S
Cl,Slt
C
Cl
S
Cl
E
D
G
F
1 cm
G
500 µm
H
500 µm

Fig. 2.7.—Facies association 2. **A)** Laminated, olive-grey claystone (C_l) sporadically interlaminated with lenticular siltstones (Slt), very thin-bedded, small-scale hummocky cross-stratified sandstone (S) and intraclastic conglomerate (C). **B)** Small-scale hummocky cross-stratified, very thin-bedded sandstone (S) interlaminated with lenticular siltstone (Slt). **C)** Small-scale hummocky cross-stratified, thin-bedded sandstone (S) within laminated claystone background (C_l). **D)** Gutter cast (G) filled with obliquely laminated fine-grained sandstone. Lens cap is 5 cm across. **E)** Bedding plane of intraclasic conglomerate (C_i) showing asymmetrical dunes. **F)** Poorly sorted intraclastic conglomerate (C_i) composed of subangular to subrounded lime mud pebbles and silty matrix. **G)** Thin section photomicrograph of intraclastic conglomerate (C_i) composed of subrounded lime mud pebbles and silty matrix. **H)** Thin section photomicrograph showing the abrupt change of sedimentation from mud lime to very fine-grained calcareous sandstone (S). Burrow in lime mud scoured and cast by sand.

2.5.6. *Facies S: Small-Scale Hummocky Cross-Stratified Sandstone*

Description.–Very fine-grained, silty, very thin-bedded sandstone beds are less than 4 cm thick and display small-scale hummocky cross-stratification, symmetrical ripples on upper surfaces and sharp erosive bases (Figs. 2.7A–C and E; also 2.8A, B and E, 2.9A and B). The wavelengths of hummocks are up to ~30 cm. Common wrinkle marks (Fig. 2.9H) and rare molds of trilobite sclerites (Fig. 2.9G), including locally near-complete thoraces (Fig. 2.9I) are present on bed tops. Tool marks are present on some of the bed soles. Horizontal burrows belong to *Monomorphichnus* isp., cf. *Trichophycus* isp., *Palaeophycus* isp., *Helminthoidichnites tenuis*, *Treptichnus* isp., and cf. *Rusophycus* isp., and vertical burrows are represented by *Skolithos* isp. and *Arenicolites* isp. (Fig. 2.9D–F).

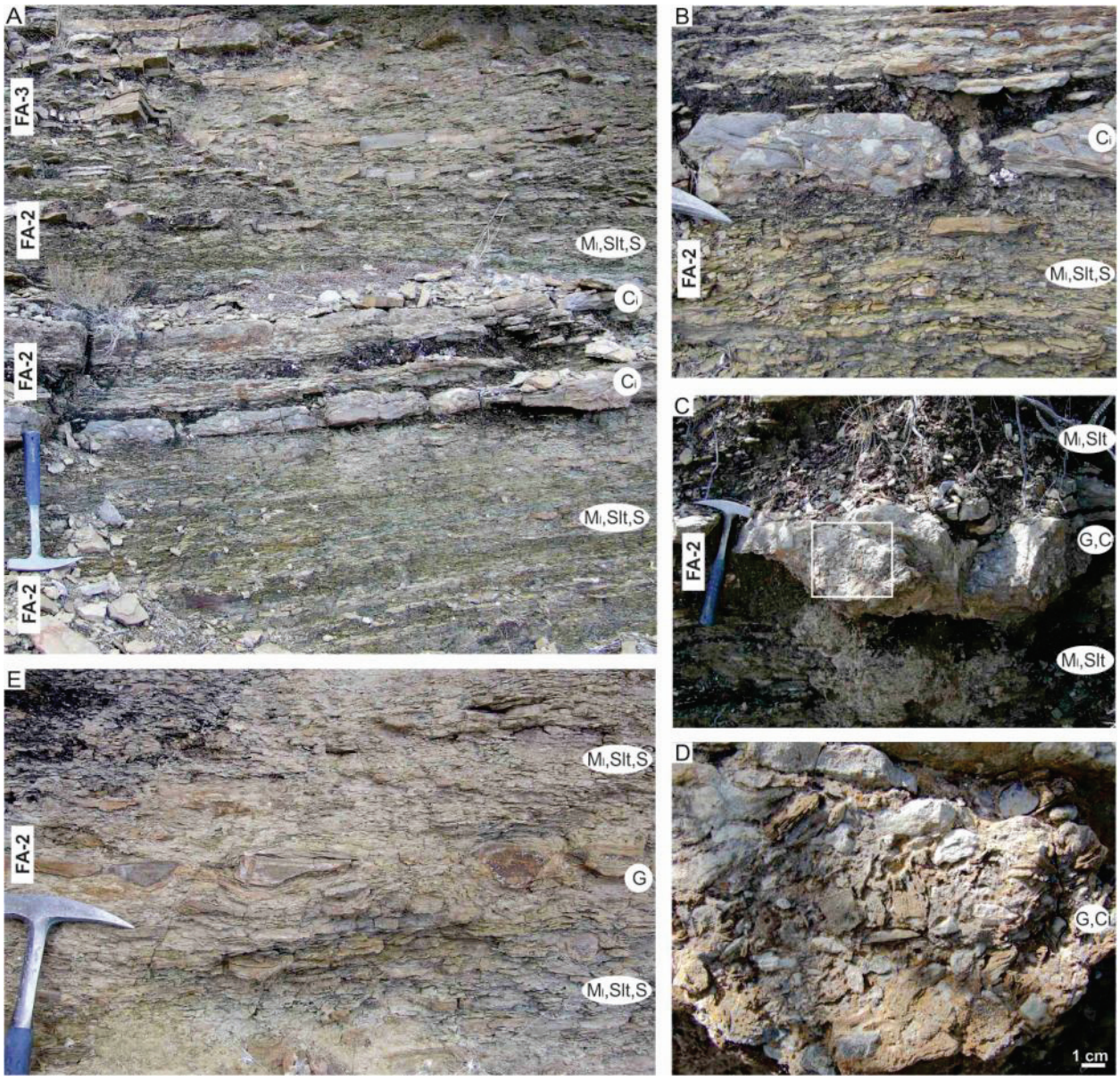

Fig. 2.8.—Facies association 2. **A)** Laminated lime mudstone (M_l) sporadically interlaminated with lenticular siltstones (Slt) and small-scale hummocky cross-stratified, thin-bedded sandstone (S) and two beds of intraclastic conglomerate (C_i). **B)** Laminated lime mudstone (M_l) occasionally interlaminated with lenticular siltstone (Slt) overlain by intraclastic conglomerate (C_i) composed of subrounded mud lime pebbles and tabular sandstone pebbles. **C)** Large gutter cast (G) intercalated with laminated lime mudstone (M_l) and lenticular siltstone (Slt). Rectangle outlines area shown in Figure 2.8D. **D)** Detail of Figure 2.8C showing varied composition of the gutter cast filled with intraclastic conglomerate (C_i) which consists of subangular tabular lime mud and sandstone pebbles. **E)**

Laminated lime mudstone (M_l) locally interlaminated with lenticular siltstone (Slt). Bed rich in gutter casts (G) filled with fine-grained sandstone.

Interpretation.–These sandstones are interpreted as relatively distal tempestites. Microbial mats have been invoked for creating wrinkle marks (e.g., Hagadorn and Bottjer 1997; Schieber 1999; Noffke et al. 2001; Buatois et al. 2014). Arguably they expanded during times of sediment surface stability. Microbial mats may have prevented disarticulation of trilobite exoskeletons in some cases.

2.5.7. *Facies G: Gutter Casts*

Description.–Gutter casts include both symmetrical and asymmetrical forms that are 3–10 cm in depth and 6–20 cm in width. They are composed of fine-grained sandstone with parallel lamination, low-angle cross-lamination, and ripple cross-lamination (Figs. 2.7D, 2.8E; also Fig. 9C). The low-angle cross-lamination dips at right angles from one side of the gutter. Some upper surfaces are covered with wave ripples whose crests are oriented parallel to the gutter axis (Fig. 2.9C). Gutter casts are oriented northeast–southwest and east–west. Rare gutter casts that reach 30 cm in depth and 60 cm in width contain carbonate and calcareous sandstone intraclasts (Fig. 2.8C and D). These large gutter casts occur in laminated claystone (C_l) and laminated lime mudstone (M_l), and lenticular siltstone (Slt) facies.

Interpretation.–Gutter casts record anomalous sea-floor erosion by offshore-directed bottom currents caused by storm (Myrow 1992; Mángano et al. 2002) or tsunami off-surge (Pratt 2001a; Pratt et al. 2012). Tsunami generation is unlikely for the Abrigo Formation, given the lack of associated seismites and outsized scours in the most proximal facies. These

currents were oriented approximately normal to the shoreline, although in the Triassic Muschelkalk of the Germanic Basin they have been reconstructed as oriented nearly parallel to the shoreline, which is suggestive of controls other than simply downslope-directed currents (Knaust and Langbein, 1995). The low-angle cross-lamination is common in gutter casts and records small-scale lateral accretion away from the side of the scour (e.g., Rees et al. 2014). Oscillation ripple cross-lamination at the top records wave action independent of the bottom currents.

2.5.8. *Facies C_i: Intraclastic Conglomerate*

Description.–Laterally extensive, tabular beds, 10–40 cm thick, of generally poorly sorted intraclastic conglomerate exhibit sharp erosive bases (Figs. 2.7A and E–G, 2.8A–D, 2.9A, also Fig. 14E). Small, low-relief, asymmetrical dunes with ~20 cm spacing are locally present on upper surfaces (Fig. 2.7E). The intraclasts are composed of rounded to subrounded and locally subangular lime mudstone pebbles (Fig. 2.7F and G), and flat, subrounded, commonly laminated, fine-grained calcareous sandstone pebbles. Intraclasts do not display any specific orientation such as imbrication or rosettes. The matrix is composed of micrite, bioclasts, peloids, and fine-grained quartz sand and silt.

Interpretation.–Strong erosive events scoured wide areas, reworking early-cemented sediment at the sediment–water interface and mixing it with unlithified carbonate grains and quartz sand. Lateral transportation was probably limited, meaning that these are essentially autochthonous deposits, although the tabular aspect of the beds suggests no shaping by strong

oscillatory currents. Lime mud was placed into suspension during storms and, as the storms waned in intensity, pumped by gentle wave action into the pores around the settled intraclasts.

This is a common facies in the Proterozoic and Cambro-Ordovician record, which is usually interpreted to be related to storms (e.g., Markello and Read 1982; Demicco 1985; Westrop 1989; Osleger and Read 1991; Saltzman 1999; Myrow et al. 2004, 2012; Kwon et al. 2006; Eoff 2014b). Some intraclastic conglomerate beds that display deep, erosive bases have been interpreted as created by strong off-shore currents or wave-action generated by tsunamis (Pratt 2001a, 2002; Pratt and Bordonaro 2007; Pratt et al. 2012). These examples formed in settings of low-intensity storm activity and, as exceptional events, are more plausibly distinguished from storm deposits. However, because the Abrigo Formation was deposited in a wave-dominated setting with evidence for a relatively high frequency of storms, and because of the tabular shape of beds, generally rounded nature, and chaotic orientation of the intraclasts, scour and reworking by storm waves is more likely. Moreover, the absence of seismites (e.g., Pratt 1994, 2001a, 2002) argues against a local tsunami-induced origin.

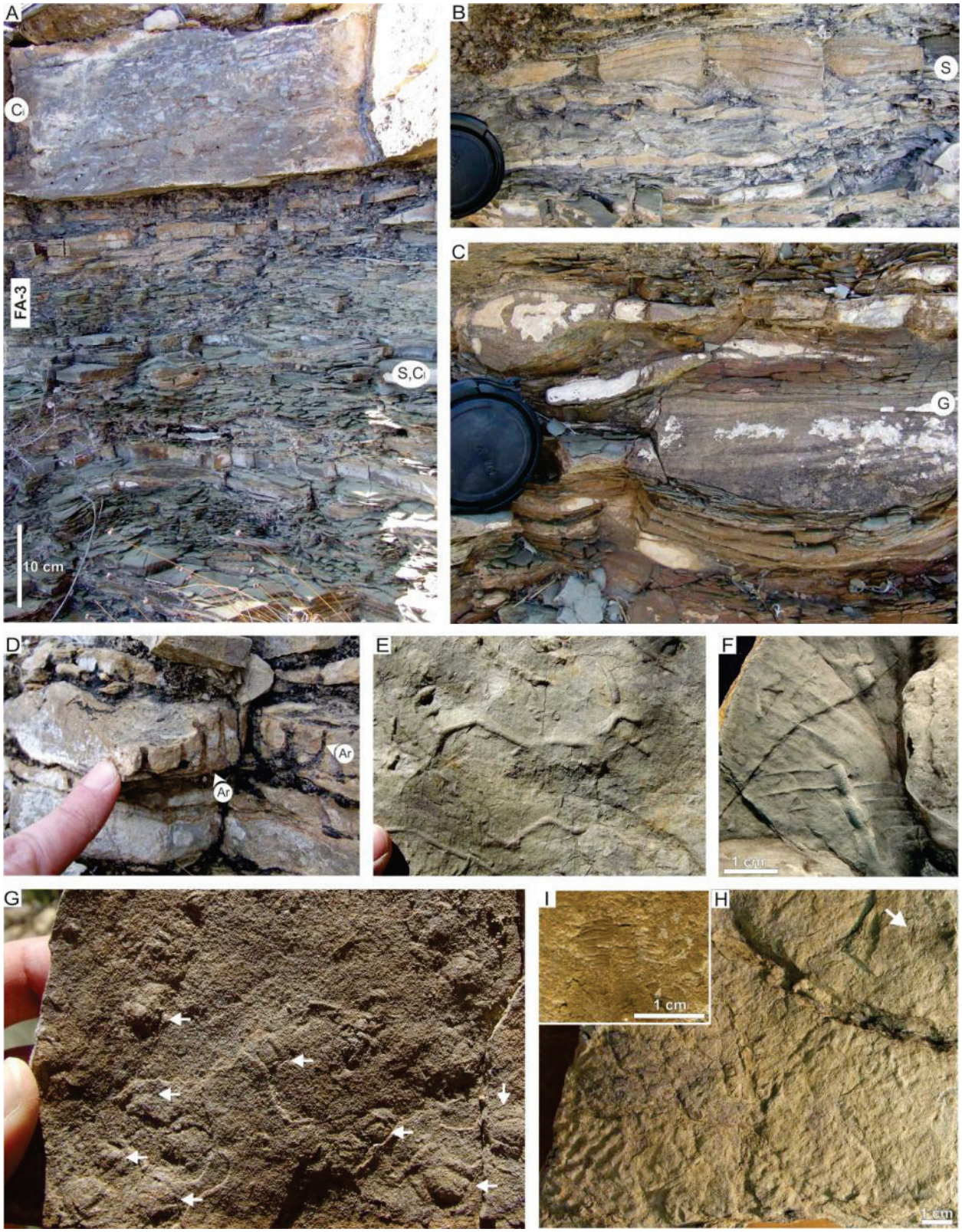

Fig. 2.9.—Facies association 3. **A)** laminated, olive-grey claystone (C_l) interbedded with small-scale hummocky cross-stratified, very thin-bedded, tabular sandstones (S). The complex is overlain by the intraclastic conglomerate

(C_i). **B)** Small-scale hummocky cross-stratified sandstone (S). **C)** Gutter casts (G) filled in with fine-grained sandstone displaying wave ripple cross-lamination in its upper part. **D)** Small-scale hummocky cross-stratification (S) with *Arenicolites* isp. **E)** *Treptichnus* isp. (S). **F)** *Monomorphichnus* isp. (S). **G)** Molds of trilobite cranidia (arrows) preserved on upper plane of fine-grained sandstone (S). **H)** Bedding plane of fine-grained sandstone covered with wrinkle marks (S). **I)** Close-up of upper right corner of **H** showing mold of part of trilobite thorax (arrow).

2.5.9. *Facies S_{HCS}: Hummocky Cross-Stratified Sandstone*

Description.–This facies consists of thin to medium beds of very fine- to fine-grained sandstone and calcareous sandstone that display irregular thicknesses and sharp erosive bases. Hummocky cross-stratification is dominant in the thicker beds, and asymmetrical and symmetrical ripples are more common in thinner beds (Fig. 2.10A, C–E). Symmetrical ripples are, in rare cases, present on the top of the hummocks (Fig. 2.10D). Hummock wavelengths are 0.5–1.5 m and amplitudes are 5–10 cm. Ripple wavelengths are 8–15 cm and amplitudes are 0.5–1 cm. Unidirectional ripples reveal southwest and west paleocurrent directions. Wrinkle marks are locally present (Fig. 2.10B). Vertical traces are represented by *Skolithos* isp. Bed soles are rich in tool marks and trace fossils belonging to *Palaeophycus* isp. and *Trichophycus* isp.

Interpretation.–Sandstone beds with hummocky cross-stratification record strong storm events. Ripples on hummock tops were formed by waves that reworked the surface after storm intensity decreased (e.g., Dott and Bourgeois 1982). Asymmetrical ripples and well developed tool marks indicate unidirectional currents. The close association of unidirectional with oscillatory cross-lamination has been taken as evidence for the presence of geostrophic currents (e.g., Swift et al. 1986; Midtgaard 1996). On the other hand, geostrophic flow might be regarded

as unlikely well in the cratonic interior. In the Abrigo Formation, unidirectional flows could have formed by the draining of shallower areas as storms waned.

Vertical dwelling traces belong to the *Skolithos* ichnofacies, the dominance of which reveals organisms' preferences for sandy substrates and high abundances of organic particles kept in suspension in the well-oxygenated water column by waves and currents (Buatois and Mángano 2011). *Palaeophycus* isp. and *Trichophycus* isp. belong to the *Cruziana* ichnofacies and represent a fair-weather suite that developed under stable, low-energy conditions between storm activity.

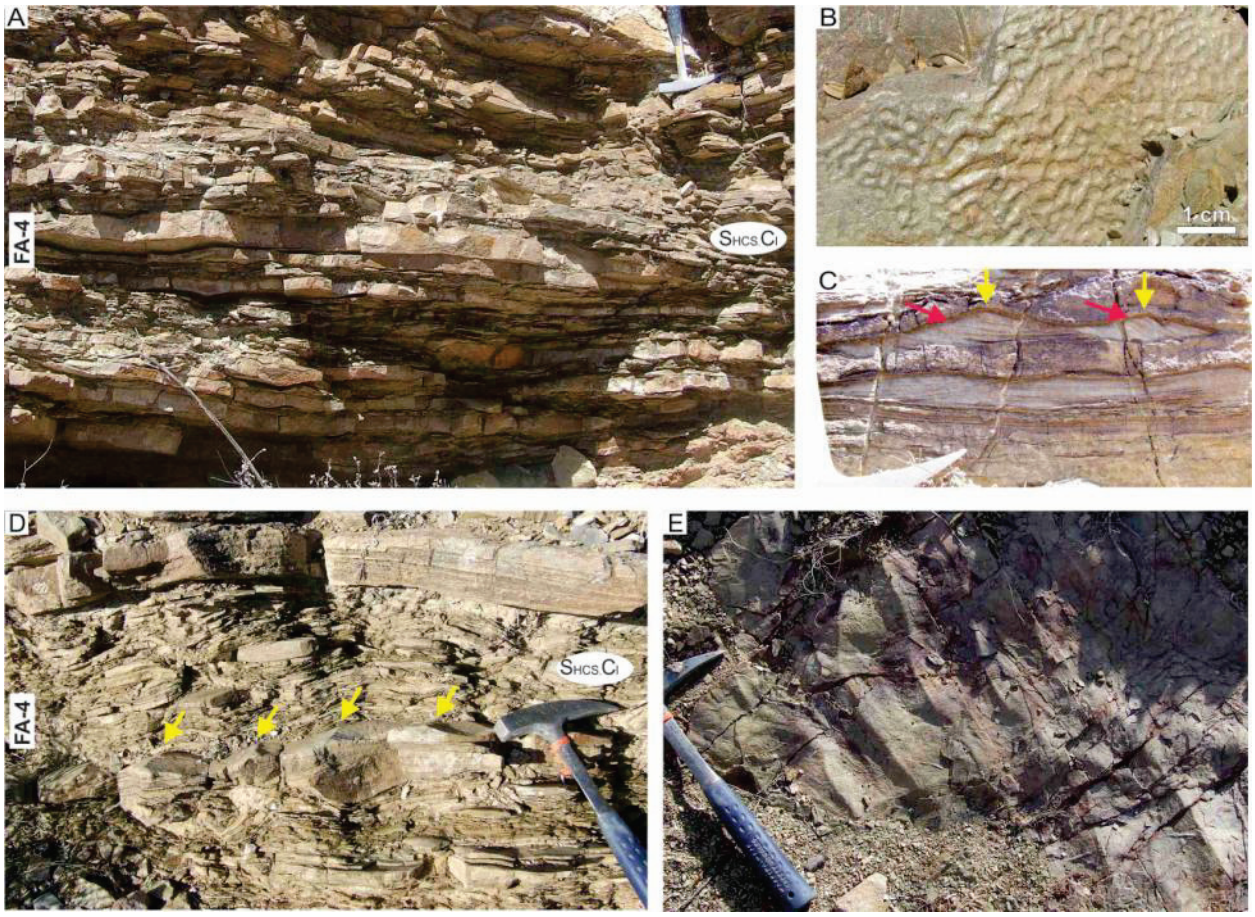

Fig. 2.10.—Facies association 4. **A)** Hummocky cross-stratified sandstone (S_{HCS}) interbedded with laminated olive-grey claystone (C_l). **B)** Wrinkle marks preserved on sandstone bedding plane. **C)** Top of hummocky cross-stratified sandstone overlain by two thin beds with wave-ripple cross-lamination, followed by a rippled bed showing

unidirectional flow from left to right (red arrows) and symmetrical crests reworked by oscillatory currents (yellow arrows). **D)** Hummocky cross-stratified sandstone (S_{HCS}) interbedded with laminated olive-grey claystone (C_l). Wave ripples overprinted the top of the hummocky cross-stratified bed (arrows). **E)** Wave ripples (S_{HCS}).

2.5.10. *Facies MW: Lime Mudstone and Wackestone*

Description.–Lime mudstone and wackestone beds range from 5 to 10 cm in thickness (Fig. 2.11A–E), with rare wave ripples evident (Fig. 2.11A). Beds with well-defined, locally dolomitized *Thalassinoides* isp. galleries are developed sporadically (Figs. 2.11B and C; also Fig. 2.12G). In some cases, these are filled by grainstone identical to the overlying bed belonging to facies GP (Fig. 2.12G). Some bedding surfaces have small amounts of trilobite sclerites that are disarticulated but usually not fragmented and abraded.

Interpretation.–This facies records deposition below fair weather wave base. The ripples suggest that at least some of the lime mud was in the form of silt-sized peloids (e.g., Demicco 1985; Palma et al. 2009). Tranquil conditions allowed sporadic bioturbation by a *Thalassinoides*-producing ichnofauna, most probably arthropods. Grainstone filling *Thalassinoides* indicates coarse sediment pumped into the empty galleries during subsequent storms. The burrows represent the *Glossifungites* ichnofacies, which typically characterizes firm substrates. Firmground development suggests reduced accumulation rate, in that the sediment was stable for sufficient time for some consolidation to occur, possibly involving incipient cementation.

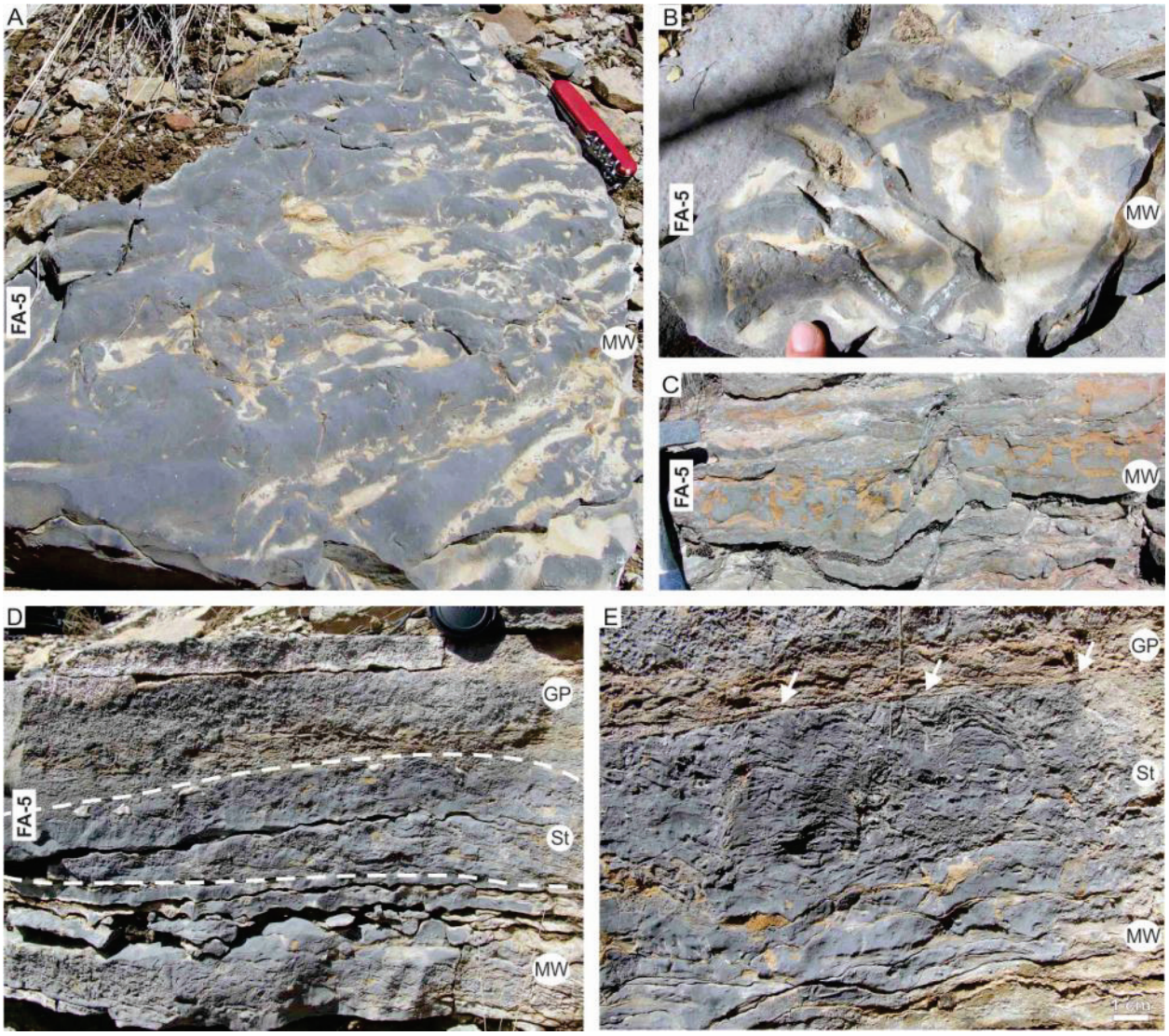

Fig. 2.11.—Facies association 5. **A)** Wave ripples on bedding plane of the lime mudstone and wackestone (M_w). **B)** Bedding plane with exhumed network of *Thalassinoides* isp. **C)** Firmground with *Thalassinoides* isp. **D)** Stromatolite above the lime mudstone and wackestone (MW) overlain by bioclastic grainstone and packstone (GP). **E)** Stromatolite and erosive contact with overlying bioclastic grainstone (GP) (arrows).

2.5.11. *Facies St: Stromatolite*

Description.–Stromatolites occur only at one horizon in French Joe Canyon (Fig. 2.3). They form laterally linked domes 3–4 cm in diameter that locally developed irregular mounds

reaching 10 cm thick (Fig. 2.11D and E). The stromatolite bed overlies lime mudstone (MW), and is overlain by sharp, erosive based oolitic–oncolitic packstone (P_o) and bioclastic grainstone and packstone (GP).

Interpretation.–A brief interval of sea-floor stability, low sedimentation rate, and clear water with minimal clay and silt input promoted the growth of wavy microbial laminae and low-relief stromatolites (e.g., Pratt et al. 2012). This period was followed by an abrupt, storm-related sedimentation event (facies P_o and GP) that brought an end to stromatolite accretion.

2.5.12. *Facies GP: Bioclastic Grainstone and Packstone*

Description.–This facies is composed of slightly sandy bioclastic grainstone and packstone beds that are generally 2–15 cm thick and rarely up to 30 cm thick (Figs. 2.12D and G, also Fig. 2.13I and J), displaying sharp, erosive bases, locally with gutter casts (G). Bioclasts commonly show normal grading. They consist of disarticulated and commonly abraded trilobite sclerites, along with lingulate (phosphatic) brachiopods and helcionelloid microgastropods in some beds (Fig. 2.13I).

Interpretation.–The taphonomic character of bioclasts indicates abrasion on the sea floor caused by protracted reworking (e.g., Pratt and Bordonaro 2007). Similar bioclast-dominated layers in the lower and middle Cambrian of southern Sweden are interpreted as migrating, low-relief sheets (Álvaro et al. 2010). By contrast, well-sorted grainstone with gutter casts has been interpreted as from erosion at the shoreface transition and transportation into deeper water by storm-generated flow (Myrow 1992). Significant transportation seems unlikely for facies GP because of the hydrodynamic resistance caused by the shape of trilobite sclerites

and brachiopod valves. Thus they represent the in situ benthic community (Pratt and Bordonaro 2007, 2014).

2.5.13. *Facies P_o: Oolitic–Oncolitic Packstone*

Description.–Oolitic packstone and minor grainstone locally contain significant amounts of oncoids, bioclasts, and intraclasts (Figs. 2.12A–C and E–G; also Fig. 2.13A–H). Packstone beds with sharp erosive bases are 5–15 cm in thickness. Oncoids range from 0.5 to 1 cm in diameter, and sporadically up to 2 cm. Nuclei are small oobiomicrite intraclasts, aggregates of ooids and peloids, and trilobite bioclasts (Fig. 2.13A–H). Ooids are medium to coarse sand-sized and although most are recrystallized, some retain a radial cortex. Lobate, coarse sand- to granule-sized aggregates consisting of grapestones of oomicrite (Fig. 2.13B) and oobiopelmicrite (Fig. 2.13C) co-occur with ooids. Peloids are silt- to very fine sand-sized, rounded to subrounded and composed of uniform and clotted micrite (Fig. 2.13A–D). Isolated peloids are rare but aggregates of peloids are moderately common. Intraclasts composed of pelmicrite and micrite are rounded to subrounded, subequant to tabular, and are 1 mm to 2 cm in size. Bioclasts include trilobite sclerites and sclerite fragments, and lingulate brachiopods. Glauconite grains are present locally. This facies is commonly interbedded with bioclastic grainstone and packstone (GP).

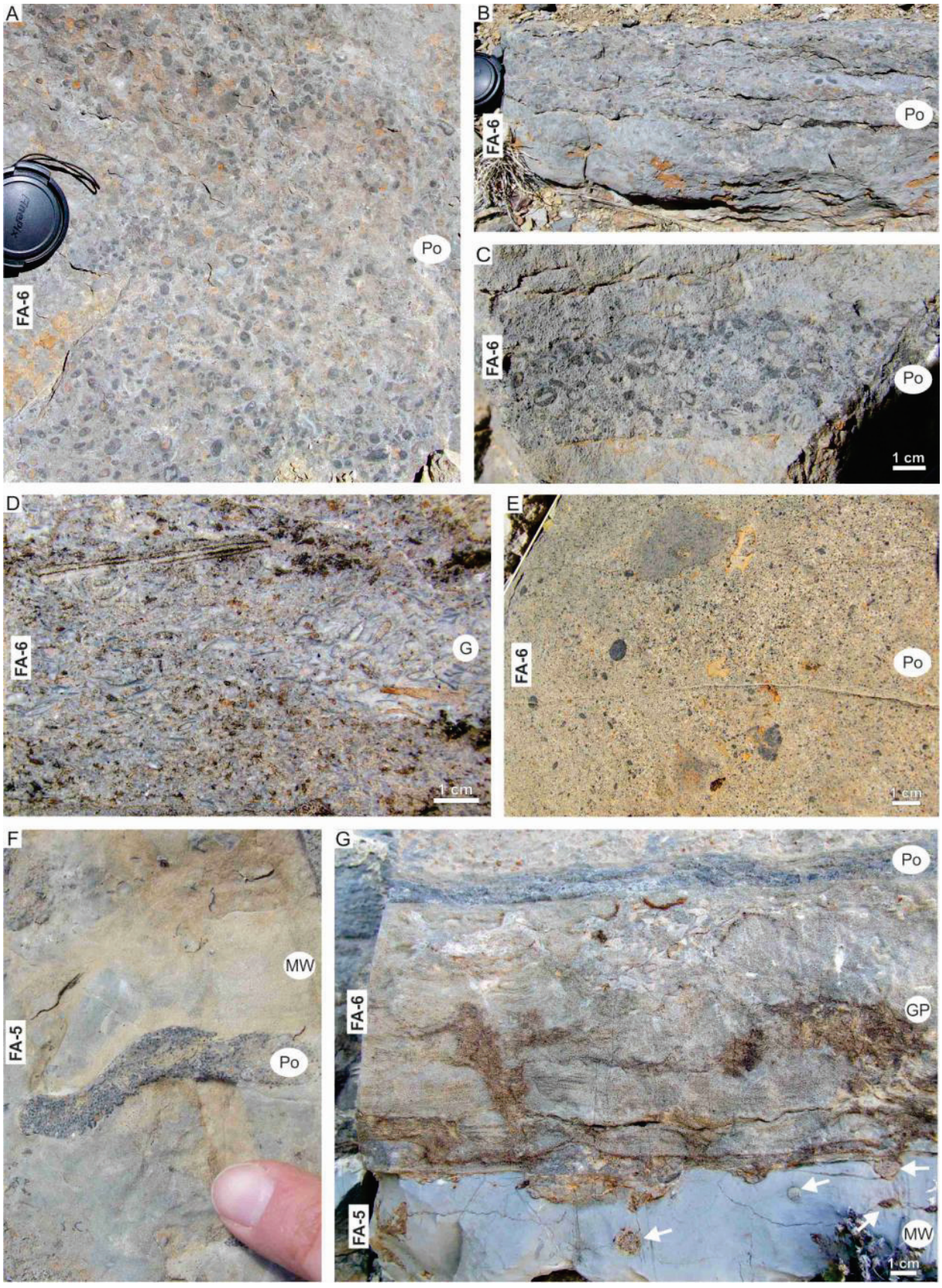
A
Po
FA-6
B
FA-6
Po
C
FA-6
Po
1 cm
D
FA-6
G
1 cm
E
FA-6
Po
1 cm
F
MW
FA-5
Po
G
Po
FA-6
GP
FA-5
MW
1 cm

Fig. 2.12.—Facies association 6. **A)** Bedding plane of oolitic–oncolitic packstone (P_o). **B)** Bed of oolitic–oncolitic packstone (P_o). **C)** Bed of oolitic–oncolitic packstone (P_o). **D)** Bioclastic grainstone (GP). **E)** Oolitic packstone (P_o). **F)** Wackestone (MW) burrowed by *Planolites* isp. filled in with oolite. **G)** Mudstone (MW) firmground, overlain by bioclastic grainstone and packstone (GP) that is, in turn, overlain by oolitic–oncolitic packstone (P_o). Grainstone-filled galleries belonging to *Thalassinoides* isp. (arrows).

Interpretation.– As this facies appears in relatively thin beds and is composed of mixed ooids, oncoids, bioclasts and intraclasts, it is interpreted to have formed by erosion and re-deposition of locally lithified sediment, rather than in situ accumulation. Interbedding with bioclastic grainstone and packstone (GP) is further evidence that the oolitic sediment was washed from small shoals in nearby shallower areas and re-deposited seaward by storm-generated currents. A similar process was invoked for middle Cambrian oolites by Kwon et al. (2006) and Brett et al. (2009).

Ooidal coatings on peloidal nuclei and the presence of oopelmicrite aggregates suggest that the factors that favored their formation were complex and involved several steps. Initially, peloids and ooids were deposited together under relatively high-energy conditions, although perhaps in separate locales or at different times in the same locale. Lime mud formed under lower energy conditions, and ooids were transported and dispersed into muddy areas. In some cases, suspended lime mud was washed in between the ooid and peloid framework grains during waning storm action or later weak turbulence. Subsequently, partial lithification took place, followed by erosion and transport.

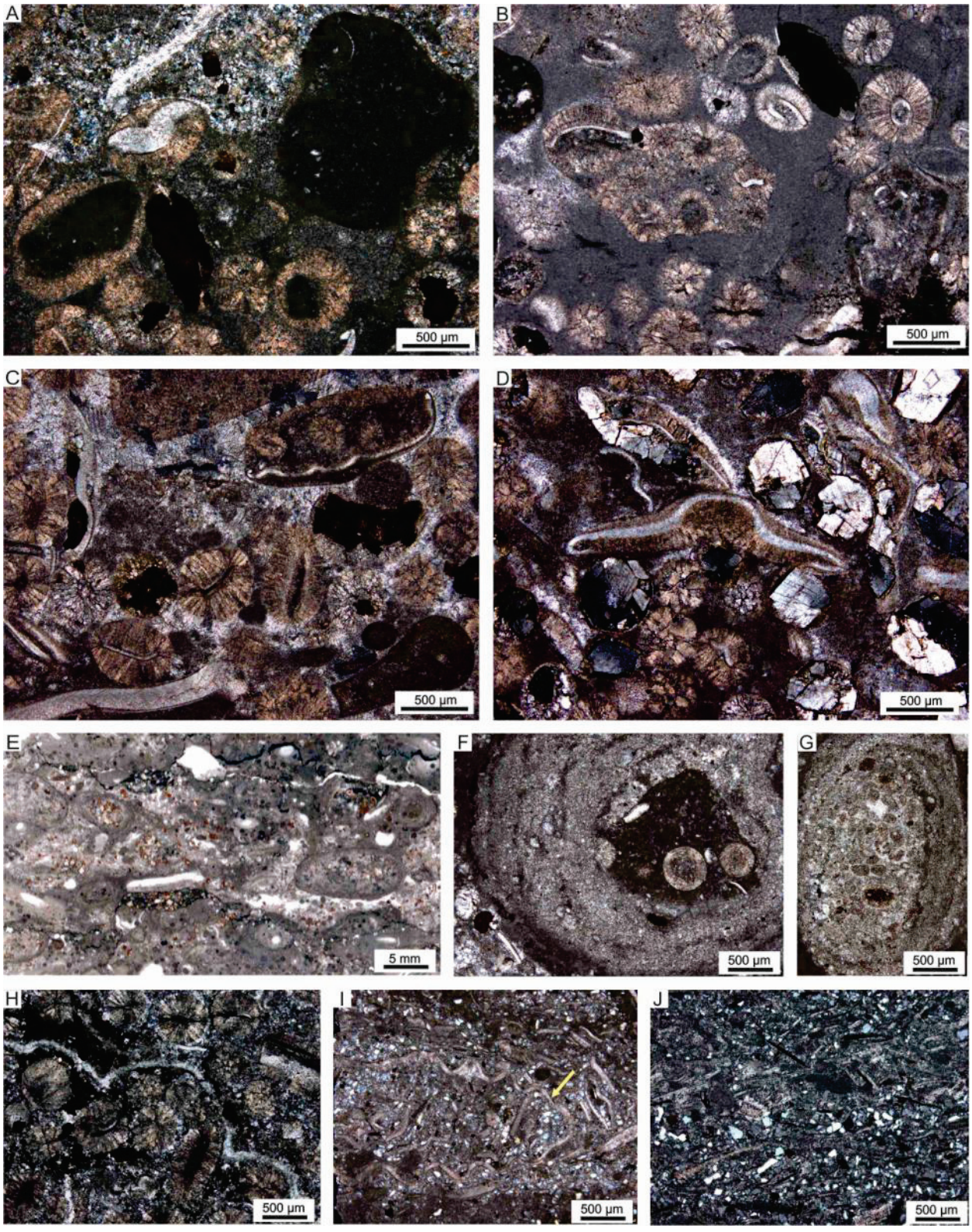
A
500 µm
B
500 µm
C
500 µm
D
500 µm
E
5 mm
F
500 µm
G
500 µm
H
500 µm
I
500 µm
J
500 µm

Fig. 2.13.—Thin section photomicrographs of facies association 6. **A)** Oobiomicrite–oobiosparite (in upper part of photograph) composed of radial ooids formed around peloids and trilobite sclerites. The ooids occur together with trilobite sclerites and subrounded granules. **B)** Oomicrite with ooid grapestone. **C)** Oobiosparite with lumps composed of ooids and trilobite sclerites. **D)** Oobiomicrite, trilobite sclerites enveloped by radially arranged calcite crystals; some ooids are recrystallized. **E)** Onco-oobiomicrite **F)** Oncoid with the nuclei formed by intraclast (oobiomicrite). **G)** Oncoid whose nuclei consists of of ooids and peloids. **H)** Oobiosparite, trilobite sclerite (cephalon with well defined glabella). **I)** Biomicrite with gastropod (arrow), trilobite sclerites and silty matrix. **J)** Mixed hybrid of fine-grained biomicrite and medium to fine sand-size quartz grains.

2.5.14. *Facies S_{AHCS}: Amalgamated Hummocky Cross-Stratified Sandstone*

Description.–This facies consists of fine-grained, yellowish-gray to brown weathering medium-bedded, hummocky cross-stratified, locally calcareous sandstone (Fig. 2.14A–E). Scours occur at the bases of some beds, and internal erosional surfaces are sporadically present. Rippled tops are rare. Hummock wavelength is 1–3 m and amplitude is 5–20 cm. Burrows are limited to rare vertical forms represented by *Skolithos* isp. The total thickness of hummocky cross-stratified sandstone packages differs significantly from section to section, from 5 m (French Joe Canyon) up to 55 m (Nugget Canyon).

Interpretation.–The presence of hummocky cross-stratification indicates wave action generated during storm events, including wave-generated surges (Dott and Bourgeois 1982; Hunter and Clifton 1982; Cheel and Leckie 1993; Plint 2010; Eoff 2014b). Scours at the bases of sandstone beds indicate strong erosive flows (e.g., Buatois and Mángano 2003). The limited presence of vertical burrows is likely due to intensity and frequency of storms that limited colonization by infaunal populations despite the appropriate sandy substrate.

Fig. 2.14.—Facies association 7. **A)** Resistant interval of amalgamated hummocky cross-stratified sandstones (S_{AHCS}). **B)** Amalgamated hummocky cross-stratified sandstones (S_{AHCS}). **C)** Transverse section through hummocky cross-stratified sandstone (S_{AHCS}). **D)** Amalgamated, hummocky cross-stratified calcareous sandstones (S_{AHCS}) **E)** Lens of intraclastic conglomerate (C_i) (circled with dashed line) preserved between hummocky cross-stratified calcareous sandstones. Hammer length is 30 cm.

2.5.15. *Facies S_{TCS}: Trough Cross-Stratified Sandstone*

Description.–Gray- to brown-weathering, amalgamated, trough cross-stratified, coarse- to very coarse-grained, locally calcareous sandstone forms beds ranging from 0.5 to 2 m thick (Fig. 2.15A–F). Beds have sharp and erosive bases, and are normally graded, with pebbles

present at some of their bases (Fig. 2.15D). The total thickness of these sandstone intervals ranges from 10 m to 50 m. Pelmatozoan ossicles are locally present in discrete laminae. Scattered *Skolithos* isp. and *Diplocraterion* isp. burrows are present (Fig. 2.15E and F).

Interpretation.–The presence of large-scale cross-stratification suggests that this facies was deposited on a relatively high-energy coast (e.g., Clifton et al. 1971; Olsen et al. 1999). Shoreface sand was transported as three-dimensional dunes produced by onshore-directed shoaling waves and also by storm-enhanced longshore and offshore currents from off-surge (Runkel 1994; Byers and Dott 1995; Runkel et al. 1998). The limited presence of vertical burrows is likely due to continuously migrating bedforms, which resulted in sparse infaunal development (Desjardins et al. 2010), although locally protected sites were colonized by pelmatozoans. This is the shallowest facies examined in this study.

Fig. 2.15.—Facies association 8. **A)** Amalgamated trough cross-stratified sandstone (S_{TCS}) forming resistant beds in Nugget Canyon. **B)** Very thick-bedded set of coarse to very coarse-grained, trough cross-stratified sandstone (S_{TCS}).**C)** Thick-bedded set of coarse to very coarse-grained, trough cross-stratified calcareous sandstone (S_{TCS}). **D)** Pebbles in the bottom part of the trough cross-stratified sandstone (S_{TCS}). **E)** Bedding plane with dense *Skolithos* isp. (Sk) and *Diplocraterion* isp. (Di) assemblage. **F)** *Skolithos* isp. (Sk) and *Diplocraterion* isp. (Di) in trough cross-stratified sandstone (S_{TCS}).

Table 2.1.—Lithofacies and facies associations of the Abrigo Formation.

Facies	Lithology and sedimentary structures	Depositional processes	Facies association	Sedimentary environment
M_n Nodular lime mudstone	Thin-bedded nodular lime mudstones with intercalated silty lime mudstone laminae. Oscillation ripples sporadically present. Macrofossils absent, but bioturbation locally abundant.	Deposited from suspension fall-out under uniform, low energy conditions.	1	Lower offshore
R_i Intraclastic rudstone	Thin lenses of intraclastic rudstone consisting of tabular, rounded lime mudstone pebbles, in shallow troughs between the ripple crests on the top surfaces of beds of facies M_n.	Deposited within the reach of storms that scoured and reworked incipiently cemented lime mud floor .	1	Lower offshore
C_l Laminated claystone	Olive-gray, parallel-laminated claystone.	Deposited from a suspension fall-out of clay in a low-energy environment.	2 3 4	Lower offshore Upper offshore Offshore transition
M_l Laminated lime mudstone	Gray, parallel-laminated lime mudstone.	Deposited under low energy conditions; lime mud from suspension fall-out.	2 3 4	Lower offshore Upper offshore Offshore transition
Slt Lenticular siltstone	Thin lenses of siltstone with erosive bases.	Deposited by distal storm events.	2	Lower offshore
S Small-scale hummocky cross-stratified sandstone	Very fine-grained, silty, very thin-bedded sandstone, displaying combined-flow ripple cross-lamination, symmetrical ripple tops, small-scale hummocky cross-stratification, and sharp erosive bases. Tool marks and wrinkle marks locally present.	Deposited during high-energy periods recorded as distal tempestites.	2 3	Lower offshore Upper offshore
G Gutter casts	Symmetrical and asymmetrical forms, filled with fine-grained sandstone, rarely carbonate and calcareous sandstone intraclasts. Some upper surfaces with wave ripples.	Sea-floor erosion by offshore-directed bottom currents caused by drainage from storm surge.	2 3 4	Lower offshore Upper offshore Offshore transition
C_i Intraclastic conglomerate	Laterally extensive, tabular beds of intraclasts with sharp erosive bases. Intraclasts composed of mixed, rounded to subrounded and locally subangular lime	Storm-related erosion scouring wide areas and reworking sediment that was cementing under the	2 3 4, 5 7	Lower offshore Upper offshore Offshore transition Lower/middle shoreface

	mudstone pebbles and flat, subrounded, often laminated, fine-grained calcareous sandstone pebbles.	sediment–water interface.	8	Upper shoreface
S_{HCS} Hummocky cross-stratified sandstone	Thin- to medium-bedded, very fine- to fine-grained sandstone or calcareous sandstone, with hummocky cross-stratification, combined-flow ripple cross-lamination, and symmetrical ripples.	Deposited during strong storm events, with ripples on hummock tops formed by gentler wave action.	4	Offshore transition
MW Lime mudstone and wackestone	Thin-bedded lime mudstone and wackestone beds, locally with wave ripples and firmgrounds.	Deposited under fair-weather and tranquil conditions.	5	Offshore transition
St Stromatolite	Laterally linked domes 3–4 cm in diameter that locally develop irregular mounds up to 10 cm thick.	Accreted when sea-floor was stable, with reduced clay and silt sedimentation.	5	Offshore transition
GP Bioclastic grainstone and packstone	Thin- to medium-bedded, erosionally based, often normally graded, bioclastic grainstone and packstone.	Reworked by storms and oscillatory currents during storms.	6	Offshore transition
P_o Oolitic–oncolitic packstone	Thin- to medium-bedded, oolitic–oncolitic packstone containing sporadic bioclasts and intraclasts, with sharp erosive bases.	Derived from high-energy shoals and transported offshore by storm currents.	6	Offshore transition
S_{AHCS} Amalgamated hummocky cross-stratified sandstone	Fine-grained, yellowish-gray to brown-weathering, medium-bedded, hummocky cross-stratified sandstone, with rare *Skolithos* burrows.	Deposited during strong wave action generated during storm events and wave-generated surges.	7	Lower/middle shoreface
S_{TCS} Trough cross - stratified sandstone	Gray- to brown-weathering, trough cross-stratified, coarse to very coarse-grained, locally calcareous sandstone. Bed bases sharp and erosive. Normally graded with quartzite pebbles present locally at their bases.	Deposited under high-energy with transportation as three-dimensional dunes mainly by storm-enhanced currents.	8	Upper shoreface

2.6. FACIES ASSOCIATIONS (FA)

Eight facies associations had been recognized leading to the interpretation of the depositional environments

2.6.1. *Facies Association 1*

Description.–FA1 is composed of nodular lime mudstone (M_n) with sporadic lenses of intraclastic rudstone (R_i) (Fig. 2.6A–F).

Interpretation.–The lime mud in FA1 is interpreted as having been deposited from suspension fall-out in a low-energy environment above storm-wave base. Rare wave ripples and sporadic lenses of intraclastic rudstone attest to the effects of higher energy events which, however, played a subordinate role. This facies association is considered to be the most seaward in the Abrigo Formation, having been deposited in the distal lower offshore setting.

2.6.2. *Facies Association 2*

Description.–FA2 consists of laminated claystone (C_l) or laminated lime mudstone (M_l) sporadically interlaminated with lenticular siltstone (Slt) and small-scale hummocky cross-stratified, very thin-bedded sandstone (S) (Figs. 2.7A–H, 2.8A–E). The sandstone/mudstone ratio ranges from 1:5 to 1:10. Gutter casts (G) and intraclastic conglomerate (C_i) are relatively common.

Interpretation.–The lime mud and clay were deposited by suspension fall-out in a low-energy environment. Dominance of horizontal burrows reflects an accumulation of organic

detritus in the sediment under low energy, fair-weather conditions (Buatois and Mángano, 2003). However, local presence of sharp-based, thin siltstone and sandstone beds with oscillatory cross-lamination, gutter casts, and intraclastic conglomerate indicates distal storm deposits. Siliciclastic sediment could have been remobilized from shallower areas and carried seaward suspended in plumes. This facies association is interpreted as having been deposited above storm wave base in a lower offshore setting, but somewhat shallower than FA1.

2.6.3. *Facies Association 3*

Description.–FA3 consists of laminated claystone (C_l) or laminated lime mudstone (M_l), interbedded with small-scale hummocky cross-stratified, very thin-bedded, laterally extensive sandstone beds (S) (Fig. 2.9A–H). Gutter casts (G) and intraclastic conglomerate beds (C_i) are common. Sandstone/mudstone ratio ranges between 1:2 and 1:3.

Interpretation.–This facies association records alternation of event deposition punctuating clay and lime mud suspension and deposition in a low-energy setting. Thin and erosive-based sandstone beds with oscillatory and unidirectional ripple cross-lamination and gutter casts are interpreted as distal tempestites. The rounding of carbonate pebbles in intraclastic conglomerate indicates that the sediment was probably repeatedly reworked. The abundant and comparatively diverse ichnofauna belonging to *Cruziana* ichnofacies reflects relative environmental stability and low sedimentation rate. However, vertical, dwelling traces indicate that there was suspended organic matter in the water column. This facies association is interpreted as having been deposited above storm-wave base in an upper offshore environment.

2.6.4. *Facies Association 4*

Description.–FA4 consists of hummocky cross-stratified sandstone (S_{HCS}) regularly interbedded with laminated claystone (C_l) (Fig. 2.10A–E). Gutter casts (G) and intraclastic conglomerate (C_i) are present. The sandstone/mudstone ratio is 1:1–2:1.

Interpretation.–This facies association was deposited by suspension fall-out during tranquil conditions alternating with the effects of storms which transported sand from nearshore areas and reworked it by oscillatory currents. Fair-weather deposits had a low preservation potential in the storm-dominated setting. A storm-related trace-fossil assemblage belonging to the *Skolithos* ichnofacies alternates with a fair-weather *Cruziana* suite. FA4 is interpreted as having been deposited in an offshore transition setting.

2.6.5. *Facies Association 5*

Description.–FA5 is composed of lime mudstone and wackestone (MW) with a stromatolite bed (St) in one instance, and is commonly found in alternation with FA6 (Fig. 2.11A–E).

Interpretation.–This facies association was deposited under fair-weather conditions and variable sedimentation rates, at times temporarily reduced. The seafloor was swept frequently by storms, which shifted substantial amounts of sediment, sometimes exposing hitherto buried layers. This led to the occasional formation of firmgrounds, which were then overlain by bioclastic grainstone and packstone (GP) (Fig. 2.12F and G). FA5 is interpreted as having been

formed in fair-weather conditions during intervals between storm events in an offshore transition environment.

2.6.6. *Facies Association 6*

Description.–FA6 is composed of bioclastic grainstone and packstone (GP), oolitic–oncolitic packstone (P_o) and minor intraclastic conglomerate (C) (Figs. 2.12A–G, 2.13A–J). It commonly alternates with FA5.

Interpretation.–Bioclasts, ooids, and oncoids formed around fair-weather wave base and were reworked by oscillatory currents during storms. FA6 is interpreted as having been deposited in an offshore transition setting.

2.6.7. *Facies Association 7*

Description.–This facies association forms units of amalgamated hummocky cross-stratified sandstone (S_{AHCS}) (Fig. 2.14A–E). Thin beds of intraclastic conglomerate (C_i) are interbedded in rare instances (Fig. 2.14E). This facies association is commonly transitional and overlain by FA8.

Interpretation.–These sandstones represent a proximal setting and record high-energy oscillatory- and probably combined-flows produced during storms. Claystone laminae separating individual sandstone tempestites are typical of deposition on a shelf that experienced alternating storm and fair-weather conditions, such that during tranquil episodes mud-sized particles settled

out of suspension and occasionally escaped erosion (e.g., Runkel et al. 2008). FA7 is interpreted as having been deposited in a middle and lower shoreface environment.

2.6.8. *Facies Association 8*

Description.–FA8 consists of the amalgamated trough cross-stratified sandstone (S_{TCS}) (Fig. 2.15A–F), locally with intraclastic conglomerate (C_i).

Interpretation.–This facies association overlies FA7 and commonly forms the top of the Abrigo Formation where it represents the shallowest recorded deposits formed by the migration of three-dimensional dunes. It is interpreted as having been accumulated in an upper shoreface setting, in common with many similar trough cross-stratified sandstone facies (e.g., Olsen et al. 1999, Clifton, 2006).

2.7. SEDIMENTARY ENVIRONMENT

Previous studies concluded that deposition during the middle and late Cambrian was dominated by very shallow peritidal conditions everywhere across the region (Lochman-Balk 1971), and the Abrigo Formation itself was deposited in an intertidal and supratidal setting (Hayes 1975, 1978). However, the lack of desiccation cracks and distinctive microbial laminites (e.g., Pratt 2010) indicates that tidal flats did not accrete in this area. Moreover, the absence of characteristic features related to tidal effects, such as herringbone cross-lamination, ‘tidal’ or flaser bedding, double mud drapes, and tidal bundles (e.g., Pratt and James 1986; Dalyrmple

2010; Gattolin et al. 2013), as well as specific subtidal sandbodies (Desjardins et al. 2012), exclude a significant role for tides in deposition.

Instead, the Abrigo Formation is interpreted to have been deposited in two main settings on a wave-dominated ramp or shelf: (1) shoreface, above fair-weather wave base; (2) offshore, below fair-weather wave base and above storm wave base (Fig. 2.16). A significant proportion of the formation was deposited under intermittent storm influence. Large- and small-scale hummocky cross-stratified sandstone, oscillatory ripples, intraclastic conglomerate, gutter casts, and sharp bases of bioclastic grainstone and packstone deposits point to the effects of storms as agents of both scour and deposition. The regional bathymetric gradient was low, and as a result, storm events transported very fine-grained sand and silt much farther seaward than in regions with higher gradient (Runkel et al. 2007).

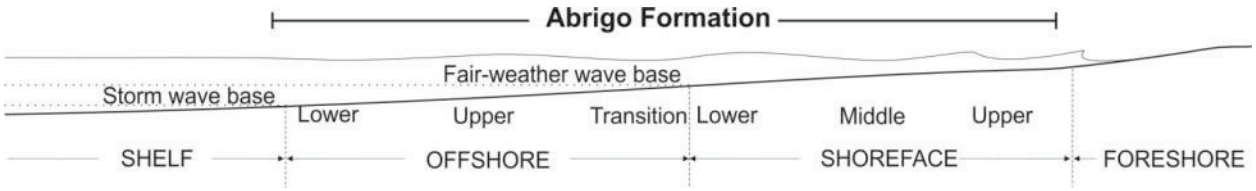

Fig. 2.16.—Idealized bathymetric profile showing the main depositional settings recognized in the Abrigo Formation (modified after Walker and Plint 1992).

2.7.1. *Depositional Model*

The mixed carbonate–siliciclastic Abrigo Formation was deposited in the nearshore setting that paleogeographically and paleobathymetrically belongs to the inner detrital belt. The depositional model for this system described from interior and western Laurentia incorporates a typical suite of nearshore siliciclastic facies containing features that document the importance of

both wave- and tide-dominated currents in the depositional system (Runkel et al. 1998; Myrow et al. 2003; Runkel et al. 2007, Myrow et al. 2012, Runkel et al. 2012, Eoff 2014b). Nearshore marine facies dominated by fine- to coarse-grained, hummocky, swaley, trough and planar cross-stratified sandstone are typical of deposition above the fair-weather wave base in a shoreface setting. They grade into mixed siliciclastic and carbonate deposits farther offshore. These offshore deposits consist of very fine-grained sandstone, siltstone, and shale, interbedded with carbonate facies that range from grainstone to lime mudstone. They are dominated by normally graded tempestites with small-scale hummocky cross-stratification that represent storm-generated deposition below fair-weather wave base.

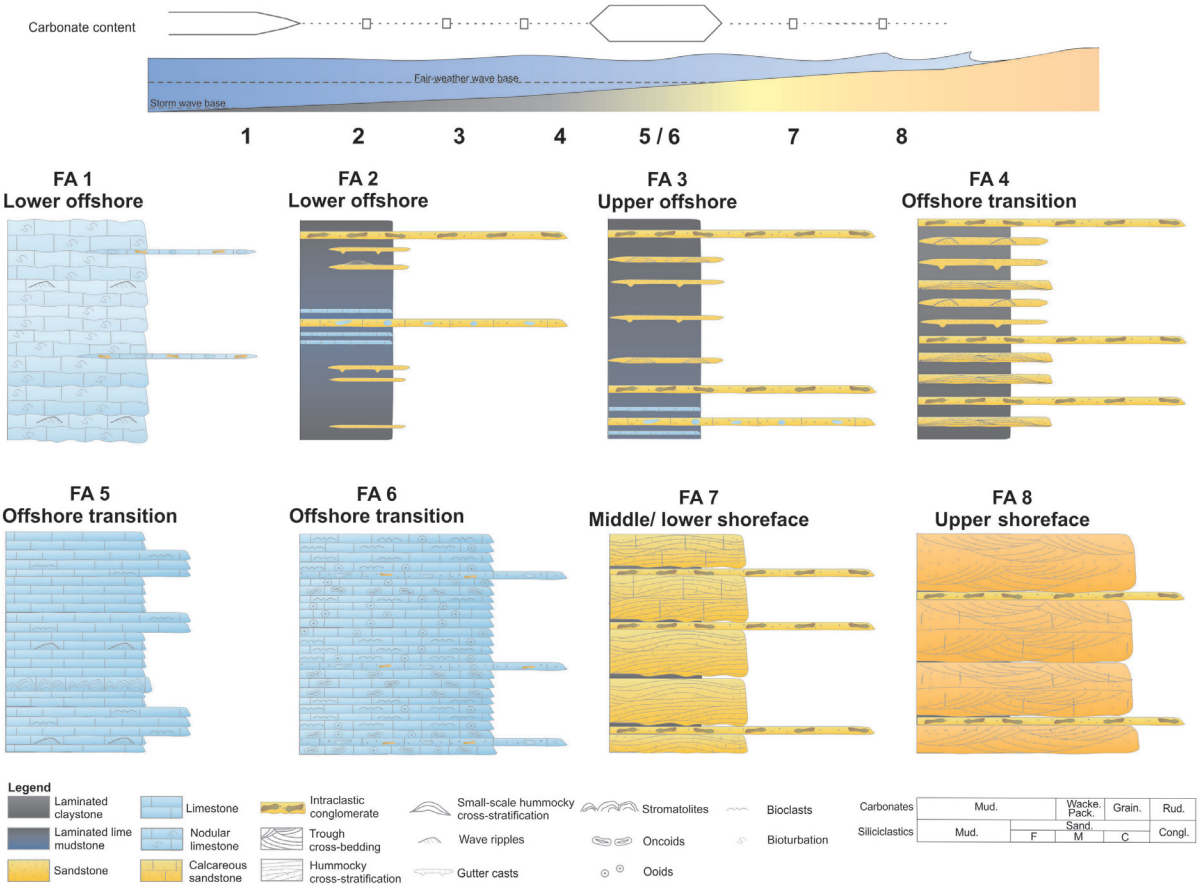

Fig. 2.17.—Diagram illustrating idealized stratigraphic sections displaying facies associations and their distribution with respect to the bathymetric profile.

The shoreface facies of the Abrigo Formation are similar to inner detrital belt deposits elsewhere in that they consist of amalgamated fine to medium-grained hummocky cross-stratified (S_{AHCS}) and coarse-grained trough cross-stratified sandstone (S_{TCS}). The major departure from these examples is in the facies arrangement (Figs. 2.17 and 2.18). Directly below fair-weather wave base in the offshore transition setting, it was dominated by carbonate deposition rather than fine-grained siliciclastic sediments. Thick intervals of carbonate facies include lime mudstone and wackestone (MW) that were deposited during fair-weather conditions, punctuated by relatively frequent storm events recorded by bioclastic grainstone and packstone (GP) and redeposited oolitic–oncolitic packstone (P_o).

Similar to other Cambrian examples, the upper and lower offshore settings are represented by mixed siliciclastic–carbonate deposits, but in the Abrigo Formation these are dominated by siliciclastic facies including claystone (C_l), lenticular siltstone (Slt), small-scale hummocky cross-stratified, thin-bedded sandstone (S), and hummocky cross-stratified sandstone (S_{HCS}). Carbonate facies are subordinate, comprising lime mudstone (M_l) and rarely wackestone (MW) and packstone (GP). In the most distal part of the lower offshore, nodular lime mudstone (M_n) accumulated.

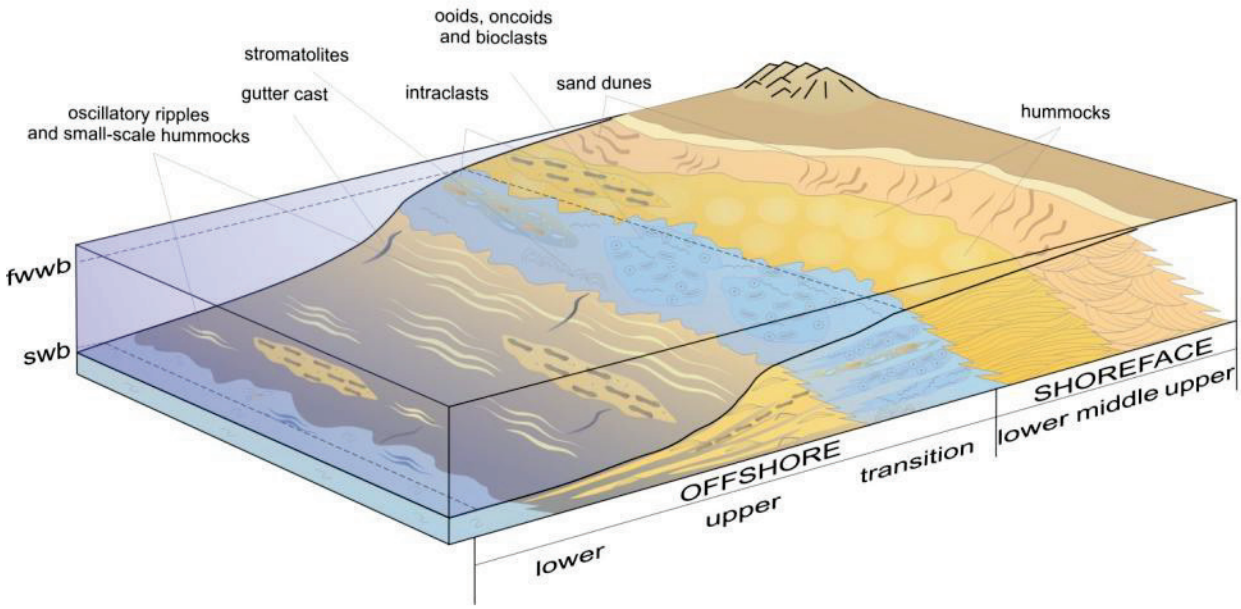

Fig. 2.18.—Facies model for the mixed carbonate–siliciclastic system showing the main depositional settings recognized in Abrigo Formation. Symbols the same as for Figures 2.5 and 2.17; fwwb = fair-weather wave base, swb = storm wave base.

The differences between the Abrigo Formation and other Cambrian inner detrital belt examples lies in relative dominance of carbonate versus siliciclastic sediment in the offshore transition setting. This reflects periods when clastic, especially clay, input decreased, such that carbonate production was promoted in shallow areas just below fair-weather wave base. The abundance of firmgrounds indicates episodically suppressed carbonate productivity and starvation of siliciclastic material. The mixed carbonate–siliciclastic deposits in the upper Carboniferous of northern Texas show a similar depositional pattern (Yancey 1991).

By virtue of its position, the carbonate-dominated zone may not have constituted a barrier to the movement of fine-grained siliciclastic sediment farther offshore. One possibility is that fine-grained siliciclastic sediment was delivered by wave-enhanced sediment gravity flows of fluid mud (e.g., Macquaker et al. 2010; Plint 2014; Kämpf and Myrow 2014). As demonstrated for the Great Barrier Reef off northern Queensland, coeval deposition of siliciclastic and

carbonate sediment is common, but even a wide reefal platform does not preclude siliciclastic sediment from passing through the reef tract to the slope and basin in form of gravity flows (Francis et al. 2007). Alternatively, Yancey (1991) invoked episodic throughput of fine-grained sediment moving in storm-generated suspension clouds or plumes to areas beyond the carbonate zone without interfering with the carbonate factory in its wake. Another hypothesis is that mud could have been deposited first in discrete areas, such as in proximity to a delta some distance from the study area, and then be transported by the longshore currents, thereby skirting the carbonate-depositing zone. Longshore processes may indeed be the main mechanism for transport of siliciclastic sediment (McNeill et al. 2004). Starvation of siliciclastic sediment delivery could also have been governed by shifts in fluvial input, and/or vagaries in wind activity if it is being carried directly from the nearby land surface.

Intensified siliciclastic influx terminated carbonate production and triggered progradation of the sandy shoreface in the latter phases of deposition of the Abrigo Formation, including that above the Sauk II–Sauk III boundary. The thickest sandstone deposits are in the northern part of the study area, which suggests that siliciclastic material was supplied from that direction, presumably reflecting the location of the shoreline. The lower part of the Abrigo Formation at French Joe Canyon and Ajax Hill is dominated by lower offshore facies, whereas at Johnny Lyon Hills and Rattlesnake Ridge upper offshore deposits form thicker and more numerous intervals, which suggests that the former two localities represent the more distal area. Additionally, a northwest–southeast shoreline orientation is supported by paleocurrent data that reveal sediment transport towards the southwest and west, which represent offshore transport combined with some longshore drift, consistent with generalized regional paleocurrent patterns (Stewart et al. 2001). There is no evidence for a major delta in the region, suggesting that siliciclastic sediment

was delivered by westward-flowing rivers from their sources in southwestern New Mexico (Amato and Mack 2012), and was subsequently transported offshore.

2.8. STRATIGRAPHIC EVOLUTION

Compared to a pure carbonate platform or an entirely siliciclastic shelf, a sequence-stratigraphic packaging of a mixed carbonate–siliciclastic deposit involves the additional factor of the effects of siliciclastic mud on the carbonate factory, on top of sea-level change and accommodation potential (Catuneanu et al. 2011).

2.8.1. *Sequence Stratigraphic Model*

The mixed carbonate–siliciclastic succession in the Abrigo Formation records the lateral migration and accretion of eight, more or less contemporaneous facies associations through time. The unit can be divided into six distinct phases that are interpreted to reflect changing rates of relative sea-level rise and fall and the corresponding influence on the carbonate factory (Figs. 2.5, 2.19). The succession starts in *Bolaspidella* Biozone time with transgression and deposition of a fine-grained offshore facies over the shallow-marine Bolsa Quartzite. This overall deepening and retrogradational trend comprises a transgressive systems tract, and during the maximum flooding phase lime mud sedimentation dominated.

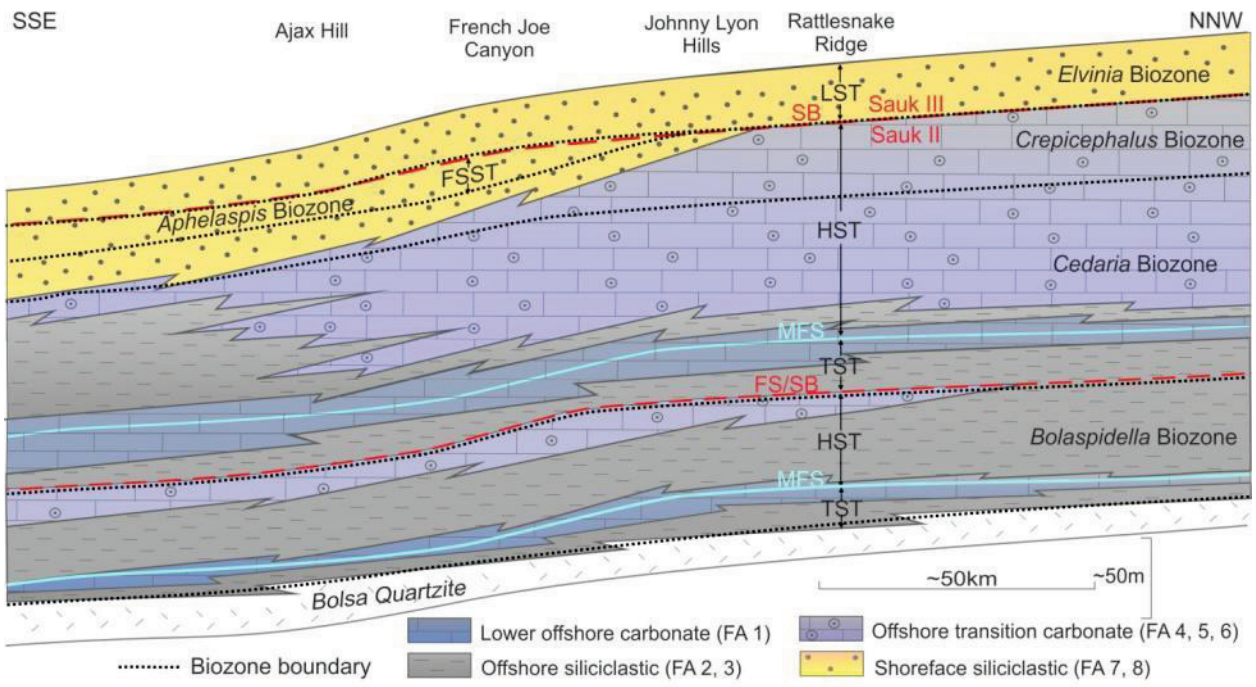

Fig. 2.19. — Generalized SSE–NNW-oriented stratigraphic cross-section across the inner detrital belt in southeastern Arizona, showing distribution of facies associations, trilobite biostratigraphy, and sequence stratigraphy. Abbreviations for sequence-stratigraphic nomenclature are the same as those in Figure 2.5.

Aggradation and subsequent progradation of a number of coarsening- and thickening-upwards intervals reflect deposition in the lower offshore followed by gradual shoaling to the upper offshore and offshore transition setting. This succession comprises a highstand systems tract. The individual shallowing-upward intervals cannot be correlated laterally with certainty because of the substantial distance between outcrops and lateral facies changes.

A sequence boundary is placed above the shallow-water bioclastic and oolitic–oncolitic grainstones and packstones around the base of the *Cedaria* Biozone, implying a sea-level fall that left no lowstand deposits in the area. In addition, this surface represents a flooding surface at the base of the succeeding transgressive systems tract. Maximum transgression in early *Cedaria* Biozone time is interpreted to coincide with the thick units of nodular lime mudstone, reflecting

low-energy, suspension fall-out and only episodic intraclastic rudstone formation across the region by bottom-impinging waves. Similarly, in the Upper Mississippi Valley area maximum flooding intervals are distinguished at the regional scale by landward-thinning tongues of carbonate strata within what are otherwise siliciclastic-dominated offshore facies (Runkel et al. 2007).

Subsequently, the stacking pattern becomes aggradational. This transition, with a few asymmetric coarsening-upward intervals, marks a change from a transgressive to a highstand systems tract. Sedimentation during the latter *Cedaria* Biozone and *Crepicephalus* Biozone time interval was dominated by carbonate deposition in an offshore transition setting. During the latter part of the highstand, the southern portion saw progradation of sand that accumulated in the lower to upper shoreface. Then, sea-level fall in *Aphelaspis* Biozone time led to the development of a falling stage systems tract that lies above and basinward of the highstand systems tract. It is recorded by a second phase of progradation of erosive-based shoreface sands (Plint and Nummedal 2000).

Shoreface sandstone in the uppermost Abrigo Formation provides a record of the Sauk II–Sauk III hiatus. It broadly correlates with the peak of the Steptoean Positive Carbon Isotope Excursion (SPICE) event recognized in Laurentia (Saltzman et al. 1998; Runkel et al. 1998; Saltzman et al. 2004), Kazakhstan, China, and Australia (Saltzman et al. 2000). It is evidence for a period of erosion or non-deposition within the long-term Sauk sequence of Sloss (1963). This event was marked by an influx of quartz sand during a sea-level lowstand, in the inner detrital belt of the interior of Laurentia and the middle carbonate belt closer to its margin (Runkel et al. 2008; Saltzman et al. 2004; Morgan 2012). In the Abrigo Formation this sequence boundary is marked at Rattlesnake Ridge by the quartz-pebble lag. However, in the other sections the

lithological expression of this boundary remains cryptic, because it separates coarse-grained sandstones that are lithologically and mineralogically similar. Nevertheless, trilobites indicative of the *Elvinia* Biozone suggests that delivery and deposition of the uppermost sandstone unit took place after the hiatus, during the subsequent lowstand phase.

2.8.2. *Inter-regional Comparison*

In the Upper Mississippi Valley area (Runkel et al. 2007, Runkel et al. 2012), the oldest trilobites belong to the *Cedaria* Biozone. The transgressive systems tract lies within the lower *Cedaria* Biozone, and the succeeding highstand systems tract is in the upper *Cedaria* and *Crepicephalus* Biozones. During *Aphelaspis* Biozone and *Dunderbergia* Biozone time, the falling-stage systems tract is characterized by sandstone progradation. This is comparable to the pattern in the Abrigo Formation. Sandstone above the Sauk II–Sauk III boundary representing the *Elvinia* Biozone were interpreted to comprise a transgressive systems tract and lowstand deposits were not distinguished (Runkel et al. 2007, 2008). Eoff (2014a), however, did recognize a subtle lowstand sandstone interval above the boundary, which is in accord with shoreface sandstones in the uppermost part of the Abrigo Formation. The substantial discrepancy between the stratigraphic thicknesses in the two regions—time-equivalent strata are generally three times greater in the Abrigo Formation—is due to exceptionally a slow subsidence rate in the northern part of the cratonic interior (Runkel et al. 2007).

There are three, broadly shallowing-upward successions termed ‘grand cycles’ expressed in the *Bolaspidella* Biozone through *Elvinia* Biozone time interval in the southern Rocky Mountains of western Canada, a region encompassing the middle carbonate belt (Aitken 1989b).

The oldest spans the *Bolaspidella* Biozone, and it may be approximately correlative with the highstand systems tract in the lower Abrigo Formation. The next youngest includes the upper *Bolaspidella* and lower *Cedaria* Biozones. Spencer and Demicco (2002) recognized five sequence boundaries in these two grand cycles. The succeeding grand cycle formed in the upper *Cedaria*, *Crepicephalus* and *Aphelaspis* biozones, and this could potentially correlate with the upper Abrigo Formation hightstand systems tract. However, comparison is hampered because these grand cycles are not precisely dated due to dearth of trilobite collections in thick limestone units capping them; they are vastly thicker in the Rocky Mountains, having been deposited near the margin of that part of Laurentia.

In western Newfoundland two shallowing-upward grand cycles have been recognized from the same approximate time interval in the transition between the inner detrital belt and middle carbonate belt. The lowest includes the *Bolaspidella* and lower *Cedaria* biozones, while the second spans the upper *Cedaria* through *Dunderbergia* biozones and embraces the Sauk II–Sauk III hiatus, with the succeeding grand cycle beginning at the base of the *Elvinia* Biozone (Chow and James, 1987). The sequence stratigraphic framework of Cowan and James (1993) , however, is not equivalent to these grand cycle subdivisions. The *Bolaspidella* Biozone is represented by a highstand terminated by a sea-level fall. This may correlate with the sequence boundary in the lower Abrigo Formation. The lower *Cedaria* Biozone is represented by a lowstand systems tract capped by a flooding surface and followed by a highstand. Below the *Crepicephalus* Biozone is another sequence boundary, and the succeeding lowstand to hightstand systems tracts include the *Crepicephalus* through *Elvinia* biozones and the Sauk II–Sauk III hiatus. In the Abrigo Formation, no lowstand systems tract is recognized in *Crepicephalus* and *Aphelaspis* biozone time, and instead a highstand systems tract developed and was overlain by a

falling stage systems tract in the *Aphelaspis* Biozone. The Sauk II–Sauk III hiatus is regarded as a sequence boundary. The poor biostratigraphic control in the Newfoundland succession and the dominance of peritidal facies make it difficult to compare it with the shoreface and offshore facies of the Abrigo Formation.

In the middle carbonate belt and adjacent inner detrital belt of the southern Appalachians, Glumac and Walker (2000) also placed a sequence boundary in the *Bolaspidella* Biozone. The overlying stratigraphy implies that this was followed by transgressive and succeeding highstand systems tracts. This may correlate with similar development in the middle part of the Abrigo Formation. Another sea-level fall recognized in the upper part of the *Cedaria–Crepicephalus* Biozone combined, however, is not recorded in the Abrigo Formation. Overlying strata were considered to comprise a transgressive systems tract followed by a highstand systems tract in the *Aphelaspis* Biozone to the Sauk II–Sauk III hiatus. This is not present in the Abrigo Formation.

The only sequence-stratigraphic elements that may correlate over a large portion of Laurentia are possibly one sequence boundary in the *Bolaspidella* Biozone and the Sauk II–Sauk III hiatus. The stratigraphic architecture in different coeval regions is governed by other phenomena in addition to sea-level, including variation in crustal flexure, sedimentation rate, and paleoclimate, such that distinguishing continental-scale events is mostly elusive.

2.8.3. *Carbonate Versus Siliciclastic Sedimentation*

Sediment supply and accommodation space are the principal controls for mixed carbonate–siliciclastic depositional systems. Sediment supply, as controlled by relief and erosion of the hinterland, and climate, determines the supply of siliciclastic sediment to a sedimentary basin (e.g., Catuneanu et al. 2009, 2011). Absence of land plants before the Silurian favored the

development of braided fluvial systems and coarser siliciclastic input into shallow seas relatively close to the land surface (Dalrymple et al. 1985; Dott 2003). During the middle and late Cambrian, Laurentia was located astride the equator, and while it is not possible to evaluate humidity, the absence of evaporites in the part of the craton (Boucot et al. 2013, p. 30) suggests that the region was not especially arid where the Abrigo Formation was deposited.

Carbonate deposition is controlled by many, partly interconnected factors, including climate, mud influx and turbidity, salinity, temperature, nutrient supply, water depth, turbulence, sea-level, and biotic evolution (Tucker, 2003; Schlager 2005; Pomar and Hallock 2008). In addition to allochems like ooids and bioclasts, warm supersaturated seawater typically leads to precipitation of copious amounts of lime mud. Evolutionary controls on the origin of lime mud may have been especially important. In modern tropical areas much is derived from the disaggregation of benthic calcareous algae, but at other times microbial activity may have been the primary source (Pratt, 2001b; Pratt et al. 2012). Significant input of siliciclastic sediment, especially silt and clay, and enhanced nutrient supply cause deterioration of the carbonate factory. Nevertheless, coeval deposition of siliciclastic and carbonate sediment can still occur, as it does off northern Queensland (Francis et al. 2007).

Varying proportions of carbonate versus siliciclastic deposits in the Abrigo Formation indicate a variable influx of terrigenous material over a period of changing accommodation space, which had a significant impact on carbonate production. Admixed quartz sand in grainstone suggests that minor amounts of coarse siliciclastic sediment are not especially deleterious. However, during the highstand of the lower part of the Abrigo Formation, fine-grained siliciclastic sediment supply dominated and suppressed carbonate productivity. Transgression led to an upward transition into the carbonate-rich upper parts of the intervals, as

the input of siliciclastic sediment decreased. The depletion of siliciclastic sediment here was related to the eastward migration of the shoreline as transgression progressed. During maximum flooding, the carbonate factory became dominant and lime mud was deposited in the distal parts of the lower offshore. The subsequent infilling of accommodation space in proximal areas by siliciclastic sediment provided a foundation shallow enough for a variety of carbonate facies to be deposited in the offshore transition setting (Warzeski et al. 1996).

The highest rate of carbonate production, which easily caught up to the increased accommodation space, took place during the early phase of the highstand in the upper part of the Abrigo Formation and resulted in rapid aggradation and progradation of shallow-marine carbonate deposits. This was followed by progradation of the shoreface which suppressed carbonate production well below the Sauk II–Sauk III hiatus.

The mixed carbonate–siliciclastic system recorded in the Abrigo Formation shows that siliciclastic sediment input and dispersal are not only restricted to the falls in sea level. Siliciclastic sedimentation appears to have dominated the transgressive systems tract and late phase of the highstand. Carbonate sedimentation, therefore, did not dominate the entire highstand systems tract as is commonly interpreted (e.g., Mack and James 1986; Choi 1998; Rankey et al. 1999; Kwon et al. 2006). Instead, in the Abrigo Formation it predominated during late phase of the transgressive systems tract and the early highstand phase.

Two general types of sequences have been distinguished in mixed carbonate–siliciclastic systems (Tucker 2003; Catuneanu et al. 2011). In lower carbonate–upper siliciclastic sequences the fine- to coarse-grained siliciclastic highstand deposits occur above transgressive carbonates. This type of sequence is common in the upper Paleozoic of North America (e.g., Soreghan 1997; Rankey et al. 1999; Miller and Eriksson 2000; Smith and Read 2001) and northern England

(Tucker 2003). By contrast, in lower mudrock–upper carbonate sequences, transgressive siliciclastics—dominantly mudrocks—comprise the lower part of the units, before highstand carbonate deposition. They are common throughout the geological record and examples include the Cambrian–Ordovician grand cycles of Laurentia (Aitken 1997; Chow and James 1987; Glumac and Walker 2000; Osleger and Read 1991), Carboniferous of North America (Elrick and Read 1991), Triassic Muschelkalk of western Europe (e.g., Aigner 1985), Triassic of the Austrian Alps (Sanders and Höfling 2000), Quaternary of Egypt (Tucker, 2003). The Abrigo Formation, however, cannot be classified simply according to either of these types. First, carbonate facies occur both in the lower, as well as in the upper part of sequence representing transgressive and highstand deposits. Secondly, although carbonate facies dominate during a highstand, the late stage of the highstand is taken over by siliciclastic deposition.

Thus, the Abrigo Formation suggests a departure from the traditional view of the tropical carbonate factory, whereby carbonate sediments were generated by a single carbonate factory in inshore areas with lime mud preferentially transported offshore (e.g., Aurell et al. 1988). The Cambrian inner detrital belt here appears to have consisted of two carbonate factories, the distal offshore one dominated by pelagic lime mud production, and the nearshore one in which a variety of carbonate particle types was generated on the sea floor, including lime mud, ooids, oncoids, and bioclasts. These areas were separated by a proximal offshore zone of siliciclastic sedimentation of muds and fine sands. Paleogeographically, the offshore carbonate factory of the Abrigo Formation eventually graded seaward into the middle carbonate belt, assuming one did exist to the southwest (cf. Aitken 1989a; Myrow et al. 2012).

The vertical facies distribution in the Abrigo Formation does not appear to be organized into a recognizable pattern of small-scale cycles like those perceived for other inner detrital belt

examples (Myrow et al. 2012). Thus, the repetition and alternation of facies at the meter scale cannot be confidently explained as due to bathymetric changes caused by short-term fluctuations in siliciclastic sediment supply during shoreline advance and retreat plus variation in climate.

2.9. CONCLUSIONS

The Abrigo Formation is a middle to late Cambrian mixed carbonate–siliciclastic unit that crops out in southeastern Arizona. It records deposition in the inner detrital belt during the Sauk transgression. In addition to the clay, silt and sand derived from the adjacent land surface, the carbonate constituents include lime mud, bioclasts, ooids, oncoids, and intraclasts, all allochems typical of Cambrian–Ordovician limestones. The unit was formed solely in a shallow-marine setting, dominated by storms, with no evidence of patch-reef development, strong tidal activity, or restricted conditions of elevated salinity.

The Abrigo Formation consists of fifteen sedimentary facies, which comprise eight facies associations representing lower offshore, upper offshore, offshore transition, lower/middle shoreface, and upper shoreface. The stratigraphic succession can be divided into six distinct phases associated with large-scale relative sea-level fluctuations. An initial flooding over shallow-marine Bolsa Quartize forming the transgressive systems tract was terminated by maximum flooding, and a subsequent highstand systems tract developed during *Bolaspidella* Biozone time. The second sequence starts with another transgressive systems tract, and is overlain by a final highstand systems tract during the *Cedaria* and *Crepicephalus* biozones. The uppermost part of the second sequence represents a falling stage systems tract developed during *Aphelaspis* Biozone time. The presence of *Elvinia* Biozone trilobites near the base of the highest

sandstone unit suggests that delivery and deposition of these sands took place during the lowstand that followed the Sauk II–Sauk III hiatus. The sequence-stratigraphic architecture of the Abrigo Formation is broadly comparable to, but far thicker than, coeval strata in the Upper Mississipi Valley. In other areas, apart from the hiatus it is difficult to correlate the sequence boundaries.

Sedimentary dynamics of the inner shelf of this part of Cambrian Laurentia were controlled by storm-induced wave action and offshore flows. The differences between the Abrigo Formation and other Cambrian inner detrital belt examples in relative dominance of carbonate versus siliciclastic strata in the offshore transition setting is interpreted to reflect periods when siliciclastic input was depleted, such that increasing accommodation and reduction of clay and possibly nutrients promoted carbonate production. Clay and silt bypassed the nearshore carbonate-depositing zone. Siliciclastic sediment input and dispersal were not only restricted to the falls in sea level, but appear to have dominated the transgressive systems tract and late phase of the highstand. Thus, carbonate sedimentation does not dominate the entire highstand systems tract but, rather, only during the late phase of the transgressive and early highstand phase. Because of this, the general facies scheme of sequences differs from the two general types of mixed siliciclastic–carbonate sequences that have been distinguished elsewhere. Mixed carbonate–siliciclastic sedimentation in the early Paleozoic inner detrital belt is revealed to have been a complex interplay of processes, not all of which are clearly understood and not all of which have direct modern analogs. It does point, however, to a fundamental role for biotic evolution in the dynamics of the carbonate factory through time.

2.10. ACKNOWLEDGMENTS

This paper derives from doctoral research by MŁ under the supervision of BRP. Funding was provided by Natural Sciences and Engineering Research Council of Canada Discovery Grants awarded to BRP. Special thanks to F.A. Sundberg who provided information on field localities, and M.G. Mángano and L.A. Buatois for discussion. We are grateful to local ranchers for their hospitality, and S. Fisher, C. Edwards, and E. Nordquist for field assistance. We thank P.M. Myrow, A.C. Runkel, and an anonymous reviewer for commenting on the manuscript.

2.11. REFERENCES

Adams, R.D., and Grotzinger, J.P., 1996, Lateral continuity of facies and parasequences in middle Cambrian platform carbonates, Carrara Formation, southeastern California, U.S.A: Journal of Sedimentary Research, v. 66, p. 1079–1090.

Aigner, T., 1985, Storm Depositional Systems: Lecture Notes in Earth Sciences, 3. Springer, Berlin, 174 p.

Aitken, J. D., 1978, Revised models for depositional grand cycles, Cambrian of the southern Rocky Montains, Canada: Bulletin of Canadian Petroleum Geology, v. 26, p. 515–542.

Aitken, J.D., 1989a, Birth, growth and death of the Middle Cambrian Cathedral carbonate lithosome, Southern Rocky Mountains: Bulletin of Canadian Petroleum Geology, v 37, p. 316–333.

Aitken, J.D. 1989b. The Sauk sequence – Cambrian to Lower Ordovician miogeosyncline and platforms, *in* Ricketts, B.D., ed., Western Canada Sedimentary Basin, a Case History, p. 105–119. Canadian Society of Petroleum Geologists, Calgary.

Aitken, J.D., 1997, Stratigraphy of the Middle Cambrian platformal succession, southern Rocky Mountains. Geological Survey of Canada Bulletin 398, 322 p.

Álvaro, J.J., Ahlberg, P., and Axheimer, N., 2010, Skeletal carbonate productivity and phosphogenesis at the lower–middle Cambrian transition of Scania, southern Sweden: Geological Magazine, v. 147, p. 59–76.

Amato, J.M., Boullion, A.O., Serna, A.M., Sanders, A.E., Farmer, G.L., Gehrels, G.E., and Wooden, J.L., 2008, The evolution of the Mazatzal province and the timing of the Mazatzal orogeny: Insights from U-Pb geochronology and geochemistry of igneous and metasedimentary rocks in southern New Mexico: Geological Society of America Bulletin, v. 120, p. 328–346.

Amato, J.M., and Mack, G.H., 2012, Detrital zircon geochronology from the Cambrian Ordovician Bliss Sandstone, New Mexico: Evidence for contrasting Grenville-age and Cambrian sources on opposite sides of the Transcontinental Arch: Geological Society of America Bulletin, v. 124, p. 1826–1840.

Aurell, M., Bádenas, B., Bosence, D.W.J., and Waltham, D.A., 1988, Carbonate production and offshore transport on a Late Jurassic carbonate ramp (Kimmeridgian, Iberian basin, NE Spain): evidence from outcrops and computer modelling, *in* Wright, V.P., and Burchette, R.P., eds., Carbonate Ramps. Geological Society, London, Special Publication 149, p. 137–161.

Boucot, A.J., Chen X., and Scotese, C.R., 2013, Phanerozoic paleoclimate: An atlas of lithologic indicators of climate. SEPM Concepts in Sedimentology and Paleontology 11, 478 p.

Brett, C.E., Allison, P.A., Desantis, M.K., Liddell, W.D., and Kramer, A., 2009, Sequence stratigraphy, cyclic facies, and lagerstätten in the Middle Cambrian Wheeler and Marjum

formations, Great Basin, Utah: Palaeogeography, Palaeoclimatology, Palaeoecology, v. 277, p. 9–33.

Bryant, D.L., 1968, Diagnostic characteristics of the Paleozoic formations of southeastern Arizona: Arizona Geological Society, Southern Arizona Guidebook III, p. 33–47.

Buatois, L.A., and Mángano, M.G., 2003, Sedimentary facies and depositional evolution of the Upper Cambrian to Lower Ordovician Santa Rosita Formation in northwest Argentina: Journal of South American Earth Sciences, v. 16, p. 343–363.

Buatois, L.A., and Mángano, M.G., 2011, Ichnology: Organism–Substrate Interactions in Space and Time: Cambridge University Press, Cambridge, 358 p.

Buatois, L.A. Narbonne, G.M., Mángano, M.G., Carmona, N.B., and Myrow, P., 2014, Ediacaran matground ecology persisted into the earliest Cambrian. Nature Communications, v. 5, article 3544, 5 p.

Byers, C.W., and Dott, R.H., jr., 1995, Sedimentology and depositional sequences of the Jordan Formation (Upper Cambrian), northern Mississippi Valley: Journal of Sedimentary Research, v. B65, p. 289–305.

Carlson, M.P., 1999, Transcontinental Arch—A pattern formed by rejuvenation of local features across central North America: Tectonophysics, v. 305, p. 225–233.

Catuneanu, O., Abreu, V., Bhattacharya, J.P., Blum, M.D., Dalrymple, R.W., Eriksson, P.G., Fielding, C.R., Fisher, W.L., Galloway, W.E., Gibling, M.R., Giles, K.A., Holbrook, J.M., Jordan, R., Kendall, C.G.St.C., Macurda, B., Martinsen, O.J., Miall, A.D., Neal, J.E., Nummedal, D., Pomar, L., Posamentier, H.W., Pratt, B.R., Sarg, J.F., Shanley, K.W., Steel, R.J., Strasser, A., Tucker, M.E., and Winker, C., 2009, Toward the standardization of sequence stratigraphy: Earth-Science Reviews, v. 92, p. 1–33.

Catuneanu, O., Galloway, W.E., Kendall, C.G.St.C., Miall, A.D., Posamentier, H.W., Strasser, A., and Tucker, M.E., 2011, Sequence stratigraphy: methodology and nomenclature: Newsletters on Stratigraphy v. 44, p. 173–245.

Cheel, R.J., and Leckie, D.A., 1993, Hummocky cross-stratification: Sedimentology Review, v. 1, p. 103–122.

Chen, J. Chough, S.K., Han Z., and Lee, J.H., 2011, An extensive erosion surface of a strongly deformed limestone bed in the Gushan and Chaomidian formations (late Middle Cambrian to Furongian), Shandong Province, China: Sequence-stratigraphic implication: Sedimentary Geology, v. 233, p. 129–149.

Choi, D.K., 1998, The Yongwol Group (Cambrian–Ordovician) redefined: a proposal for the stratigraphic nomenclature of the Choson Supergroup: Geosciences Journal, v. 2, p. 220–234.

Chow, N., and James, N.P., 1987, Cambrian Grand Cycles: A northern Appalachian perspective: Geological Society of America Bulletin, v. 98, p. 418–429.

Chow, N., and James, N.P., 1992, Synsedimentary diagenesis of Cambrian peritidal carbonates; evidence from hardgrounds and surface paleokarst in the Port au Port Group, western Newfoundland: Bulletin of Canadian Petroleum Geology, v. 40, p. 115–127.

Clifton, H.E., 2006, A re-examination of facies models for clastic shorelines, *in* Posamentier, H.W., and Walker, R.G., eds., Facies Models Revisited: SEPM Special Publication 84, p. 293–337.

Clifton, H.E., Hunter, R.E., and Phillips, R.L., 1971, Depositional structures and processes in the non-barred high-energy nearshore: Journal of Sedimentary Petrology, v. 41, p. 651–670.

Cooper, J.R., and Silver, L.T., 1964, Geology and ore deposits of the Dragoon quadrangle, Cochise County, Arizona: U.S. Geological Survey Professional Paper 416, 196 p.

Cowan, C.A., and James, N.P., 1993, The interactions of sea-level change, terrigenous sediment influx and carbonate productivity as controls of Upper Cambrian Grand Cycles of western Newfoundland: Geological Society of America Bulletin, v. 105, p. 1576–1590.

Dalrymple, R.W., Narbonne, G.M., and Smith, L., 1985, Eolian action in the distribution of Cambrian shales in North America: Geology, v. 13, p. 607–610.

Demicco, R.V., 1985, Platform and off-platform carbonates of the Upper Cambrian of western Maryland, U.S.A: Sedimentology, v. 32, p. 1–22.

Desjardins, P.R., Mángano, M.G., Buatois, L.A., and Pratt, B.R. 2010, *Skolithos* pipe rock and associated ichnofabrics from the southern Rocky Mountains, Canada: colonisation trends and environmental controls in an Early Cambrian sand-sheet complex: Lethaia, v. 43, p. 507–528.

Desjardins, P.R., Buatois, L.A., Pratt, B.R., and Mángano, M.G., 2012, Sedimentological–ichnological model for tide-dominated shelf sandbodies: Lower Cambrian Gog Group of western Canada: Sedimentology, v. 59, p. 1452–1477.

Dott, R.H., jr., 2003, The importance of eolian abrasion in supermature quartz sandstones and the paradox of weathering on vegetation-free landscapes: Journal of Geology, v. 111, p. 387–405.

Dott, R.H., jr., and Bourgeois, J., 1982, Hummocky stratification: significance of its variable bedding sequences: Geological Society of America Bulletin, v. 93, p. 663–680.

Einsele, G., and Ricken, W. 1991, Limestone–marl alternations—an overview, *in* Einsele, G., Ricken, W., and Seilacher, A. eds., Cycles and Events in Stratigraphy: Springer, Berlin, p. 23–47.

Elrick, M., and Read, J.F., 1991, Cyclic ramp-to-basin carbonate deposits, Lower Mississippian, Wyoming and Montana: a combined field and computer modelling study: Journal of Sedimentary Petrology, v. 61, p. 1194–1224.

Eoff, J.D., 2014a, Sequence stratigraphy of the upper Cambrian (Furongian; Jiangshanian and Sunwaptan) Tunnel City Group, Upper Mississippi Valley:Transgressive assumptions of cratonic flooding: Sedimentary Geology, v. 302, p. 87-101.

Eoff, J.D., 2014b, Sedimentary facies of the upper Cambrian (Furongian; Jiangshanian and Sunwaptan) Tunnel City Group, Upper Mississippi Valley: new insight on the old stormy debate: Sedimentary Geology, v. 302, p. 102-121.

Epis, R.C., and Gilbert, C.M., 1957, Early Paleozoic strata in southeastern Arizona: American Association of Petroleum Geologists Bulletin. v. 41, p. 2223–2242.

Fan, S., Swift, D.J.P., Traykovski, P., Bentley, S., Borgeld, J.C., Reed, C.W., and Niedoroda, A.W., 2004, River flooding, storm resuspension, and event stratigraphy on the northern California shelf: observations compared with simulations: Marine Geology, v. 210, p. 17–41.

Francis, J.M., Dunbar, G.B., Dickens, G.R., Sutherland, I.A., and Droxler, A.W., 2007, Siliciclastic sediment across the North Queensland margin (Australia): A Holocene perspective on reciprocal versus coeval deposition in tropical mixed siliciclastic–carbonate systems: Journal of sedimentary Research, v. 77, p. 572–586.

Gattolin, G., Breda, A., and Preto, N., 2013, Demise of Late Triassic carbonate platforms triggered the onset of a tide-dominated depositional system in the Dolomites, Northern Italy: Sedimentary Geology, v. 297, p. 38-49.

Gilluly, J., 1956, General geology of central Cochise County, Arizona: U.S. Geological Survey Professional Paper 281, 169 p.

Glumac, B., and Walker, K.R., 2000, Carbonate deposition and sequence stratigraphy of the terminal Cambrian grand cycle in the southern Appalachians, U.S.A: Journal of Sedimentary Research, v. 70, p. 952–963.

Goldring, R., 1995, Organisms and the substrate: response and effect, in Bosence, D.W.J., and Allison, P.A., eds., Marine Paleoenvironmental Analysis from Fossils: Geological Society of London, Special Publication 83, p. 151–180.

Hayes, P.T., 1975, Cambrian and Ordovician rocks of southeastern Arizona and New Mexico and westernmost Texas: U.S. Geological Survey Professional Paper 873, 98 p.

Hayes, P.T., 1978, Cambrian and Ordovician rocks of southeastern Arizona and southwestern New Mexico: New Mexico Geological Society Guidebook, 29th Field Conference Land of Cochise, p. 165–173.

Hayes, P.T., and Landis, E.R., 1965, Paleozoic stratigraphy of the southern part of the Mule Mountains, Arizona: U.S. Geological Survey Bulletin 1201–F, 43 p.

Hips, K., 1998, Lower Triassic storm-dominated ramp sequence in northern Hungary: an example of evolution from homoclinal through distally steepened ramp to Middle Triassic flat-topped platform, *in:* Wright, V.P., and Burchette, T.P., eds., Carbonate Ramps. Geological Society, London, Special Publication 149, p. 315–338.

Hunter, R.E., and Clifton, H.E., 1982, Cyclic deposits and hummocky cross-stratification of probable storm origin in Upper Cretaceous rocks of the Cape Sebastian area, southwestern Oregon: Journal of Sedimentary Petrology, v. 52, p. 127–144.

Kämpf J., and Myrow P.M., 2014, High-density mud suspensions and cross-shelf transport: on the mechanism of gelling ignition: Journal of Sedimentary Research, v. 84, p. 215–223.

Kelley, V.C., and Silver C., 1952, Geology of the Caballo Mountains: University of New Mexico Publications in Geology, v. 4, 286 p.

Knaust, D., and Langbein, R., 1995, Pot Casts in the Upper Muschelkalk (Middle Triassic) of Weimar/Thuringia - Composition, Microfabrics and Diagenesis: Facies, v. 33, p. 151–166.

Krieger, M.H., 1961, Troy Quartzite (younger Precambrian) and Bolsa and Abrigo formations (Cambrian), northern Galiuro Mountains, southeastern Arizona: U.S. Geological Survey Professional Paper 424–C, p. 160–164.

Krieger, M.H., 1968, Stratigraphic relations of the Troy Quartzite (younger Precambrian) and the Cambrian formations in southeastern Arizona: Arizona Geological Society, Southern Arizona, Guidebook III, p. 23–42.

Kwon, Y.K., Chough, S.K., Choi, D.K., and Lee, D.J., 2006, Sequence stratigraphy of the Taebeck Group (Cambrian–Ordovician), mideast Korea: Sedimentary Geology, v. 192, p. 19–55.

Li, Z.X., Bogdanova, S.V. , Collins, A.S., Davidson, A., De Waele, B., Ernst, R.E., Fitzsimons, I.C.W., Fuck, R.A., Gladkochub, D.P., Jacobs, J., Karlstrom K.E., Lu, S., Natapov, L.M, Pease V., Pisarevsky S.A., Thrane K., Vernikovsky V., 2008, Assembly, configuration, and break-up history of Rodinia: a synthesis: Precambrian Research, v.160, p. 179–210.

Lochman-Balk, C., 1971, The Cambrian of the craton of the United States, *in* Holland, C.D., ed., Cambrian of the New World: Wiley, New York, p. 79-167.

Mack, G.H., 2004, The Cambro-Ordovician Bliss and Lower Ordovician El Paso Formations, southwestern New Mexico and west Texas: *in* Mack, G.H., and Giles, K.A., eds., The Geology of New Mexico: A Geologic History: Canada, New Mexico Geological Society Special Publication 11, p. 35–44.

Mack, G.H., and James, W.C., 1986, Cyclic sedimentation in the mixed siliciclastic–carbonate Abo–Hueco transition zone (Lower Permian), southwestern New Mexico: Journal of Sedimentary Petrology, v. 56, p. 635–647.

Macquaker, J.H.S., and Gawthorpe, R.L., 1993, Mudstone lithofacies in the Kimmeridge Clay Formation, Wessex Basin, southern England: implications for the origin and controls of the distribution of mudstones: Journal of Sedimentary Petrology, v. 63, p. 1129–1143.

Macquaker, J.H.S., Bentley, S.J., and Bohacs, K.M., 2010, Wave-enhanced sediment gravity flows and mud dispersal across continental shelves: Reappraising sediment transport processes operating in ancient mudstone successions: Geology, v. 38, p. 947–950.

Mángano, M.G., Buatois, L.A., West, R.R., and Maples, C.G. 2002, Ichnology of a Pennsylvanian equatorial tidal flat—The Stull Shale member at Waverly, eastern Kansas: Kansas Geological Survey Bulletin 245, p. 133 p.

Markello, J.R., and Read, J.F., 1982, Upper Cambrian intrashelf basin, Nolichucky Formation, southwest Virginia Appalachians: American Association of Petroleum Geologists Bulletin, v. 66, p. 860–878.

Mata, S.A., and Bottjer D.J, 2011, Origin of Lower Triassic microbialites in mixed carbonate-siliciclastic successions: Ichnology, applied stratigraphy, and the end-Permian mass extinction: Palaeogeography, Palaeoclimatology, Palaeoecology, v. 300, p. 158–178.

McNeill, D.F., Cunningham, K.J., Guertin, L.A., and Anselmetti, F.S., 2004, Depositional themes of mixed carbonate-siliciclastics in the south Florida Neogene: Application to ancient deposits: *in* Grammer, G.M., Harris, P.M., and Eberli, G.P., eds., Integration of Outcrop and Modern Analogs in Reservoir Modeling: AAPG Memoir 80, p. 23– 43.

Midtgaard, H., 1996, Inner-shelf to lower shoreface hummocky sandstone bodies with evidence for geostrophic-influenced combined flow, Lower Cretaceous, West Greenland: Journal Sedimentary Research, v. 66, p. 343–353.

Miller, D.J., and Eriksson, K.A., 2000, Sequence stratigraphy of Upper Mississippian strata in the Central Appalachians: a record of glacio-eustasy and tectono-eustasy in a foreland basin setting: American Association of Petroleum Geologists Bulletin, v. 84, p. 210–233.

Morgan, W.A., 2012, Sequence stratigraphy of the great American carbonate bank, *in* Derby, J.R., Fritz, R.B., Longacre, S.A., Morgan, W.A., and Sternbach, C.A., eds., The Great American Carbonate Bank: The Geology and Economic Resources of the Cambrian–Ordovician Sauk Megasequence in Laurentia: American Association of Petroleum Geologists Memoir 98, p. 37–82.

Munnecke, A., and Samtleben, C., 1996, The formation of micritic limestones and the development of limestone–marl alternations in the Silurian of Gotland, Sweden: Facies, v. 34, p. 159–176.

Myrow, P.M., 1992, Pot and gutter casts from the Chapel Island Formation, southeast Newfoundland: Journal of Sedimentary Petrology, v. 62, p. 992–1007.

Myrow, P.M., Taylor, J.F., Miller, J.F., Ethington, R.L., Ripperdan, R.L., and Allen, J., 2003, Fallen arches: dispelling myths concerning Cambrian and Ordovician paleogeography of the Rocky Mountain region: Geological Society of America Bulletin, v. 115, p. 695–713.

Myrow, P.M., Tice, L., Archuleta, B., Clark, B., Taylor, J.F., and Ripperdan, R.L., 2004, Flat-pebble conglomerate: its multiple origins and relationship to metre-scale depositional cycles: Sedimentology, v. 51, p. 973–996.

Myrow, P.M., Taylor, J. F., Runkel, A. C., and Ripperdan, R. L., 2012, Mixed siliciclastic–carbonate upward-deepening cycles of the Upper Cambrian inner detrital belt of Laurentia: Journal of Sedimentary Research, v. 82, p. 216–231.

Noffke, N., Gerdes, G., Klenke, T., and Krumbein, W.E., 2001, Microbially induced sedimentary structures—A new category within the classification of primary sedimentary structures: Journal of Sedimentary Research, v. 71, p. 649–656.

Olsen, T.R, Mellere, D., and Olsen, T., 1999, Facies architecture and geometry of landward-stepping shoreface tongues: the Upper Cretaceous Cliff House Sandstone (Mancos Canyon, south-west Colorado): Sedimentology, v. 46, p. 603–625.

Osleger, D.A., and Montañez, I.P., 1996, Cross-platform architecture of a sequence boundary in mixed siliciclastic–carbonate lithofacies, Middle Cambrian, southern Great Basin, USA: Sedimentology, v. 43, p. 197–217.

Osleger, D.A., and Read, J.F., 1991, Relation of eustasy to stacking patterns of meter-scale carbonate cycles, Late Cambrian, U.S.A.: Journal of Sedimentary Petrology, v. 61, p. 1225–1252.

Page, W.R., Gray, F., Iriondo, A., Miggins, D., Blodgett, R.B., Maldonado, F., and Miller, R.J., 2010. Stratigraphy and Mesozoic–Cenozoic tectonic history of northern Sierra Los Ajos and adjacent areas, Sonora, Mexico: Journal of South American Earth Sciences, v. 29, p. 557–571.

Palma, R.M., Kietzmann D.A., Adamonis S., and López Gómez J., 2009, Oxfordian reef architecture of the La Manga Formation, Neuquén Basin, Mendoza Province, Argentina: Sedimentary Geology, v. 221, p. 127–140.

Palmer, A.R., 1960, Some aspects of the early Upper Cambrian stratigraphy of White Pine County, Nevada and vicinity, *in* Boettcher, J.W., and Sloan, W.W., eds., Guidebook to the Geology of East Central Nevada, Intermountain Association of Petroleum Geologists, 11th Annual Field Conference, p. 53–58.

Palmer, A.R., 1981, Subdivision of the Sauk sequence, *in* Taylor, M.E., ed., Short Papers for the Second International Symposium on the Cambrian System: U.S. Geological Survey Open-File Report 81–743, p. 160–162.

Peterhänsel, A., and Pratt, B.R., 2008, The Famennian (Upper Devonian) Palliser platform of western Canada—architecture and depositional dynamics of a post-extinction giant. In: Pratt, B.R., and Holmden, C., eds., The Dynamics of Epeiric Seas. Geological Association of Canada, Special Paper 48, p. 247–281.

Plint, A.G., 2010, Wave- and storm-dominated shoreline and shallow-marine systems, *in* James, N.P., and Dalrymple, R.W., eds., Facies Models 4: Geological Association of Canada, St. John's, p. 167–200.

Plint, A.G., 2014, Mud dispersal across a Cretaceous prodelta: Storm-generated, wave-enhanced sediment gravity flows inferred from mudstone microtexture and microfacies: Sedimentology, v. 61. p. 609–647.

Plint, A.G., and Nummedal, D., The falling stage systems tract: recognition and importance in sequence stratigraphic analysis *in* Hunt, D., and Gawthorpe, R. L., eds., Sedimentary Responses to Forced Regressions: Geological Society, London, Special Publications 172, p. 1–17.

Pratt, B.R., 1994, Seismites in the Mesoproterozoic Altyn Formation (Belt Supergroup), Montana: A test for tectonic control of peritidal carbonate cyclicity: Geology, v. 22, p. 1091–1094.

Pratt, B.R., 2001a, Oceanography, bathymetry and syndepositional tectonics of a Precambrian intracratonic basin: Integrating sediments, storms, earthquakes and tsunamis in the Belt

Supergroup (Helena Formation, c. 1.45 Ga), western North America: Sedimentary Geology, v. 141–142, p. 371–394.

Pratt, B. R., 2001b, Calcification of cyanobacterial filaments: *Girvanella* and the origin of lower Paleozoic lime mud: Geology, v. 29, p. 763–766.

Pratt, B.R., 2002, Storms versus tsunamis: Dynamic interplay of sedimentary, diagenetic, and tectonic processes in the Cambrian of Montana: Geology, v. 30, p. 423–426.

Pratt, B.R., 2010, Peritidal carbonates, *in* James, N.P., and Dalrymple, R.W., eds., Facies Models 4: Geological Association of Canada, St. John's, p. 401–420.

Pratt, B.R., and James, N.P., 1986, The St. George Group (lower Ordovician) of western Newfoundland: tidal flat island model for carbonate sedimentation in epeiric seas: Sedimentology, v. 33, p. 313–343.

Pratt, B.R., and Bordonaro, O.L., 2007, Tsunamis in a stormy sea: Middle Cambrian inner shelf limestones of western Argentina: Journal of Sedimentary Research, v. 77, p. 256–262.

Pratt, B.R., and Bordonaro, O.L., 2014, Early middle Cambrian trilobites from La Laja Formation, Cerro El Molle, Precordillera of western Argentina: Journal of Paleontology, v. 88, p. 906–924.

Pratt, B.R., Raviolo, M.M., Bordonaro, O.L., 2012, Carbonate platform dominated by peloidal sands: Lower Ordovician La Silla Formation of the eastern Precordillera, San Juan, Argentina: Sedimentology, v. 59, p. 843–866.

Rankey, E. C., Bachtel S. L., and Kaufman J., 1999, Controls on stratigraphic architecture of icehouse mixed carbonate-siliciclastic systems; a case study from the Holder Formation (Pennsylvanian, Virgilian), Sacramento Mountains, New Mexico, *in* Harris, P.M., Saller,

A.H., and Simo, J.A., eds., Advances in Carbonate Sequence Stratigraphy: Application to Reservoirs Outcrops and Models: SEPM Special Publication 63, p. 127–150.

Ransome, F.L., 1904, Geology and ore deposits of the Bisbee quadrangle, Arizona: U.S. Geological Survey Professional Paper 21, 168 p.

Rees, A.J., Thomas, A.T., Lewis, M., Hughes, H.E., and Turner, P., 2014, Lithostratigraphy and palaeoenvironments of the Cambrian in SW Wales, *in* Rees, A.J., Thomas, A.T., Lewis, M., Hughes, H.E., and Turner, P., eds., The Cambrian of SW Wales: Towards a United Avalonian Stratigraphy. Geological Society Memoir 42, p. 33–100.

Runkel, A.C., 1994, Deposition of the uppermost Cambrian (Croixan) Jordan Sandstone, and the nature of the Cambrian– Ordovician boundary in the Upper Mississippi Valley, Geological Society of America Bulletin, v. 106, p. 492–506.

Runkel, A.C., McKay, R.M., and Palmer, A.R., 1998, Origin of a classic cratonic sheet sandstone: Stratigraphy across the Sauk II–Sauk III boundary in the Upper Mississippi Valley: Geological Society of America Bulletin, v. 110, p. 188–210.

Runkel, A.C., Miller, J.F., McKay, R.M., Palmer, A.R., and Taylor, J.F., 2007, High-resolution sequence stratigraphy of lower Paleozoic sheet sandstones in central North America: The role of special conditions of cratonic interiors in development of stratal architecture: Geological Society of America, Bulletin, v. 119, p. 860–881.

Runkel, A.C., Miller, J.F., McKay, R.M., Palmer, A.R., and Taylor, J.F., 2008, The record of time in cratonic interior strata: does exceptionally slow subsidence necessarily result in exceptionally poor stratigraphic completeness?, *in* Pratt, B.R., and Holmden, C., eds., Dynamics of Epeiric Seas: Geological Association of Canada, Special Paper 48, p. 341–362.

Runkel, A.C., McKay, R.M., Cowan, C.A., Miller, J.F., and Taylor, J.F., 2012, The Sauk

megasequence in the cratonic interior of North America: Interplay between a fully developed inner detrital belt and the central great American carbonate bank, *in* Derby, J.R., Fritz, R.B., Longacre, S.A., Morgan, W.A., and Sternbach, C.A., eds., The Great American Carbonate Bank: The Geology and Economic Resources of the Cambrian–Ordovician Sauk Megasequence in Laurentia: American Association of Petroleum Geologists Memoir 98, p. 1001–1011.

Sabins, F.F., jr., 1957, Stratigraphic relations in the Chiricahua and Dos Cabezas mountains, Arizona: American Association of Petroleum Geologists Bulletin, v. 41, p. 466– 510.

Salad Hersi, O., Lavoie, D., and Nowlan, G.S., 2002, Stratigraphy and sedimentology of the Upper Cambrian Strites Pond Formation, Philipsburg Group, southern Quebec, and implications for the Cambrian platform in eastern Canada: Bulletin of Canadian Petroleum Geology, v. 50, p. 542–565.

Saltzman, M.R., 1999, Upper Cambrian carbonate platform evolution, *Elvinia* and *Taenicephalus* zones (pterocephaliid–ptychaspid biomere boundary), northwestern Wyoming: Journal of Sedimentary Research, v. 69, p. 926–938.

Saltzman, M.R., Runnegar, B., Lohmann, K.C., 1998, Carbon isotope stratigraphy of Upper Cambrian (Steptoean Stage) sequences of the eastern Great Basin: record of a global oceanographic event. Geological Society of America Bulletin, v. 110, p. 285–297.

Saltzman, M.R., Brasier, M.D., Ripperdan, R.L., Ergaliev, G.K., Lohmann, K.C., Robison, R.A., Chang, W.T., Peng, S., and Runnegar, B., 2000, A global carbon isotope excursion during the Late Cambrian: relation to trilobite extinctions, organic-matter burial and sea level: Palaeogeography, Palaeoceanography, Palaeoclimatology, v. 162, p. 211–223.

Saltzman, M.R., Cowan, C.A., Runkel, A.C., Runnegar, B., Steward, M.C., and Palmer, A.R., 2004, The Late Cambrian SPICE ^{13}C event and the Sauk II–III regression: New evidence from Laurentian basins in Utah, Iowa, and Newfoundland: Journal of Sedimentary Research, v. 74, p. 366–377.

Sanders, D., and Höfling, R. 2000, Carbonate deposition in mixed siliciclastic–carbonate environments on top of an orogenic wedge (Late Cretaceous, Northern Calcareous Alps, Austria): Sedimentary Geology, v. 137, p. 127–146.

Schieber, J., 1999, Microbial mats in terrigenous clastics: the challenge of identification in the rock record: Palaios, v. 14, p. 3–12.

Schlager, W., 2005, Carbonate sedimentology and sequence stratigraphy: SEPM Concepts in Sedimentology and Paleontology 8, 200 p.

Sloss, L.L., 1963, Sequences in the cratonic interior of North America: Geological Society of America Bulletin, v. 74, p. 93–114.

Smith, L.B., and Read, J.F., 2001, Discrimination of local and global effects on Upper Mississippian stratigraphy, Illinois Basin, U.S.A.: Journal of sedimentary Research, v. 71, p. 985–1002.

Soreghan, G.S., 1997, Walther's law, climate change and upper Paleozoic cyclostratigraphy in the ancestral Rocky Mountains: Journal of Sedimentary Research, v. 67, p. 1001–1004.

Spencer, R.J., and Demicco, R.V., 2002, Facies and sequence stratigraphy of two Cambrian grand cycles: implications for Cambrian sea level and origin of grand cycles: Bulletin of Canadian Petroleum Geology, v. 50, p. 478–491.

Stewart, J.H., Gehrels, G.E., Barth, A.P., Link, P.K., Christie-Blick, N., and Wrucke, C.T., 2001, Detrital zircon provenance of Mesoproterozoic to Cambrian arenites in the western United

States and northwestern Mexico: Geological Society of America Bulletin, v. 113, p. 1343–1356.

Stoyanow, A.A., 1936, Correlation of Arizona Paleozoic formations: Geological Society of America Bulletin, v. 47, p. 459–540.

Swift, D.J.P., Han, G., and Vincent, C.E., 1986, Fluid processes as sea-floor response on a modern storm-dominated shelf: Middle Atlantic shelf of North America. Part I: the storm-current regime, *in* Knight, R.J., and McLean, J.R., eds., Shelf Sands and Sandstones: Canadian Society of Petroleum Geologists Memoir 11, p. 99–119.

Taylor, J.F., Repetski, J.E., Loch, J.D., and Leslie, S.A., 2012, Biostratigraphy and chronostratigraphy of the great American carbonate bank, *in* Derby, J.R., Fritz, R.B., Longacre, S.A., Morgan, W.A., and Sternbach, C.A., eds., The Great American Carbonate Bank: The Geology and Economic Resources of the Cambrian–Ordovician Sauk Megasequence in Laurentia: American Association of Petroleum Geologists Memoir 98, p. 15–35.

Torsvik, T.H., and Cocks, L.R.M., 2013, New global paleogeographical reconstructions for the early Palaeozoic and their generation, *in* Harper, D.A.T., and Servais, T., eds., Early Palaeozoic Biogeography and Palaeogeography: Geological Society of London , Memoirs, 38, p. 5–24.

Tucker, M.E., 2003, Mixed clastic–carbonate cycles and sequences: Quaternary of Egypt and Carboniferous of England: Geologica Croatica, v. 56, p. 19–37.

Walker, R.G., and Plint, A.G., 1992, Wave- and storm-dominated shallow marine systems, *in* Walker R.G., and James, N.P., eds., Facies Models: Response to Sea-Level Change: Geological Association of Canada, St. John's, p. 219–238.

Warzeski, R.E., Cummingham, K.J., Ginsburg, R.N., Anderson, J.B., and Ding, Z.-D., 1996, A Neogene mixed siliciclastic and carbonate foundation for the Quaternary carbonate shelf, Florida Keys: Journal of Sedimentary Research, v. 66, p. 788–800.

Westphal, H., Munnecke, A., Böhm, F., and Bornholdt, S., 2008, Lime-marl alternation in epeiric sea limestone–marl alternations in epeiric sea settings—witnesses of environmental changes or diagenesis?, *in* Pratt, B.R., and Holmden, C., eds., Dynamics of Epeiric Seas: Geological Association of Canada Special Paper 48, p. 389–406.

Westrop, S.R., 1989, Facies anatomy of an Upper Cambrian grand cycle: Bison Creek and Mistaya formations, southern Alberta: Canadian Journal of Earth Sciences, v. 26, p. 2292–2304.

Yancey, T.E., 1991, Controls on carbonate and siliciclastic sediment deposition on a mixed carbonate–siliciclastic shelf (Pennsylvanian Eastern Shelf of north Texas): Kansas Geological Survey Bulletin 233, p. 263–272.

CHAPTER 3

MARJUMAN AND STEPTOEAN (MIDDLE AND UPPER CAMBRIAN) TRILOBITES OF THE ABRIGO FORMATION, SOUTHEASTERN ARIZONA.

3.1. ABSTRACT

One hundred eighty-two collections, yielding some 940 trilobite remains have been recovered from the Abrigo Formation of southeastern Arizona. They represent 69 species belonging to 42 genera. Eight new species are identified: *Blairella* n. sp., *Camaraspis* n. sp., *Modocia* n. sp., *Crepicephalus* n. sp., *Coosia* n. sp., *Bolaspidella* n. sp., *Paracedaria* n. sp., *Llanoaspis* n. sp. Fossils range in age from early Marjuman to late Steptoean (Guzhangian through Paibian). They were collected from four measured sections across a distance of 170 km: Ajax Hill, French Joe Canyon, Johnny Lyon Hills, and Rattlesnake Ridge. They are assigned to five biostratigraphic zones: *Bolaspidella*, *Cedaria*, *Crepicephalus*, *Aphelaspis*, and *Elvinia* Zones. In addition, two subzones are recognized, the *Cedaria eurycheilos* Subzone defined in the upper part of the *Cedaria* Zone and the *Coosella helena* Subzone recognized in the upper part of the *Crepicephalus* Zone. The fauna is overwhelmingly dominated by ptychoparioids; agnostoids are virtually absent. Eight trilobite biofacies are defined from generic relative abundance data: *Ehmaniella, Olenoides–Bolaspidella, Blairella, Eldoradia, Modocia–Paracedaria, Cedaria, Coosella–Coosina,* and *Camaraspis*. These are taken to represent a temporal succession of species living under relatively nearshore conditions dominated by mixed siliciclastic–carbonate sedimentation.

3.2. INTRODUCTION

Half a billion years ago the broad epeiric sea that progressively covered most of Laurentia created a generalized three-fold depositional pattern: outer detrital belt, middle carbonate belt, and inner detrital belt (Palmer 1960) (Fig. 3.1). The outer detrital belt and middle carbonate belt have been studied extensively in a wide variety of locations, and the trilobite fauna has been well documented (e.g., Demicco 1985; Pratt and James 1986; Osleger and Read 1991; Pratt, 1992; Osleger and Montañez 1996; Aitken 1997; Glumac and Walker 2000; Salad Hersi et al. 2002). The inner detrital belt, representing the mixed carbonate–siliciclastic setting, has been studied especially in the Upper Mississippi Valley (Runkel et al. 2008; Runkel et al. 2012; Eoff 2014a, b), but otherwise is relatively poorly understood with respect to facies distribution, the variable role of the 'carbonate factory,' and its trilobite fauna. Published Cambrian biostratigraphic schemes provide a mosaic of zonations applicable to a variety of depositional environments ranging from peritidal to open shelf and slope. Trilobite distribution in shallow-marine, storm-dominated deposits in the inner detrital belt remain to be determined in detail.

The middle and upper Cambrian Abrigo Formation of southeastern Arizona is a mixed carbonate–siliciclastic unit, and thus it offers an opportunity to explore sedimentation and faunal relationships in the inner detrital belt in a subequatorial location in what was western Laurentia (Torsvik and Cocks 2013). The unit has been described only in a reconnaissance manner (e.g., Gilluly 1956; Hayes 1975), and consequently the paleoenvironmental and biostratigraphic contexts have been only broadly outlined. The identification of the trilobite fauna was mostly just to the genus level and was provided by A. R. Palmer (Gilluly, 1956; Cooper and Silver, 1964) and Taylor *in* Hayes, 1975) (Table.1).

This study provides a taxonomic account and documents the distribution of the trilobite fauna in the Marjuman and Steptoean interval (Guzhangian–Paibian). A biostratigraphic zonal scheme is erected that should be broadly applicable to the inner detrital belt of Laurentia. These zones are integrated with the pattern of trilobite biofacies characterized for the shallow-marine storm-dominated environment, and combined with a detailed lithofacies analysis of the Abrigo Formation, aid in the evaluation of the overall ecologic controls on faunal distribution.

3.3. STUDY AREA

The study area is located in southeastern Arizona, on the southwestern side of the North American craton. The study is based on six measured sections totalling 1066 m of stratigraphy that were logged in a bed-by-bed detail. This includes identification of sedimentary textures and structures, paleocurrent measurements, preliminary recognition of the ichnofossils present, determination of degree of bioturbation and detailed analysis of facies. Trilobite collections were made concurrently. A number of other, previously described sections (Gilluly 1956; Hayes and Landis 1965; Hayes 1975; Krieger 1961; Hayes 1978) were field-checked. In addition to observations made at the hand-lens level, some two dozen rock samples were slabbed and polished, and 30 thin sections were prepared.

Trilobite collections were made in four of the measured sections: (1) Ajax Hill located on the eastern hillside of the Ajax Hill in Tombstone Hills, 31^{o}40’N, 110^{o}04’W; (2) French Joe Canyon: situated on the southeastern hillside of the Cape peak in the Whetstone Mountains, 31^{o}49’ N, 110^{o}24’W; (3) Rattlesnake Ridge: accessible from the Three Links Ranch 32^{o} 12’N, 110^{o} 11’W; (4) Johnny Lyon Hills: accessible from the Three Links Ranch, from a dirt road in Tres Alamos Wash, located on the southeastern hillside of the Keith Peak in Johnny Lyon Hills (32^{o} 06’N,

110° 13'W) (Fig. 2.3). One hundred eighty-two fossil-bearing samples from the Marjuman and Steptoean interval were collected and processed by splitting and mechanical preparation in the laboratory. Over 940 trilobite remains have been recovered.

3.4. SEDIMENTARY ENVIRONMENTS

The mixed carbonate–siliciclastic Abrigo Formation of middle and late Cambrian age, which crops out in southeastern Arizona, was deposited during the Sauk transgression in the craton interior landward of the passive margin of Laurentia. It overlies shallow-marine sandstone of the Bolsa Quartzite, which mantled the Precambrian land surface. The Abrigo Formation consists of ten distinct rock types: claystone, siltstone, sandstone, lime mudstone, wackestone, bioclastic grainstone, packstone, oolitic packstone, oncolitic packstone, and intraclastic conglomerate. These comprise fifteen lithofacies, which are grouped into eight facies associations. They represent an array of shallow-marine environments that were dominated by wave and storm activity. The interpreted paleoenvironments include lower offshore, upper offshore, offshore transition, and lower, middle and upper shoreface (Łabaj and Pratt, submitted).

Deposition of the Abrigo Formation started with transgressive lower offshore carbonates overlying shallow-marine, high-energy sandstones comprising to the Bolsa Quartzite. This was followed in *Bolaspidella* Zone time by accumulation of highstand deposits, recorded initially by mixed siliciclastic and carbonate sedimentation in the offshore setting, and then carbonate-dominated deposition in an offshore-transition setting. Subsequent flooding in early *Cedaria* Zone time resulted in a landward shift of facies, reduction of siliciclastic input, and dominance of clay and lime mud sedimentation under somewhat deeper water conditions. This phase led to

deposition of the transgressive systems tract. Progressive shallowing and aggradation during the next highstand phase in late *Cedaria* and early *Crepicephalus* Zone time was accompanied by a further decrease in siliciclastic input and a switch to pure carbonate deposition in a mainly offshore-transition setting. This was followed, in late *Crepicephalus* Zone time by renewed coarse siliciclastic input and progradation of the sandy shoreface which terminated the highstand systems tract. Subsequent progradation of proximal shoreface sand in *Aphelaspis* Zone time characterized the falling stage systems tract. Presence of *Elvinia* Zone trilobites near the base of the succeeding lowstand shoreface sandstone reveals that the widely recognized Sauk II–Sauk III hiatus is recorded in southeastern Arizona.

3.5. BIOSTRATIGRAPHY

The Abrigo Formation consists of carbonate and siliciclastic rocks deposited in shallow-marine wave- and storm-dominated setting and for that reason significant parts of the sections lack fossils or are only sparsely fossiliferous. Hence, establishing new zones based on species occurence in the Abrigo Formation was unachievable. The generalized genus-based biozonation established for the Marjuman–Steptoean interval in North America is recorded in the Abrigo Formation. It consists of the *Bolaspidella, Cedaria*, *Crepicephalus*, *Aphelaspis* and *Elvinia* zones (Howell et al., 1944; Lochman-Balk and Wilson, 1958) named from Great Basin of Utah–Nevada (Palmer, 1971, 1972), Upper Mississippi Valley (Lochman-Balk, 1971), as well as the southern Appalachians (Rasetti, 1965). However, in two intervals where the fossils are more common, two subzones were defined: the *Cedaria eurycheilos* Subzone in the upper part of *Cedaria* Zone, and the *Cosella helena* Subzone in the upper part of *Crepicephalus* Zone. The

trilobite-based units are assemblage zones, the boundaries of which are defined by the lowest documented presence of one or more diagnostic species.

3.5.1. Marjumian Stage

3.5.1.1. *Bolaspidella* Zone

The *Bolaspidella* Zone is the oldest assemblage of species recovered from the Abrigo Formation. It comprises the following assemblage of species: *Brachyaspidion rynchina* Miller, 1936b; ?*Ehmaniella* sp.; *Olenoides nevadensis* (Meek, 1870); *Modocia oweni* (Meek and Hayden, 1861); *Modocia* sp., *Modocia dubia* (Resser, 1938a); *Solenopleurella quadrata* Rasetti, 1963; *Bolaspidella* n. sp.; *Blairella crassimarginata* Rasetti, 1965b; *Blairella* n. sp.; *Marjumia* cf. *M. typa* Walcott, 1916b; *Alokistocare americanum* (Walcott, 1916a). Representatives of the *Bolaspidella* Zone have been found in all of the measured sections, in the lowest part of the Abrigo Formation where it is dominated by claystones, siltstones and thin beds of fine-grained sandstones interbedded sporadically with thin beds of lime mudstone. These rocks have been interpreted as deposited in the offshore environment. The lower portion is marked by the presence of *B. rynchina,* ?*Ehmaniella* sp., *M. oweni, Modocia* sp., and *M. dubia. Brachyaspidion rynchina* was recognized by Robison (1964) in the Wheeler Formation of Utah, and also reported from the lower part of the *Bolaspidella* Zone, being part of the *Bathyuriscus fimbriatus* Subzone. *Solenopleurella quadrata*, *Bolaspidella*. n. sp., *B. crassimarginata*, *Blairella* n. sp., *M. typa*, *A. americanum* are distinctive for the upper part of this subzone.

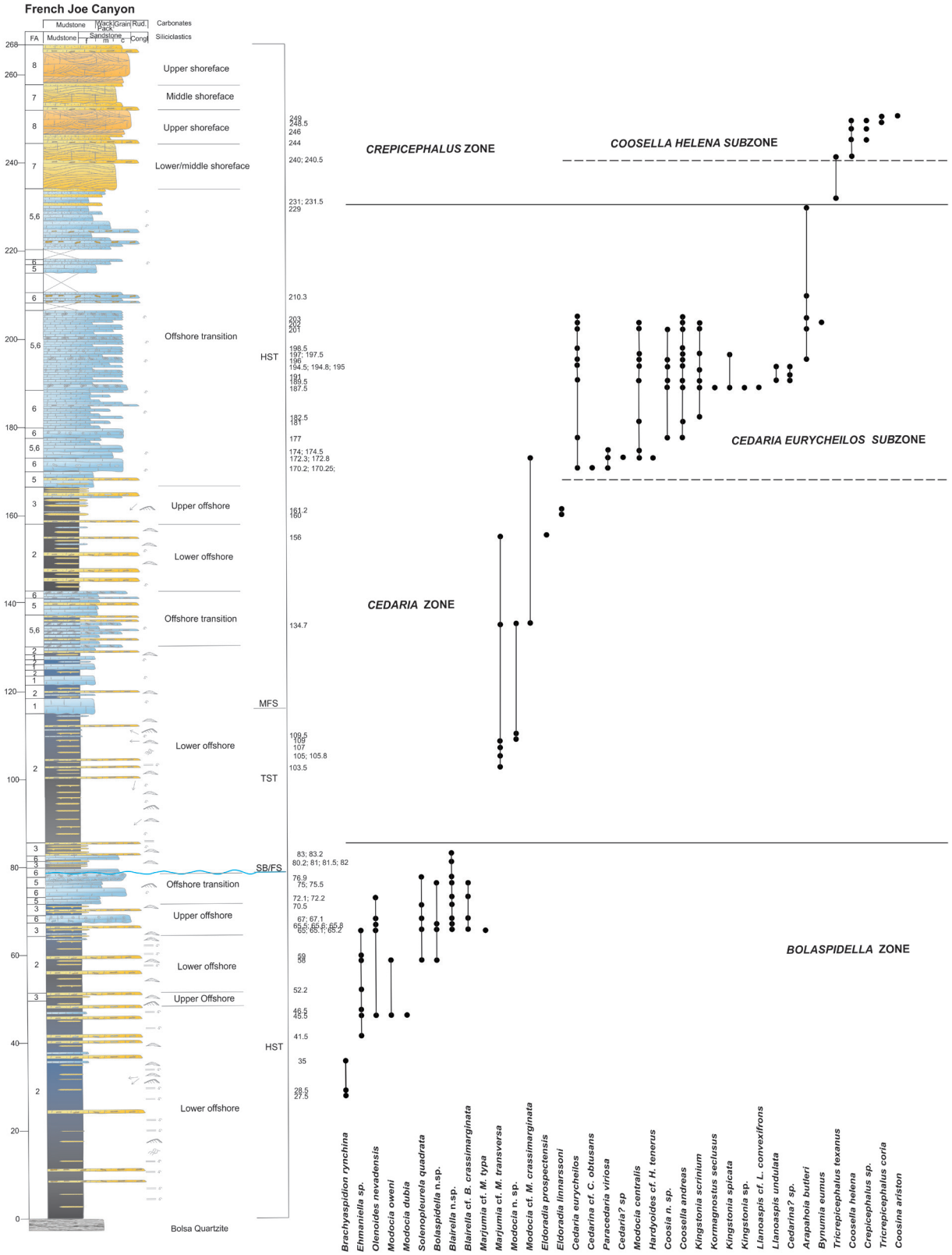

Fig. 3.1. Stratigraphic section of French Joe Canyon and species range chart with biostratigraphic units. Symbols the same as for Figures 3.3.

Marjumia typa is present in the *Bolaspidella contracta* Subzone of Robison (1964) from the Wheeler Formation and in the Abrigo Formation from the upper part of *Bolaspidella* Zone. Species of *Bolaspidella*, *Marjumia*, *Modocia* and *Olenoides* in other units permit the general correlation with the *Bolaspidella* Zone in the Abrigo Formation. *M. oweni* and the species of *Bolaspidella* indicate that it is equivalent to *Bolaspidella* Zone from the Riley Formation of Texas (Palmer, 1954). The *Bolaspidella* Zone of the Abrigo Formation hosts species of several genera in common with the *Bolaspidella* Zone from central Appalachians recognized by Rasetti, 1965b such as *Blairella*, *Solenopleurella, Olenoides* and *Alokistocare*.

3.5.1.2. *Cedaria* Zone

The lower part of the *Cedaria* Zone is represented by*: Modocia* n. sp.*; Marjumia* cf. *M. transversa* (Palmer, 1968); *Marjumia* cf. *M. typa* Walcott, 1916b; *Modocia* cf. *M. crassimarginata* Rasetti, 1965; *Eldoradia prospectensis* (Walcott, 1884); and *E. linnarssoni* (Walcott, 1884).

The *Cedaria eurycheilos* Subzone is distinguished in the upper part of *Cedaria* Zone. The lower boundary is defined by the first appearance of *Cedaria C. eurycheilos* Palmer, 1954 and the subzone is characterized by the following assemblage of species: *C. eurycheilos* Palmer, 1954; *Cedarina* cf. *C. obtusans* Duncan *in* Lochman and Duncan, 1944; *Paracedaria viriosa* Lochman and Hu, 1962; *Paracedaria* n. sp.; *Cedarina*? sp.; *Cedaria*? sp.; *Modocia centralis* (Whitfield 1877); *Hardyoides* cf. *H. tenerus* (Walcott, 1916a); *Coosia* n. sp.; *Coosella andreas* (Walcott, 1916b); *Kingstonia spicata* Lochman, 1940; *K. scrinium* (Raymond, 1937); *Kingstonia* sp.; *Kormagnostus seclusus* (Walcott, 1884); *Llanoaspis undulata* Lochman, 1938a; *Llanoaspis* cf. *Ll. convexifrons* Rasetti, 1961; *Arapahoia butleri* (Stoyanow, 1936); *Bynumia eumus* Walcott,

1924; *Ll. peculiaris* (Resser, 1938a); and *Tricrepicephalus coria* (Walcott, 1916a). Representatives of the *Cedaria eurycheilos* Subzone occur in all the measured sections in the upper part of the Abrigo Formation where it is dominated by grainstones and packstones interbedded with wackestones deposited in the offshore transition environment. *Arapahoia butleri,* and *K. seclusus* are distinctive for the upper part of this subzone. The lower portion is marked by the presence of *C. obtusans* and *P. viriosa*. This subzone can be correlated with the upper part of *Cedarina*-*Cedaria* Zone defined in the Riley Formation of Texas (Palmer, 1954) that is characterized by the presence of *C. eurycheilos.*

The presence of *A. butleri* suggests a correlation with the middle and upper *Cedaria* Subzone of Lochman and Duncan (1944) from Montana. The *Cedaria eurycheilos* Subzone maybe correlatable with the *Cedaria minor* and *Cedaria selwini* zones of Pratt (1992) as recognized in the Rabittketle Formation of the Mackenzie Mountains on the basis of the shared presence of *K. seclusus.* The presence of *C. andreas* suggests a correlation with *Cedaria* Zone of Rasetti (1965) from the central Appalachians.

3.5.1.3. *Crepicephalus* Zone

The *Crepicephalus* Zone is thin in the Abrigo Formation and has been found in all of the measured sections, in the upper part of the Abrigo Formation dominated by grainstones and packstones of the offshore transition, as well as, hummocky cross-stratified calcareous sandstones of middle shoreface and trough cross-stratified calcareous sandstones of upper shoreface environment. The lower part is characterized by a single collection from French Joe Canyon containing *Tricrepicephalus texanus* (Shumard 1861).

The presence of *T. texanus* suggests a correlation with the *Coosella* Zone defined by Palmer (1954) in the Riley Formation of Texas, the *Crepicephalus* Zone of Lochman and Duncan (1944) in the Pilgrim Formation of Montana, and the *Cedaria prolifica* Zone of Pratt (1992) in the Rabbitkettle Formation of the Mackenzie Mountains.

The *Coosella helena* Subzone is distinguished within the upper part of the *Cedaria* Zone, the lower boundary is defined by the first appearance of the *C. helena* Lochman 1938b in the upper Abrigo Formation. This subzone is characterized in addition by the presence of *Kingstonia scrinium* (Raymond, 1937); *Coosina ariston* (Walcott, 1916b); *Crepicephalus* sp.; *Crepicephalus* n. sp.; *Crepicephalus* cf. *C. iowensis* (Owen 1852); *Llanoaspis undulata* Lochman, 1938a; *Ll. modesta* Lochman, 1938a; *T. coria* (Walcott, 1916a); *Crepicephalus exutus* Resser, 1938a; *Glaphyraspis parva* (Walcott, 1899); and *Llanoaspis* n. sp. The presence of *Coosina ariston* in the *Coosella helena* Subzone in all of the measured sections makes it correlatable with the *Coosina* (*Maryvillia*) Zone of Palmer (1954) from Texas, which is defined by the presence of *C. ariston.*

The *Coosella helena* Subzone is an equivalent of the upper part of the *Crepicephalus* Zone as recognized by Stitt and Perfetta (2000) in the Deadwood Formation of South Dakota, by the presence of *C. ariston, L. undulata, T. coria,* and *K. scrinium*.

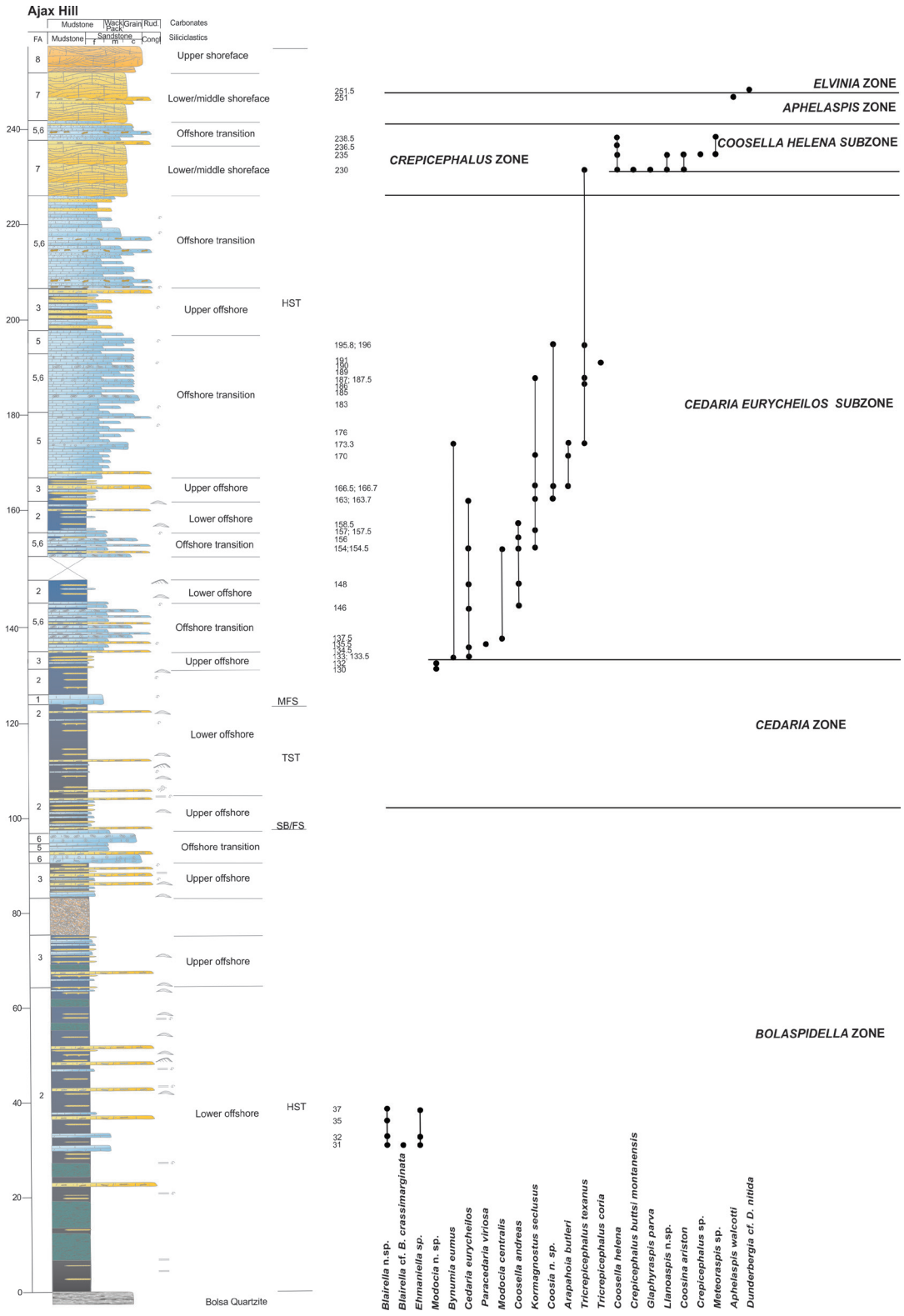

Fig. 3.2. Stratigraphic section of Ajax Hill and species range chart with biostratigraphic units. Symbols the same as for Figures 3.3.

It is, however, difficult to correlate this subzone with the *Cedaria* species-based zones of the Mackenzie Mountains defined by Pratt (1992). It may be partly an equivalent to the *Cedaria brevifrons* Zone. However, only *K. scrinium* in the *Cedaria brevifrons* Zone occurs in the *Coosella helena* Subzone. *Kingstonia scrinium* is also present in the *Cedaria eurycheilos* Subzone of the Abrigo Formation. The presence of *C. ariston* suggests a correlation with *Crepicephalus* Zone of Rasetti (1965) in the Nolichucky Formation from the central Appalachians.

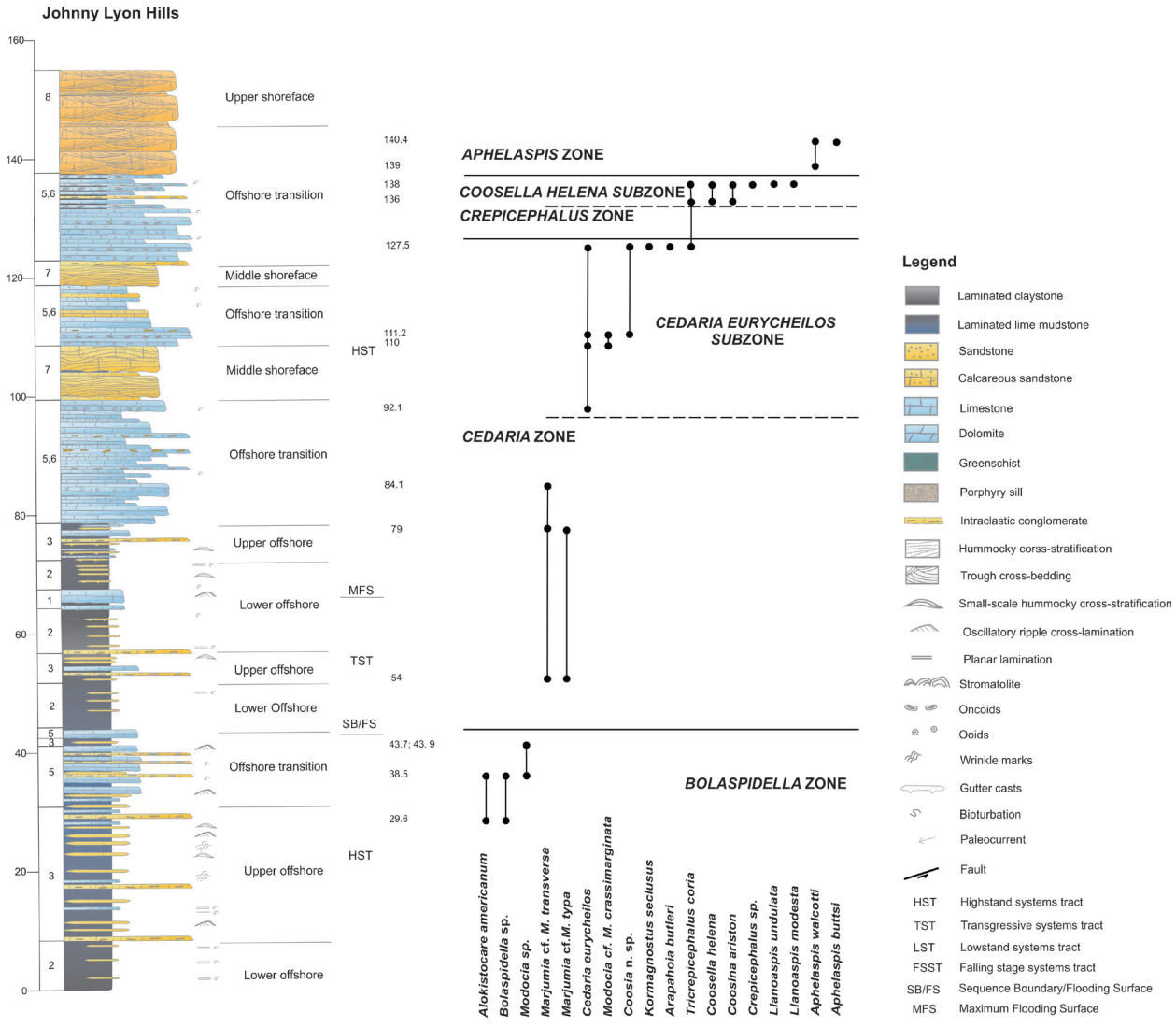

Fig. 3.3. Stratigraphic section of Johnny Lyon Hills and species range chart with biostratigraphic units.

3.5.2. Steptoean Stage

3.5.2.1. *Aphelaspis* Zone

Representatives of *Aphelaspis* Zone are present in the Ajax Hill and Johnny Lyon Hills sections in the upper part of the Abrigo Formation dominated by grainstones and packstones of offshore transition, as well as hummocky cross-stratified calcareous sandstones and trough-cross stratified calcareous sandstones of middle and upper shoreface settings, respectively. This zone is represented by *Aphelaspis walcotti* Resser, 1938 and *A. buttsi* (Kobayashi, 1936). It is correlatable with the *Aphelaspis* Zone of Palmer (1954) on the basis of the presence of *A. walcotti* which corresponds to the *Aphelaspis* Zone of Lochman and Duncan (1944). The presence of *A. walcotti* suggests a correlation with the *Aphelaspis* Zone of Rasetti (1965) from the central Appalachians. The striking faunal change has been known to exist in the Laurentian fauna at the base of the *Aphelaspis* Zone, where the boundary between Marjumiid and Pterocephaliid biomeres reflects non-evolutionary discontinuity in the fossil record, being considered to represent the worldwide extinction event (Palmer, 1984). The cause of it is still unclear. The rise of the oceanic thermocline has been suggested as a factor causing the invasion of cooler waters onto the shelf (Palmer, 1965b, 1984; Stitt, 1971, 1975, 1977). Nevertheless, Westrop and Ludvigsen (1987) disagreed with the idea of cool and poorly oxygenated waters originating from the ocean, noting the lack of sedimentological evidence for the environmental change.

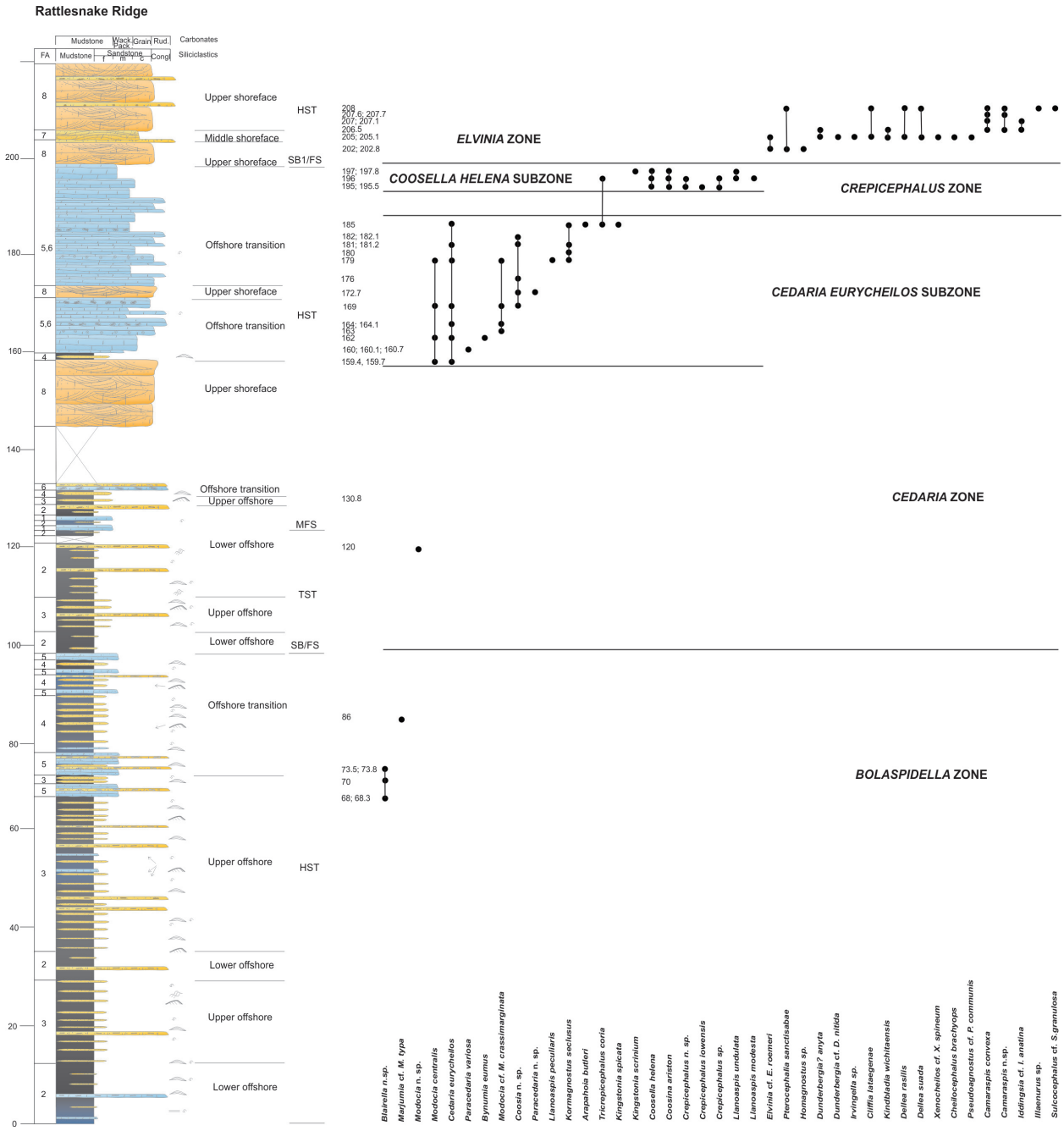

Fig. 3.4. Stratigraphic section of Rattlesnake Ridge and species range chart with biostratigraphic units. Symbols the same as for Figures 3.3.

3.5.2.2. *Elvinia* Zone

Representatives of the *Elvinia* Zone occur in trough-cross stratified calcareous sandstones in the Rattlesnake Ridge and Ajax Hill sections in the upper part of the Abrigo Formation deposited in the middle and upper shoreface setting. Species include *Elvinia* cf. *E. roemeri* (Shumard, 1861); *Pterocephalia sanctisabae* Roemer, 1849; *Homagnostus* sp.; *Dunderbergia*? cf. *D. anyta* (Hall and Whitfield, 1877); *D.* cf. *D. nitida* (Hall and Whitfield,1877); *Irvingella* sp.; *Cliffia lataegenae* (Wilson, 1949); *Kindbladia wichitaensis* (Resser, 1942); *D. rasilis* Westrop, 1986; *Dellea suada* (Walcott,1890); *Xenocheilos* sp. cf. *X. spineum* Wilson, 1951; *Cheilocephalus brachyops* Palmer, 1965; *Pseudagnostus* cf. *P. communis* (Hall and Whitfield, 1877); *Camaraspis convexa* (Whitfield, 1878); *Camaraspis* n. sp.; *Iddingsia* cf. *I. anatina* Resser, 1942; *Illaenurus* sp.; and *Sulcocephalus* sp.

The *Elvinia* Zone in the Abrigo Formation can be correlated directly with the *Elvinia* Zone in the Bison Creek Formation from southern Alberta and British Columbia (Westrop, 1986). Moreover, more than a half of the species in this portion of the Abrigo Formation have been reported from the *Xenocheilos* sp. cf. *X. spineum* Fauna that occurs in the upper part of the *Elvinia* Zone in the southern Canadian Rocky Mountains. There are strong similarities with the *Elvinia* Zone in the Wilberns Formation of Texas described by (Wilson, 1949). Common to both southeastern Arizona and Texas, as well as the Reagan Sandstone of Oklahoma (Stitt, 1971), are: *C. convexa, E. roemeri, K. wichitaensis, I. anatina*, *P. sanctisabae* and *C. lataegenae*. The *Elvinia* Zone in the Abrigo Formation can be correlated with the Ore Hill Member of the Gatesburg Formation in the central Appalachians on the basis of the presence of *C. convexa, E. roemeri, I. anatina*, *K. wichitaensis, D. suada, X.* sp. cf. *X. spineum, and C. lataegenae*. The presence of *E. roemeri, P. sanctisabae*, *C. lataegenae*, *D. suada, X. spineum* suggests that the B and C units of the Davis

Formation in Missouri (Kurtz, 1975) correlate with the *Elvina* Zone of the Abrigo Formation. The correlation can be made also with the *Elvinia* Zone from the Wonewoc Formation in Minnesota (Bell et al., 1952), the Open Door Limestone in Wyoming (Deland and Shaw, 1956), Dry Creek and Sage members of the Snowy Range Formation of Montana and Wyoming (Grant, 1965), and Dunderberg Formation of Nevada and Utah (Palmer, 1965). The presence of species like *E. roemeri, C. lataegenae, D. nitida* in the *Proceratopyge rectispinata* Fauna from the Mackenzie Mountains (Pratt, 1992) indicates a general correlation with *Elvinia* zone, although this fauna is restricted to a deeper water setting.

The *Irvingella major* Subzone of the *Elvinia* Zone has not been recognized in the Abrigo Formation.

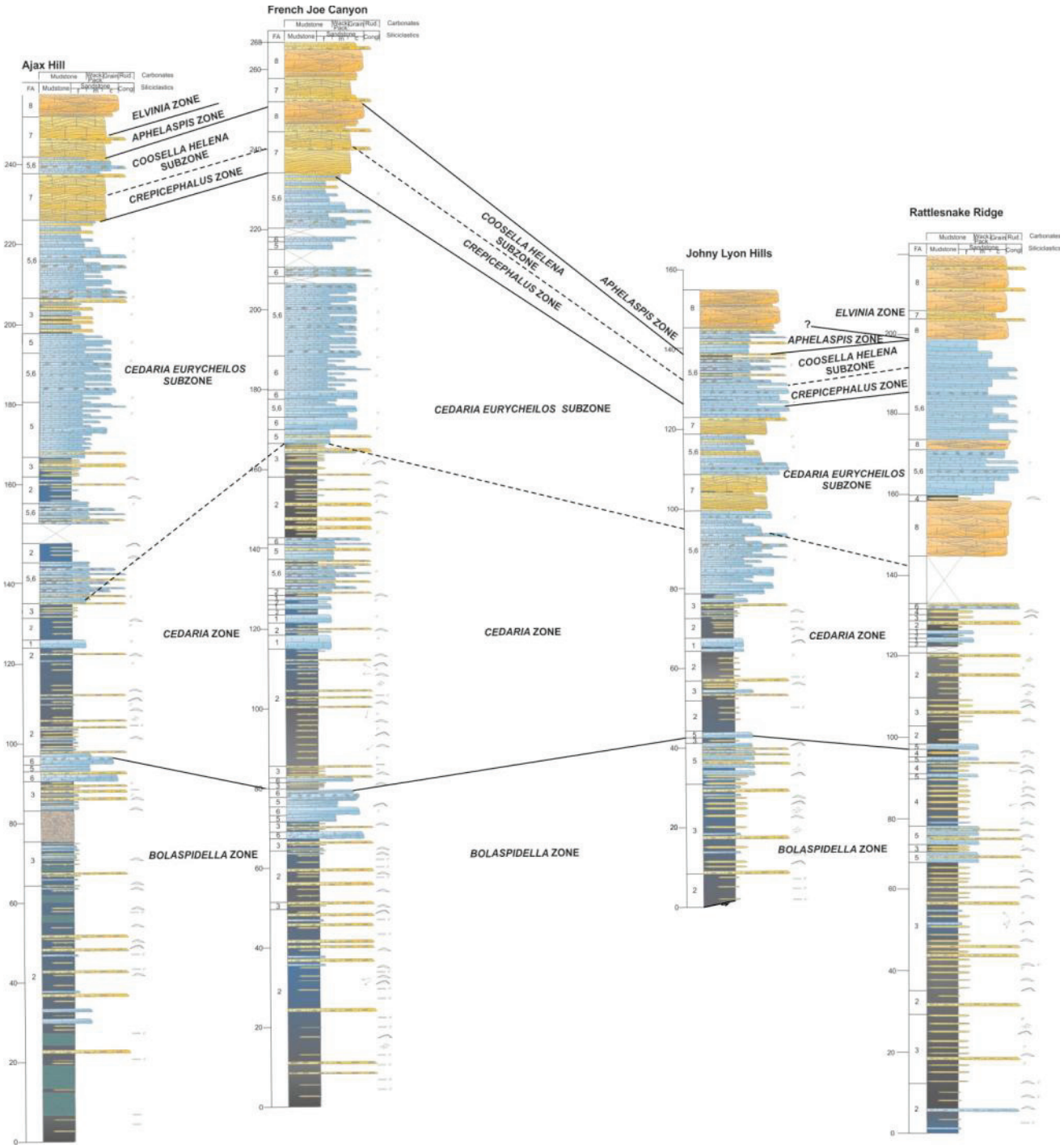

Fig. 3.5. Biostratigraphic correlation of Ajax Hill, French Joe Canyon, Johnny Lyon Hills, and Rattlesnake Ridge sections, Abrigo Formation. Symbols the same as for Figures 3.3.

3. 6. TRILOBITE BIOFACIES

Sedimentological data indicate that the trilobite taxa recovered from the Abrigo Formation are essentially autochthonous accumulations of species that inhabited a range of environments ranging from lower offshore to upper shoreface.

Biofacies are defined on the base of relative abundance of trilobite genera in individual or grouped collections made in intervals of seemingly uniform lithofacies or lithofacies assemblages (Figs. 3.6–3.9). The biofacies are therefore taken as reflecting benthic communities usually within individual biostratigraphic zones (Ludvigsen, 1978; Westrop 1992; Pratt, 1992; Melzak and Westrop, 1994, Amati and Westrop, 2006). These communities are in turn considered as reflecting the sedimentary environment in the context of evolutionary replacement of the fauna (Fig. 3.10).

Because the number of fossiliferous horizons is not great and some collections are sparse, these biofacies are readily apparent and do not need to be supported by statistical manipulation (cf. Ludvigsen et al., 1986). Eight biofacies are recognized and determined within the following zones on the basis of the number of cranidia.

3.6.1. Lower Marjuman: *Ehmaniella, Olenoides–Bolaspidella,* and *Blairella* biofacies. These are defined in this interval of the Abrigo Formation.

The *Ehmaniella* biofacies is recognized in the lowest portion of French Joe Canyon and Ajax Hill sections, that was deposited the most offshore setting. This biofacies occurs in laminated lime mudstone sporadically intercalated with lenticular siltstone and small-scale hummocky cross-stratified, thin-bedded sandstone. These deposits formed above storm wave base in a lower

offshore setting. The *Ehmaniella* biofacies seems to represent a unique assemblage with low diversity due to ecological stress.

***Bolaspidella* Zone**

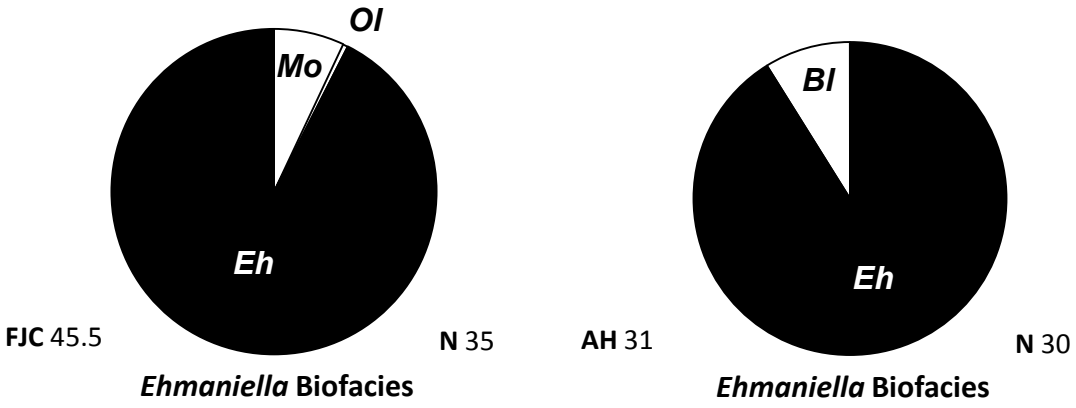

A

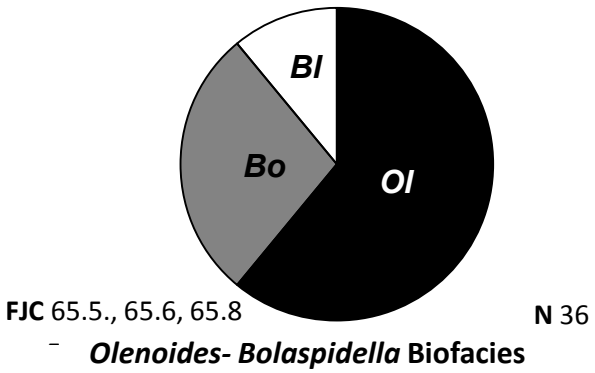

B

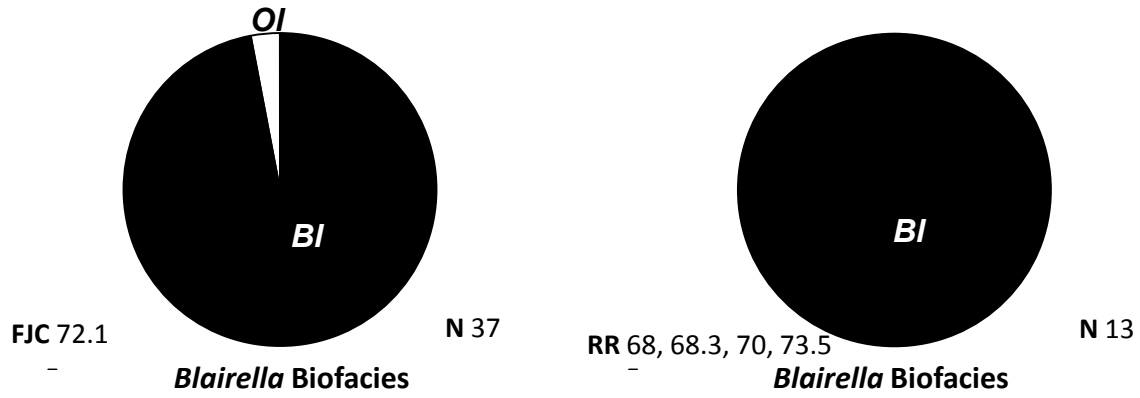

C

Fig. 3.6. Abundance of lower Marjuman trilobite genera in the *Bolaspidella* Zone. A. Two collections from the *Ehmaniella* Biofacies. B. One collection from the *Olenoides-Bolaspidella* Biofacies. C. Two collections from the *Blairella* Biofacies. *Eh = Ehmaniella*; *Mo = Modocia*; *Ol = Olenoides*; *Bo = Bolaspidella*; *Bl = Blairella*. Blank areas remaining minor taxa. Collection number at lower left of each pie diagram which reflects the meters above the base of the Abrigo Formation; number of taxa counted at lower right. FJC= French Joe Canyon, JLH= Johnny Lyon Hills, RR= Rattlesnake Ridge, AH=Ajax Hill.

The *Olenoides–Bolaspidella* biofacies is recognised only in the French Joe Canyon section in laminated lime mudstone, interbedded with small-scale hummocky cross-stratified, thin-bedded, laterally extensive sandstone. These deposits were deposited above storm-wave base in an upper offshore environment.

The *Blairella* biofacies occurs in French Joe Canyon and Rattlesnake Ridge sections within laminated lime mudstone, interbedded with small-scale hummocky cross-stratified, thin-bedded, laterally extensive sandstone of upper offshore setting. Small amounts of trilobite sclerites that

are disarticulated but usually not fragmented and abraded are preserved on some of the bedding surfaces.

This biofacies is present as well in lime mudstone and wackestone interbedded with bioclastic grainstone and packstone formed close to the fair-weather wave base, in the offshore transition environment. Bioclasts commonly show normal grading and consist of disarticulated and commonly abraded trilobite sclerites.

***Cedaria* Zone**

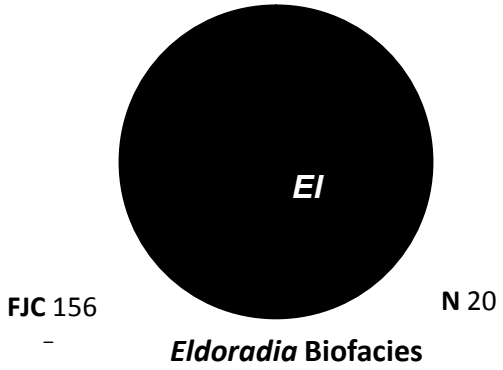

A

***Cedaria eurycheilos* Subzone**

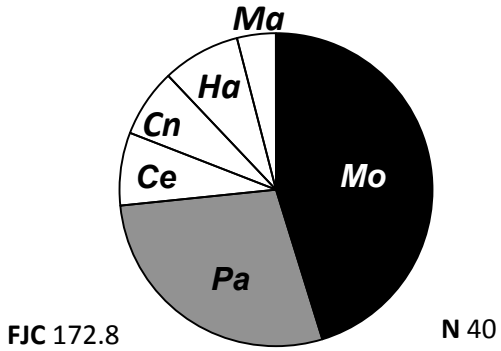

B

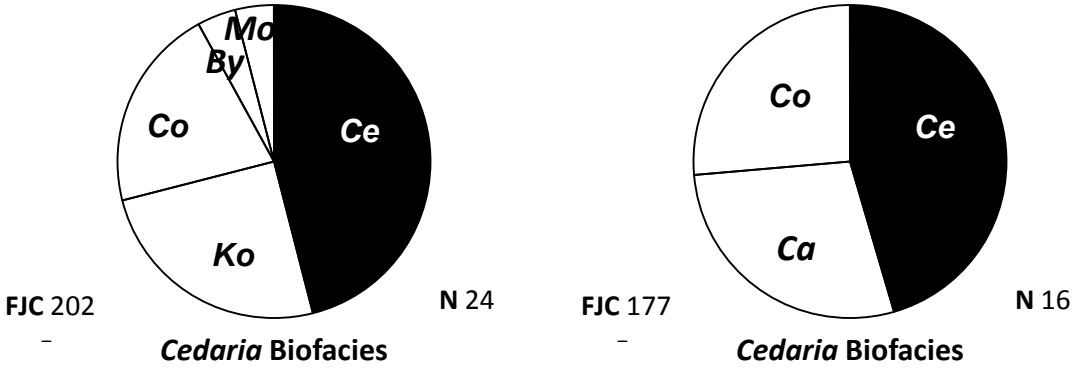

C

Fig. 3.7. Abundance of upper Marjuman trilobite genera. A . One collection from the *Eldoradia* Biofacies developed in *Cedaria* Zone. B. One collection of *Modocia-Paracedaria* Biofacies developed in *Cedaria eurycheilos* Subzone. C. Two collections of *Cedaria* Biofacies developed in *Cedaria eurycheilos* Subzone. *Ce = Cedaria*; *Cn = Cedarina; Ko = Kormagnostus*; *Co = Coosella*; *Ca = Coosia*; *Pa =Paracedaria*; *By = Bynumia*; *Mo = Modocia*.

3.6.2. Upper Marjuman: *Eldoradia, Modocia–Paracedaria, Cedaria,* and *Coosella–Coosina*.

The *Eldoradia* biofacies is composed entirely of the eponymous genus and was found developed only in the French Joe Canyon section in laminated lime mudstone sporadically interbedded with lenticular siltstone and small-scale hummocky cross-stratified, thin-bedded sandstone deposited in the lower offshore. It may represent a increase of the ecological stress characteristic of somewhat deeper-water conditions. *Eldoradia* also dominated the faunal assemblage in western Newfoundland (Lochman, 1938b).

The *Modocia–Paracedaria* biofacies occurs in the French Joe Canyon section, in lime mudstone and wackestone interbedded with bioclastic grainstone and packstone, and oolitic–oncolitic packstone. These deposits formed in an offshore transition setting around fair-weather wave base and were reworked by oscillatory currents during storms. It represents the most diverse community that became established in favourable conditions between the storm activity.

The *Cedaria* biofacies is represented also by a diverse assemblage in all the sections, in lime mudstone and wackestone interbedded with bioclastic grainstone and packstone, and oolitic–oncolitic packstone. These deposits formed close to fair-weather wave base in an offshore transition setting. The *Cedaria* biofacies in the Abrigo Formation seems to be similar in the composition to the assemblages reported from other subtidal and peritidal limestones of Laurentia (e.g., Lochman and Duncan, 1944; Lochman, 1950; Palmer, 1954a; Westrop, 1992). A *Cedaria*-dominated assemblage has been described by Pratt (1992) from the deep-water Rabbitkettle Formation which suggests fairly broad ecological tolerance for the component species. The sparse presence of agnostoids in the Abrigo Formation supports the generally

proposed concept that they were adapted to deeper water, being commonly recognized from outer shelf and slope settings (e.g., Robison, 1976; Pratt, 1992; Pratt and Bordonaro, 2014).

***Crepicephalus* Zone**

***Coosella helena* Subzone**

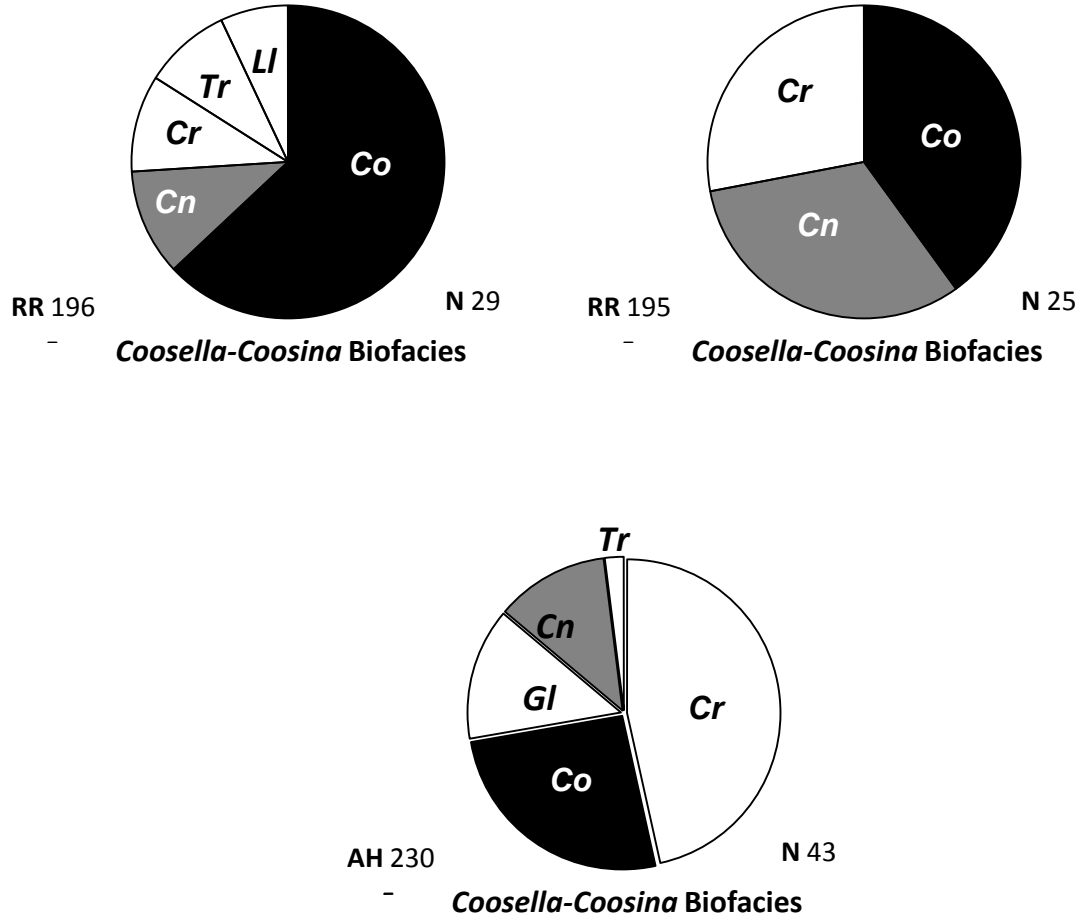

Fig. 3.8. Distribution of trilobite genera in three collections from *Coosella* - *Coosina* Biofacies developed in *Crepicephalus* Zone, *Coosella helena* Subzone of the Upper Marjuman. *Co* = *Coosella*; *Cn* = *Coosina*; *Cr* = *Crepicephalus*; *Tr* = *Tricrepicephalus*; *Ll* = *Llanoaspis*; *Gl* = *Glaphyraspis*.

Coosella–Coosina biofacies occurs across the area. In Rattlesnake Ridge and Johnny Lyon Hills sections it has been distinguished in lime mudstone and wackestone interbedded with bioclastic grainstone and packstone, and oolitic–oncolitic packstone deposited in offshore transition setting. In French Joe Canyon and Ajax Hill it has been recognised in amalgamated hummocky cross-stratified calcareous sandstone and amalgamated trough cross-stratified calcareous sandstone deposited above fair-weather wave base in the shoreface setting. Bioclastic limestones containing *Coosella* and *Coosina* in the Big Cove Member of western Newfoundland (Westrop, 1992) represent the same biofacies developed in a similar setting as in the Abrigo Formation. Species belonging to *Coosella* and *Coosina* are common in shallow subtidal to peritidal environments (Palmer, 1954b, Lochamn and Duncan, 1944; Stitt and Perfetta, 2000).

3.6.3. Upper Steptoean. The *Camaraspis* biofacies is recognised in the uppermost part of the Abrigo Formation at Ajax Hill and Rattlesnake

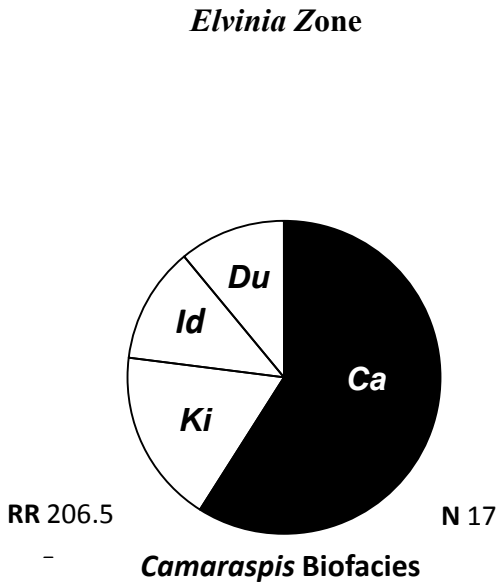

Fig. 3.9. Distribution of trilobite genera in the collection from *Camaraspis* Biofacies developed in *Elvinia* Zone of the upper Steptoean. *Ca = Camaraspis*; *Ki = Kindbladia*; *Id = Iddingsia*; *Du = Dunderbergia*.

Ridge in amalgamated trough cross-stratified calcareous sandstone deposited in shoreface environment. Similarly, the coeval shallow-water assemblage in the Reagan Sandstone of Oklahoma is dominated by *Camaraspis* (Stitt, 1971). This biofacies resembles the *Xenocheilos–Kindbladia* Biofacies of Westrop (1986) from the Lyell Formation; as well as assemblages described from the basal Wilberns Formation of central Texas (Wilson, 1949); the Dunderberg Formation of Nevada–Utah (Palmer, 1965); the Snowy Range Formation of southwestern Montana and northwestern Wyoming (Grant, 1965); and the Davis Formation of Missouri (Kurtz, 1975).

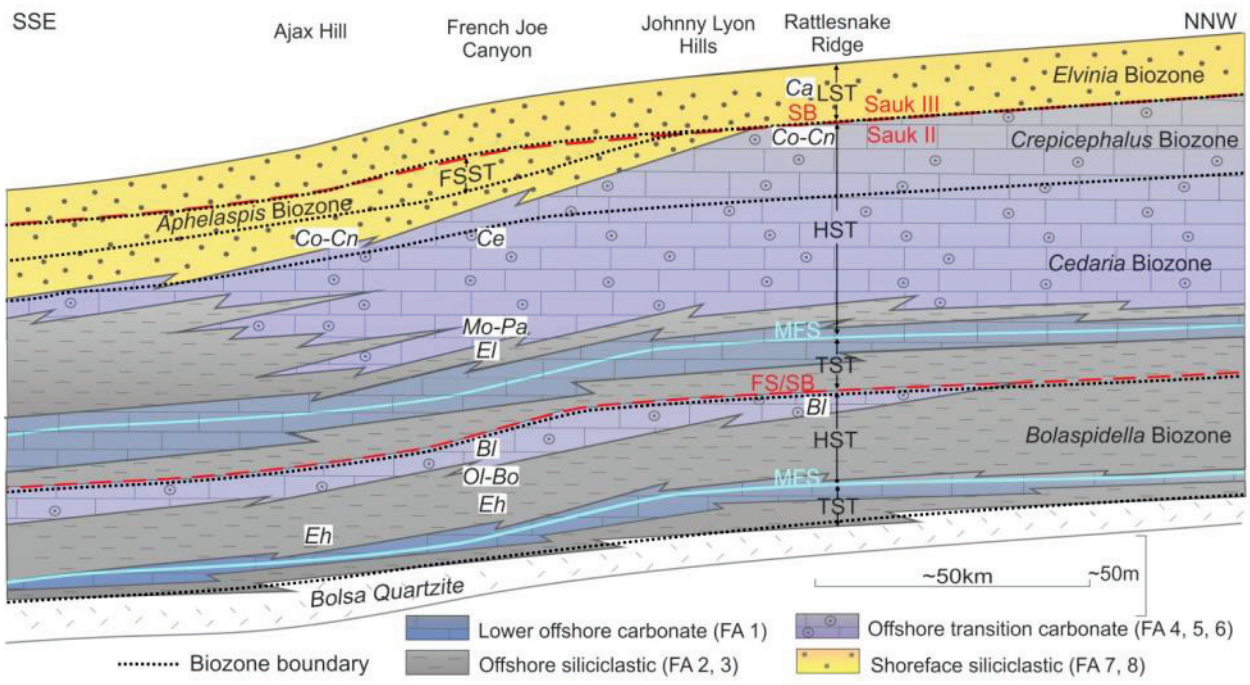

Fig. 3.10 . — Generalized SSE–NNW-oriented stratigraphic cross-section across the inner detrital belt in southeastern Arizona, showing distribution of facies associations, sequence stratigraphy, trilobite biostratigraphy, and biofacies. *Eh=Ehmaniella, Ol-Bo=Olenoides-Bolaspidella, Bl=Blairalla, El=Eldoradia, Mo-Pa=Modocia-Paracedaria, Ce=Cedaria, Co-Cn=Coosella- Coosina, Ca=Camaraspis*.

3.7 SYSTEMATIC PALEONTOLOGY

Phylum ARTHROPODA Latreille, 1829

Class UNCERTAIN

Order AGNOSTIDA Salter, 1864

Family AGNOSTIDAE M'Coy, 1849

Subfamily AGNOSTINAE M'Coy, 1849

Genus *Homagnostus* Howell, 1935

Type species. *Agnostus pisiformis* var. *obesus* Belt, 1867, Lower Lingula Flags, Wales (by original designation).

Remarks. See Pratt (1992) for discussion of this genus.

Homagnostus sp.

Pl. 1, fig. 17

Occurrence. Abrigo Formation, southeastern Arizona, *Elvinia* Zone.

Material. 1 cephalon.

Remarks. A cephalon with moderately inflated and slightly anteriorly tapering glabella, slight depression in front of the anterior glabellar lobe and lack of preglabellar median furrow. It

resembles *H. obesus* (Belt, 1867). However, Westrop and Eoff (2012) revised this species partitioning it into two morphotypes *H.* cf. *H. obesus* and *H.* cf. *H. alaskensis* Palmer 1968 on the basis of the morphology of pygidial axis, expression of glabellar furrows, and extent of the effacement of preglabellar median furrow. The specimen from the Abrigo Formation lacks a preglabellar median furrow, which excludes it from *H.* cf. *H. obesus* according to Westrop and Eoff (2012). The lack of the pygidium precludes a species determination.

Subfamily KORMAGNOSTINAE Pratt, 1992

Genus *Kormagnostus* Resser, 1938

Type species. Agnostus seclusus Walcott, 1884, Nolichucky Formation, Tennessee (by synonymy with *Kormagnostus simplex* Resser, 1938; Robison, 1988, p. 45).

Remarks. The concept of this genus by Westrop et al. (1996, p. 812) is followed here.

Kormagnostus seclusus (Walcott, 1884)

Pl. 1, figs. 1–15

1884 *Agnostus seclusus* Walcott, p. 25, pl. 9, fig. 14.

1988 *Kormagnostus seclusus*, Robison, p. 45, fig. 11.5–15 (see for synonymy).

1992 *Kormagnostus seclusus*, Pratt, p. 31, figs. 1–3, 14–29.

1996 *Kormagnostus* cf. *K. seclusus*, Westrop et al., p. 814, fig.13.1–13.5.

2000 *Kormagnostus seclusus*, Stitt and Perfetta, p. 203, fig. 6.1–6.4.

Holotype. A cephalon from the Hamburg Limestone, Nevada (Walcott, 1884, pl. 9, fig. 14; Palmer, 1954a, pl. 13 fig. 1).

Material. 18 cephala, 15 pygidia.

Occurence. Abrigo Formation, southeastern Arizona, *Cedaria* Zone, *Cedaria eurycheilos* Subzone; widespread in Laurentia, upper Steptoean; Greenland, Holm Dal Formation; Kazakhstan, *Kormagnostus simplex* Zone; Siberia, Sakhayan and Nganasanian horizons; Argentina, Cerro Solitario, Estancia San Isidro olistoliths, Upper Cambrian; China, Chefu Formation, *Formosagnostus formosus-Distazeris* Zone to *Liostracina bella-Ammagnostus sinensis* Zone, and *Ammagnostus integriceps-Chatiania* Zone.

Remarks. This species of *Kormagnostus* demonstrates wide intraspecific variation not only in the Abrigo Formation but also in previously described occurrences (Pratt, 1992). The variation is present in pygidia and predominantly in the shape of posterior pygidial axis. In collections from the Abrigo Formation the morphology of axis varies from parallel-sided to posteriorly expanding, but no stratigraphic pattern is apparent.

Subfamily PSEUDAGNOSTINAE Whitehouse, 1936

Genus *Pseudoagnostus* Jaekel, 1909

Type species. *Agnostus cyclopyge* Tullberg, 1880, Andrarum Limestone, Sweden (by original designation).

Pseudagnostus cf. *P. communis* (Hall and Whitfield, 1877)

Pl. 1, fig. 16

1877 *Agnostus communis* Hall and Whitfield, p. 228, pl. 1, figs. 28, 29.

1955 *Pseudagnostus communis*, Palmer, p. 94, pl.19, figs. 16, 19–21; pl. 20, figs. 4–10 (see for synonymy).

1992 "*Pseudagnostus communis*", Pratt, p. 34, p. 5, figs. 10–34 (see for synonymy).

2012 *Pseudagnostus* cf. *P. communis*, Westrop and Eoff, p. 209, figs. 6.1–6.12, 7.1–7.9, 8.1–8.13 (see for synonymy).

Occurrence. Abrigo Formation, southeastern Arizona *Elvinia* Zone; widespread in North America, upper Steptoean.

Material. 1 pygidium.

Remarks. There has been two approaches to defining this species. Westrop and Eoff (2012, p. 209) maintained a stricter view of its attributes and consequently limited its range to Laurentia. By contrast, Pratt (1992, p. 34) took a broader view, but at the same time placed it under open nomenclature as "*Pseudagnostus communis*", signaling that it needed a thorough revision. Westrop and Eoff (2012) also placed their material under an open nomenclature. The single pygidium recovered cannot contribute to the debate.

Class TRILOBITA Walch, 1771

Order CORYNEXOCHIDA Kobayashi, 1935

Family DORYPYGIDAE Kobayashi, 1935

Genus *Olenoides* Meek, 1877

Type species. *Paradoxides*? *nevadensis* Meek, 1870, Wheeler Formation, Utah (by original designation).

Remarks. The concept of this genus by Robison (1964, p. 537) is followed here. The various species of *Olenoides* are distinguished largely on the basis of number and the relative length of the pygidial border spines.

Olenoides nevadensis (Meek, 1870)

Pl. 4, figs. 1–16

1870 *Paradoxides*? *nevadensis* Meek, p. 62. 1877, p. 1, fig. 5.

1971 *Olenoides nevadensis*, Robison, p. 799, pl. 89, figs. 13–15 (see for synonymy).

Holotype. Thorax and pygidium from the Wheeler Formation, Utah (Meek, 1870, p. 62; Palmer, 1954a, pl. 14, fig. 9).

Diagnosis. *Olenoides* with short pygidial margin bearing four pairs of spines; two anterior pairs are of medium length; third pair are much longer and wider; posterior pair are short.

Occurrence. Abrigo Formation, southeastern Arizona, *Bolaspidella* Zone; Wheeler Formation, Utah, middle Cambrian, Hamburg Formation, Eureka district, Nevada.

Material. 11 cranidia, 6 pygidia, 6 hypostomes.

Remarks. The hypostome of this species has not been previously described, but it resembles that of other species of *Olenoides*. The distinguishing characteristics of the species are the strong development of the third pair of marginal spines, and the weak development of the fourth pair.

Order PTYCHOPARIIDA Swinnerton, 1915

Suborder PTYCHOPARIINA Richter, 1933

Family ALOKISTOCARIDAE Resser, 1939

Genus *Ehmaniella* Resser, 1937

Type species. Crepicephalus (*Loganellus*) *quadrans* Hall and Whitfield, 1877, Ute Formation (by original designation).

Remarks. The generic concept in Sundberg (1994, p. 53) is followed here. Material in the Abrigo Formation, however, cannot contribute to a discussion about the usefulness of subspecies.

Ehmaniella sp.

Pl. 2, figs. 1–5

Occurrence. Abrigo Formation, southeastern Arizona, *Bolaspidella* Zone.

Material. 39 cranidia.

Remarks. Cranidia from the Abrigo Formation agree in general with *Ehmaniella.* They display a subrectangular, gently tapered, anteriorly truncated glabella, with four faint glabellar furrows. The preglabellar field is slightly convex and moderately downsloping, A well-developed anterior border furrow defines a moderately long, slightly convex anterior border with few terrace lines at its anterior margin. The occipital ring is long and the fixed cheeks are wide. The exfoliated exoskeleton shows a pitted surface. They resemble *E. fronsplanata fronsplanata* Sundberg, 1994, differing in possessing a longer preglabellar field and a palpebral ridge that is more transverse. From *E. whitei* Robison and Babcock, 2011, they differ in their more subrectangular glabella and lack of an occipital spine. These cranidia are left under open nomenclature.

Genus *Blairella* Rasetti, 1965b

Type species. Blairella crassimarginata Rasetti, 1965b, Pleasant Hill Formation, Pennsylvania (by original designation).

Remarks. Two species of *Blairella* have been described: *B. crassimarginata* Rasetti, 1965b and *B. triangularis* Rasetti, 1965b. This genus has been known only from cranidia. One additional species is erected here, including the first described pygidium and free cheek for this genus.

Blairella cf. *B. crassimarginata* Rasetti 1965b

Pl. 1, figs. 18–22

1965b *Blairella crassimarginata* Rasetti, p. 1012, pl. 120, figs. 11–14.

Holotype. A cranidium from the Pleasant Hill Formation, Pennsylvania (Rasetti, 1965b, pl. 120, figs. 11–13).

Diagnosis. Blairella with subconical glabella and deep and wide axial furrows. Shallow but long anterior border furrow with slight median indentation. Long occipital ring.

Occurrence. Abrigo Formation, southeastern Arizona, *Bolaspidella* Zone; Pleasant Hill Formation, Pennsylvania, upper middle Cambrian.

Material. 58 cranidia.

Remarks. Cranidia from the Abrigo Formation closely resemble the holotype of *B. crassimarginata*. However they display a more convex glabella, slightly wider axial furrows and a faint medial indentation in the anterior border furrow. Because an appreciation of intraspecific variation is lacking in the Pleasant Hill Formation, cranidia are left under open nomenclature.

Blairella n. sp.

Pl. 2, figs. 6–16

Holotype. A cranidium from the Abrigo Formation, sotheastern Arizona (Pl. 2, figs. 10).

Diagnosis. Blairella with subrectangular, tapered, anteriorly truncated glabella, moderately long occipital ring.

Description. Glabella is subrectangular and tapered in outline, anteriorly truncated, with four faint glabellar furrows. Preglabellar field convex, downsloping. Convex anterior border. Moderately long occipital ring. Free cheek with moderately long genal spine. Small, transverse

pygidium. Pygidial axis with three axial rings and rounded terminal piece, reaching the narrow posterior margin. Prosopon smooth or finely granulate.

Occurrence. Abrigo Formation, southeastern Arizona, *Bolaspidella* Zone.

Material. 58 cranidia, 12 pygidia, 3 free cheeks.

Remarks. Blairella n. sp. differs from *B. crassimarginata*, Rasetti, 1965b in having shallower and narrower axial furrows, and a shorter preglabellar field and anterior border. From *B. triangularis* Rasetti, 1965b it differs in its shorter and gently rounded, rather than triangular, posteriorly occipital ring, narrower fixed cheeks and longer glabella.

Genus *Alokistocare* Lorenz, 1906

Type species. *Conocephalites subcoronatus* Hall and Whitfield, 1877, Ute Formation, Utah (by original designation).

Alokistocare americanum (Walcott, 1916a)

Pl. 3, figs. 1–11

1916a *Acorcephalites americanus* Walcott, p. 177, pl. 24, figs. 2, 2a, 2b, 3, 3a, 3b.
1989 *Alokistocare americanum*, Schwimmer, p. 486, figs. 2.11–2.16, 2.18–2.20 (see for synonymy).

Holotype. A cranidium from the Conasauga Formation, Georgia (Walcott, 1916a, pl. 24, fig. 2).

Occurrence. Abrigo Formation, southeastern Arizona, *Bolaspidella* Zone; Conasauga Formation, Georgia, *Bolaspidella* Zone.

Material. 26 cranidia.

Remarks. This species is characterized by a conical to subconical, anteriorly truncated glabella bearing three pairs of glabellar furrows, well-defined axial furrows, moderately long preglabellar area with a preglabellar median swelling, long anterior border, prominent, and strongly arched palpebral lobe extending from antero-latteral corner of glabella. The surface is covered with coarse tubercles with two rows of tubercles placed on glabella. Early holaspid stage cranidia show shorter preglabellar area, shorter anterior border and less convex fixed cheeks. The appreciation of this species by Schwimmer (1989), allowing for fairly wide morphological variation, is followed here.

Superfamily OLENACEA Burmeister, 1843

Family ELVINIIDAE Kobayashi, 1935

Subfamily ELVINIINAE Kobayashi, 1935

Genus *Elvinia* Walcott, 1924

Type species. *Dikelocephalus roemeri* Shumard, 1861, Wilberns Formation, central Texas (by original designation).

Elvinia cf. *E. roemeri* (Shumard, 1861)

Pl. 5, fig. 11

1861 *Dikelocephalus roemeri* Shumard, p. 220.

1965 *Elvinia roemeri*, Palmer, p. 44, pl. 3, figs. 9, 11, 14, 16 (see for synonymy).

1986 *Elvinia roemeri*, Westrop, p. 62, pl. 30, figs. 14–16 (see for synonymy).

1992 *Elvinia roemeri*, Pratt, p. 48, pl. 11, figs. 1, 2 (see for synonymy).

Neotype. A cranidium from the Wilberns Formation, central Texas (Walcott, 1925, pl. 17, figs. 9, 10; Bridge and Girty, 1937, pl. 69, fig. 9; selected by Walcott, 1925, p. 88).

Occurrence. Abrigo Formation, southeastern Arizona, *Elvinia* Zone; Rabbittkettle Formation, Mackenzie Mountains, *Proceratopyge rectispinata* Fauna; widespread in North America, *Elvinia* Zone; upper Cambrian Precordillera Argentina.

Material. 1 cranidium, 1 pygidium.

Remarks. The absence of coarse granulate prosopon in the cranidium from the Abrigo Formation suggests it belongs to *E. roemeri*. The only other species in this genus is *E. granulata* Resser, 1942b which is characterized by granulate prosopon. Material is too limited, however, to make a firm identification.

Genus *Irvingella* Ulrich and Resser *in* Walcott, 1924

Type species. Irvingella major Ulrich and Resser *in* Walcott, 1924, Franconia Formation, Wisconsin (by original designation).

Irvingella sp.

Pl. 4, fig. 17

Occurrence. Abrigo Formation, southeastern Arizona, *Elvinia* Zone.

Material. 1 cranidium.

Remarks. The cranidium from the Abrigo Formation resembles *I. flohri* Resser, 1942b by the possession of a glabella that is convex and truncated anteriorly, a faint second pair of glabellar furrow, and a short preglabellar area. It differs from *I. major* Walcott, 1924 in its glabella that is less convex transversely and longitudinally. *Irvingella transversa* Palmer, 1965 has much longer fixed cheeks.

Genus *Dunderbergia* Hall and Whitfield, 1877

Type species. Crepicephalus (*Loganellus*) *nitidus* Hall and Whitfield, 1877, Dunderberg Formation, Nevada (by original designation).

Remarks. The concept of Palmer (1960, p. 65; 1965, p. 39) is followed here.

Dunderbergia cf. *D. nitida* (Hall and Whitfield) 1877

Pl. 3, figs. 14–16

1877 *Crepicephalus* (*Loganellus*) *nitidus* Hall and Whitfield, p. 212, pl. 2, fig. 8.

1965 *Dunderbergia nitida*, Palmer, p. 41, pl. 4, figs. 1, 2, 5, 6 (see for synonymy).

1992 *Dunderbergia nitida*, Pratt, p. 49, pl. 11, figs. 31, 32.

Lectotype. A cranidium from the Dunderberg Formation, Nevada (selected by Palmer, 1960, pl. 4, fig. 15).

Occurrence. Abrigo Formation, southeastern Arizona, *Elvinia* Zone; Rabbitkettle Formation, Mackenzie Mountains, *Proceratopyge rectispinata* Fauna; Dunderberg Formation, Nevada, middle and upper *Dunderbergia* and *Elvinia* zones.

Material. 8 cranidia.

Remarks. Cranidia from the Abrigo Formation conform to this species outlined by Palmer (1960, p. 67; 1965, p. 41), in lacking prosopon. However, open nomenclature is applied because they display a narrower glabella and wider axial furrows.

Dunderbergia? cf. *D. anyta* (Hall and Whitfield, 1877)

Pl. 3, figs. 12, 13

1877 *Crepicephalus* (*Loganellus*) *anytus* Hall and Whitfield, p. 219, pl. 2, figs. 19–21.
1965 *Dunderbergia*? *anyta*, Palmer, p. 39, pl. 4, figs. 8, 10, 14–16 (see for synonymy).

Occurrence. Abrigo Formation, southeastern Arizona, *Elvinia* Zone; Dunderberg Formation and Johns Wash Limestone, Nevada, *Dunderbergia* Zone.

Material. 2 cranidia.

Remarks. These cranidia resemble *Dunderbergia*? *anyta* Palmer, 1965 (pl. 4, figs. 8, 10) by their low cranidial and glabellar convexity, narrow fixed cheeks, wide preglabellar field, and truncated subrectangular glabella with faint glabellar furrows. Palmer, 1965 placed this species to *Dunderbergia* because of the narrow cranidial border and slight median bend of the border furrow. However the granulate prosopon differs from that of other specimens assigned to this species.

Subfamily DOKIMOCEPHALINAE Kobayashi, 1935

Remarks. The concept of this subfamily as outlined by Westrop (1986, p. 59) is followed here.

Genus *Sulcocephalus* Wilson, 1948

Type species. Talbotina candida Resser, 1942b, Wilberns Formation, central Texas (by original designation).

Sulcocephalus sp.

Pl. 3, fig. 17

Occurrence. Abrigo Formation, southeastern Arizona, *Elvinia* Zone;

Material. 1 cranidium.

Remarks. A single incomplete cranidium from the Abrigo Formation resembles *Sulcocephalus granulosus* (Wilson, 1951) by its possession of a tapered glabella that is rounded anteriorly, well-incised lateral glabelar furrows, and tuberculate prosopon. It is too poorly preserved, however, to make positive identification.

Genus *Kindbladia* Frederickson, 1949

Type species. *Berkeia wichitaensis* Resser, 1942b from the Honey Creek Limestone, Oklahoma (by original designation).

Kindbladia wichitaensis Resser, 1942b

Pl. 5, figs. 1–3

1942b *Kindbladia wichitaensis* Resser, p. 92, pl. 15, figs. 31–33.

1951 *Kindbladia wichitaensis*, Wilson, p. 645, pl. 92, figs. 23, 24 (see for synonymy).

1971 *Kindbladia wichitaensis*, Stitt, p. 19, pl. 2, fig. 9 (see for synonymy).

1986 *Kindbladia wichitaensis*, Westrop, p. 61, pl. 28, figs. 6–8.

Holotype. A cranidium from the Honey Creek Limestone, Whichita Mountains, Oklahoma (Resser, 1942b, pl. 15, figs. 31, 32).

Occurrence. Abrigo Formation, southeastern Arizona, *Elvinia* Zone; widespread in North America, *Elvinia* Zone.

Material. 4 cranidia.

Remarks. Cranidia of this species are characterized by a slightly tapering glabella that is rounded anteriorly, deeply impressed axial furrows, and two pairs of well-impressed and one pair of faint lateral glabellar furrows, and a well-defined anterior border furrow with three shallow depressions. It bears an occipital node. It differs from *K. affinis* (Walcott, 1884) by having a

greater preglabellar field-anterior border ratio. However, the difference is not remarkable that species may be a synonym of *K. wichitaensis* (Resser, 1942b).

Genus *Dellea* Wilson, 1949

Type species. *Dellea wilbernsensis* Wilson, 1949 from the Wilberns Formation, central Texas (by original designation; =*Ptychoparia suada* Walcott, 1890).

Dellea rasilis Westrop, 1986

Pl. 5, figs. 4, 5

1986 *Dellea rasilis* Westrop, p. 59, pl. 28, figs. 1–5.

Holotype. A cranidium from the Bison Creek Formation, southern Alberta (pl. 28, figs. 4, 5).

Occurrence. Abrigo Formation, southeastern Arizona *Elvinia* Zone; Lyell and Bison Creek formations, southern Alberta, *Xenocheilos* cf. *spineum* Fauna.

Material. 2 cranidia.

Remarks. These cranidia with their smooth surface, convex anteriorly rounded glabella that lacks lateral glabellar furrows, and convex preglabellar field are most similar to *D. suada* (Walcott, 1890) and *D. snoburgensis* (Wilson, 1951). However they differ from those species by having a narrower, more tapered glabella and more convex preglabelar field, and agree well with *D. rasilis*.

Dellea suada (Walcott, 1890)

Pl. 5, figs. 6–10

1890 *Ptychoparia suada* Walcott, p. 274, pl. 21, fig. 9.

1951 *Dellea suada,* Wilson, p. 636, pl. 91, figs. 4–10, 18, 20–23, 25, 26 (see for synonymy).

1975 *Dellea suada*, Kurtz, p. 1037, pl. 2, figs. 12-17 (see for synonymy).

Holotype. A cranidium from the Wilberns Formation, central Texas (Walcott, 1890, pl. 21, fig. 9 [drawing], Wilson, 1951, pl. 91, fig. 25).

Occurrence. Abrigo Formation, southeastern Arizona, *Elvinia* Zone; widespread in North America, *Elvinia* Zone.

Material. 4 cranidia.

Remarks. This is the most widespread species of *Dellea* and exhibits a moderately convex glabella and downsloping preglabellar field and anterior part of the fixed cheek. It differs from *D. rasilis* Westrop, 1986 by having a wider glabella and fainter lateral glabellar furrows. *Dellea saratogensis* (Resser, 1942b) possesses coarse granulate prosopon. *Dellea forteyi* Pratt, 1992 differs in having a short nearly transverse anterior border and anteriorly slightly truncated glabella.

Genus *Iddingsia* Walcott, 1924

Type species. *Ptychoparia similis* Walcott, 1884 from the Windfall Formation, Nevada (by original designation).

Remarks. Westrop (1986) revised this genus and considered *Plataspella* as a junior synonym of *Iddingsia*. Valid species appear to be *I. similis* (Walcott, 1884); *I. robusta* (Walcott, 1884); *I. concava* Kobayashi 1938; *I. anatina* Resser, 1942b; *I. missouriensis* Resser, 1942b; *I. utahensis* Resser, 1942b; *I. occidentalis* Deland and Shaw, 1956; *I. intermedia* Palmer, 1965; and *I. relativa* Palmer, 1968.

Iddingsia cf. *I. anatina* Resser, 1942b

Pl. 5, figs. 12–16

1942b *Iddingsia anatina* Resser, p. 89, pl. 17, figs. 1, 2.

1971 *Plataspella anatina*, Stitt, p. 19, pl. 1, fig. 10 (see for synonymy).

1986 *Iddingsia anatina*, Westrop, p. 61, pl. 29, figs. 2–6.

Holotype. A cranidium from the Honey Creek Limestone, Oklahoma (Resser 1942b, pl. 17, figs. 1, 2).

Material. 2 cranidia, 3 pygidia, 1 free cheek.

Description. *Iddingsia* with cranidium having a subrectangular glabella with three lateral glabellar furrows, downsloping preglabellar field, shallow and broad anterior border furrow, and long anterior border. Occipital ring bearing occipital spine. Transverse pygidium displays broad axis and three axial rings and terminal piece. Two pairs of well-developed pleural and interpleural furrows. The third pair is faint. Pygidium expands into small posterolateral flanges. Posterior margin very short and convex. Finely granulated prosopon.

Occurence. Abrigo Formation, southeastern Arizona, *Elvinia* Zone; Bison Creek Formation, southern Alberta, *Xencheilos* cf. *spineum* Fauna; Honey Creek Limestone, Oklahoma, *Elvinia* Zone.

Remarks. Cranidia from the Abrigo Formation closely resemble *I. anatina* Resser, 1942b except they exhibit better defined lateral glabellar furrows and deeper axial furrows. *Iddingsia anatina* is characterized by its long occipital spine. Although, the cranidia from the Abrigo Formation show an indentation in posterior margin of the occipital ring suggesting an occipital spine that has broken off, but its incomplete preservation precludes positive identification.

Family PTEROCEPHALIIDAE Kobayashi, 1935

Subfamily APHELASPIDINAE Palmer, 1960

Genus. *Aphelaspis* Resser, 1935

Type species. *Aphelaspis walcotti* Resser, 1938a, Nolichucky Formation, Virginia (by original designation)

Remarks. The approach to this genus as outlined by Pratt (1992) is followed here. Żylińska (2015) discussed the occurrence of *Aphelaspis* on a global scale.

Aphelaspis walcotti Resser, 1938a

Pl. 6, figs. 1–9

1938a *Aphelaspis walcotti* Resser, p. 59, pl. 13, fig. 14.

1954b *Aphelaspis walcotti,* Palmer, p. 746, pl. 84, figs. 2, 4–8 (see for synonymy).

Holotype. A cranidium from the Nolichucky Formation, Virginia (Resser, 1938a, p. 59, pl. 13, fig. 14).

Occurrence. Abrigo Formation, southeastern Arizona, *Aphelaspis* Zone; widespread in North America*, Aphelaspis* Zone.

Material. 19 cranidia, 3 pygidia, 2 free cheeks.

Remarks. This species of *Aphelaspis* exhibits a moderately rounded anterior border, long and shallow anterior border furrow, and indistinct or very faint lateral glabellar furrows. The pygidium is transverse and semi-elliptical in outline, with a flat, moderately wide border. It differs from *A. buttsi* (Kobayashi, 1936) in having longer and narrower preglabellar field and shallower anterior border furrow. *Aphelaspis subditus* Palmer, 1962b exhibits longer anterior border, and longer and less transverse pygidium. *Aphelaspis brachyaspis* Palmer*,* 1962b has shorter preglabellar field.

Aphelaspis buttsi (Kobayashi, 1936)

Pl. 5, fig. 21

1936 *Proaulacopleura buttsi* Kobayashi, p. 93, pl. 15, fig. 6.

1965 *Aphelaspis buttsi*, Palmer, p. 59, pl. 8, figs. 14–16 (see for synonymy).

Holotype. A cranidium from the McKay Group, British Columbia, (Kobayashi, pl. 15, fig. 6).

Occurence. Abrigo Formation, southeastern Arizona, *Aphelaspis* Zone; Dunderberg Formation, Nevada, *Aphelaspis* Zone; McKay Group, southern British Columbia, *Dunderbergia* Zone.

Material. 11 cranidia, 3 pygidia, 2 free cheeks.

Remarks. *Aphelaspis buttsi* is similar to *A. walcotti*, except it has a wider and shorter preglabellar field, deeper anterior border furrow and deeper glabellar furrows. It displays the shortest pygidial border of any species assigned to *Aphelaspis*. *Aphelaspis haguei* (Hall and Whitfield, 1877) and *A. subditus* Palmer, 1962b have a slightly inflated preglabellar field.

Subfamily PTEROCEPHALIINAE Kobayashi, 1935

Remarks. Recent phylogenetic analysis of Pterocephaliinae (Hopkins, 2011) suggests the subfamily embraces four genera: *Cernuolimbus* Palmer, 1960; *Sigmocheilus* Palmer, 1960, *Pterocephalia* Roemer, 1849; and *Strigambitus* Palmer 1965 plus questionably assigned genera described from China: *Beigongia* Qiu *in* Qiu et al., 1983; *Dikelocephalioides* Qian, 1994; *Dikelocephalites* Sun, 1935; *Dingxiangaspis* Zhang, in Qiu et al., 1983; *Jubileia* Kobayashi, 1938; *Prodikelocephalites* Yuan and Yin, 1998; *Yokusenia* Kobayashi, 1935; and *Zhenania* Luo, 1983. Because *Camaraspis* Ulrich and Resser, 1924, *Pulchricapitus* Kurtz, 1975, and *Pelicephalus* Kurtz, 1975 do not possess the concave border that defines the Pterocephaliinae (Palmer, 1965b, p. 57) they were excluded from this subfamily.

Genus *Pterocephalia* Roemer, 1849

Type species. *Pterocephalia sanctisabae* Roemer, 1849 from the Wilberns Formation, central Texas (by original designation).

Remarks. *Pterocephalia* is distinguished from other pterocephaliines by its exceptionally long anterior border. Five other species have been assigned to *Pterocephalia*: *P. concava* Palmer, 1960; *P. constricta* Palmer, 1968; *P. elongata* Palmer, 1960; *P. norfordi* Chatterton and Ludvigsen, 1998; and *P. occidens* (Walcott, 1884).

Pterocephalia sanctisabae Roemer, 1849

Pl. 5, figs. 17–20

1949 *Pterocephalia sanctisabae* Roemer, p. 421.

1986 *Pterocephalia sanctisabae*, Westrop, p. 57, pl. 27, figs. 16–21 (see for synonymy).

1989 *Pterocephalia sanctisabae,* Hohensee and Stitt, p. 874, figs. 5.13–5.15 (see for synonymy).

Syntypes. Cranidia from the Wilberns Formation, central Texas, illustrated by Bridge and Girty (1937, pl. 67, figs. 1a–d).

Diagnosis. Cranidia of *P. sanctisabae* are characterized by very long anterior border and sub-rectangular glabella. Pygidia are characterized by a large number of axial rings and pleural furrows, and long posterior border.

Occurrence. Abrigo Formation, southeastern Arizona, *Elvinia* Zone; widespread in North America, *Elvinia* Zone.

Material. 2 cranidia, 1 pygidium.

Remarks. *Pterocephalia concava* Palmer, 1954b differs from *P. sanctisabae* by having rounded anterior border, rounded, inflated glabella, smaller number of axial rings and pleural ridges. *Pterocephalia elongata* Palmer, 1960 exhibits an elongate and subquadrate pygidial outline. *Pterocephalia norfordi* Chatterton and Ludvigsen, 1998 has a wide, transverse pygidium and the longest anterior border of all described species of the genus

Genus *Camaraspis* Ulrich and Resser, 1924

Type species. *Arionellus* (*Agraulos*) *convexus* Whitfield, 1878 from the Wonewoc Formation,Wisconsin (by original designation).

Remarks. Currently *Camaraspis* contains three species: *C. convexa* (Whitfield, 1878); *C. parabola* Frederickson, 1948; and *C. berkeyi* Resser, 1935. One new species is described from the Abrigo Formation.

Camaraspis convexa (Whitfield, 1878)

Pl. 7, figs. 1–8

1878 *Arionellus* (*Agraulos*) *convexus* Whitfield, p. 57.

1948 *Camaraspis convexa*, Frederickson, p. 798, pl. 123, figs. 12, 13 (see for synonymy).

1986 *Camaraspis convexa*, Westrop, p. 58, pl. 27, figs. 11–14 (see for synonymy).

Holotype. A cranidium from the Wonewoc Formation, Wisconsin, illustrated by Whitfield (1882, pl.1, fig. 17).

Diagnosis. *Camaraspis* with cranidium of moderate convexity and moderately well defined axial furrows. Glabella subrounded, tapering anteriorly. Pygidium with an axial lobe bearing two axial rings.

Occurrence. Abrigo Formation, southeastern Arizona, *Elvinia* Zone; widespread in North America, *Elvinia* Zone.

Material. 12 cranidia, 7 pygidia.

Remarks. Cranidia of *C. convexa* differ from those of *Camaraspis* n. sp. by the possession of an anteriorly tapering, subrounded glabella, deeper axial furrows and narrower pygidium. It differs from *C. parabola* Frederickson, 1948 by having a less convex cranidium. *Camaraspis berkeyi* Resser, 1935 has deeper axial and lateral glabellar furrows and a deeper anterior border furrow (Kurtz, 1975, p. 1034).

Camaraspis n. sp.

Pl. 7, figs. 9–18

Diagnosis. *Camaraspis* with subquadrate glabella. Cranidium strongly arched transversively and faint axial furrows. Wide, semi-elliptical pygidium with two well-defined axial rings and two to three pleural furrows.

Holotype. A cranidium from the Abrigo Formation, Rattlesnake Ridge (Pl. 7, figs.13, 14).

Occurrence. Abrigo Formation, southeastern Arizona, *Elvinia* Zone.

Description: Cranidium is semi-elliptical in outline and strongly arched transversely and longitudially. Axial furrows are weakly impressed parallel or nearly parallel, defining a subquadrate glabella. Wide frontal area is in length two-thirds that of the glabella. Faint anterior border furrow defines a short anterior border. Palpebral ridge extends to the anterio-lateral corner of glabella. Very short occipital spine recognised in some specimens. The prosopon of the cranidium and free cheek consists of fine pits. Lateral border of free cheek bears irregular terrace lines. Pygidium is semi-elliptical in outline. It is more than twice as wide as long. Axis consists of two well-defined rings and posteriorly rounded terminal piece. Axial field is crossed by two to three pleural furrows. Border comprises a short rim.

Material. 11 cranidia, 5 pygidia, 9 free cheeks.

Remarks. *Camaraspis* n. sp. differs from other species of the genus in its subquadrate glabella and longer and wider frontal area. The pygidium is wider with well-defined marginal rim. *Camaraspsis*. n. sp. differs from *C. convexa* and *C. berkeyi* by having a broader cranidium, a quadrate glabella, shallower lateral glabellar furrows, and longer frontal area. *Camaraspis parabola* has the most inflated cranidium with faint axial furrows.

Superfamily ILLAENURACEA Vogdes, 1890

Family ILLAENURIDAE Vogdes, 1890

Genus *Illaenurus* Hall, 1863

Type species. *Illaenurus quadratus* from the St. Lawrence and Jordan formations, Wisconsin (by original designation).

Remarks. The concept of this genus outlined by Westrop (1986) is followed here.

Illaenurus sp.

Pl. 7, fig. 19

Material. 1 cranidium.

Occurrence. Abrigo Formation, southeastern Arizona, *Elvinia* Zone.

Remarks. The single cranidium resembles *I. priscus* Resser, 1942b in its slightly arched cranidium that is subquadrate in outline, very shallow axial, faint palpebral ridge, and palpebral lobe that is located opposite the cranidial midlength. Posterior sutures are abruptly divergent. The single cranidium is left under open nomenclature.

Family SOLENOPLEURIDAE Angelin, 1854

Genus *Solenopleurella* Poulsen, 1927

Type species. *Solenopleurella ulrichi* Poulsen, 1927, from the Cape Wood Formation, northwestern Greenland (by original designation).

Remarks. Resser (1938a, 1945) named five more species: *S. buttsi; S. minor; S. virginica; S. diligens; and S. porcata*. Rasetti (1963) considered that those species together with *S. gaspensis*

(Kindle, 1942) are not congeneric with the type species and referred them to *Spencella* Rasetti, 1963.

Solenopleurella quadrata Rasetti, 1963

Pl. 6, figs. 14–16

1963 *Solenopleurella quadrata* Rasetti, p. 590, pl. 70, figs. 9–12.

Diagnosis. *Solenopleurella* with convex, sub-quadrate, commonly anteriorly indented glabella bearing two to three pairs of weakly impressed lateral glabellar furrows. Preglabellar field absent. Occipital furrow deep. Occipital ring long, lacking occipital spine. Anterior border furrow well incised, defining moderately long, nearly straight anterior border. Prosopon granulate. Pygidium unknown.

Holotype. A cranidium from the Lévis Formation, Quebec (Rasetti, 1963, pl. 70, figs. 10–12).

Occurrence. Abrigo Formation, southeastern Arizona, *Bolaspidella* Zone; Lévis Formation, Quebec (middle Cambrian boulder).

Material. 5 cranidia.

Remarks. *Solenopleurella quadrata* is characterized by subquadrate, inflated glabella with nearly parallel axial furrows, short anterior border furrow and faint lateral glabellar furrows. *Solenopleurella elatifrons* Rasetti, 1965b has deeper lateral glabellar furrows, a longer anterior border furrow, a deeper and longer occipital furrow, a longer and better impressed posterior border furrow, and prosopon is lacking. *Solenopleurella transversa* Rasetti, 1965b differs in

possessing a tapered, less convex glabella. It also lacks prosopon. *Solenopleurella ulrichi* Poulsen, 1927 possesses a truncated glabella with well-impressed lateral glabellar furrows and moderately long occipital ring.

Superfamily UNCERTAIN

Family MARJUMIIDAE Kobayashi, 1935

Remarks. Pratt (1992, p. 60) and Melzak and Westrop (1994, p. 975) concluded that *Marjumia* Walcott, 1916b and *Modocia* Walcott, 1924 are closely related and a generic distinction based on presence or absence of pygidial spines is artificial. Furthermore, Melzak and Westrop (1994, p. 975) considered *Modocia* as a junior synonym of *Marjumia*. Robison and Bobcock (2011, p. 29) agreed with Melzak and Westrop (1994, p. 975) that full cladistic analysis of marjumiid genera is needed but they continued to recognise *Modocia* as a valid genus. This approach is followed here.

Genus *Marjumia* Walcott, 1916b

Type species. *Marjumia typa* Walcott, 1916b, Marjum Formation, Utah (by original designation).

Marjumia cf. *M. transversa* (Palmer, 1968)

Pl. 8, figs. 1–3

1968 *Modocia transversa* Palmer, p. 65, pl. 5, figs. 1–5.

1994 *Marjumia* cf. *transversa*, Melzak and Westrop, p. 978, pl. 1, figs. 7–13.

Holotype. A cranidium from the Jones Ridge Limestone, east-central Alaska (Palmer, 1968, pl. 5, fig. 5).

Occurrence. Abrigo Formation, southeastern Arizona, *Cedaria* Zone; Jones Ridge Limestone, east-central Alaska, middle Cambrian; Pika Formation, southwestern Alberta, *Plagiura* cf. *P. retracta* Zone.

Material. 13 cranidia.

Remarks. Specimens from the Abrigo Formation are most similar to *M. transversa* but differ in having a more tapered glabella like that of the cranidia described by Melzak and Westrop, 1994).

Marjumia cf. *M. typa* Walcott, 1916b

Pl. 8, figs. 4–8

1916b *Marjumia typa* Walcott, p. 401, pl. 65, figs. 4, 4a, 4b.

1944 *Marjumia typa*, Shimer and Shrock, pl. 258, fig. 17.

1964 *Marjumia typa*, Robison, p. 549, pl. 87, figs. 1–4.

Holotype. A complete exoskeleton from the Marjum Formation, Utah (Walcott, 1916b, pl. 65, fig. 4).

Occurrence. Abrigo Formation, southeastern Arizona, *Cedaria* zone; Marjum and Wheeler formations, Utah, *Bolaspidella contracta* Subzone, *Bolaspidella* Zone.

Material. 10 cranidia

Remarks. Cranidia from the Abrigo Formation are most similar to *M. typa* Walcott, 1916b. However they differ in having a subtrapezoidal glabella that is less rounded anteriorly, and a shorter preglabellar field. No pygidia have been recovered and thus the material is left under open nomenclature.

Genus *Modocia* Walcott, 1924

Type species. *Arionellus* (*Crepicephalus*) *oweni* Meek and Hayden, 1861, Deadwood Formation, South Dakota (by original designation).

Remarks. The approach outlined by Palmer (1954, p. 762) is followed here.

Modocia centralis (Whitfield, 1877)

Pl. 9, figs. 5–15

1877 *Crepicephalus* (*Loganellus*) *centralis* Whitfield, p.10.

1956b *Modocia centralis*, Shaw, p. 141 (see for synonymy).

1956 *Modocia centralis*, Deland and Shaw, p. 358, pl. 64, fig. 10.

1961 *Modocia centralis*, Lochman and Hu, p. 136, pl.29, figs. 1–39.

1998 *Modocia centralis*, Stitt, p. 1038, figs. 6.15–6.20, 6.23.

Holotype. A cranidium from the Deadwood Formation, South Dakota (Whitfield, 1877, p. 10).

Occurrence. Abrigo Formation, southeastern Arizona, *Cedaria eurycheilos* Subzone, *Cedaria* Zone; Riley Formation, central Texas, *Bolaspidella* Zone; Deadwood Formation, South Dakota, *Cedarina dakotaensis* Zone.

Material. 18 cranidia, 4 pygidia, 6 free cheeks.

Remarks. This species is characterized mainly by a long preglabellar field, relatively long anterior border and well-defined anterior border furrow. Prosopon is tuberculate. Fixed cheeks are wider than those of *M. dubia* Resser, 1938a.

Modocia oweni (Meek and Hayden, 1861)

Pl. 9, figs. 3, 4

1861 *Arionellus oweni* Meek and Hayden, p. 436.

1924 *Modocia oweni*, Walcott, p. 59, pl. 12, fig. 7.

1925 *Modocia oweni*, Walcott, p. 106, pl. 116, fig. 1–3 (see for synonymy).

1954 *Modocia* cf. *M. oweni*, Palmer, p. 763, pl.97, figs. 3, 4, 6.

1998 *Modocia oweni*, Stitt, p. 1038, pl. 6, figs. 21, 22, 24–26.

Holotype. A cranidium from Deadwood Formation, South Dakota (Meek and Hayden, 1861, p. 436).

Occurrence. Abrigo Formation, southeastern Arizona, *Bolaspidella* Zone; Riley Formation, central Texas, *Bolaspidella* Zone; Deadwood Formation, South Dakota, *Cedarina dakotaensis* Zone.

Material. 2 cranidia.

Remarks. This species is characterized mainly by a long preglabellar field, relatively long anterior border and well-defined anterior border furrow. Fixed cheeks are wider than those of *M. dubia*. It differs from *M. centralis* (Whitfield, 1877) by its narrower cranidium and narrower fixed cheeks.

Modocia dubia (Resser, 1938a)

Pl. 9, figs. 1, 2

1938a *Ehmania dubia* Resser, p. 75, pl. 9, figs. 18, 19.

1965 *Modocia dubia*, Rasetti, p. 107, pl. 1, figs. 22–26.

1992 *Modocia dubia*, Pratt, p. 60, pl. 20, figs. 1, 2.

Holotype. A pygidium from the Nolichucky Formation, Tennessee (Resser, 1938a, pl. 9, fig. 19).

Occurrence. Abrigo Formation, southeastern Arizona, *Bolaspidella* Zone; Rabbitkettle Formation, *Cedaria minor* Zone; Nolichucky and Maryville formations, Tennessee, *Cedaria* Zone.

Material. 2 cranidia.

Remarks. Cranidia of this species are characterized by a narrow preglabellar field, relatively long anterior border and well-defined anterior border furrow. Fixed cheeks are narrower than in the other species of this genus.

Modocia cf. *M. crassimarginata* Rasetti, 1965a

Pl. 8, figs. 14–23

1965a *Modocia crassimarginata,* Rasetti, p. 109, pl. 2, figs. 1–9.

Holotype. A cranidium from Maryville Formation, Tennessee (Rasetti, 1965a, p. 109, pl. 2, figs. 1–3).

Occurrence. Abrigo Formation, southeastern Arizona, *Cedaria eurycheilos* Subzone, *Cedaria Z*one; Maryville Formation, Tennessee, *Cedaria* Zone.

Material. 15 cranidia, 9 pygidia.

Remarks. The specimens from the Abrigo Formation resemble *M. crassimarginata* in the inflated glabella, short, narrow fixed cheeks, and pygidium with short and moderately long posterior border with a small median indentation. Nevertheless, pygidia from the Abrigo Formation exhibit faint pleural furrows and are more convex than those assigned to this species by Rasetti (1965a).

Modocia n. sp.

Pl. 8, figs. 9–13

Diagnosis. *Modocia* with glabella bearing three to four glabellar furrows, outlined by well-developed and wide axial and preglabellar furrows.

Holotype. A cranidium from the Abrigo Formation, southeastern Arizona (Pl. 8, fig. 11).

Occurrence. Abrigo Formation, southeastern Arizona, *Cedaria* Zone.

Material. 29 cranidia, 2 pygidia.

Description. Glabella bears three to four glabellar furrows. It is outlined by well-developed and wide axial and preglabellar furrows. Occipital furrow is anteriorly curved sagitally. Pygidium has broad, rounded axis, that is composed of two rings and short terminal piece. It displays smooth pygidial margin.

Remarks. *Modocia* n. sp. differs from other species of this genus by having a subtrapezoidal glabella, wide and well-developed axial and preglabellar furrows, and a long, anteriorly curved occipital furrow.

Family TRICREPICEPHALIDAE Palmer, 1954b

Genus *Meteoraspis* Resser, 1935

Type species. *Ptychoparia metra* Walcott, 1890, Bonneterre Formation, Missouri (by original designation).

Remarks. Meteoraspis species differ from one another in the length and width of the posterior and lateral pygidial margins, the width and shape of pygidial spines and shape of glabella.

Meteoraspis sp.

Pl. 9, fig. 16

Occurrence. Abrigo Formation, southeastern Arizona, *Cedaria eurycheilos* Subzone, *Cedaria* Zone.

Material. 1 pygidium.

Remarks. The pygidium exhibits a pair of wide spines extending posteriorly slightly inward from the postero-lateral margin. The pygidial axis has three axial rings and a terminal piece. The pleural field is narrow. It resembles *M. metra* (Walcott, 1890).

Genus *Tricrepicephalus* Kobayashi, 1935

Type species. *Arionellus* (*Bathyurus*) *texanus* Shumard, 1861, Riley Formation, central Texas (by original designation).

Remarks. Palmer (1954b, p. 754) recognized three species, the tuberculate *T. coria* (Walcott, 1916a), *T. texanus* (Shumard, 1861) with a non-tuberculate glabella, and *T. tripunctatus* (Whitfield, 1876) with an occipital spine. Pratt (1992, p. 62) argued that the variable presence of tubercules is not a valid criterion for specific differentiation and he considered two species assigned to *T coria* and *T. texanus* as synonyms. However, the Abrigo Formation yielded specimens of *T. texanus* with non-tuberculate prosopon of the glabella, lateral border of free cheek and pygidium, as well as specimens of *T. coria* covered with tubercules. That agrees with Palmer's (1954b) concept, which is therefore followed here.

Tricrepicephalus coria (Walcott, 1916a)

Pl. 10, figs. 1–9

1916a *Crepicephalus coria* Walcott, p. 206, pl. 33, figs. 3a–g.

1954b *Tricrepicephalus coria*, Palmer, p. 755, pl. 81, figs. 1–4, 6 (see for synonymy).

1992 *Tricrepicephalus texanus*, Pratt, p. 62, pl. 21, figs. 1–7 (see for synonymy).

2000 *Tricrepicephalus coria*, Stitt and Perfetta, p. 212, figs. 9.20–9.27.

Holotype. A cranidium from the Weeks Formation, Utah (Walcott, 1916a, pl. 33, fig. 3b).

Occurrence. Abrigo Formation, southeastern Arizona, *Cedaria eurycheilos* Subzone, *Cedaria* Zone, and *Coosella helena* Subzone, *Crepicephalus* Zone; Riley Formation, *Coosella* and *Maryvillia* zones; Deadwood Formation, South Dakota, *Cedarina dakotaensis* and *Crepicephalus* zones; widespread in North America, *Cedaria* and *Crepicephalus* zones.

Material. 12 cranidia, 3 pygidia, 5 free cheeks.

Remarks. Cranidia, free cheeks and pygidia of this species are evenly covered with tubercules and this is true for specimens from the Abrigo Formation. Palmer (1954b, p. 755) adopted a somewhat broad species concept based on significant intraspecific morphological variability, especially in length and shape of the anterior border and character of the pits in the anterior border furrow. Specimens from the Abrigo Formation have a rather short preglabellar field, long and narrow pits in the anterior border. An occipital spine is absent.

Tricrepicephalus texanus (Shumard, 1861)

Pl. 10, figs. 10–17

1861 *Arionellus* (*Bathyurus*) *texanus* Shumard, p. 218.

1954b *Tricrepicephalus texanus* Palmer, p. 755, pl. 81, fig. 9 (see for synonymy).

Neotype. Type specimens from the Riley Formation, central Texas were destroyed and a neotype has yet to be designated.

Occurrence. Abrigo Formation, southeastern Arizona, *Cedaria eurycheilos* Subzone, *Cedaria* Zone, and *Coosella helena* Subzone, *Crepicephalus* Zone; Riley Formation *Coosella* Zone, widespread in North America, *Cedaria* and *Crepicephalus* zones.

Material. 10 cranidia, 2 pygidia, 2 free cheeks.

Remarks. The surface of the preglabellar field and fixed cheeks is covered unevenly with tubercules. The glabella, anterior border and lateral border of the free cheeks are smooth. The pygidium bears thick spines that are also bereft of tubercules. This species differs consistently from *T. coria* in the contrasting distribution of tubercles.

Family CREPICEPHALIDAE Kobayashi, 1935

Remarks. The concept of this family by Pratt (1992, p. 62) is followed here.

Genus *Crepicephalus* Owen, 1852

Type species. Dikelocephalus? *iowensis* Owen, 1852, Eau Claire Formation, Minnesota (designated by Walcott, 1886, p. 206).

Remarks. The concept of this family outlined by Pratt (1992, p. 62) is followed here.

Crepicephalus exutus Resser, 1938a

Pl. 11, fig. 1–8

1938a *Crepicephalus exutus* Resser, p. 73, pl. 11, fig. 40.

Diagnosis. *Crepicephalus* with transverse pygidium, long and nearly straight posterior margin and narrow and moderately long spines that are posteriorly divergent.

Holotype. A pygidium from the Nolichucky Formation, Alabama (Resser, 1938a, pl. 11, fig. 40).

Occurrence. Abrigo Formation, southeastern Arizona, *Crepicephalus* Zone; Nolichucky Formation, Alabama, upper Cambrian.

Description. The cranidium exhibits sub-conical glabella, moderately long preglabellar field and anterior border, moderately wide fixed cheeks, and moderately wide, slightly convex occipital ring. The pygidium is broadly transverse with long posterior margin covered with terrace lines. Narrow and convex pygidial axis bears three to four axial rings and a terminal piece. Wide pleural field is crossed by three pleural furrows. The pair of narrow and moderately long pygidial spines are posteriorly divergent from the posterolateral corners. The prosopon is densely granulate.

Material. 8 cranidia, 7 pygidia.

Remarks. This species was founded on a single pygidium. The Abrigo Formation provides cranidia for the first time, and they are typical for the genus. The pygidium resembles that of *C. explicatus* Resser, 1938a but differs in having straighter posterior margin and longer and narrower border spines. *Crepicephalus buttsi* Resser, 1938a displays posteriorly divergent spines but the posterior pygidial margin is convex outward. *Crepicephalus buttsi montanensis* Lochman in Lochman and Duncan, 1944 displays a shorter posterior margin.

Crepicephalus sp.

Pl. 11, figs. 9–11

Occurrence. Abrigo Formation, southeastern Arizona, *Coosella helena* Subzone. *Crepicephalus* Zone.

Material. 7 pygidia.

Remarks. The seven pygidia from the Abrigo Formation agree in general with a number of species of *Crepicephalus*, displaying pleural fields that are wider than the axis, moderately short posterior border, straight posterior margin, and narrow, moderately short posterolateral spines directed posteriorly. They resemble *C. rabbitkettlei* Pratt, 1992 in their straight posterior margin and moderately short posterolateral spines, directed posteriorly. However, they have a narrower pleural field that is slightly wider than the pygidial axis.

Crepicephalus n. sp.

Pl. 11, figs. 12–16

Diagnosis. *Crepicephalus* with short, and moderately wide pygidial axis bearing five axial rings; pleural field moderately wide, equal or slightly wider in width to pygidial axis, crossed by four pleural furrows. Posterior border moderately short; posterior margin curving anteriorly. Posterolateral spines short, directed posteriorly.

Holotype. A pygidium from the Abrigo Formation, southeastern Arizona (Pl. 11, fig. 16).

Occurrence. Abrigo Formation, southeastern Arizona, *Coosella helena* Subzone, *Crepicephalus* Zone.

Material. 7 pygidia.

Remarks. The pygidium of *Crepicephalus* n. sp. is characterised by anteriorly curving posterior margin, short spines and moderately wide pleural field. It differs from that of *C. australis* Palmer, 1954b by its narrower pygidium, shorter and wider pygidial axis and narrower pleural field. *Crepicephalus micans* (Resser, 1938a) and *C. nitida* (Resser, 1938a) have narrow and long axis, reaching posterior margin and very short posterior border. *Crepicephalus convergens* Rasetti, 1965a displays wider posterolateral spines located closer to the median line, whereas *C. discrepans* (Duncan *in* Lochman and Duncan, 1944) shows a shorter pygidial axis and a longer posterior border.

Crepicephalus cf. *C. iowensis* (Owen, 1852)

Pl. 11, fig. 17

1852 *Dikelocephalus*? *iowensis* Owen, p. 575, pl. 1, fig. 4, pl. 1A , fig. 13.

1916a *Crepicephalus iowensis*, Walcott, p. 207, pl. 29, figs. 1, 2, 2a–f (see for synonymy).

1944 *Crepicephalus iowensis*, Shimer and Shrock, pl. 262, figs. 7, 8.

1992 *Crepicephalus* cf. *C. iowensis*, Westrop, p. 236, figs. 12.3, 12.4, 12.9.

Holotype. A pygidium from the Eau Claire Formation, Minnesota (Owen 1852, pl. 1, fig. 4, pl. 1A, fig. 13).

Occurrence. Abrigo Formation, southeastern Arizona, *Coosella helena* Subzone, *Crepicephalus* Zone; Petit Jardin Formation, western Newfoundland; Eau Claire and Dresbach formations, Wisconsin and Minnesota.

Material. 1 pygidium.

Remarks. A single pygidium from the Abrigo Formation resembles that of *C. iowensis* (Owen, 1852) by its pair of divergent, thick posterolateral spines, mindful, however, of some debate about the original material on which this species was based (Pratt, 1992, p. 63).

Genus *Coosella* Lochman, 1936

Type species. *Coosella prolifica* Lochman, 1936, Bonneterre Dolomite, Missouri (by original designation).

Remarks. Westrop (1992, p. 239) reviewed the differences between *Coosella*, *Coosia* and *Coosina* which include rather similar species.

Coosella helena Lochman, 1938b

Pl. 13, figs. 11–19

1938b *Coosella helena* Lochman, p. 468, pl. 57, figs. 10–15.

1992 *Coosella helena,* Westrop, p. 239, figs. 13.1–13.7 (see for synonymy).

Holotype. A cranidium from the Petit Jardin Formation, western Newfoundland (Lochman, 1938, pl. 57, figs. 10, 15).

Occurrence. Abrigo Formation, southeastern Arizona, *Coosella helena* Subzone, *Crepicephalus* Zone; Petit Jardin Formation, western Newfoundland.

Material. 39 cranidia, 24 pygidia, 1 hypostome.

Diagnosis. Coosella with wide, subconical glabella, short preglabellar area with well-defined but short anterior border furrow. Convex, moderately long anterior border bearing terrace lines. Broad pygidium with shallow median indentation. Pygidial axis with four axial rings and the terminal piece.

Remarks. *Coosella beltensis* Lochman (*in* Lochman and Duncan 1944), *C. widnerensis* (Resser, 1938a) and *C. texana* Resser, 1942b possess a longer preglabellar field and anterior border furrow. *Coosella prolifica* Lochman, 1938 and *C. andreas* (Walcott, 1916b) possess deeper median indentation on the posterior margin of the pygidium.

Coosella andreas (Walcott, 1916b)

Pl. 12, figs. 1–11

1916b *Blountia andreas* Walcott, p. 398, pl. 64, fig. 2, 2'.

1938 *Coosella andreas*, Resser, p. 70, pl. 13, fig. 11.

1965 *Coosella andreas*, Rasetti, p. 48, pl. 1, figs. 1–4.

Holotype. A cranidium from the Maryville Formation, Tennessee (Walcott, 1916b, p. 398, pl. 64, figs. 2, 2').

Occurrence. Abrigo Formation, southeastern Arizona, *Cedaria eurycheilos* Subzone, *Cedaria* Zone; Maryville and Nolichucky formations, Tennessee, *Cedaria* Zone.

Material. 23 cranidia, 22 pygidia.

Remarks. The cranidium of *C. andreas* is characterized by its short preglabellar field, short and well-defined anterior border furrow, and relatively long, convex anterior border. The pygidium possesses a short axis bearing two axial rings and terminal piece. The pleural field is convex. The deep median indentation and convexity of the pygidium makes this species distinguishable from other species of *Coosella*.

Genus *Coosia* Walcott, 1911

Type species. *Coosia superba* Walcott, 1911, Conasauga Formation, Alabama (by original designation).

Remarks. This genus is characterized by a long, flat anterior cranidial border separated from shorter preglabelar field by shallow anterior border furrow, and a pygidium with a broad concave border and relatively narrow pleural field.

Coosia n. sp.

Pl. 13, figs. 1–10

Diagnosis. *Coosia* with elongate cranidium; narrow, nearly parallel-sided, anteriorly rounded, convex glabella; fixed cheeks narrow, anterior border long, narrow and flat.

Holotype. A cranidium from the Abrigo Formation, southeastern Arizona (pl. 13, fig. 1).

Occurrence. Abrigo Formation, southeastern Arizona, *Cedaria eurycheilos* Subzone, *Cedaria* Zone.

Description. Cranidium is elongate and narrow. Nearly parallel-sided glabella is convex and rounded anteriorly. Lateral glabellar furrows are absent. Anterior border is long and one and a half to twice as long as the preglabellar field, and separated from it by a short, shallow anterior border furrow. Anterior facial suture is slightly divergent. Fixed cheeks are narrow with small palpebral lobes that are strongly arcuate and located opposite to the glabellar midlength. Occipital ring furrow is shallow and relatively short. Posterolateral fixed cheek is narrow. Pygidium is semi-circular in outline. Narrow pygidial axis bears five axial rings and a terminal piece. The pleural field is narrow and crossed by four pleural furrows. Border is wide, smooth and concave.

Material. 19 cranidia, 6 pygidia.

Remarks. The characteristic features that distinguish *Coosia* n. sp. from other species is the long cranidium with a long and narrow, nearly parallel-sided glabella, less divergent anterior facial suture, and long and narrow anterior field and anterior border. The pygidium with its longer and narrower axis possesses more axial rings.

Genus *Coosina* Rasetti, 1956

Type species. *Maryvillia ariston* Walcott, 1916b, Maryville Formation, Tennessee (by original designation).

Remarks. The concept outlined by Westrop (1992, p. 239) is followed here. This genus includes the species with effaced cranidia whose glabellae barely rise above the fixed cheeks. Unlike *Coosia* and *Cossella*, the pygidial border is narrow. Seven valid species appear to be: *C. ariston* (Walcott, 1916b), *C. amage* (Walcott, 1916b), *C. wyomingensis* (Resser, 1937), *C. utahensis* (Resser, 1942b), *C. violaensis* (Resser, 1942b), *C. marjumensis* (Resser, 1942), *C. kindlei* (Westrop, 1992).

Coosina ariston (Walcott, 1916b)

Pl. 12, figs. 1–11

1916b *Maryvillia ariston* Walcott, p. 401, pl. 64, fig. 5.

1954a *Maryvillia cf. M. ariston*, Palmer, p. 723, pl. 79, figs. 6–9.

1956 *Coosina ariston,* Rasetti, p. 1268 (see for synonymy).

1960 *Coosina ariston*, Robison, p. 19, pl. 2, figs. 13–16.

1960 *Coosina ariston*, Lochman and Hu, p. 816, pl. 97, figs. 15–20.

1961 *Coosina ariston*, Rasetti, p. 111, pl. 21, figs. 12–13.

1965a *Coosina ariston*, Rasetti, p. 51, pl. 7, fig. 27.

2000 *Coosina ariston*, Stitt and Perfetta, p. 208, fig. 8.1–8.3.

Diagnosis. Glabella anteriorly tapering and truncated. Lateral glabellar furrows absent or present as faint four pairs of depressions. Moderately long, slightly convex anterior border. Long, occipital furrow, gently anteriorly curved sagitally.

Holotype. A cranidium from Maryville Formation, Tennessee (Walcott, 1916b, pl. 64, fig. 5, 5').

Occurrence. Abrigo Formation, southeastern Arizona, *Coosella helena* Subzone, *Crepicephalus* Zone; Riley Formation, central Texas, *Crepicephalus* and *Maryvilla* zones; Nolichucky and Maryville formations, Tennessee and Virginia, *Crepicephalus* Zone; Pilgrim Formation, Montana, *Crepicephalus* Zone; Deadwood Formation, South Dakota, *Crepicephalus* Zone.

Material. 37 cranidium, 8 pygidia.

Remarks. The complicated history of this species is explained by Rasetti (1956). It is characterized by low cranidial convexity, long and shallow anterior border furrow, narrow and shallow axial furrows, and a semi-circular pygidium. *Coosina amage* (Walcott, 1916b) differs from *C. ariston* in the shape of the glabella, which is rounded antriorly rather than truncated, deeper axial furrows and shorter anterior boarder furrow.

Family ASAPHISCIDAE Raymond, 1924

Subfamily KINGSTONIINAE Kobayashi, 1933

Remarks. Inclusion here of *Brachyaspidion* Miller, 1936b expands the concept of this subfamily as previously summarized by Pratt (1992, p. 67). This genus shows a relationship with other genera included in this subfamily, expressed by a cranidium of similar outline and wide, convex pygidium.

Genus *Kingstonia* Walcott, 1924

Type species. *Kingstonia apion* Walcott, 1924, Maryville Formation, Tennessee (by original designation).

Remarks. This genus was discussed in detail by Pratt (1992, p. 67).

Kingstonia spicata Lochman, 1940

Pl. 13, figs. 23–25

1940 *Kingstonia spicata* Lochman, p. 34, pl. 4, figs. 1–9.

1956 *Kingstonia spicata*, Deland and Shaw, p. 556, pl. 63, fig. 17.

1962 *Kingstonia spicata*, Lochman and Hu, p. 15, pl. 4, figs. 1–11, 13–28.

1983 *Kingstonia spicata*, Hu, p. 227, fig. 2, pl. 1, figs. 14–33.

1998 *Kingstonia spicata*, Stitt, p. 1041, pl. 1, fig. 7.14– 7.16.

Diagnosis. *Kingstonia* with triangular pygidium terminating in a long, thick posterior spine; pygidial axis with eight or nine axial rings visible on exfoliated specimens.

Holotype. A cranidium from the Bonneterre Dolomite, Missouri (Lochman, 1940, pl. 4, figs. 2–4).

Occurrence. Abrigo Formation, southeastern Arizona, *Cedaria eurycheilos* Subzone, *Cedaria* Zone; Bonneterre Dolomite, Missouri, *Cedaria* Zone; Park Shale, Wyoming, *Cedaria* Zone; Deadwood Formation, South Dakota, *Cedarina dakotaensis* Zone.

Material. 6 pygidia.

Remarks. Holaspid pygidia from the Abrigo Formation differ from those described by Lochman (1940) by the presence of nine instead of eight axial rings. Late meraspid forms display narrow pleural fields that taper posteriorly and merge into the posterior spine. Holaspid forms show wider pleural fields, gently transforming posteriorly into the posterior spine. No cranidia or free cheeks were recovered.

Kingstonia scrinium (Raymond, 1937)

Pl. 13, figs. 20–22

1937 *Kingstonia scrinium* Raymond, p. 1113, pl. 3, fig. 6.

1952 *Kingstonia scrinium*, Shaw, p. 472, pl. 57, figs. 46–48.

1992 *Kingstonia scrinium*, Pratt, p. 68, pl. 25, figs. 12–20.

2000 *Kingstonia scrinium*, Stitt and Perfetta, p. 213, fig. 10.12.

Holotype. A pygidium from the Rockledge Conglomerate, northern Vermont (Raymond, 1937, pl. 3, fig. 6).

Occurrence. Abrigo Formation, southeastern Arizona, *Cedaria eurycheilos* Subzone, *Cedaria* Zone, and *Coosella helena* Subzone. *Crepicephalus* Zone; Rabbitkettle Formation, Mackenzie Mountains, *Cedaria brevifrons* Zone; Rockledge Conglomerate, Vermont; Deadwood Formation, South Dakota, *Crepicephalus* Zone.

Material. 5 pygidia.

Remarks. The pygidia from the Abrigo Formation are characterized by their long, subtriangular outline and eight to nine axial rings. Pygidia of *K. scrinium* are more elongated then those of *K. walcotti*. The pygidial axis of *K. scrinium* tapers posteriorly, whereas in *K. walcotti* it is more parallel-sided.

Kingstonia sp.

Pl. 13, fig. 26

Occurrence. Abrigo Formation, southeastern Arizona, *Cedaria eurycheilos* Subzone, *Cedaria* Zone.

Material. 1 pygidium.

Remarks. With its subtriangular outline this pygidium is similar to that of *K. walcotti*, but the axial furrows taper posteriorly rather than being nearly parallel.

Genus *Bynumia* Walcott, 1924

Type species. *Bynumia eumus* Walcott, 1924, Sullivan Formation, southern Alberta (by original designation).

Remarks. This genus of Kingstoniinae differs from *Kingstonia* by having a pointed anterior margin, lacking an anterior border, and having reduced convexity of the pygidium.

Bynumia eumus Walcott, 1924

Pl. 14, figs. 10–15

1924 *Bynumia eumus* Walcott, p. 54, pl. 14, fig. 3.

1992 *Bynumia* cf. *B. eumus*, Pratt, p. 68, pl. 25, fig. 21 (see for synonymy).

1998 *Bynumia eumus*, Stitt, p. 1041, pl. 7, figs. 18–21.

Diagnosis. *Bynumia* with triangular cranidium, sharply pointed cranidial margin; subrectangular glabella.

Lectotype. A cranidium from the Sullivan Formation, Alberta (Walcott, 1925, pl. 17, fig. 4; Resser, 1942b, pl. 9, figs. 5, 6; designated by Resser, 1942b).

Occurrence. Abrigo Formation, southeastern Arizona *Cedaria eurycheilos* Subzone, *Cedaria* Zone; Rabbitkettle Formation, Mackenzie Mountains, *Cedaria minor* Zone (?) and *Cedaria brevifrons* Zone; Sullivan Formation, southern British Columbia and Alberta; Pilgrim Formation, Montana, *Cedaria Zone*; DuNoir Limestone, Wyoming *Cedaria Zone*; Deadwood Formation, South Dakota, *Cedarina dakotensis* Zone.

Material. 2 cranidia, 7 pygidia.

Remarks. *Bynumia eumus* exhibits the distinctive triangular cranidium and pointed anterior margins that characterize this genus. Pratt (1992) observed some intraspecific variation and considered most previously described *Bynumia* species to be synonyms.

Genus *Brachyaspidion* Miller, 1936b

Type species. *Brachyaspis rynchina* Miller, 1936a, Gros Ventre Formation, Wyoming.

Diagnosis. Kingstoniinae with cranidium subtrapezoidal to semi-elliptical in outline. Subtrapezoidal glabella. Convex anterior border. Pygidium subtriangular to elliptical in outline

Remarks. The name *Brachyaspidion* Miller 1936a was created to substitute *Brachyaspis* Miller 1936b which was preoccupied. The genus has been previously known from cranidia only. The Abrigo Formation yielded a pygidium and a hypostome. The genus differs from *Kingstonia* in having a smaller glabella that is subtrapezoidal in outline rather than subquadrate to subrectangular, wide and often deeper anterior border furrow, long occipital furrow, fewer axial rings.

Brachyaspidion rynchina Miller, 1936b

Pl. 14, figs. 1–9

1936a *Brachyaspis rynchina* Miller, p. 28, pl. 8, fig. 7.

1936b *Brachyaspidion rynchina*, Miller, p. 417.

1964 *Brachyaspidion sulcatum* Robison, p. 545, pl. 86, figs. 4–6.

Diagnosis. *Brachyaspidion* with subtriangular pygidium moderately short and convex. Axis consists of four axial rings and a terminal axial piece. Lack of occipital spine.

Holotype. A cranidium from the Gros Ventre Formation, Wyoming illustrated by Miller (1936, pl. 8, fig. 7).

Occurrence. Abrigo Formation, southeastern Arizona, *Bolaspidella* Zone; Wheeler Formation, Utah, *Bathyuriscus fimbriatus* Subzone, *Bolaspidella* Zone; Gros Ventre Formation, Wyoming.

Description. Cranidium is subtriangular in outline, moderately arched transversely and convex. Subtrapezoidal glabella is rounded anteriorly. Preglabellar field is very short or absent. Anterior boarder furrow varies from well defined to shallow, and curved forward. Subtriangular pygidium is moderately short and convex, in length half that of width. Axis consists of four axial rings and a terminal axial piece. Axis furrows are anteriorly divergent. Pleural fields are crossed by two deeply impressed pleural furrows in the anterior portion and two shallow toward the posterior. Border is poorly defined. Anterior margins are arched posteriorly. Hypostome is round with solid anterior lobe. Posterior lobe is significantly smaller. Triangular anterior wings are fairly massive, tapering posteriorly.

Material. 10 cranidia, 1 pygidium, 1 hypostome.

Remarks. This species previously has been known from cranidia only. The hypostome differs from other known natant hypostomes of generalized morphology (Whittington, 1988a; Fortey,

1990) by having a prominent anterior lobe significantly exceeding the posterior one in size and big anterior wings. In addition, the anterior lobe is round in outline rather than oval as in most natant hypostomes.

Even among specimens coming from the same bed, material from the Abrigo Formation shows variation in the width of fixed cheeks, depth of anterior boarder furrow, and depth of the axial furrows. *Brachyaspidion sulcatum* Robison, 1964 was erected on the basis of slightly better defined axial furrows and deeper anterior boarder furrow in comparison to *B. rynchina*. However, variation in depth of the furrows may result from intraspecific variation as well as vagaries of preservation which are clearly noticeable in partially exfoliated specimens from the Abrigo Formation, suggesting that these are not valid criteria for specific differentiation. For that reason *B. sulcatum* Robison, 1964 is assigned here as synonymous with *B. rynchia*. *B. rynchina* differs from *B. spinosum* Rasetti, 1946 and *B. microps* Robison, 1971 by lacking an occipital spine. The pygidium is subtriangular in outline whereas in *B. microps* is elliptical. The pygidial axis is transversely wider than that of *B. microps*.

Family CHEILOCEPHALIDAE Shaw, 1956

Genus *Cheilocephalus* Berkey, 1898

Type species. Cheilocephalus saintcroixensis Berkey, 1898, St. Lawrence Formation, Minnesota (by original designation).

Cheilocephalus brachyops Palmer, 1965

Pl. 15, fig. 6

1965 *Cheilocephalus brachyops* Palmer, p. 30, pl. 1, figs. 12–15, 17.

2008 *Cheilocephalus* cf. *C. brachyops*, Westrop et al., p. 734, figs. 1a–1l, 2a–2i, 3a–3f (see for synonymy).

Holotype. A cranidium from the Johns Wash Limestone, Nevada (Palmer, 1965, pl. 1, fig. 12).

Occurrence. Abrigo Formation, southeastern Arizona, *Elvinia* Zone; Rabbitkettle and Broken Skull formations, *Parabolinoides calvilimbata* Fauna and upper Steptoean, respectively; Johns Wash Limestone, Nevada, *Prehousia* to *Elvinia* zones; Nolichucky Formation, Tennessee, upper *Aphelaspis* Zone; Collier Shale, Oklahoma, *Elvinia* Zone.

*Material.*1 cranidium.

Remarks. This species of *Cheilocephalus* differs from other species of this genus by lacking a preglabellar field, having a short anterior border furrow, a concave anterior border and a rectangular glabella. The cranidium is covered by small granules. *Cheilocephalus brachyops* resembles *C. wichitaensis*. However, *C. wichitaensis* possesses a subquadrate glabella.

Family LONCHOCEPHALIDAE Hupé, 1955

Genus *Glaphyraspis* Resser, 1937

Type species. *Liostracus parvus* Walcott, 1899, Gallatin Limestone, Wyoming (by original designation).

Remarks. The concept of the genus as outline by Palmer (1965b) and Pratt (1992) is followed here.

Glaphyraspis parva (Walcott, 1899)

Pl. 15, figs. 1–5

1899 *Liostracus parvus* Walcott, p. 463, pl. 65, fig. 6.

1992 *Glaphyraspis parva*, Pratt, p. 71, pl. 26, figs. 13–22 (see for synonymy).

2000 *Glaphyraspis parva*, Stitt and Perfetta, p. 218, fig. 12.21–12.25.

Holotype. A cranidium from Gallatin Limestone, Wyoming (Walcott, 1899, pl. 65, fig. 6).

Occurrence. Abrigo Formation, southeastern Arizona, *Coosella helena* Subzone, *Crepicephalus* Zone; Rabbitkettle Formation, *Glyptagnostus reticulatus* Zone, Mackenzie Mountains; widespread in North America, *Crepicephalus* and *Aphelaspis* zones.

Material. 5 cranidia.

Remarks. The expanded concept of this species as defined by Pratt (1992) is followed here. *Glaphyraspis parva* from the Abrigo Formation is characterized by a convex, subquadrate, anteriorly indented glabella bearing three pairs of deeply incised and one pair of shallow lateral glabellar furrows. The anterior border furrow is well incised defining a short, convex anterior border.

Family NORWOODIIDAE Walcott,1916

Genus *Hardyoides* Kobayashi, 1938

Type species. *Hardyoides minor* Kobayashi, 1938, McKay Group, British Columbia (by original designation).

Hardyoides cf. *H. tenerus* (Walcott, 1916a)

Pl. 15, figs. 7–9

1916a *Norwoodia tenera* Walcott, p. 172, pl. 28, figs. 2, 2a–g.

1992 *Hardyoides* cf. *H. tenerus*, Pratt, p. 76, pl. 28, figs. 22–29 (see for synonymy).

1998 *Hardyoides tenerus*, Stitt, p. 1039, figs. 7.11–7.13.

Lectotype. A complete exoskeleton from the Weeks Formation, Utah (Walcott, 1916a, pl. 28, fig. 2b; selected by Pratt, 1992).

Occurrence. Abrigo Formation, southeastern Arizona, *Cedaria eurycheilos* Subzone, *Cedaria* Zone; widespread in North America, upper Marjuman.

Material. 3 cranidia.

Remarks. Cranidia of *H, tenerus* from the Abrigo Formation agree well with the lectotype from Utah in the convex, elongate, subrectangular glabella, short, equally divided frontal area, wide free cheeks, and the palpebral lobes which are positioned slightly posteriorly from the anterolateral corners of the glabella. The occipital ring is not completely preserved in any of the specimens from the Abrigo Formation which makes it impossible to determine the presence of

the occipital spine. Nevertheless, as described by Pratt (1992) the occipital spine is so delicate that is very often broken during sampling. For this reason open nomenclature is appropriate.

Genus *Xenocheilos* Wilson, 1949

Type species. X*enocheilos minutum* Wilson, 1949 from the Wilberns Formation, central Texas (by original designation).

Remarks. The concept of this genus as outlined by Westrop (1986, p. 79) is followed here.

Xenocheilos cf. *X. spineum* Wilson, 1951

Pl. 16, figs. 15, 16

1951 *Xenocheilos spineum* Wilson, p. 649, pl. 95, figs. 15–17

1956 *Xenocheilos spineum*, Deland and Shaw, p. 560, pl. 65, figs. 4, 6, 13.

1975 *Xenocheilos spineum*, Kurtz, p. 1033, pl. 4, figs. 27–29.

1986 *Xenocheilos* cf. *spineum*, Westrop, p. 79, pl. 29, figs. 11–14.

Holotype. A cranidium from the Ore Hill Member of the Gatesburg Formation, Pennsylvania (Wilson, 1951, pl.95, figs. 15, 16).

Occurrence. Abrigo Formation, southeastern Arizona, *Elvinia* Zone; Ore Hill Member of the Gatesburg Formation, Pennsylvania, *Elvinia* Zone; Davis Formation, Missouri, *Elvinia* Zone;

Open Door Limestone, Wyoming, *Elvinia* Zone; Lyell and Bison Creek formations, southern Alberta, *Elvinia* Zone.

Material. 2 cranidia.

Remarks. *Xenocheilos* cf. *X. spineum* from Arizona resembles closely *X*. cf. *spineum* from Alberta (Westrop, 1986). Nevertheless, in comparison to the holotype of *X. spineum* (Wilson, 1951, pl. 95, figs. 15, 16) it possesses better defined axial furrows that become wider posteriorly, and they have a longer anterior border. *Xenocheilos minutum* Wilson, 1949 has an anteriorly tapering glabella. *Xenocheilos. granulosus* Palmer, 1965 and *X. orthos* Kurtz, 1975 has less convex fixed cheeks.

Family MENOMONIIDAE Walcott, 1916b

Remarks. The concept of this family as outlined by Robison (1964, p. 552) is followed here, although Pratt (1992) resurrected *Hysteropleura* as a valid genus which was sustained by Westrop and Ludvigsen (2000).

Genus *Bolaspidella* Resser, 1937

Type species. *Ptychoparia housensis* Walcott, 1886, Wheeler Formation, Utah (by original designation).

Remarks. The concept of this genus as established by Robison (1964) and Robison and Babcock (2011) is followed here.

Bolaspidella n. sp.

Pl. 16, figs. 1–12

Diagnosis. *Bolaspidella* with small, anteriorly tapering, truncated glabella. Convex occipital ring, longer on median line. Convex, nearly straight to gently arched anterior border longest on median line.

Holotype. A cranidium from the Abrigo Formation, southeastern Arizona (Pl. 16, figs.1, 2).

Occurrence. Abrigo Formation, southeastern Arizona, *Bolaspidella* Zone.

Description: Cranidium is subtrapezoidal in outline and moderately arched transversively and longitudially. Glabella is small but prominent, tapering forward and truncated anteriorly. It bears three pairs of narrow lateral glabellar furrows. Occipital ring is longer on median line and well-defined by narrow occipital furrow. Anterior border is convex, nearly straight and longer on median line. Fixed cheeks are broad and each bears gently arched posteriorly palpebral ridge. Palpebral ridges extend nearly out from anterolateral corners of glabella. Palpebral lobes are prominent and located opposite glabellar midlenght. Dorsal surface is covered with small tubercles. Pygidium is small. Axial lobe is well defined and slightly tapered posteriorly. It nearly reaches posterior margin and bears four axial ring furrows. Gently convex pleural field is crossed by three pleural furrows. Meraspid cranidium is subtrapezoidal in outline. Glabella slightly taper interiorly but not as much as in holaspid forms. Glabellar axial furrows meet anterior border furrow so there is no preglabellar field present. Dorsal surface is covered with tubercles.

Material. 12 cranidia, 2 pygidia.

Remarks. *Bolaspidella* n. sp. differs from other species of the genus in its tapering, anteriorly truncated glabella and nearly transeverse anterior border. It lacks an occipital spine. *Bolaspidella drumensis* Robison, 1964 and *B. macgerriglei* (Raymond, 1937) exhibit a subrectangular glabella and an occipital spine. *Bolaspidella lucieae* Polusen, 1927 posses a small occipital node. *Bolaspidella* n. sp. differs from *B. contracta* Robison, 1964 in having a longer preglabellar field, and from *B. burnetensis* (Walcott, 1890)*, B. prooculis* Palmer, 1954b and *B. wellsvillensis* (Lochman and Denson *in* Lochman and Duncan, 1944) in having wider fixed cheeks and a straight and shorter anterior border.

Bolaspidella sp.

Pl. 16, figs. 13–14

Occurrence. Abrigo Formation, southeastern Arizona, *Bolaspidella* Zone.

Material. 3 cranidia.

Remarks. Cranidia assigned to *Bolaspidella* without a species designation are subtrapezoidal in outline and possess a subrectangular glabella and prominent palpebral lobes located slightly anterior to glabellar mid-length. These cranidia agree with *Bolaspidella* except in their more arched anterior border furrow and narrower fixed cheeks.

Family BOLASPIDIDAE Howell *in* Moore, 1959

Remarks. This family proposed by Howell *in* Moore (1959) is distinguished by the presence of an inflated area or boss in the preglabellar field, along with a tapering, subtriangular glabella. This taxon contains *Bolaspis* Resser, 1935; *Acrocephalops* Poulsen, 1927; *Rawlinsella* Shaw, 1956; and *Eldoradia* Resser, 1935

Genus *Eldoradia* Resser, 1935

Type species. *Ptychoparia*? *linnarssoni* Walcott, 1884 (by original designation).

Remarks. The concept of this genus as defined by Palmer (1954a, p. 76) is followed here. Two valid species appear to be *E. linnarssoni* (Walcott, 1884) and *E. prospectensis* (Walcott, 1884). *Eldoradia dunbari* Lochman, 1938b was excluded by Palmer (1954a) on the basis of a lack of a preglabellar median boss and short frontal area. *Eldoradia lata* Resser, 1935 had been synonymized with *E. linnarssoni* by Palmer (1954a).

Eldoradia linnarssoni (Walcott, 1884)

Pl. 17, figs. 8–13

1884 *Ptychoparia*? *linnarssoni* Walcott, p. 47, pl. 9, figs. 18, 18a.

1916a *Alokistocare linnarssoni*, Walcott, p. 185, pl. 25, figs. 7, 7a.

1935 *Eldoradia linnarssoni*, Resser, p. 27.

1935 *Eldordia lata* Resser, p. 27

1954a *Eldoradia linnarssoni*, Palmer, p. 77, pl. 16 figs. 9, 10.

Diagnosis. Eldoradia with small, conical, anteriorly truncated glabella and broad and strongly convex fixed cheeks and strongly convex oval boss. Lack of anterior border.

Holotype. A cranidium from the Secret Canyon Shale, Nevada (Walcott, 1884, pl. 9, figs. 18, 18a).

Occurence. Abrigo Formation, southeastern Arizona, *Cedaria* Zone; Secret Canyon shale, Eureka district, Nevada.

Material. 11 cranidia, 1 free cheek.

Remarks. This species is defined by a small, conical, anteriorly truncated glabella bearing three pairs of faint, lateral glabellar furrows, and broad and strongly convex fixed cheeks. Preglabellar area with strongly convex oval boss separated from the glabella, prominent palpebral lobes extend transversally from the anterolateral corners of the glabella. This species from the Abrigo Formation differs from *E. prospectensis* by lacking an anterior border, and having strongly convex fixed cheeks well elevated above the smaller, conical glabella.

Eldoradia prospectensis (Walcott, 1884)

Pl. 17, figs. 1–7

1884 *Ptychoparia*? *prospectensis* Walcott, p. 46, pl. 9, fig. 20.

1916a *Alokistocare prospectense*, Walcott, p. 186, pl. 25, fig. 8.

1954a *Eldoradia prospectensis*, Palmer, p. 77, pl. 16, fig. 8.

Diagnosis. *Eldoradia* with broad fixed cheeks of elevation equal to that of the glabella, and small boss in the preglabellar field, and short anterior border furrow.

Holotype. A cranidium from the Prospect Mountain Formation, Nevada (Walcott, 1884, pl. 9, fig. 20).

Occurence. Abrigo Formation, southeastern Arizona, *Cedaria* Zone; Prospect Mountain Formation and Secret Canyon Shale, middle Cambrian, Nevada.

Materials. 20 cranidia.

Remarks. This species possesses a subconical, truncated glabella, three faint lateral glabellar furrows, broad fixed cheeks of elevation equal to that of the glabella, a small swelling or boss in the preglabellar field adjacent to or slightly separated from the glabella, short anterior border furrow. It differs from *E. linnarssoni* by the presence of anterior border and a subconical glabella.

Family CEDARIIDAE Raymond, 1937

Genus *Cedaria* Walcott, 1924

Type species. Cedaria prolifica Walcott, 1924, Conasauga Formation, Alabama (by original designation).

Remarks. The concept of this genus as outlined by Palmer (1962, p. F–24) and Pratt (1992, p. 79) is followed here.

Cedaria eurycheilos Palmer, 1954b

Pl. 18, figs. 1–14

1954b *Cedaria eurycheilos,* Palmer, p.726, pl. 80, figs. 5–7.

Diagnosis. Cedaria with anteriorly rounded, subrectangular glabella, wide, flat anterior border and well-impressed anterior border furrow. Prosopon finely granulated. Pygidium semicircular with very wide border.

Holotype. A cranidium from Riley Formation, centralTexas, (Palmer, 1954b, pl. 80, fig. 7).

Occurrence. Abrigo Formation, southeastern Arizona, *Cedaria eurycheilos* Subzone, *Cedaria* Zone; Riley Formation, central Texas, *Cedarina–Cedaria* Zone.

Material. 22 cranidia, 16 pygidia.

Remarks. Cedaria eurycheilos is distinguished from other species of *Cedaria* by its long anterior border and long posterior pygidial border. The facial suture is less divergent than in most *Cedaria* species, and so is the lack of pits in the anterior border furrow and the finely granulated prosopon.

Cedaria? sp.

Pl. 19, figs. 14, 17, 18

Occurrence. Abrigo Formation, southeastern Arizona, *Cedaria eurycheilos* Subzone, *Cedaria* Zone.

Remarks. Pygidia from the Abrigo Formation, assigned questionably to *Cedaria*, possess a semicircular pygidium with axis bearing 5 to 6 axial rings and a terminal piece which reaches the posterior border furrow. Broad pleural fields are nearly effaced. These pygidia agree with *Cedaria* and resemble *C. major* because of the wide border. However the specimens from the Abrigo Formation show a posteriorly rounded terminal piece and a better defined border furrow than that present in other species of the genus.

Genus *Cedarina* Lochman, 1940a

Type species. *Cedarina vale* Lochman, 1940a, Bonneterre Dolomite, Missouri (by original designation).

Remarks. The concept of this genus outlined by Adrain et al., 2009 is followed here.

Cedarina cf. *C. obtusans* Duncan *in* Lochman and Duncan, 1944

Pl. 19, fig. 13

1944 *Cedarina obtusans* Duncan *in* Lochamn and Duncan, p. 91, pl. 16, figs. 30–37.

Holotype. A cranidium from the Pilgrim Formation, Montana, *Cedaria* Zone (Duncan *in* Lochman and Duncan, 1944, pl. 16, fig. 34).

Material. 1 cranidium

Occurrence. Abrigo Formation, southeastern Arizona, *Cedaria* Zone, *Cedaria eurycheilos* Subzone; Pilgrim Formation, Montana, *Cedaria* Zone.

Remarks. An incomplete cranidium from the Abrigo Formation displays a very long, subtriangular anterior border, well-impressed, short anterior margin furrow, and an anteriorly rounded glabella.

Cedarina? sp.

Pl. 19, figs. 15, 16

Occurrence. Abrigo Formation, southeastern Arizona, *Cedaria eurycheilos* Subzone, *Cedaria* Zone.

Material. 2 pygidia.

Remarks. Pygidia from the Abrigo Formation, assigned questionably to *Cedarina*, possess a transverse pygidium with a prominent axis bearing 5 axial rings and a terminal piece. The axis reaches the border furrow. The pleural field is gently convex as in other species of *Cedarina*, and the wide, flat border narrows slightly where it reaches the axis.

Subfamily RAYMONDININAE Clark, 1924

Genus *Paracedaria* Duncan *in* Lochman and Duncan, 1944

Type species. Pilgrimia montanensis Duncan *in* Lochman and Duncan, 1944, Pilgrim Formation, Montana (by original designation).

Diagnosis. Cranidium subtrigonal to subrectangular rounded anteriorly. Anterior border triangular or rounded. Well-impressed anterior border furrow slightly curved or curved backward on axial line forming median inbend. It can bear a row of small pits. Transverse pygidium with well-impressed pleural furrows.

Remarks. Valid species appear to be *P. montanensis* (Duncan *in* Lochman and Duncan, 1944); *P. tarda* Lochman and Hu, 1962; *P. viriosa* Lochman and Hu, 1962; and P. n. sp. *Paracedaria* differs from *Cedaria* Walcott, 1924 by its narrow frontal area, less divergent anterior facial suture, and its transverse pygidium with well-impressed pleural furrows.

Paracedaria viriosa Lochman and Hu, 1962

Pl. 19, figs. 1–8

1962 *Paracedaria viriosa* Lochman and Hu, p. 26, pl. 1 figs. 14–58.

Diagnosis. *Paracedaria* with subrectangular, rounded anteriorly glabella. Anterior border furrow curved backward on axial line forming median inbend, bearing a row of small pits. Anterior border triangular.

Holotype. A cranidium from the DuNoir Limestone, Wyoming, *Cedaria* Zone (Lochman and Hu, 1962, pl. 1, figs. 55, 58).

Occurrence. Abrigo Formation, southeastern Arizona, *Cedaria eurycheilos* Subzone, *Cedaria* Zone; DuNoir Limestone, Wyoming, *Cedaria* Zone.

Material. 11 cranidia, 4 pygidia.

Description. Glabella is subrectangular, rounded anteriorly. It bears three glabellar furrows. Preglabellar field is narrow to moderate. Well-impressed anterior border furrow curved backward on axial line forming median inbend, bearing a row of small pits. Anterior border is triangular. Palpebral lobes are strongly arcuate, located anteriorly of glabellar midlength. Dorsal surface is covered with small tubercles. Transverse pygidium has well-impressed four pleural furrows. Axial lobe is strongly convex with four axial rings and terminal piece. Pleural furrows are bend backwards.

Remarks. *Paracedaria viriosa* Lochman and Hu, 1962 differs from *P. montanensis* (Duncan *in* Lochman and Duncan, 1944) and *P*. n. sp. in its subrectangular, anteriorly rounded glabella and triangular anterior border. *P. tarda* Lochman and Hu, 1962 shows long and deep anterior border furrow.

Paracedaria n. sp.

Pl. 19, figs. 9–12

Diagnosis. A species of *Paracedaria* with strongly convex subconical glabella, lacking glabellar furrows, wide occipital ring reaching half of the glabella length, narrow preglabellar field. Anterior border gently rounded.

Holotype. A cranidium from the Abrigo Formation, southeastern Arizona (Pl. 19, fig. 11).

Occurrence. Abrigo Formation, southeastern Arizona, *Cedaria eurycheilos* Subzone, *Cedaria* Zone.

Material. 3 cranidia.

Remarks. Paracedaria n. sp. differs from *P. viriosa* Lochman and Hu, 1962 in its subconical glabella lacking glabellar furrows, well-impressed but short anterior border furrow, lack of pits on the anterior border furrow, gently arched anterior border. Very wide occipital ring and wider lateral border furrow, smooth dorsal surface. *Paracedaria tarda* Lochman and Hu, 1962 displays a well-impressed and wide anterior border furrow, subrectangular glabella and wider fixed cheeks. *Paracedaria montanensis* (Duncan *in* Lochman and Duncan, 1944) exhibits a conical glabella, wider preglabellar field and anterior border furrow, long and wide posterolateral fixed cheek, and the prosopon is finely tuberculate.

Family LLANOASPIDIDAE Lochman *in* Lochman and Duncan, 1944

Remarks. The concept of this family and subfamily as outlined by Pratt (1992, p. 83) is followed here.

Subfamily LLANOASPIDINAE Lochman *in* Lochman and Duncan, 1944

Genus *Llanoaspis* Lochman, 1938a

Type species. *Llanoaspis modesta* Lochman, 1938a, Riley Formation, central Texas (by original designation).

Remarks. The *Llanoaspis* species differ from one another in convexity and width of the anterior border, trace of the anterior border furrow, degree of inflation of the glabella, shape of the pygidium, and length of flanges on the pygidial border. Seven valid species appear to be *L. peculiaris* (Resser, 1938a), *L. virginica* (Resser, 1938a), *L. clinchensis* (Resser, 1938a), *L. modesta* Lochman, 1938a, *L. undulata* Lochman, 1938a, *L. dorothea* Lochman *in* Lochman and Duncan, 1944, and *L. convexifrons* Rasetti, 1961. Five species including one new species are present in the Abrigo Formation.

Llanoaspis modesta Lochman, 1938a

Pl. 20, figs. 1, 2

1938a *Llanoaspis modesta* Lochman, p. 81, pl. 17, figs. 9–14.
1992 *Llanoaspis modesta*, Pratt, p. 83, pl. 32, figs. 9–11 (see for synonymy).

Diagnosis. *Llanoaspis* with anterior border furrow transverse, tangent to anterior end of subrectangular to rounded anteriorly glabella. Anterior border gently concave. Anterior margin pointed.

Holotype. A cranidium from the Riley Formation, central Texas (Lochman, 1938a, pl. 17, figs. 10, 14).

Occurrence. Abrigo Formation, southeastern Arizona, *Coosella helena* Subzone, *Crepicephalus* Zone; Rabbitkettle Formation, Mackenzie Mountains, *Cedaria prolifica* Zone; Riley Formation, central Texas, *Crepicephalus* and *Coosella* zones (Palmer,1954b); Nolichucky Formation, Tennessee and Virginia, *Crepicephalus* Zone; possibly Orr Formation, Utah, *Crepicephalus* Zone.

Material. 2 cranidia,

Remarks. These cranidia resemble those assigned to *L. modesta* by Pratt (1992, p. 83). Similarly, they exhibit gently concave anterior border which confirms that this species is not characterized by a convex anterior border as held by Lochman (1938a, p. 81) and Palmer (1954b, p. 737).

Llanoaspis undulata Lochman, 1938a

Pl. 20, figs. 3–6

1938a *Llanoaspis undulata* Lochman, p. 81, pl. 17, figs. 24–26.

1938a *Genevievella rogersvillensis* Resser, p 78, pl. 15, figs. 16–18.

1944 *Llanoaspis montanensis* Lochman, p. 67, pl. 7, figs. 14, 15.

1954b *Llanoaspis undulata*, Palmer, p. 738, pl. 82, figs. 6, 7.

2000 *Llanoaspis undulata*, Stitt and Perfetta, p. 217, pl. 7, fig. 8.

Diagnosis. *Llanoaspis* with gently convex, subrectangular glabella. Anterior border furrow transverse, tangent to anterior end of glabella. Pygidium expanded posterolaterally outward.

Holotype. A cranidium from the Riley Formation, central Texas (Lochman, 1938a, pl. 17, fig. 24).

Occurrence. Abrigo Formation, southeastern Arizona, *Coosella helena* Subzone, *Crepicephalus* Zone; Riley Formation, central Texas, *Crepicephalus* and *Maryvilla* zones (Palmer, 1954b); Nolichucky Formation, Tennessee and Virginia, *Crepicephalus* Zone; Pilgrim Formation, Montana, *Crepicephalus* Zone; Deadwood Formation, South Dakota, *Crepicephalus* Zone.

Material. 2 cranidia, 4 pygidia.

Remarks. Cranidia of *L. undulata* are very similar to those belonging to *L. modesta*. However, they exhibit rounded anterior margins whereas in *L. modesta* they tend to be slightly pointed. Significant differences are in the shape of pygidia which are more transverse and have smaller marginal flanges.

Llanoaspis peculiaris (Resser, 1938a)

Pl. 20, fig. 15

1938a *Genevievella peculiaris* Resser, p. 78, pl. 15, figs. 6, 7.
1954b *Llanoaspis peculiaris*, Palmer, p. 737, pl. 82, fig. 5.

Diagnosis. *Llanoaspis* with subquadrate, rounded anteriorly, inflated glabella. Anterior border furrow transverse, tangent to anterior end of glabella. Anterior border convex.

Holotype. A cranidium from the Nolichucky Formation, Tennessee and Virginia (Resser, 1938a, pl. 15, figs. 6).

Occurrence. Abrigo Formation, southeastern Arizona, *Cedaria eurycheilos* Subzone, *Cedaria* Zone; Riley Formation, Texas, *Coosella* Zone; Nolichucky Formation, Tennessee and Virginia, *Crepicephalus* Zone.

Material. 1 cranidium.

Remarks. *Llanoaspis peculiaris* differs from other species of the genus in its inflated, subquadrate glabella. It resembles *L. convexifrons*, except it displays a straight anterior border furrow whereas that of *L. convexifrons* curves backwards to the anterior margin of the glabella, and glabella itself is more inflated.

Llanoaspis cf. *L. convexifrons* Rasetti, 1961

Pl. 20, fig. 14

1961 *Llanoaspis convexifrons* Rasetti, p. 115, pl. 22 figs. 1–6.

Holotype. A cranidium from the Conococheague Formation, Virginia (Rasetti, 1961, pl. 22, fig. 3).

Occurrence. Abrigo Formation, southeastern Arizona, *Cedaria eurycheilos* Subzone, *Cedaria* Zone; Conococheague Formation, Virginia.

Material. 1 pygidium.

Remarks. The pygidium from the Abrigo Formation agrees with *L. convexifrons* in its subtriangular outline, well-defined, slightly tapering axis extending almost to the posterior margin, and five pairs of pleural furrows curving abruptly backward towards the posterior

margin. The dorsal surface is similarly covered with scattered tubercles. One exception is in the number of axial rings: the pygidium from the Abrigo Formation bears six axial rings and terminal piece, whereas the pygidia described by Rasseti (1961) display seven to eight axial rings. For that reason, as well as the limited number of specimens, open nomenclature is used.

Llanoaspis n. sp.

Pl. 20, figs. 7–9

Diagnosis. A species of *Llanoaspis* with tapering forward, rounded anteriorly, inflated glabella. Anterior border furrow curved back to the sides of anterior margin of glabella. Rounded anterior margin.

Holotype. A cranidium from the Abrigo Formation, Ajax Hill, Arizona, (Pl. 20, fig. 7).

Occurrence. Abrigo Formation, southeastern Arizona, *Coosella helena* Subzone, *Crepicephalus* Zone.

Description. Cranidium subquadrate in outline. Glabella is tapering forward, rounded anteriorly and inflated. Anterior border furrow gently curves back to the sides of anterior margin of glabella. Anterior margin is rounded. Anterior border is wide and concave. Pygidium expanded posterolaterlally downward into small posterolateral flanges. Strongly convex axis tapers to posterior border. It displays nine axial rings and terminal piece.

Material. 1 cranidium, 1 pygidium.

Remarks. The cranidium of *Llanoaspis* n. sp. is distinguished from other species of *Llanoaspis* by the inflated, anteriorly tapering and anteriorly rounded glabella, and wider anterior border. Similar to *L. virginica* and *L. clinchensis* the anterior border furrow curves backwards to the anterior margin of the glabella. However in *L.* n. sp. it curves to the anterolaeral corners of glabella instead of the center of the anterior margin of the glabella. The pygidium is similar to that of *L. modesta* but possesses smaller flanges on the border.

Family PHYLACTERIDAE Ludvigsen and Westrop *in* Ludvigsen et al., 1989

Genus *Cliffia* Wilson, 1951

Type species. *Acrocephalites lataegenae* Wilson, 1949, Wilberns Formation, central Texas (by original designation).

Cliffia lataegenae (Wilson, 1949)

Pl. 20, figs. 10–13

1949 *Acrocephalites lataegenae* Wilson, p. 31, pl. 10, fig. 14.

1951 *Cliffia lataegenae*, Kurtz, p. 1036, pl.4, figs. 14, 15 (see for synonymy).

1992 *Cliffia lataegenae*, Pratt, p. 88, p. 26, figs. 32, 33 (see for synonymy).

Holotype. A cranidium from Wilberns Formation, central Texas (Wilson, 1949, pl. 10, fig. 14).

Occurrence. Abrigo Formation, southeastern Arizona, *Elvinia* Zone; Rabbitkettle Formation, *Proceratopyge rectidpinata* Zone, Mackenzie Mountains; widespread in North America, *Elvinia* Zone.

Material. 2 cranidia, 1 pygidium.

Remarks. *Cliffia lataegenae* is characterized by a triangular to subtriangular, glabella with two pairs of deeply impressed lateral glabellar furrows, a long preglabellar field, and a subtriangular pygidium. *Cliffia wilsoni* Lochman, 1964 differs in having narrower anterior border, and a pygidium with a shorter pygidial axis with fewer axial rings. The cranidium of *C. magnacilis* Hohensee *in* Hohensee and Stitt, 1989 has a more quadrate glabella, longer preglabellar field and anterior border, loger palpebral lobes, and a pygidium with wider, nearly parallel-sided axis and straighter pleural furrows.

Family UNCERTAIN

Genus *Arapahoia* Miller, 1936

Type species. *Arapahoia typa* Miller 1936, Depass Formation, Wyoming (by original designation).

Remarks. Westrop (1992) described the relation of this genus to Plethopeltidae. *Arapahoia* species differ from one another in the length and width of the frontal area, and the length of the pygidium. *Arapahoia raymondi* Lochman, 1938b*, A. stantoni* Resser 1942b*,* and *A. reesidei* Resser, 1942b are regarded here as synonyms of *Arapahoia butleri* (Stoyanow, 1936).

Arapahoia butleri (Stoyanow, 1936)

Pl. 21, figs. 1–16

1936 *Hesperaspis butleri* Stoyanow, p. 469, pl. 1, figs. 8.

1938b *Arapahoia raymondi* Lochman, p. 466, pl. 57, figs. 17–26.

1942b *Arapahoia stantoni* Resser, p. 44, pl. 7, figs. 2–4.

1942b *Arapahoia reesidei* Resser, p. 44, pl. 7, figs. 5–9.

1965 *Arapahoia* sp., Kindle and Whittington, pl. 1, figs. 3, 4, 16.

1992 *Arapahoia raymondi,* Westrop, p. 251, fig. 17.3–17.11.

Diagnosis. A species of *Arapahoia* with short anterior border and longer preglabellar field. Occipital ring with short occipital spine. Pygidium with three or two axial rings and terminal piece.

Holotype. A cranidium from the Abrigo Formation, southeastern Arizona (Stoyanow, 1936, pl.1, figs. 8)

Occurrence. Abrigo Formation, southeastern Arizona, *Cedaria eurycheilos* Subzone, *Cedaria* Zone; Big Cove Member, Petit Jardin Formation, Newfoundland, *Cedaria* Zone.

Material. 23 cranidia, 10 pygidia, 5 free cheeks.

Remarks. *Arapahoia raymondi* Lochman, 1938b is considered here as synonymous with *A. butleri*. Even though Lochman (1938b) noted the similarities between *A. raymondi* and *A. butleri* named *A. raymondi* without any discussion that would explain any possible differences between those two species. Westrop (1992) distinguished those species on the basis of the number of axial

rings with *A. raymondi* exhibiting one axial ring and a terminal piece. The pygidia of *A. raymondi* presented by Lochman, 1938b possess two axial rings and a terminal piece. However the significant collection from the Abrigo Formation provided material that demonstrate intraspecific variation in the number of axial rings and the transition from pygidia with one axial ring to those with two. The variation applies also to the border furrow in free cheeks. In some specimens the border furrow is faint in the other is not present. There is also difference in the length of the preglabellar field. *Arapahoia stantoni* Resser, 1942b and *Arapahoia reesidei* Resser, 1942b show no obvious differences and they are placed in synonymy with *A. butleri*.

3.8. PLATES

Plate 1

Figs. 1–15. *Kormagnostus seclusus* (Walcott, 1884).

1. Pygidium (T), dorsal view, x9.5

2. Pygidium (T), dorsal view, x10

3, 4. Pygidium (T), dorsal and lateral views, x10

5. Pygidium (T/E), dorsal view, x9

6. Pygidium (T), dorsal view, x9

7. Pygidium (T), dorsal view, x10.5

8. Pygidium (T), dorsal view, x9

9. Cephalon (T), dorsal view, x10

10. Cephalon (T/E) , dorsal view, x10

11. Cephalon (T), dorsal view, x9

12, 13. Cephalon (T), dorsal and lateral views, x10

14. Cephalon (T), dorsal view, x9

15. Cephalon (T), dorsal view, x9.5

Figs. 16. *Pseudoagnostus* cf. *P. communis,* Hall and Whitfield, 1877.

16. Pygidium (T/E), dorsal view, x10.5

Figs. 17. *Homagnostus* sp.

17. Cephalon (T/E), dorsal view, x9

Figs. 18–22. *Blairella* cf. *B. crassimarginata*, Rasetti, 1965b.

18, 19. Cranidium (T), dorsal and lateral views, x3

20, 21. Cranidium (T), dorsal and lateral views, x3

21. Cranidium (T), dorsal view, x2.5

22. Cranidium (L), dorsal view, x2.5

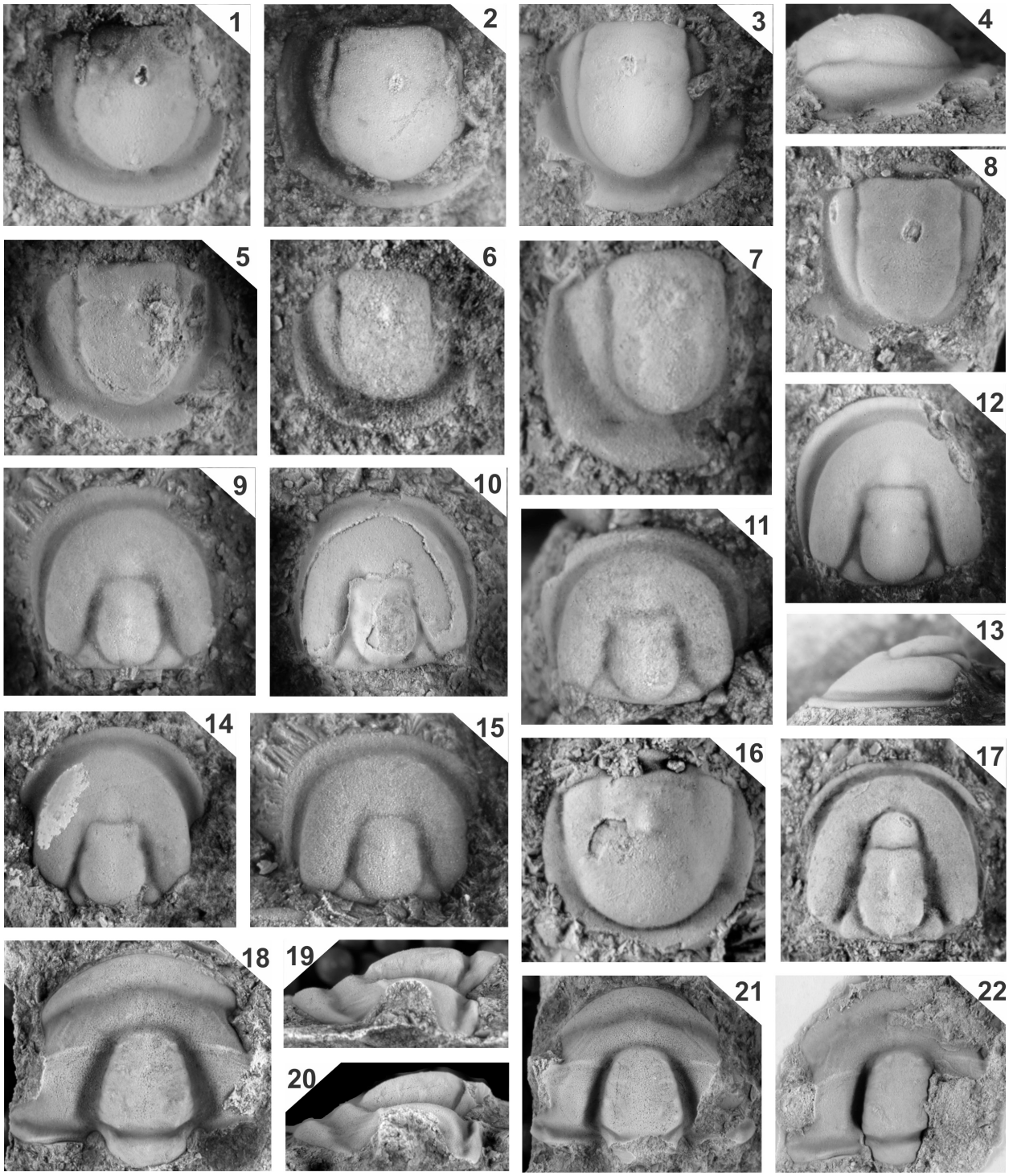

Plate 2

Figs. 1–5. *Ehmaniella* sp.

1, 2. Cranidium (E), dorsal and lateral views, x3

3. Cranidium (T), dorsal view, x 3

4. Cranidium (T), dorsal view, x3

5. Cranidium (T/E), dorsal view, x3.5

Figs. 6–16. *Blairella* n. sp.

6. Cranidium (T), dorsal view, x7.5

7. Pygidium (T), dorsal view, x8

8. Cranidium (T), dorsal view, x7

9. Cranidium (T), dorsal view, x7.5

10. Cranidium (T), holotype, dorsal view, x7.5

11. Pygidium (T), dorsal view, x8

12. Cranidium (T), dorsal view, x8

13. Free cheek (T), dorsal view, x6

14. Free cheek (T), dorsal view, x6.5

15, 16. Cranidium (T), dorsal and lateral views, x7.5

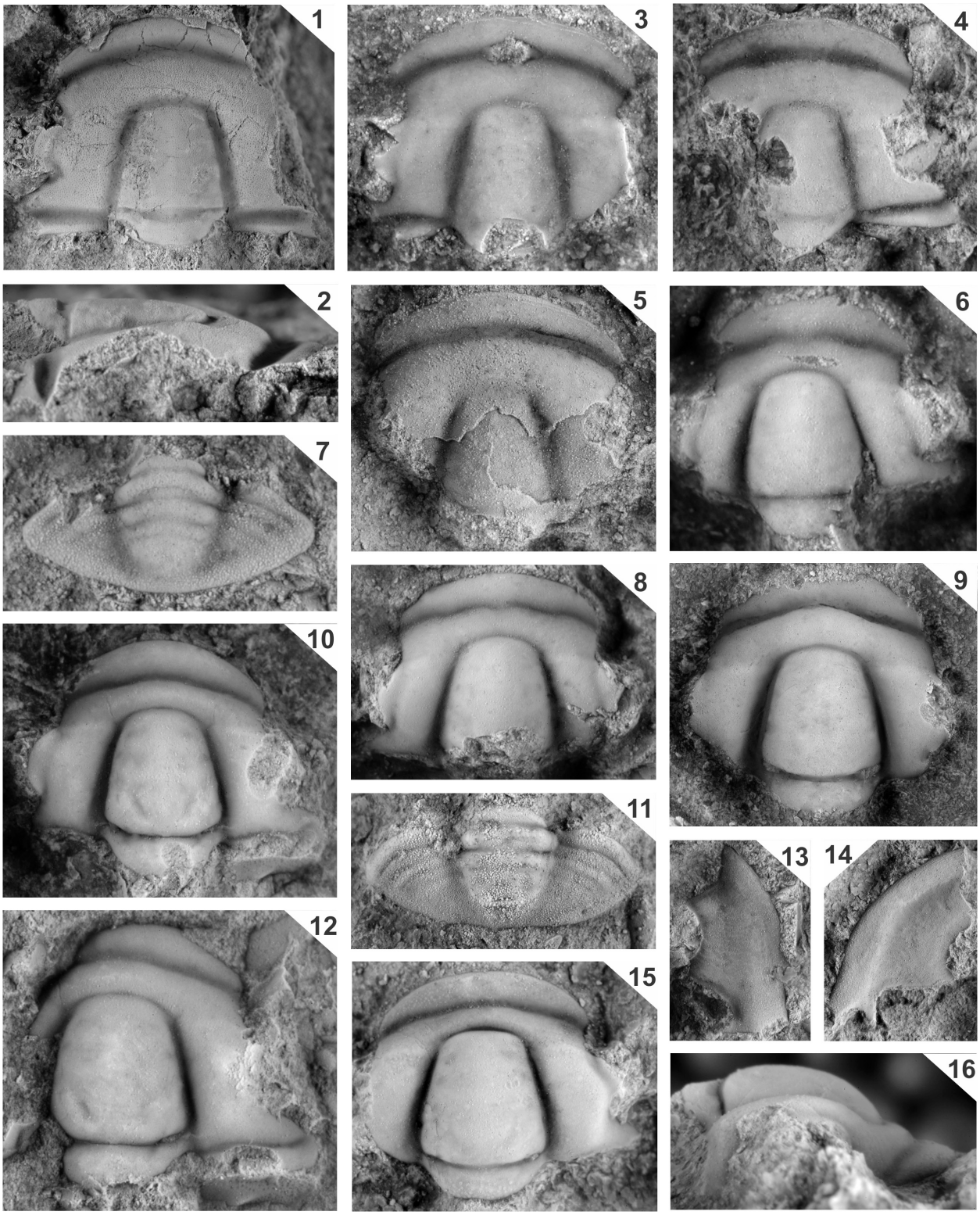
1
3
4
2
5
6
7
8
9
10
11
13
14
12
15
16

Plate 3

Figs. 1–11. *Alokistocare americanum* Walcott, 1916a.

1. Cranidium (L), dorsal view, x5

2. Cranidium (L), dorsal view, x5

3. Cranidium (L), dorsal view, x5.5

4. Cranidium (L), dorsal view, x5

5. Cranidium (T), dorsal view, x6

6. Cranidium (T), dorsal view, x8

7. Cranidium (T), dorsal view, x6

8. Cranidium (L), dorsal view, x9

9. Cranidium (L), dorsal view, x9

10. Cranidium (T), dorsal view, meraspid, x15

11. Cranidium (T), dorsal view, meraspid, x15

Figs. 12, 13. *Dunderbergia? anyta* (Hall and Whitfield, 1877).

12. Cranidium (T), dorsal view, x4

13. Cranidium (T), dorsal view, x4

Figs. 14-16. *Dunderbergia* cf. *D. nitida* (Hall and Whitfield 1877).

14. Cranidium (T/E), dorsal view, x3

15. Cranidium (T/E), dorsal view, x3

16. Cranidium (T/E), dorsal view, x3.5

Figs. 17. *Sulcocephalus* sp.

17. Cranidium (T), dorsal view, x6

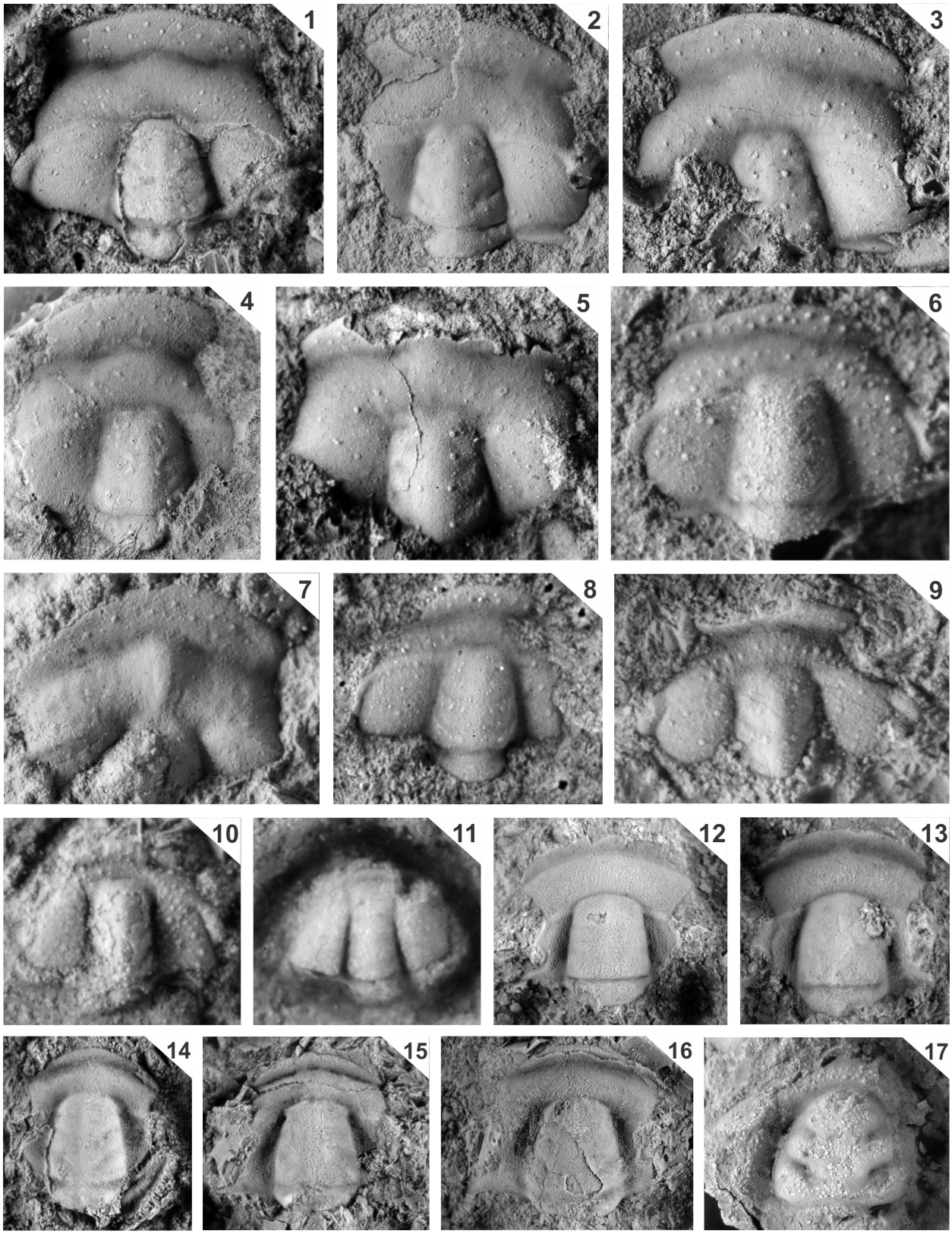
1
2
3
4
5
6
7
8
9
10
11
12
13
14
15
16
17

Plate 4

Figs. 1–16. *Olenoides nevadensis* (Meek, 1870).

1, 2. Cranidium (T), dorsal lateral views, x5

3. Cranidium (T/E), dorsal view, x5

4. Cranidium (T/E), dorsal view, x6

5. Cranidium (T), dorsal view, x6

6, 12, 13. Cranidium (T), lateral-oblique, lateral and anterior-oblique views, x 4.5

7–9. Hypostome (T), dorsal and lateral views, x1.5

10, 11. Hypostome (T) lateral and anterior views, 1.5

14. Pygidium (L), dorsal view, x7

15. Pygidium (T), dorsal view, x7.5

16. Pygidium (L), dorsal view, x10

Figs. 17. *Irvingella* sp.,

17. Cranidium (T), dorsal view, x6

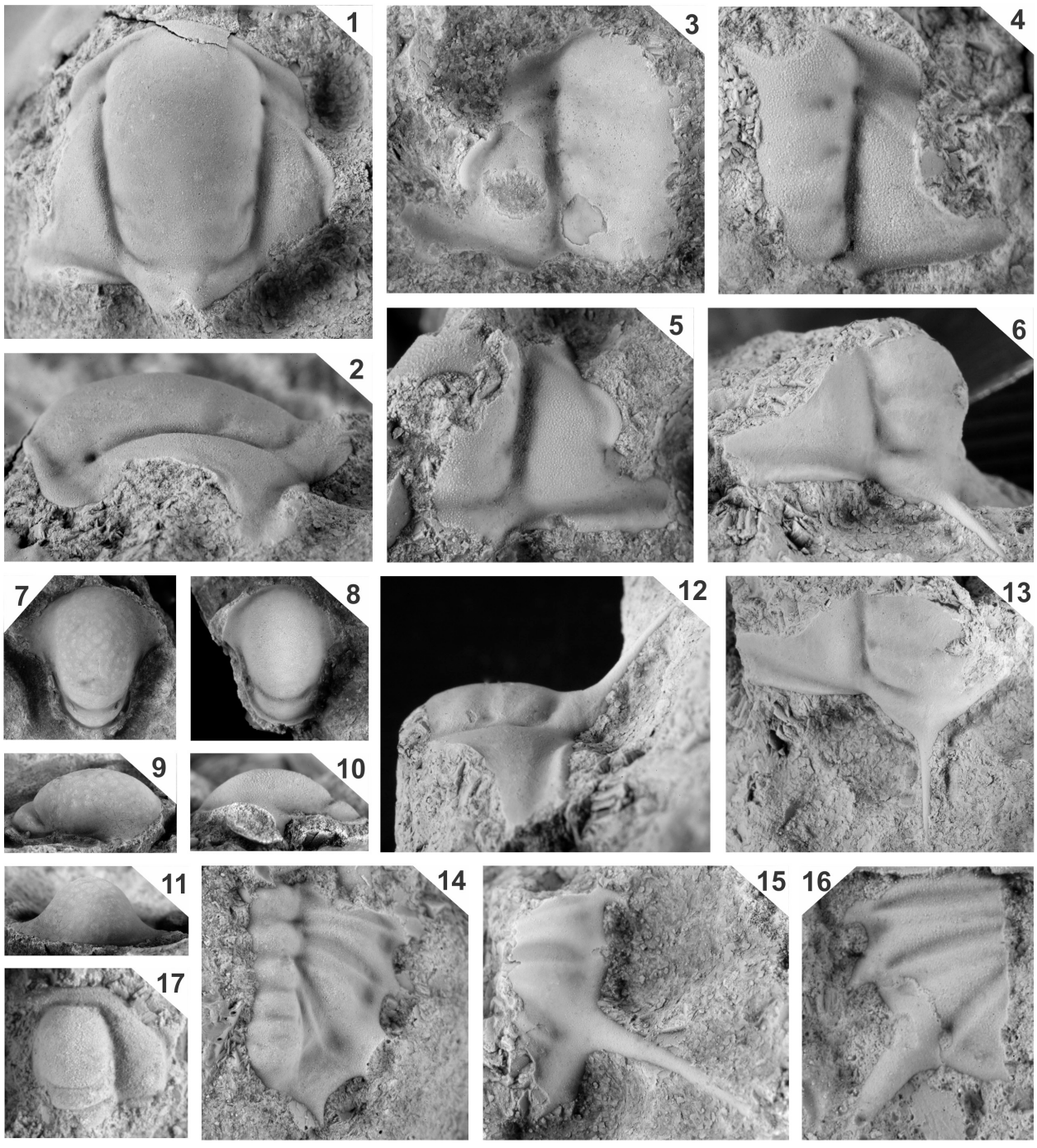
1
3
4
2
5
6
7
8
12
13
9
10
11
14
15
16
17

Plate 5

Figs. 1–3. *Kindbladia wichitaensis* (Resser, 1942).

1. Cranidium (T/E), dorsal view, x6

2. Cranidium (T/E), dorsal view, x5.5

3. Cranidium (T/E), dorsal view, x8

Figs. 4, 5. *Dellea rasilis* Westrop, 1986.

4. Cranidium (T/E), dorsal view, x7

5. Cranidium (T/E), dorsal view, x8

Figs. 6–10. *Dellea suada* (Walcott, 1890).

6, 7. Cranidium (T/E) dorsal and lateral views, x3.5

8. Cranidium (T/E), dorsal view, x4

9, 10. Cranidium (T/E), dorsal view, x4

Figs. 11. *Elvinia* cf. *E. roemeri* (Shumard, 1861).

11. Pygidium (T/E), dorsal view, x4

Figs. 12–16. *Iddingsia* cf. *I. anatina* Resser, 1942.

12. Pygidium (T), dorsal view, x4

13. Pygidium (T), dorsal view, x5

14. Cranidium (T/E), dorsal view, x4

15. Free cheek (T/E), dorsal view, x3

16. Cranidium (T/E), dorsal view, x4

Figs. 17–20. *Pterocephalia sanctisabae* Roemer, 1849.

17, 20. Cranidium (T), dorsal and lateral views, x2

18. Pygidium (T/E), dorsal view, x5

19. Cranidium (L), dorsal view, x2.5

Figs. 21. *Aphelaspis buttsi* Kobayashi, 1936.

21. Free cheek (T), dorsal view, x4

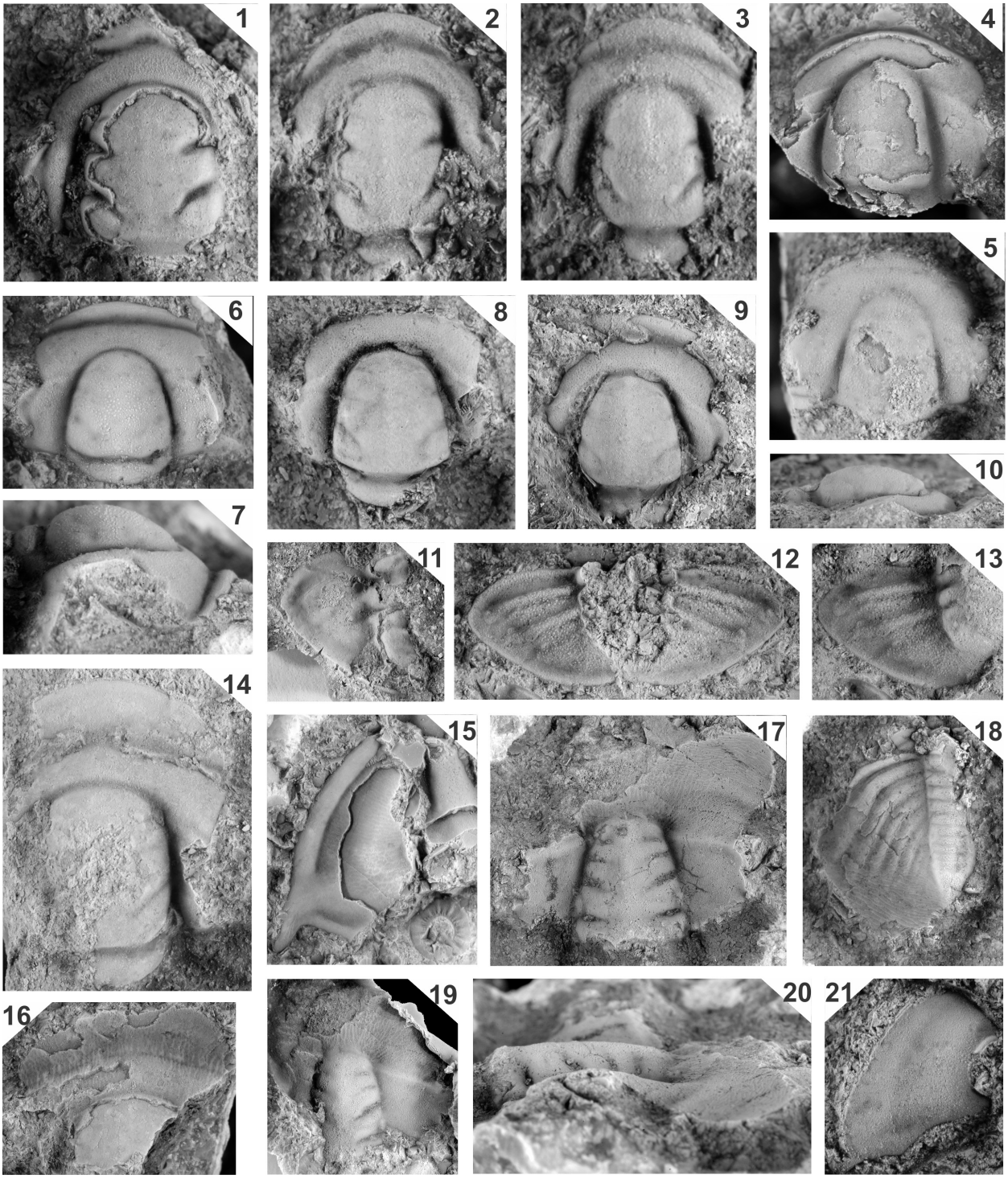

Plate 6

Figs. 1–9. *Aphelaspis walcotti* Resser, 1938.

1, 2. Cranidium (T), dorsal and lateral views, x6

3. Cranidium (L), dorsal view, x6.5

4. Cranidium (T), dorsal view, x7

5. Pygidium (T), dorsal view, x7.5

6. Cranidium (L), dorsal view, x4

7. Cranidium (L), dorsal view, x5

8. Free cheek (T), dorsal view, x4

9. Cranidium (T/E), dorsal view, x5

Figs. 10–13. *Aphelaspis buttsi* Kobayashi, 1936.

10. Pygidium (T), dorsal view, x8

11. Cranidium (T/E), dorsal view, x6

12. Cranidium (E), dorsal view, x5

13. Cranidium (T/E), dorsal view, x6

Figs. 14–16. *Solenopleurella quadrata* Rasetti, 1963.

14. Cranidium (E), dorsal view, x15

15. Cranidium (T), dorsal view, x15

16. Cranidium (T), dorsal view, x14

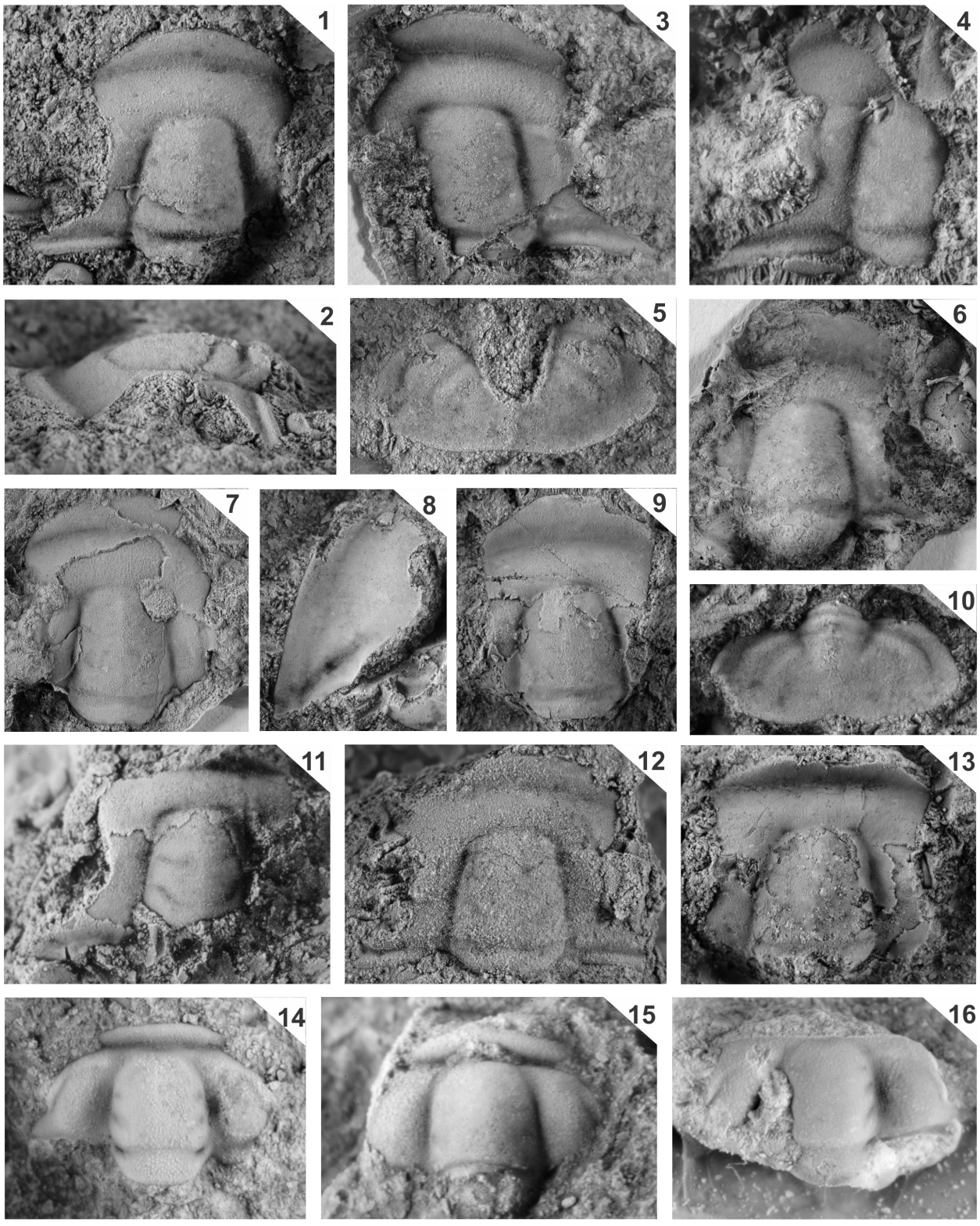
1
3
4
2
5
6
7
8
9
10
11
12
13
14
15
16

Plate 7

Figs. 1–8. *Camaraspis convexa* (Whitfield, 1878).

1. Cranidium (T), dorsal view, x5

2, 3. Cranidium (E), dorsal and lateral views, x5

4. Cranidium, meraspid (T/E), dorsal view, x7

5. Free cheek (T), dorsal view, x6

6, 7. Pygidium (T), dorsal and lateral views, x5, x6

8. Cranidium (T), dorsal view, x5.5

Figs. 9–18. *Camaraspis* n. sp.

9, 10. Cranidium (T), dorsal and lateral views, x3

11, 12. Pygidium (T), dorsal and lateral views, x2

13, 14. Cranidium (T), holotype, dorsal and lateral views, x4

15. Cranidium (T), dorsal view, x3.5

16, 17. Cranidium (T), dorsal and lateral views, x4

18. Free cheek (T), dorsal view, x3

Figs. 19. *Illaenurus* sp.

19. Cranidium (L), dorsal view, x2.5

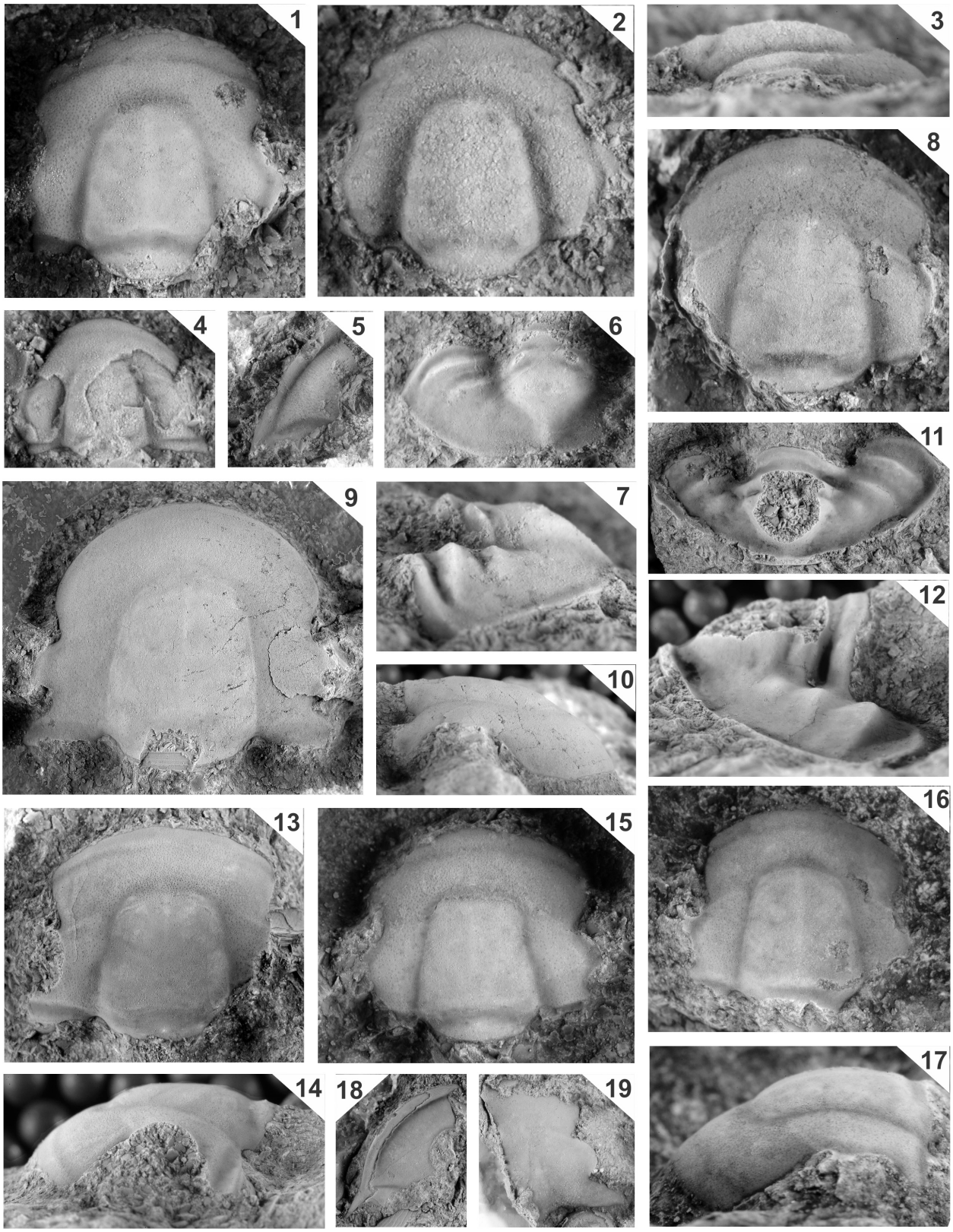
1
2
3
8
4
5
6
11
9
7
12
10
16
13
15
17
14
18
19

Plate 8

Figs. 1–3. *Marjumia* cf. *M. transversa* (Palmer, 1968).

1. Cranidium (T/E), dorsal view

2. Cranidium (E), dorsal view

3. Cranidium (T), dorsal view

Figs. 4–8. *Marjumia* cf *M. typa* Walcott, 1916b.

4. Cranidium (T/E), dorsal view

5. Cranidium (T/E), dorsal view

6. Cranidium (T/E), dorsal view

7, 8. Cranidium (T/E), dorsal and lateral views

Figs. 9–13. *Modocia* n. sp.

9. Cranidium (L), dorsal view, x5

10. Cranidium (T), dorsal view, x5.5

11. Cranidium (E), holotype, dorsal view, x8

12. Cranidium (E), dorsal view, x7.5

13. Pygidium (T), dorsal view, x4.5

Figs. 14–23. *Modocia* cf. *M. crassimarginata* Rasetti, 1965.

14, 15. Cranidium (T), dorsal and lateral views, x4.5

16. Cranidium (T), dorsal view, x4

17, 18. Cranidium (T), lateral and dorsal views, x5

19. Pygidium (T/E), dorsal view, x3

20, 21. Pygidium (T/E), dorsal and posterior views, x3

22, 23. Pygidium (T/E), dorsal and lateral views, x4

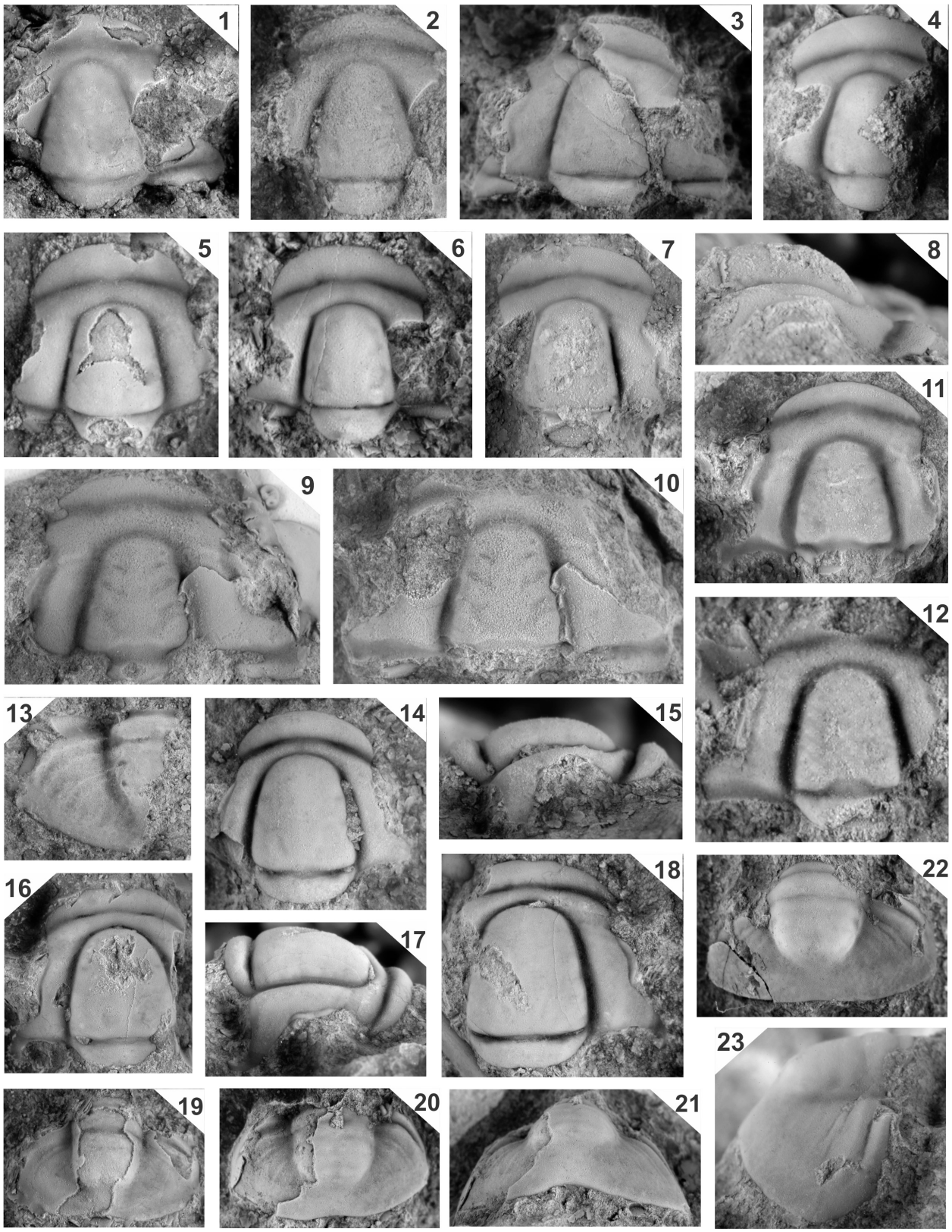
1
2
3
4
5
6
7
8
11
9
10
12
13
14
15
16
18
22
17
23
19
20
21

Plate 9

Figs. 1, 2. *Modocia dubia* (Resser, 1938a).

1. Cranidium (T), dorsal view, x3

2. Cranidium (E), dorsal view, x3.5

Figs. 3, 4. *Modocia oweni* (Meek and Hayden, 1861).

3. Cranidium (T/E), dorsal view, x3

4. Cranidium (E), dorsal view, x2.5

Figs. 5–15. *Modocia centralis* (Whitfield, 1877).

5, 6. Cranidium (T/E), dorsal and lateral views, x2.5

7. Cranidium (T), dorsal view, x2.5

8. Free cheek (T), dorsal view, x2.5

9, 10. Cranidium (T), dorsal and lateral views, x3

11. Cranidium (L), dorsal view, x2.5

12. Pygidium (T), dorsal view, x4

13. Pygidium (E), dorsal view, x3

14. Pygidium (L), dorsal view, x5

15. Pygidium (L), dorsal view, x3

Fig. 16. *Meteoraspis* sp.

16. Pygidium (T), dorsal view, x2

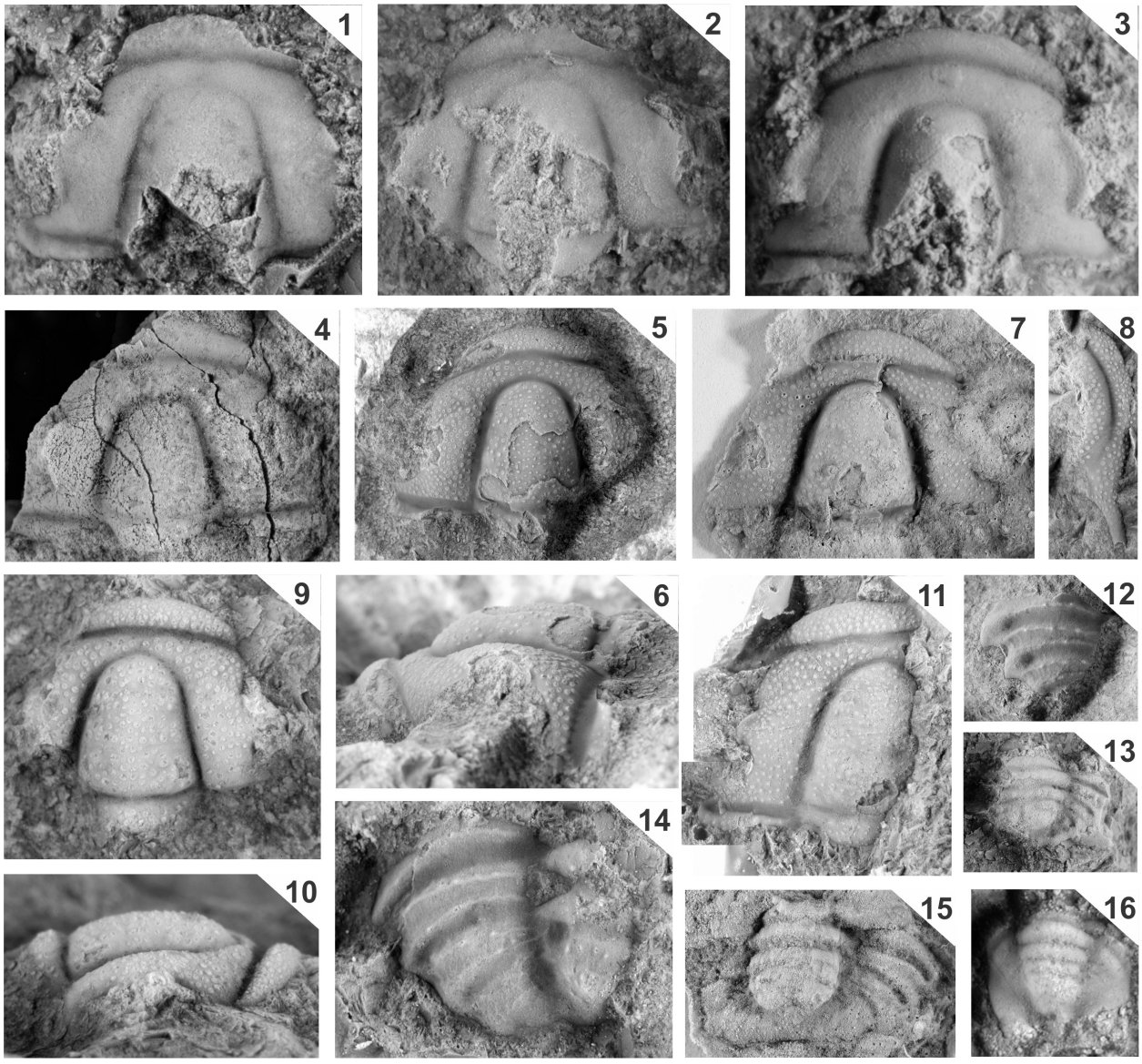
1
2
3
4
5
7
8
9
6
11
12
13
14
10
15
16

Plate 10

Figs. 1–9. *Tricrepicephalus coria* (Walcott, 1916a).

1. Cranidium (E), dorsal view, x2.5

2, 3. Cranidium (E), dorsal and lateral views, x2

4. Cranidium (T/E), dorsal view, x3

5. Free cheek (T/E), dorsal view, x2

6. Free cheek (T), dorsal view, x3.5

7, 8. Pygidium (E), dorsal and posterior-oblique views, x2.5, x3

9. Pygidium (L), dorsal view, x3

Figs. 10–17. *Tricrepicephalus texanus* (Shumard, 1861).

10. Cranidium (T/E), dorsal view, x2.5

11. Cranidium (T/E), dorsal view, x2

12. Free cheek (T), dorsal view, x5

13. Cranidium (L), dorsal view, x2.5

14. Cranidium (T/E), dorsal view, x4

15. Free cheek (T), dorsal view, x3

16. Pygidium (T/E), dorsal view, x3.5

17. Pygidium (T/E), dorsal view, x2

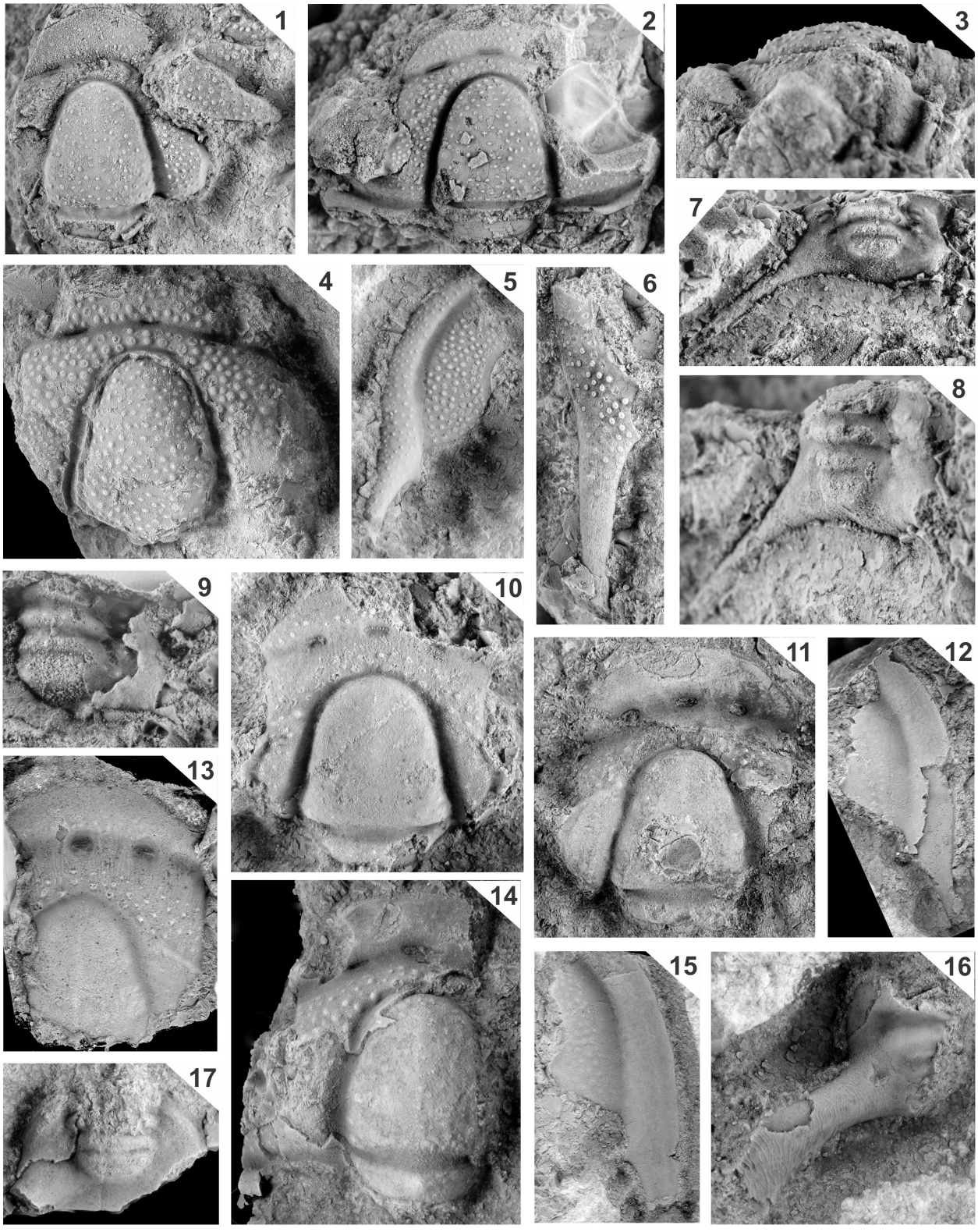
1
2
3
7
4
5
6
8
9
10
11
12
13
14
15
16
17

Plate 11

Figs. 1–8. *Crepicephalus exutus* Resser, 1938a

1. Cranidium (T/E), dorsal view, x2.5
2. Cranidium (T/E), dorsal view, x2.5
3. Cranidium (T/E), dorsal view, x3
4. Cranidium (L), dorsal view, x3
5. Pygidium (T/E), dorsal view, x5
6. Pygidium (T/E), dorsal view, x6
7. Pygidium (T/E), dorsal view, x4.5
8. Pygidium (L), dorsal view, x3

Figs. 9–11. *Crepicephalus* sp.

9. Pygidium (T), dorsal view, x3
10. Pygidium (T/E), dorsal view, x3.5
11. Pygidium (T/E), dorsal view, x3

Figs. 12–16. *Crepicephalus* n. sp.

12. Pygidium (T), dorsal view, x5
13. Pygidium (T/E), dorsal view, x5.5
14. Pygidium (T), dorsal view, x6
15. Pygidium (T), dorsal view, x6
16. Pygidium (T), holotype, dorsal view, x5.5

Figs. 17. *Crepicephalus* cf. *C. iowensis* (Owen, 1852).

17. Pygidium (T), dorsal view, x3

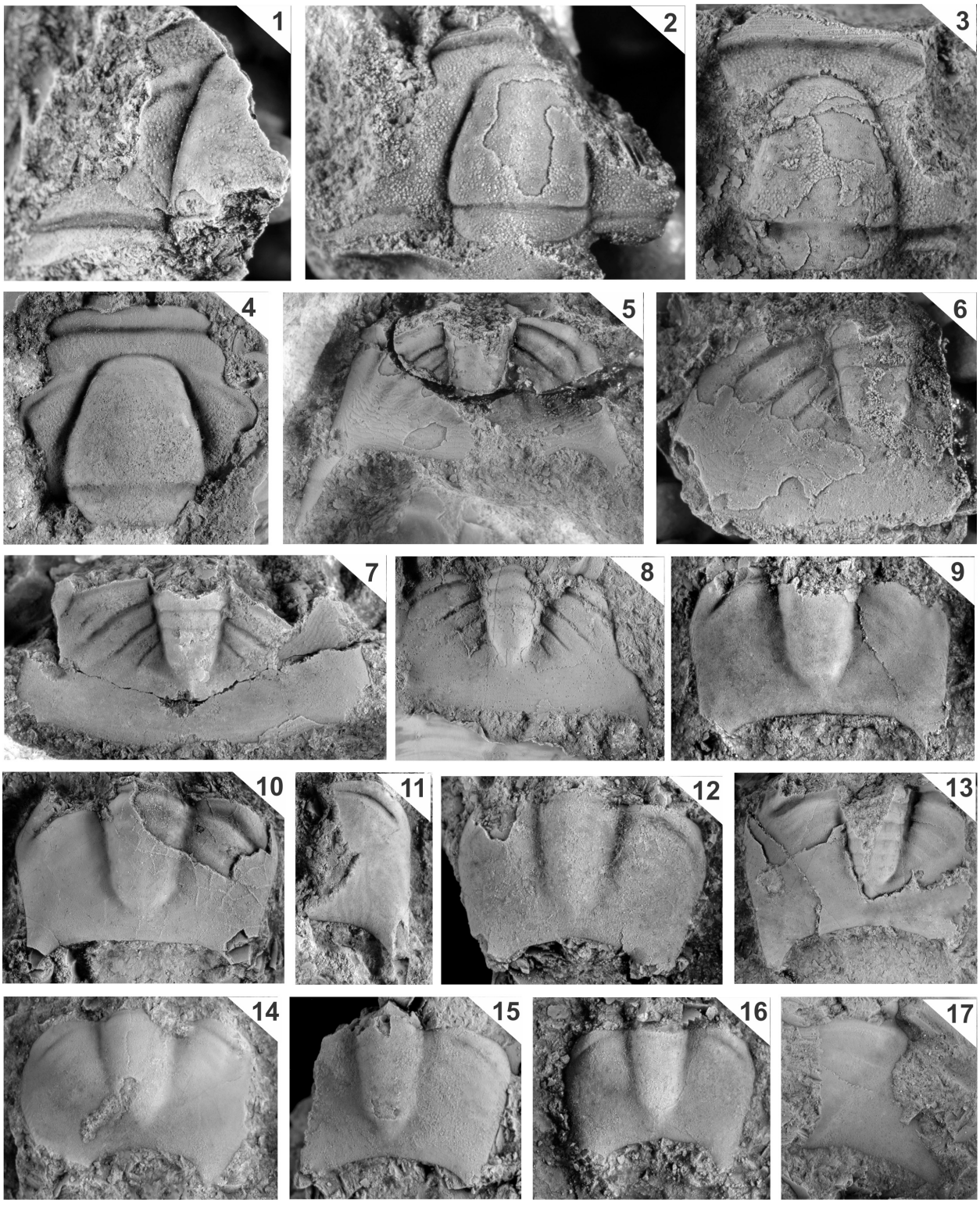
1
2
3
4
5
6
7
8
9
10
11
12
13
14
15
16
17

Plate 12

Figs. 1–11. *Coosella andreas* (Walcott, 1916).

1, 2. Cranidium (T), dorsal and lateral views, x7.5

3. Cranidium (T/E), dorsal view, x7.5

4. Cranidium (T), dorsal view, x7

5, 6. Pygidium (T), dorsal and posterior views, x4

7. Pygidium (T), dorsal view, x4

8, 9. Pygidium (T) dorsal and lateral views, x3.5

10, 11. Pygidium (T), dorsal and lateral views, x3

Figs. 12–21. *Coosina ariston* (Walcott, 1916b).

12. Cranidium (E), dorsal view, x4.5

13. Cranidium (T), dorsal view, x4

14, 15. Cranidium (E), dorsal and lateral views, x4.5

16. Cranidium (T/E), dorsal view, x3

17. Pygidium (E), dorsal view, x6

18. Cranidium (T/E), dorsal view, x3

19. Cranidium (E), dorsal view, x4

20, 21. Pygidium (E), dorsal and lateral views, x4


1
3
4
5
6
2
7
8
10
12
13
9
11
14
16
17
20
15
18
19
21

Plate 13

Figs. 1–10. *Coosia* n. sp.

1. Cranidium (T/E), holotype, dorsal view, x4

2. Cranidium (L), dorsal view, x4

3. Cranidium (T), dorsal view, x6

4. Cranidium, dorsal view, pygidium (E), anterior-oblique view, x4

5. Cranidium (T), dorsal view, x6

6. Cranidium (T), dorsal view, x5

7. Pygidium (T), dorsal view, x4

8. Pygidium (T/E), dorsal view, x4

9. Cranidium (E), dorsal view, x5

10. Cranidium (T), dorsal view, x5

Figs. 11–19. *Coosella helena* Lochman, 1938.

11, 12. Cranidium (T), dorsal and lateral views, x3

13. Cranidium (T/E), dorsal view, x3

14. Pygidium (T), dorsal view, x4

15. Hypostome (E), dorsal view, x5

16, 17. Pygidium (E), dorsal and lateral views, x4

18, 19. Cranidium (T) dorsal and lateral views, x3.5

Figs. 20–22. *Kingstonia scrinium* (Raymond, 1937).

20. Pygidium (E/T), dorsal view, x5

21. Pygidium (E/T), dorsal view, x7

22. Pygidium (E/T), dorsal view, x8

Figs. 23–25. *Kingstonia spicata* Lochman, 1940.

23. Pygidium (E), dorsal view, x3

24. Pygidium (E/T), dorsal view, x3

25. Pygidium (T), dorsal view, x2.5

Fig. 26. *Kingstonia* sp.

26. Pygidium (T), dorsal view, x9

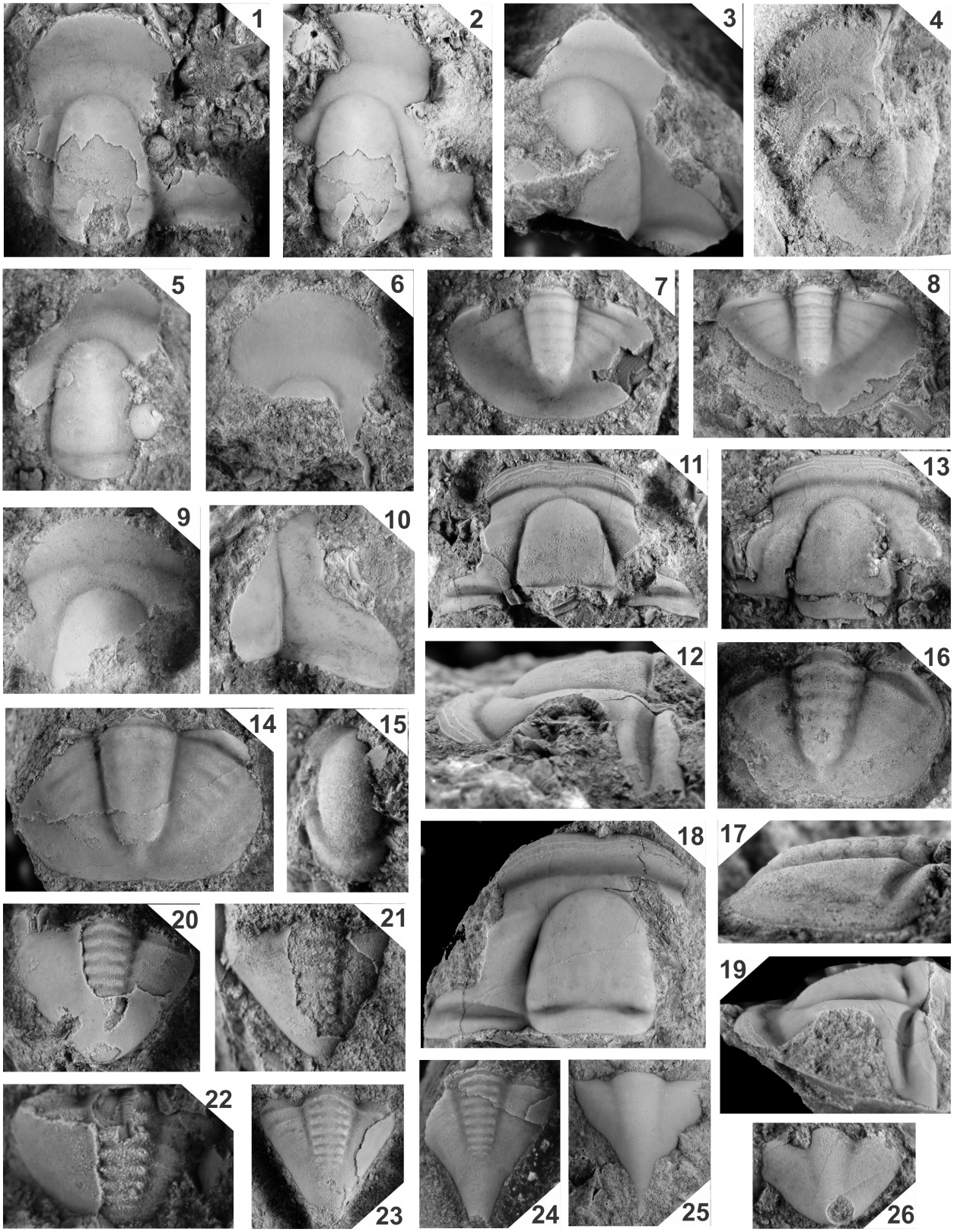
1
2
3
4
5
6
7
8
9
10
11
13
12
16
14
15
18
17
19
20
21
22
23
24
25
26

Plate 14

Figs. 1–9. *Brachyaspidion rynchina* Miller, 1936b.

1. Cranidium (E/T), dorsal view, x7.5

2. Cranidium (E/T), dorsal view, x8

3. Cranidium (T), dorsal view, x8

4. Cranidium (T), dorsal view, x8.5

5. Cranidium (E/T), dorsal view, x8.5

6., 9. Cranidium (T), dorsal and lateral views, x8

7. Pygidium (E), dorsal view, x15

8. Hypostome (E/T), dorsal view, x10

Fig.10–15. *Bynumia eumus* Walcott, 1924.

10. Cranidium (E/T), dorsal view, x9

11. Cranidium (T), dorsal view, x10

12. Pygidium (E), dorsal view, x14

13. Pygidium (T), dorsal view, x12

14. Pygidium (T), dorsal view, x12

15. Pygidium (T), dorsal view, x13

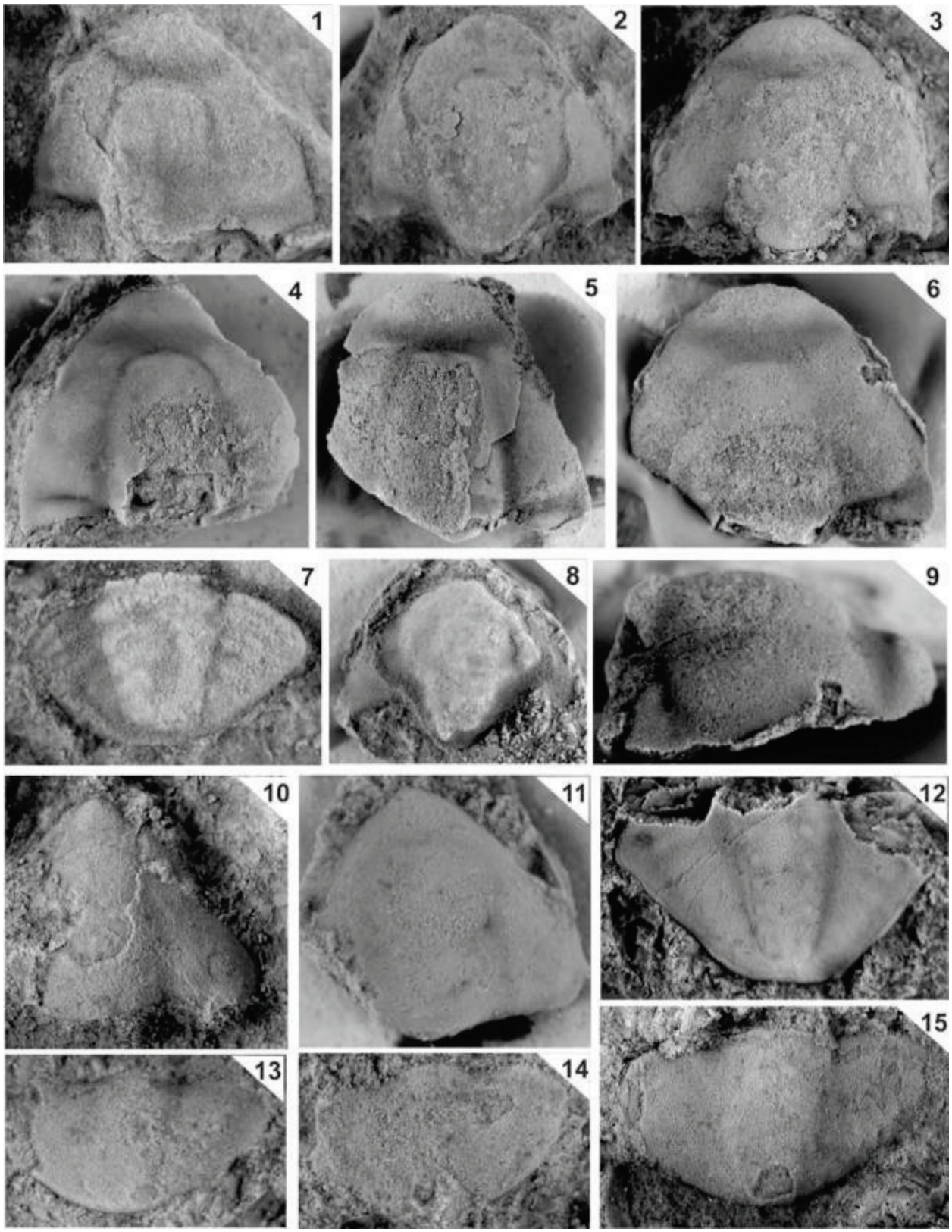
1
2
3
4
5
6
7
8
9
10
11
12
13
14
15

Plate 15

Figs. 1–5. *Glaphyraspis parva* (Walcott, 1899).

1. Cranidium (T), dorsal view, x10

2. Cranidium (T), dorsal view, x10.5

3. Cranidium (T), dorsal view, x10

4. Cranidium (T), dorsal view, x10.5

5. Cranidium (T), dorsal view, x10

Figs. 6. *Cheilocephalus brachyops* Palmer, 1965.

6. Cranidium (T), dorsal view, x5

Figs. 7–9. *Hardyoides* cf. *H. tenerus* (Walcott, 1916).

7. Cranidium (T/E), dorsal view, x12

8. Cranidium (T/E), dorsal view, x12

9. Cranidium (T), dorsal view, x13

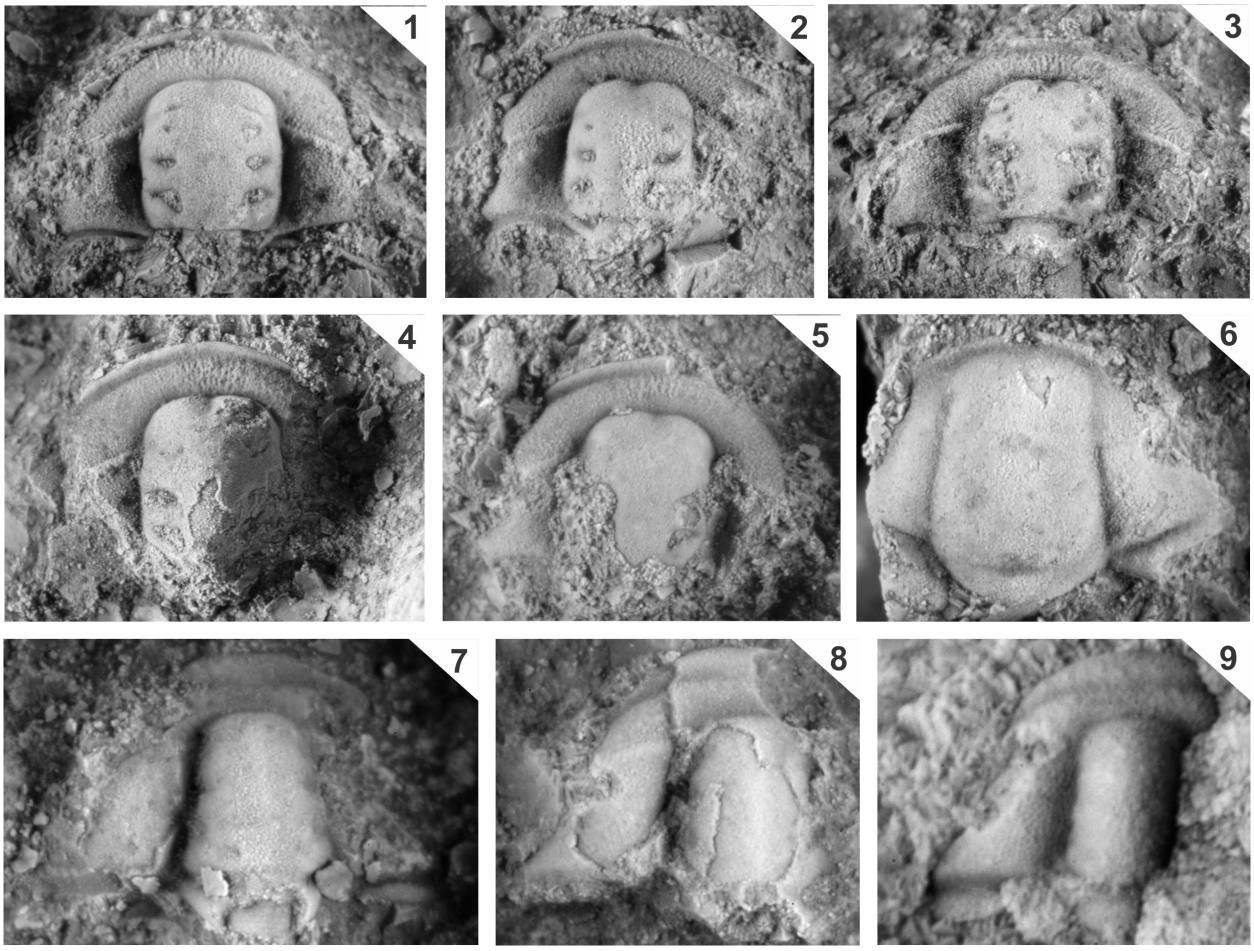
1
2
3
4
5
6
7
8
9

Plate 16

Figs. 1–12. *Bolaspidella* n. sp.

1, 2. Cranidium (T) Holotype, dorsal and lateral-oblique views, x9.5

3. Cranidium (E), dorsal view, x8.5

4, 5. Cranidium (T), dorsal and lateral views, x9

6. Cranidium (T), dorsal view, x8.5

7. Cranidium (E), dorsal view, x8

8. Cranidium (E), dorsal view, x9

9. Pygidium (L), dorsal view, x10

10. Cranidium (T). Meraspid, dorsal view, x15

11. Cranidium (E), dorsal view, x12

12. Pygidium (T), dorsal view, x10.5

Figs. 13–14. *Bolaspidella* sp.

13. Cranidium (E), dorsal view, x13

14. Cranidium (E), dorsal view, x13

Figs. 15, 16. *Xenocheilos* cf. *X. spineum* Wilson, 1951.

15. Cranidium (T/E), dorsal view, x15

16. Cranidium (T/E), dorsal view, x15

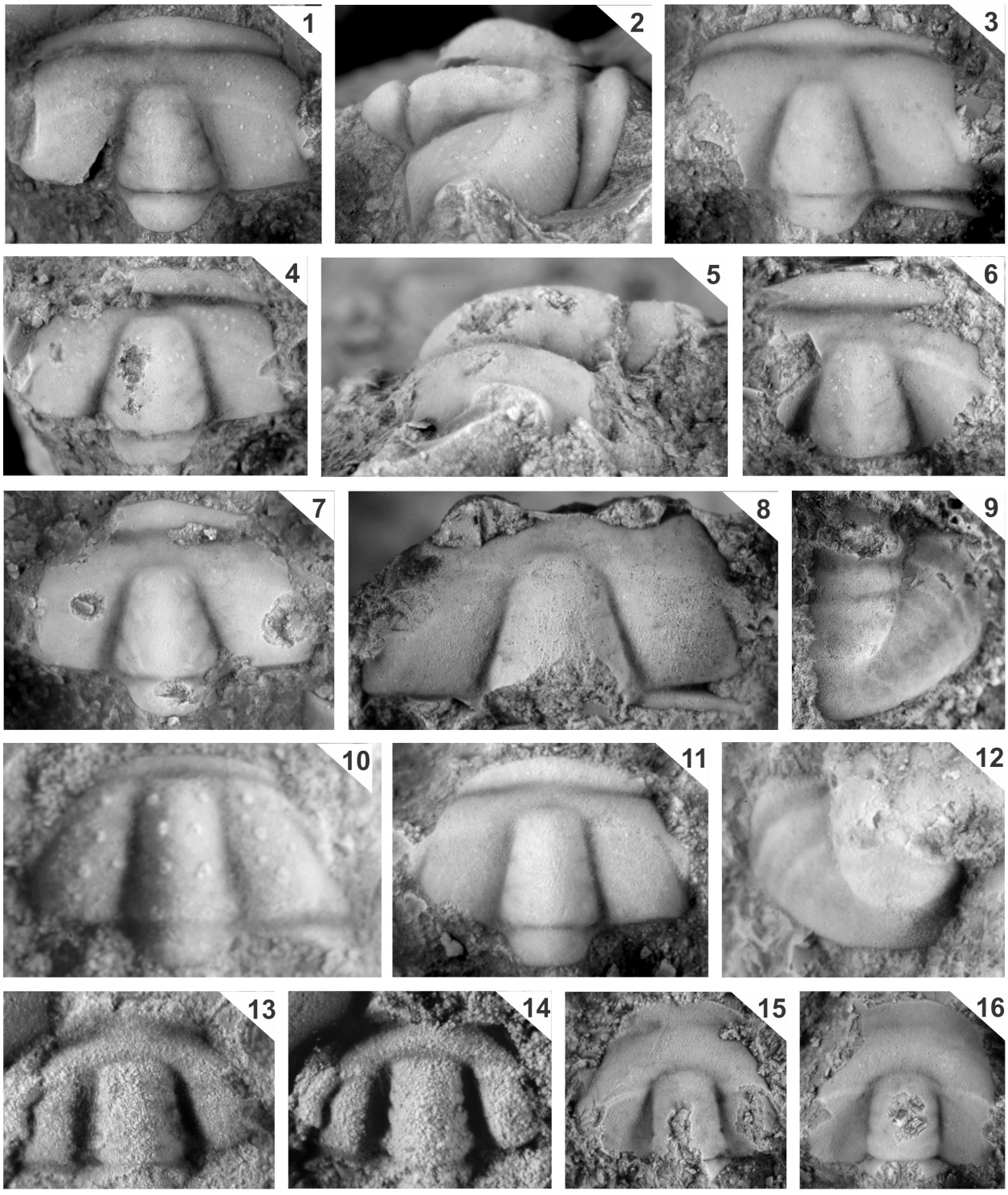
1
2
3
4
5
6
7
8
9
10
11
12
13
14
15
16

Plate 17

Figs. 1–7. *Eldoradia prospectensis* (Walcott, 1884).

1. Cranidium (E), dorsal view, x6.5

2. Cranidium (E), dorsal view, x7.5

3. Cranidium (E), dorsal view, x6.5

4. Cranidium (E), dorsal view, x7

5. Cranidium (E), dorsal view, x7

6. Cranidia (E), x4

7. Cranidia (E), x 0.5

Figs. 8–13. *Eldoradia linnarssoni* (Walcott, 1884).

8, 9. Cranidium (L), dorsal and posterior views, x3.5

10. Free cheek (E), dorsal view, x4

11, 12. Cranidia (E), dorsal and lateral views, x3

13. Cranidium (E), dorsal view, x6

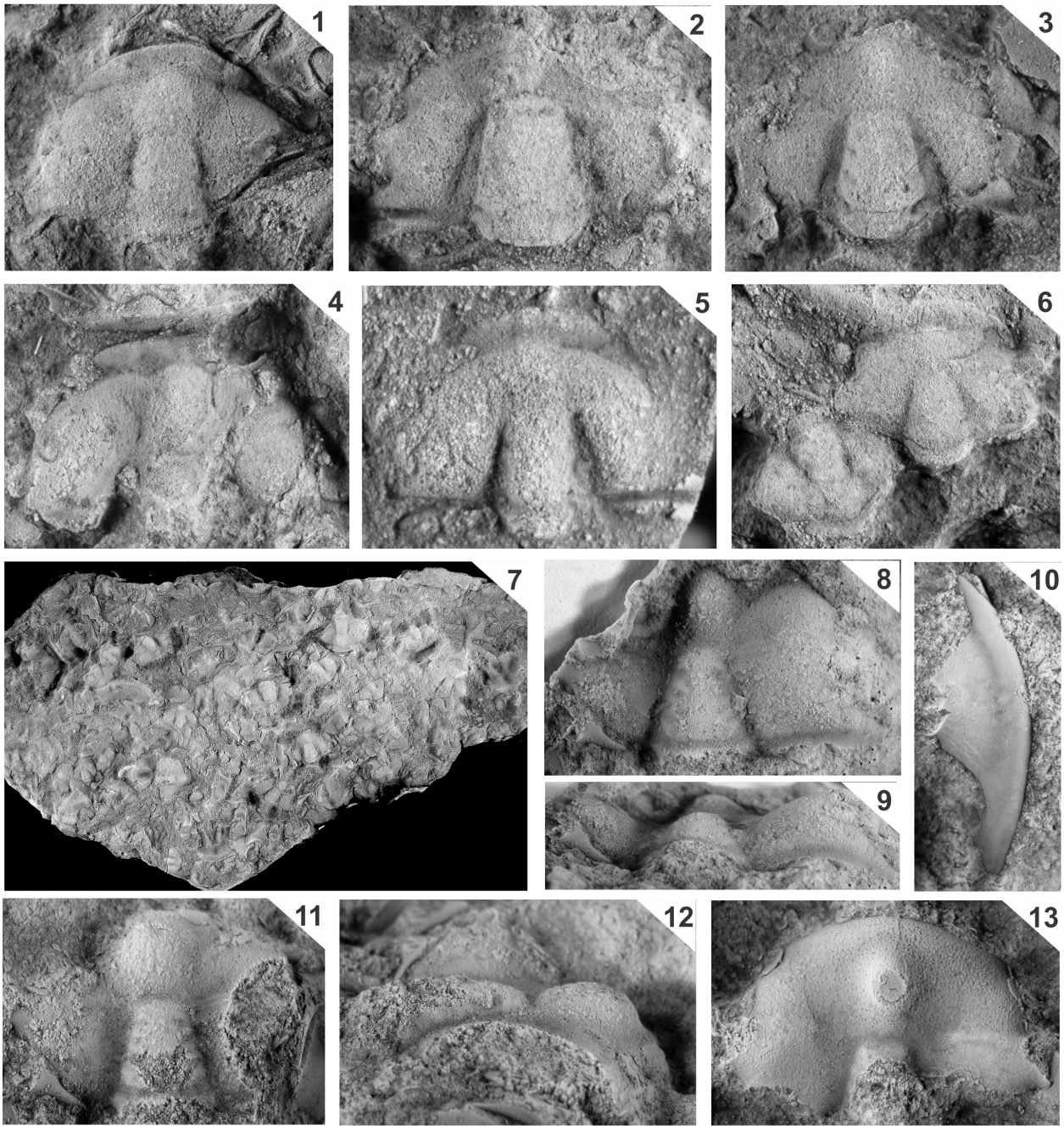
1
2
3
4
5
6
7
8
9
10
11
12
13

Plate 18

Figs. 1–14. *Cedaria eurycheilos* Palmer, 1954.

1, 2. Cranidium (T/E), dorsal and lateral views, x7,5

3. Cranidium (T/E) dorsal view, x13

4. Cranidium (T/E), dorsal view, x12

5, 6. Pygidium (T), dorsal and lateral views, x8

7. Cranidium (T), dorsal view, x12

8. Cranidium, (T), dorsal view, x10

9. Cranidium, (T), dorsal view, x9

10. Pygidium (T), dorsal view, x7.5

11. Pygidium (L), dorsal view, x8

12. Pygidium (T/E), dorsal view, x 6

13. Pygidium (T/E), dorsal view, x6.5

14. Cranidium (T/E), dorsal view, x9

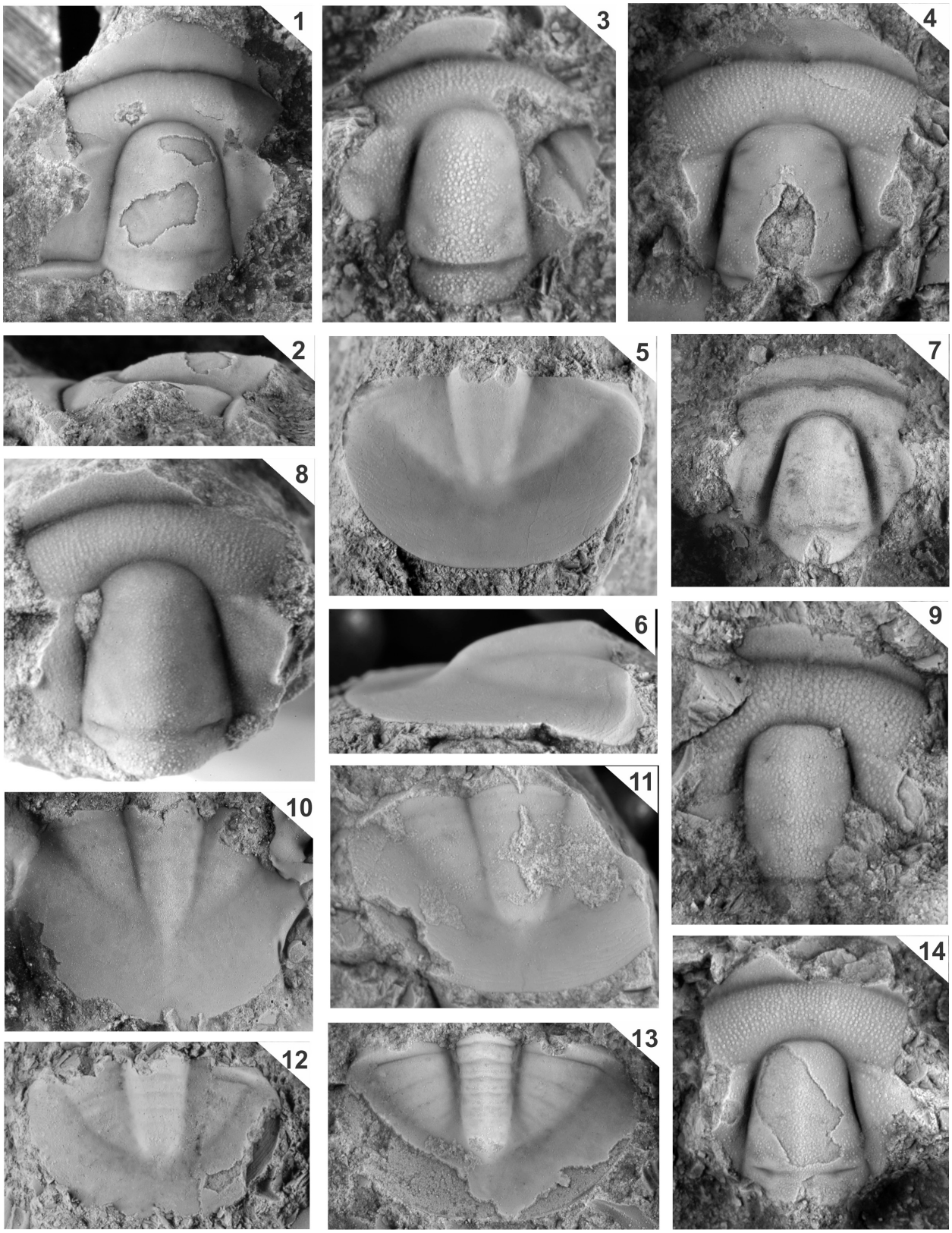
1
3
4
2
5
7
8
6
9
10
11
14
12
13

Plate 19

Figs. 1–8. *Paracedaria viriosa* Locham and Hu, 1962.

1, 2. Cranidium (T/E), dorsal and lateral views, x4

3. Cranidium (T), dorsal view, x6

4. Cranidium (T), dorsal view, x5

5. Cranidium (T), dorsal view, x5

6, 7. Pygidium (T), dorsal and lateral views, x10

8. Pygidium (L), dorsal view, x8

Figs. 9–12. *Paracedaria* n. sp.

9, 10. Cranidium (T/E), dorsal and lateral views, x4

11. Cranidium (T), holotype, dorsal view, x5.5

12. Cranidium (T), dorsal view, x5.5

Figs. 13. *Cedarina cf. C. obtusans* Duncan *in* Lochman and Duncan, 1944.

13. Cranidium (E), dorsal view, x4

Figs. 15, 16. *Cedarina*? sp.

15. Pygidium (L), dorsal view, x4

16. Pygidium (T), dorsal view, x8

Figs. 14, 17, 18. *Cedaria*? sp.

14. Pygidium (L), dorsal view, x7

17. Pygidium (T), dorsal view, x7

18. Pygidium (T), dorsal view, x7.5

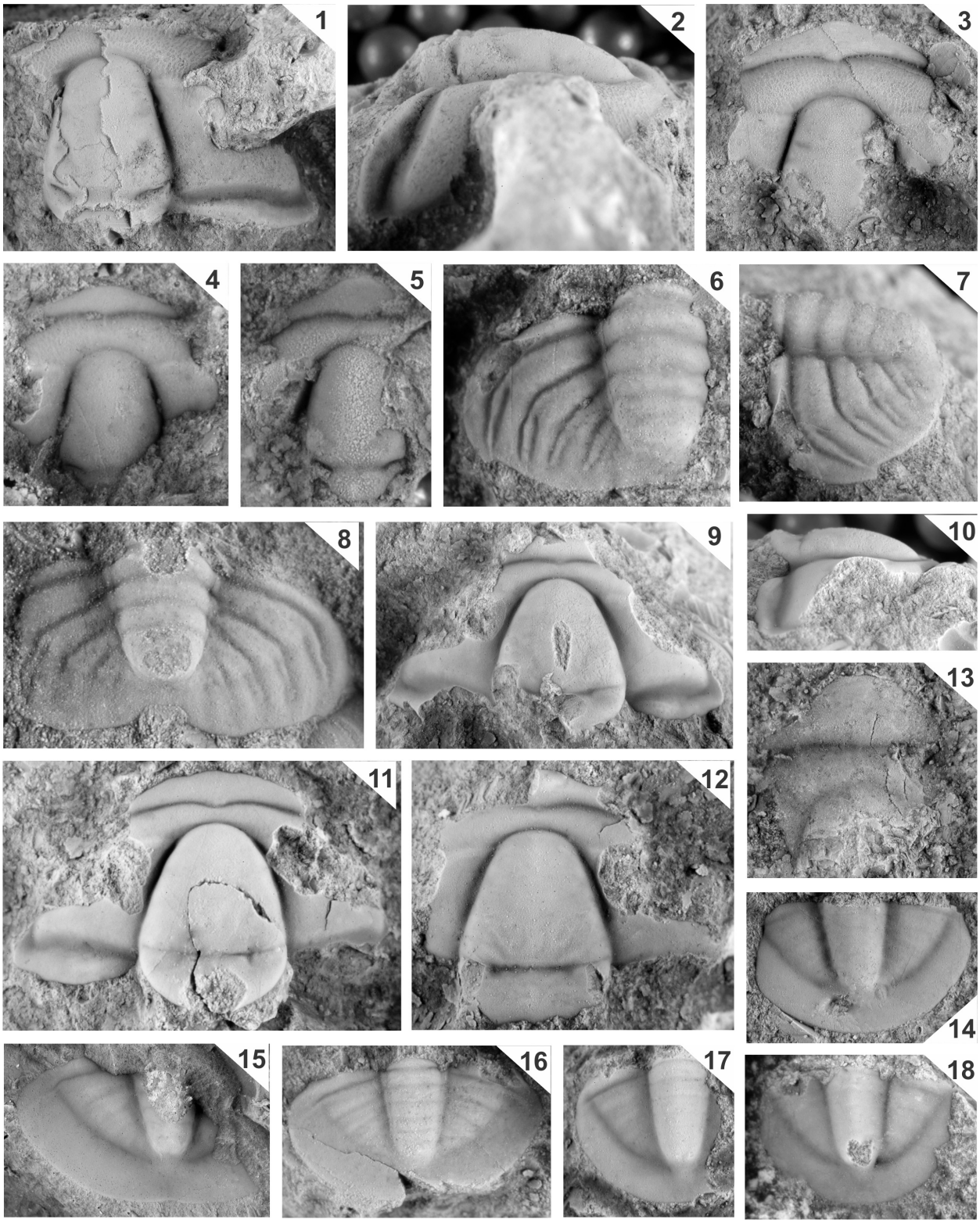
1
2
3
4
5
6
7
8
9
10
13
11
12
14
15
16
17
18

Plate 20

Figs. 1, 2. *Llanoaspis modesta* Lochman, 1938a.

1. Cranidium (T), dorsal view, x6

2. Cranidium (L), dorsal view, x8

Fig. 3-6. *Llanoaspis undulata* Lochman, 1938a.

3. Cranidium (E/T), dorsal view, x6

4. Cranidium (T), dorsal view, x7

5. Pygidium (T), dorsal view, x3.5

6. Pygidium (E/T), dorsal view, x4

Fig. 7–9. *Llanoaspis* n. sp.

7. Cranidium (T), holotype, dorsal view, x5

8, 9. Pygidium (T), dorsal and lateral views, x6

Figs. 10–13. *Cliffia lataegenae* (Wilson, 1949).

10. Cranidium (T), dorsal view, x8

11. Cranidium (T), dorsal view, x8.5

12, 13. Pygidium (T), lateral and dorsal views, x10

Fig. 14. *Llanoaspis* cf. *L. convexifrons* Rasetti, 1961.

14. Pygidium (T), dorsal view, x4

Fig. 15. *Llanoaspis peculiaris* (Resser, 1938a).

15. Cranidium (L), dorsal view, x7

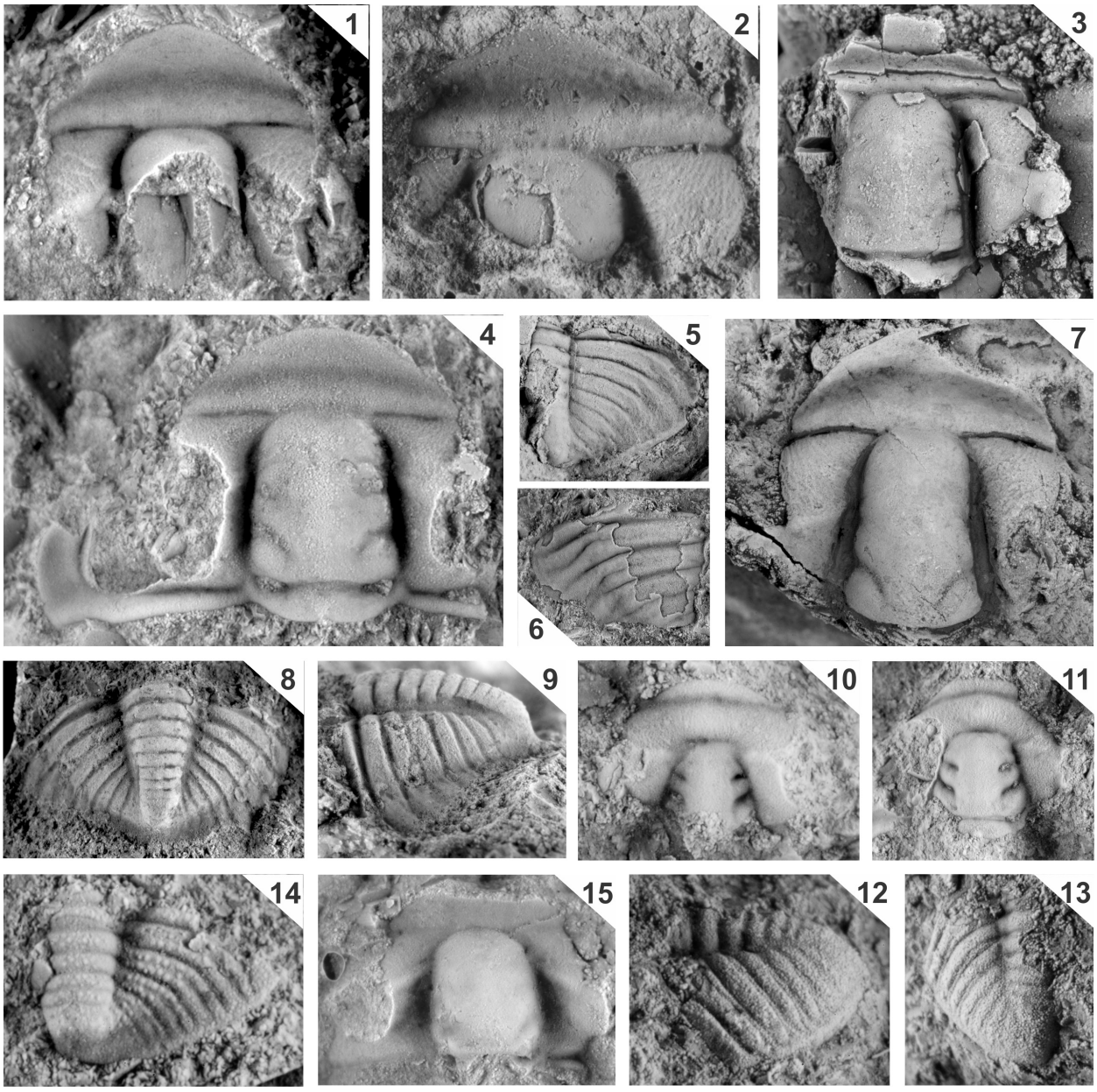
1
2
3
4
5
6
7
8
9
10
11
14
15
12
13

Plate 21

Figs. 1–16. *Arapahoia butleri* (Stoyanow, 1936).

1. Cranidium (E), dorsal view, x4

2. Cranidium (T), dorsal view, x3.5

3. Pygidium (T), dorsal view, x3.5

4, 5. Cranidium (E), dorsal and lateral views, x3

6. Cranidium (E), dorsal view, x3

7–9. Cranidium (E), lateral, dorsal, x5 and posterior-oblique views, x6

10. Pygidium (T/E), dorsal view, x4

11. Pygidium (T), dorsal view, x5

12. Pygidium (E), dorsal view, x5

13. Cranidium (E), dorsal view, x3.5

14. Free cheek (E), dorsal view, x4

15 Cranidium (T), dorsal view, x4

16. Free cheek (E), dorsal view, x2.5

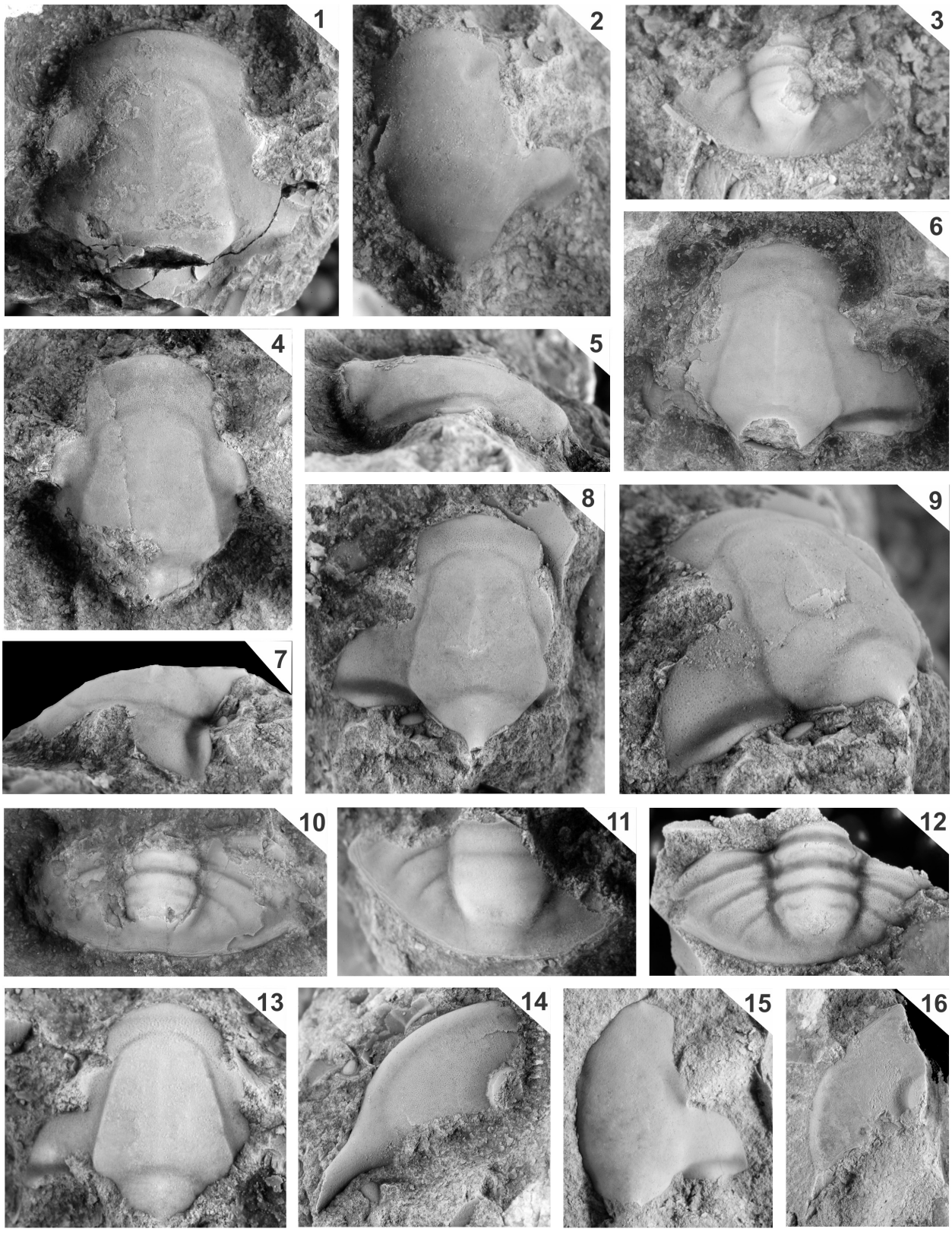
1
2
3
4
5
6
7
8
9
10
11
12
13
14
15
16

Table. 1.FauTable. 3.1. Faunal zones recognized in the Abrigo Formation from several fossil collections.

Zone	Whetstone Mountains (Gilluly, 1956)	French Joe Canyon (Hayes, 1975)	Ajax Hill (Gilluly, 1956)	Mount Martin (Hayes, 1975),	(Gilluly, 1956)	Dragoon Mountains (Gilluly, 1956)	Little Dragoon Mountains (Gilluly, 1956)	Swisshelm Mountains (Gilluly, 1956),	(Hayes, 1975)	Johnny Lyon Hills (Cooper and Silver, 1964)	Miscellaneous collections (Cooper and Silver, 1964)
post-Elvinia				*Briscoia* sp. *?Prosaukia* sp. *Rasettia* sp. *Catillicephalid* *Ptychopariid* *Drumaspis* cf. *D. walcotti* *Idahoia* sp. *Maladia* sp. *Ptychaspis* cf. *P. miniscaensis* *Agnostid* *Dikelocephalid* *Drumaspis* cf. *D. maxwelli*	*Agnostus parilis* *Drumaspis* sp. *Ellipsocephaloides?* sp. *Maladia* sp. *Pseudagnostus* sp. *Prosaukia?* sp. *Wilbernia* sp. *Billingsella* sp.					*Idahoia* sp. *Drumaspis* sp.
Elvinia								*Pterocephalia?* sp.			*Camaraspis* sp. *Dellea* sp. *Elvinia* sp. *Irvingella* sp. *Kinbladia* sp. *Linnarssonella* sp. *Pseudagnostus* sp.
Aphelaspis			*Aphelaspis walcotti* *Crepicephalus* sp.			*Bolutnia* sp. *Cheilocephalus* sp.				*Aphelaspis* sp.	
Crepicephalus			*Crepicephalus?* sp. *Brassicicephalus* sp. *Holcacephalus appalachius* *Kormagnostus* cf. *K. simplex* *Tricrepicephalus* cf. *T. coria*		*Coosella* sp. *Coosia* cf. *C. connata* *Crepicephalus* sp. *Tricrepicephalus* sp. *Kinsabia* sp. *Kormagnostus* cf. *K. simplex* *Meteoraspis* cf. *M. borealis* *Tricrepicephalus* cf. *T. coria* *Tricrepicephalus* cf. *T. texana*	*Crepicephalus sp.* *Maryvillia* cf. *M. ariston* *Tricrepicephalus sp.*				*Crepicephalus?* sp. *Llanoaspis* sp. *Coosina* sp. *Tricrepicephalus* sp.	*Crepicephalus* sp. *Llanoaspis* sp. *Coosina* sp. *Tricrepicephalus* sp.
Cedaria	*Arapahoia ransomei* *Semnocephalus centralis* *Kingstonia* sp. *Meteoraspis* cf.*M. borealis* *Pseudagnostus?* sp *Syspacheilus* cf. *S. occidens* *Dicellomus nanus* *Aspidagnostus?* sp. *Cedaria* cf .*C.nixonia* *Cedarina* cf. *C. cordillerae* *Coosia* sp. *Kormagnostus* cf.*K. simplex* *Meteoraspis* cf.*M. borealis* *Kingstonia spicata* *Menomonia?* sp.	*?Ankoura* sp. *Arapahoia* sp. *Crepicephalid* *Kingstonia* cf. *montanensis* *Kormagnostus* sp. cf. *Meteoraspis* sp. cf. *Blountia* sp. *?Brassicephalus* sp. *?Cedaria* sp.	*Ankoura?* sp. *Meteoraspis* cf. *M. borealis* *Nixonella?* cf. *N.wolfensis* *Tricrepicephalus* cf. *T. coria* *Aspidagnostus?* sp. *Coosella* sp. *Genevievella?* sp. *Nixonella* sp. *Tricrepicephalus* cf. *T. texanus* *Brasssicicephalus* sp. *Cedaria* cf . *C. nixonia* *Holcacephalus tenerus* *Kormagnostus* cf. *K. simplex* *Kingstonia* sp. *Menomonia* sp. *Arapahoia ransomei* *Cedarina* cf. *C. cordillerae* *Kingstonia spicata* *Tricrepicephalus* sp. *Semnocephalus centralis*	*Arapahoia* sp. cf. *Meteoraspis* sp. *Bynumia* sp. *Cedaria* sp. *Kormagnostus* sp. *Ptychopariid* *?Menomonia* sp. *Modocia* sp. *Cedariid*	*Cedaria* cf. *C. cordillerae* *Kormagnostus* cf. *K. simplex* *Meteoraspis* cf. *M. borealis* *Semnocephalus centralis* *Albansia?* cf. *A.?* *montanensis* *Cooselllia* sp. *Kinsabia* sp. *Ankoura* sp. *Kingstonia* sp.	*Meteoraspis cf. M. borealis* *Tricrepicephalus* cf. *T. texanus* *Arapahoia ransomei* *Kingstonia* sp. *Kingstonia spicata*	*Arapahoia ransomei* *Cedaria* cf. *C. nixonia* *Cedarina* cf. *C. cordillerae* *Kormagnostus* cf. *K. simplex* *Meteoraspis* cf. *M. borealis* *Paracedaria montanensis* *Semnocephalus centralis* *Syspacheilus* cf. *S. dunoirensis*	*Meteoraspis* sp. *Tricrepicephalus* sp. *Cedarina* cf. *C. cordillerae* *Kormagnostus* cf. *K. simplex* *Paracedaria montanensis* *Syspacheilus* cf. *S. dunoirensis* *Armonia* cf. *A. lata* *Brassicicephalus* sp. *Bynumia?* sp. *Nixonella* sp.	*Cedarina* aff. *C. obtusans* cf. *Kormagnostus* sp. *Meteoraspis* sp. cf. *Bolaspidella* sp. cf. *Modocia* sp.	*Coosia* sp. *Genevievella* sp. *Tricrepicephalus* sp. *Cedaria* sp. *Arapahoia* sp. *Kormagnostus* sp. *Densonella* sp. *Meteoraspis* sp. *Semnocephalus* sp.	*Cedaria* sp. *Coosella?* sp. *Kormagnostus* sp. *Semnocephalus* sp. *Arapahoia* sp. *Coosella?* sp. *Dicellomus* sp. *Kingstonia* sp. *Meteoraspis* sp.
Bolaspidella			*Eldoradia* sp. *Olenoides ?* sp. *Glyphaspis* sp.		*Eldoradia* sp. *Bolaspidella* sp. *Ehmania* sp.	*Eldoradia* sp. *Bolaspidella* sp. *Ehmania* sp.	*Ehmania* sp.	*Ehmania* sp.	*Eldoradia* sp.	*Ehmania* sp.	*Alokistocare* sp. *Elrathia?* sp. *Niusuia?* sp. *Olenoides* sp.

3.9. REFERENCES

Adrian, J.M.; Peters, S.E.; Westrop, S.R., 2009: The Marjuman trilobite Cedarina Lochman thoracic morphology, systematics, and new species from western Utah and eastern Nevada, USA. Zootaxa v.2218: 35-58.

Angelin, N.P., 1854. Palaeontologia scandinavica. Pars II. Crustacea formationis transitionis. Holmiae, Stockholm, pp. 21–92.

Amati, L., and Westrop, S.R., 2006. Sedimentary facies and trilobite biofacies along an Ordovician shelf to basin gradient, Viola Group, south-central Oklahoma, Palaios, 21: 516-529.

Bell, W.C., Feniak, O.W. and Kurtz, V.E. 1952. Trilobites of the Franconia Formation, southeast Minnesota. Journal of Paleontology, 26:175–198.

Belt, T. 1867. On some new trilobites from the Upper Cambrian rocks of North Wales. Geological Magazine, 4:294–295.

Berkey, C.P. 1898. Geology of the St. Croix Dalles. American Geologist, 21:270294.

Bridge, J. and Girty, G. H. 1937. A redescription of Ferdinand Roemer's Paleozoic types from Texas. United States Geological Survey Professional Paper, 186-M, pp. 239–271.

Burmeister, H. 1843. Die Organisation der Trilobiten aus ihren lebenden Verwandten entwickelt; nebst einer systematischen Uebersicht aller zeither beschriebenen Arten. Berlin. 147.

Chatterton, B.D.E. and R. Ludvigsen. 1998. Upper Steptoean (upper Cambrian) trilobites from the McKay Group of southeastern British Columbia, Canada. Paleontological Society Memoir, 49:1–43.

Clark, T.H. 1924. The paleontology of the Beekmantown Series at Levis, Quebec. Bulletins of American Paleontology, 1434.

Deland, C.R. and Shaw, A.B. 1956. Upper Cambrian trilobites from western Wyoming. Journal of Paleontology, 30:542–562.

Fortey, R.A. 1990. Ontogeny, hypostome attachment and trilobite classification. Palaeontology, 33:529–576.

Frederickson, E.A. 1949. Trilobite fauna of the Upper Cambrian Honey Creek Formation. Journal of Paleontology, 23:341–363.

Grant, R.E. 1965. Faunas and stratigraphy of the Snowy Range Formation (Upper Cambrian) in southwestern Montana and northwestern Wyoming. Geological Society of America Memoir, 96, 171 pp.

Hall, J. 1863. Supplementary note on some fossils of the lower beds of the Potsdam Sandstone of the Upper Mississippi Valley. New York State Cabinet Natural History 16th Annual Report, pp. 221–222.

Hall, J. and Whitfield, R.P. 1877. Palaeontology (Part II. Fossils of the Potsdam Group). *In* C. King. Report of the United States geological exploration of the Fortieth Parallel, v. 4, pt. II. United States Army Engineer Department Professional Papers, 18:198–302.

Hohensee, S.R. and Stitt, J.H. 1989. Redeposited *Elvinia* Zone (Upper Cambrian) trilobites from the Collier Shale, Ouachita Mountains, west‐central Arkansas. Journal of Paleontology, 63:857–879.

Hopkins, M. J. 2011. Species-level phylogenetic analysis of Pterocephaliids (Trilobita, Cambrian) from the Great Basin, western USA. Journal of Paleontology, 85 (6):1128–1153.

Howell, B.F. 1935. New Middle Cambrian agnostian trilobites from Vermont. Journal of Paleontology, 9:218–221.

Howell, B.F., Bridge, J., Deiss, C.F., Edwards, I., Lochman, C., Raasch, G.O. and Resser, C.E. 1944. Correlation of the Cambrian formations of North America. Geological Society of America Bulletin, 55:993–1003.

Hu, C.H. 1971.Ontogeny and sexual dimorphism of lower Paleozoic Trilobita. Palaeontographica Americana, 7, 155 pp.

Hu, C.H. 1983b. The Ontogenetic development of two upper Middle Cambrian trilobites from the Bonneterre Dolomite, Missouri (with a discussion on the morphologic varieties of *Cedarina vale* Lochman). Memoir of the Geological Society of China, 5:275–280.

Hupe, P. 1955. Classification des trilobites. Annales de Paleontologie, 41:91–325.

Jaekel, O. 1909. Uber die Agnostiden. Zeitschrift der deutschen geologischen Gesellschaft, 61:380–401.

Kindle, C. H. 1942. A Lower (?) Cambrian Fauna from Eastern Gaspe, Quebec. American Journal of Science, 240(9):633-641.

Kindle, C.H. and Whittington, H. B. 1965. New Cambrian and Ordovician fossil localities in western Newfoundland. Geological Society of America Bulletin, 76:683-688.

Kobayashi, T. 1933. Upper Cambrian of the Wuhutsui Basin, Liaotung, with special reference to the limit of the Chaumitian (or upper Cambrian) of eastern Asia, and its subdivision. Japanese Journal of Geology and Geography, 11:55–155.

Kobayashi, T. 1935. The Cambro-Ordovician formations and faunas of South Chosen: Palaeontology, Part III, Cambrian faunas of South Chosen with a special study on the Cambrian trilobite genera and families. Journal of the Faculty of Science, Tokyo University (sec. 2), 4:49–344, pls. 1–24.

Kobayashi, T. 1936. On the Parabolinella fauna from Province Jujuy, Argentina with a note on the Olenidae. Japanese Journal of Geology and Geography, 13:85–102.

Kobayashi, T. 1938. Upper Cambrian fossils from British Columbia with a discussion on the isolated occurrence of the so-called "Olenus" beds of Mt. Jubilee. Japanese Journal of Geology and Geography, 15:149–192.

Kurtz, V.E. 1975. Franconian (Upper Cambrian) trilobite faunas from the Elvins Group of southeast Missouri. Journal of Paleontology, 49:1009–1043.

Lochman, C. 1936. New trilobite genera from the Bonneterre Dolomite (Upper Cambrian) of Missouri. Journal of Paleontology, 10:35–43.

Lochman, C. 1938a. Upper Cambrian faunas of the Cap Mountain Formation of Texas. Journal of Paleontology, 12:72–85.

Lochman, C. 1938b. Middle and Upper Cambrian faunas from western Newfoundland. Journal of Paleontology, 12: 461–477.

Lochman, C. 1940a. Fauna of the basal Bonneterre Dolomite (Upper Cambrian) of southeastern Missouri. Journal of Paleontology, 14:1–53.

Lochman, C. 1940b. Corrections to the basal Bonneterre fauna. Journal of Paleontology, 14:515.

Lochman, C. 1950. Upper Cambrian faunas of the Little Rocky Mountains, Montana. Journal of Paleontology, 24:322–349.

Lochman, C. 1964. Upper Cambrian faunas from the subsurface Deadwood Formation, Williston Basin, Montana. Journal of Paleontology, 38:33–60.

Lochman, C. and Duncan, D. 1944. Early Upper Cambrian faunas of central Montana. Geological Society of America Special Papers, 54, 181 pp.

Lochman, C. and Hu, C.H. 1960. Upper Cambrian faunas from the northwest Wind River Mountains, Wyoming, Part I. Journal of Paleontology, 34: 793–834.

Lochman, C. and Hu, C.H. 1961. Upper Cambrian faunas from the northwest Wind River Mountains, Wyoming, Part II. Journal of Paleontology, 35:125–146.

Lochman, C. and Hu, C.H. 1962. Upper Cambrian faunas from the northwest Wind River Mountains, Wyoming, Part III. Journal of Paleontology, 36:1–28.

Lochman-Balk, C. 1971. The Cambrian of the craton of the United States. *In* Holland, C.D. (ed.). Cambrian of the New World. Wiley, New York, pp. 79–167.

Lochman-Balk, C. and Wilson, J.L. 1958. Cambrian biostratigraphy in North America. Journal of Paleontology, 32:312–350.

Lorenz,T. 1906. Beitrage zur Geologie und Palaeontologie von Ostasien unter besonderer Beruchsichtingder Provinz Schantung in China, 2 Palaeontologischer Teil. Deutsche Geologische Gesellschaf, 58:53–108.

Luo, H. 1983. New finds of trilobites from Late Cambrian in western Yunnan, p. 1–30. In Contributions to the Geology of the Qinghai-Xizang (Tibet) Plateau.

Ludvigsen, R. 1978. Middle Ordovician trilobite biofacies southern Mackenzie Mountains. In Stelck, C.R. and Chatterton, B.D.E. (eds.) Western and Arctic Canadian biostratigraphy. Geological Association of Canada Special Paper, 18, pp.1-37.

Ludvigsen, R., Westrop, S.R. and Kindle, C.H. 1989. Sunwaptan (Upper Cambrian) trilobites of the Cow Head Group, western Newfoundland, Canada. Palaeontographica Canadiana, 6, 175 pp.

Mckee E. D. and Resser C. E. 1945. Cambrian history of the Grand Canyon Region. Part 1 Stratigraphy and ecology of the Grand Canyon: Carnegie Institute Washington Publication, 563:3-168.

M'coy, F. 1849. On the classification of some British fossil Crustacea, with notices of some new forms in the University collection at Cambridge. Annals and Magazine of Natural History (London), s. 2, 4: 161–179, 330–335, 392–414.

Meek, F.G. 1870. Descriptions of fossils collected by the U.S. Geological Survey under the charge of Clarence King, esq. Proceedings of the Academy of Natural Science, Philadelphia, s. 2, 14:56–64.

Meek, F.G. 1877. Paleontology. U. S. Geol. Expl. 40th Parallel (King) 4(2):1-197.

Meek, F.G., and Hayden, F.V. 1861. Descriptions of new Lower Silurian (Primordial), Jurassic, Cretaceous and Tertiary fossils collected in Nebraska by the exploring expedition under the command of Capt. Wm. F. Reynolds, U.S. Top. Engrs; with remarks on the rocks from which they were obtained. Proceedings of the Academy of Natural Science, Philadelphia, s. 2, 5:415–447.

Melzak, A., and S. R. Westrop. 1994. Mid-Cambrian (Marjuman) trilobites from the Pika Formation, southern Canadian Rocky Mountains, Alberta. Canadian Journal of Earth Sciences, 31:969–985.

Miller, B. M., 1936a, Cambrian trilobites from northwestern Wyoming: Journal of Paleontology, 10:23–34.

Miller, B. M., 1936b. New Name for Brachyaspis Miller (Not Salter): Journal of Paleontology, 10:417.

Moore, R. C. (ed.). 1959. Treatise on Invertebrate Paleontology, Part 0, Arthropoda 1. Geological Society of America and University of Kansas Press, Lawrence, 560 p.

Owen, D.D. 1852. Report of a geological survey of Wisconsin, Iowa, and Minnesota, and incidentally a portion of Nebraska Territory. Lippincott, Grambo ~ Co., Philadelphia. 638 pp.

Palmer, A.R. 1954a. An appraisal of the Great Basin Middle Cambrian trilobites described before 1900. United States Geological Survey Professional Paper, 264–D:55–86.

Palmer, A.R. 1954b. The faunas of the Riley Formation in central Texas. Journal of Paleontology, 28:709–786.

Palmer, A.R. 1955 Upper Cambrian Agnostidae of the Eureka District, Nevada. Journal of Paleontology, 29:86–101.

Palmer, A.R. 1960. Trilobites of the Upper Cambrian Dunderberg Shale, Eureka District, Nevada. United States Geological Survey Professional Paper, 334–C:109 pp.

Palmer, A.R. 1962a. Comparative ontogeny of some opisthoparian, gonatoparian and proparian Upper Cambrian trilobites. Journal of Paleontology, 36:87–96.

Palmer, A.R. 1962b. *Glyptagnostus* and associated trilobites in the United States. United States Geological Survey Professional Paper, 374–F, 49 pp.

Palmer, A. R. 1965a. The biomere—a new kind of biostratigraphic unit. Journal of Paleontology, 39:149–153.

Palmer, A.R. 1965b. Trilobites of the Late Cambrian Pterocephaliid Biomere in the Great Basin, United States. United States Geological Survey Professional Paper, 493, 105 pp.

Palmer, A.R. 1968. Cambrian trilobites of east-central Alaska. United States Geological Survey Professional Paper, 559–B:115 pp.

Palmer, A.R. 1971. The Cambrian of the Appalachian and eastern New England regions,

eastern United States, p. 169–217. *In* C. H. Holland (ed.), Cambrian of the New World. Wiley Interscience, London.

Palmer, A.R. 1972. Upper Cambrian faunal patterns on the craton: discussion. Geological Society of America Bulletin, 83:927–930.

Poulsen, C. 1927. The Cambrian, Ozarkian and Canadian faunas of northwest Greenland. Meddelelser om Grønland, 70:233–343, pls. 14–21.

Poulsen, C. 1937: On the Lower Ordovician faunas of East Greenland. Meddelelser om Grønland, 119, 3, 72 pp.

Pratt, B. R. 1992. Trilobites of the Marjuman and Steptoean stages (Upper Cambrian), Rabbitkettle Formation, southern Mackenzie Mountains, Northwest Canada. Palaeontographica Canadiana, 9, 179 p.

Pratt, B. R. and Bordonaro, O. L. 2014. Early middle Cambrian trilobites from La Laja Formation, Cerro el Molle, Precordillera of western Argentina. Journal of Paleontology, 88:906–924.

Qian, Y.-Y. 1994. Trilobites from Middle Upper Cambrian (Changshan Stage) of north and northeast China. Palaeontologia Sinica, 183, 190 p.

Qiu, H.-A., Y.-H. Lu, Z.-L. Zhu, D.-C. Bi, T.-R. Lin, Z.-Y. Zhou, Q.-Z. Zhang, Y.-Y. Qian, T.-Y. Ju, N.-R. Han, and X.-Z. Wei. 1983. Trilobita, p. 28–254, 574–609, pl. 211–288. In Paleontological Atlas of East China, 1, Early Paleozoic Vol. Geological Publishing House, Beijing.

Rasetti, F. 1946. Early Upper Cambrian trilobites from western Gaspe. Journal of Paleontology, 20:442–462.

Rasetti, F. 1956. Revision of the trilobite genus *Maryrillia* Walcott. Journal of Paleontology, 30:1266–1269.

Rasetti, F. 1961. Dresbachian and Franconian trilobites of the Conococheague and Frederick limestones of the central Appalachians. Journal of Paleontology, 35:104–124.

Rasetti, F. 1963. Middle Cambrian ptychoparioid trilobites from the conglomerates of Quebec. Journal of Paleontology, 37:575–594.

Rasetti, F. 1965a. Upper Cambrian trilobite faunas of northeastern Tennessee. Smithsonian Miscellaneous Collections, 148(3):127

Rasetti, F. 1965b. Middle Cambrian trilobites of the Pleasant Hill Formation in central Pennsylvania. Journal of Paleontology, 39:1007–1014.

Raymond, P.E. 1924. New Upper Cambrian and Lower Ordovician trilobites from Vermont. Proceedings of the Boston Society of Natural History, 37:389–466.

Raymond, P.E. 1937. Upper Cambrian and Lower Ordovician Trilobita and Ostracoda from Vermont. Geological Society of America Bulletin, 48:1079–1146.

Resser, C.E. 1935. Nomenclature of some Cambrian trilobites. Smithsonian Miscellaneous Collections, 93(5), 46 pp.

Resser, C.E. 1937. Third contribution to nomenclature of Cambrian trilobites. Smithsonian Miscellaneous Collections, 95(22), 29 p.

Resser, C.E. 1938a. Cambrian System (restricted) of the southern Appalachians. Geological Society of America, Special Paper 15, 140 p.

Resser, C.E. 1938b. Middle Cambrian fossils from Pend Oreille Lake, Idaho. Smithsonian Miscellaneous Collections, 97(3), 12 p.

Resser, C.E. 1939a. The Spence Shale and its fauna. Smithsonian Miscellaneous Collections, 97(12), 29 p.

Resser, C.E. 1939b. The Ptarmigania strata of the northern Wasatch Mountains. Smithsonian Miscellaneous Collections, 98(24), 72 p.

Resser, C.E. 1942a. Fifth contribution to nomenclature of Cambrian fossils. Smithsonian Miscellaneous Collections, 101(15), 58 pp.

Resser, C.E. 1942b. New Upper Cambrian trilobites. Smithsonian Miscellaneous Collections, 103(5), 136 pp.

Richter, R. 1933. Crustacea. Handworterbuch der Naturwissenschaften (2nd Edition), v. 2. Jena, pp. 840–864.

Robison, R.A. 1960. Some Dresbachian and Franconian trilobites of western Utah. Brigham Young University Research Studies, 7, 59 pp.

Robison, R.A. 1964. Late Middle Cambrian faunas from western Utah. Journal of Paleontology, 38:510–566.

RobisoN, R.A. 1971. Additional Middle Cambrian Trilobites from the Wheeler Shale of Utah. Journal of Paleontology, 45:796–804.

Robison, R. A. 1976. Middle Cambrian trilobite biostratigraphy of the Great Basin. Brigham Young Geology University Studies, 23:93–109.

Robison, R.A. 1988. Trilobites of the Holm Dal Formation (late Middle Cambrian), central North Greenland. Meddelelser om Grønland, Geoscience, 20:23–103.

Robison, R.A. and Babcock L. E. 2011. Systematics, paleobiology, and taphonomy of some exceptionally preserved trilobites from Cambrian lagerstätten of Utah. University of Utah, Paleontological Contributions, No. 5, 47 p.

Roemer, F., 1849, Texas, mit beson-dered Rusksicht auf deutsche Auswanderung und die physischen Verhaltnisse des Landes: xiv, Bonn.

Rozova, A. V. 1963. Biostratigraphic scheme of the upper and uppermiddle Cambrian and new upper Cambrian trilobites. Geologiya i Geofizika, 9:3–20.

Salter, J. W. 1864. Figures and descriptions illustrative of British organic remains. Decade 11, Trilobites (chiefly Silurian). Memoirs of the Geological Survey of the United Kingdom, 1–64.

Schwimmer, D. R. 1989. Taxonomy and biostratigraphic significance of some Middle Cambrian trilobites from the Conasauga Formation in western Georgia. Journal of Paleontology, 63:484–494.

Shaw, A.B. 1952. Paleontology of northwestern Vermont. II. Fauna of the Upper Cambrian Rockledge Conglomerate near St. Albans. Journal of Paleontology, 26:458–483.

Shaw, A. B. 1956a. A Cambrian *Aphelaspis* fauna from Steele Butte, near Boulder, Wyoming. Journal of Paleontology, 30:48–52.

Shaw, A. B. 1956b. Notes on Modocia and Middle Cambrian Trilobites from Wyoming. Journal of Paleontology, 30:141-145.

Shimer, H.W. and Shrock, R.R. 1944. Index fossils of North America. Wiley, New York. 837 pp.

Shumard, B.F. 1861. The Primordial zone of Texas with descriptions of new fossils. American Journal of Science, s. 2, 32:213–221.

Stitt, J.H. 1971. Late Cambrian and earliest Ordovician trilobites, Timbered Hills and lower Arbuckle groups, western Arbuckle Mountains, Murray County, Oklahoma. Oklahoma Geological Survey Bulletin, 110, 83 pp.

Stitt, J. H. 1998. Trilobites from the Cedarina dakotaensis zone, lowermost part of the Deadwood Formation (Marjuman State, Upper Cambrian), Black Hills, South Dakota. Journal of Paleontology, 72:1030–1046.

Stitt, J. H. and P. J. Perfetta. 2000. Trilobites, biostratigraphy, and lithostratigraphy of the Crepicephalus and Aphelaspis zones, lower Deadwood Formation (Marjuman and Steptoean stages, Upper Cambrian), Black Hills, South Dakota. Journal of Paleontology, 74:199–223.

Stoyanow, A. A. 1936. Correlation of Arizona Paleozoic formations. Bulletin of the Geological Society of America, 47:459-540.

Sun, Y.-C. 1935. The Upper Cambrian trilobites faunas of North China. Palaeontologia Sinica series B, 7:93 p.

Sundberg, F. A. 1994. Corynexochida and Ptychopariida (Trilobita, Arthropoda) of the *Ehmaniella* Biozone (Middle Cambrian), Utah and Nevada. Natural History Museum of Los Angeles County, Contributions in Science, 446, 137 p.

Swinnerton, H. H. 1915. Suggestions for a revised classification of trilobites. Geological Magazine, 2:407–496, 538–545.

Tullberg, S.A. 1880. Om Agnostus arterna i de Kambriska aflagringarna vid Andrarum. Sveriges Geologiska Undersokning, s. C, 42:1–37.

Vodges, A. W. 1890. A bibliography of Paleozoic *Crustacea* from 1698 to 1889, including a list of arrangement of genera: U.S. Geological Survey Bulletin, 63, 177p.

Walch, J.E.I. 1771. Die naturgeschichte der versteinerungen, Dritter Teil. Zur erlauterung der Knorrischen Sammlung von Merkwurdigkeiten der Natur, pp. 1−235. P.J. Flestecker; Nurnberg.

Walcott, C.D. 1884. Paleontology of the Eureka District. United States Geological Survey Monographs, 8, 298 pp.

Walcott, C.D. 1886. Second contribution to the studies of the Cambrian faunas of North America. Bulletin of the U.S. Geological Survey, 30,369 p.

Walcott, C.D. 1890, Description of new forms of Upper Cambrian fossils: U. S. Nat. Mus. Proc., 13:267–279.

Walcott, C.D. 1899. Cambrian fossils of the Yellowstone National Park. United States Geological Survey Monographs, 32:440–478.

Walcott, C.D. 1911. Research in China: Smithsonian Misc. Coll., no. 4, 57:69–108.

Walcott, C.D. 1916a. Cambrian geology and paleontology III. No. 3.—Cambrian trilobites. Smithsonian Miscellaneous Collections, 64:157–256.

Walcott, C.D. 1916b. Cambrian geology and paleontology III. No. 5.—Cambrian trilobites. Smithsonian Miscellaneous Collections, 64:303–456.

Walcott, C.D. 1924. Cambrian geology and paleontology V. No. 2.—Cambrian and Ozarkian trilobites. Smithsonian Miscellaneous Collections, 75:53–60.

Walcott, C.D. 1925. Cambrian geology and paleontology V. No. 3.—Cambrian and Ozarkian trilobites. Smithsonian Miscellaneous Collections, 75:61–146.

Westrop, S.R. 1986. Trilobites of the Upper Cambrian Sunwaptan Stage, southern Canadian Rocky Mountains, Alberta. Palaeontographica Canadiana, 3,179 pp.

Westrop, S. R. 1992. Upper Cambrian (Marjuman-Steptoean) Trilobites from the Port au Port Group, Western Newfoundland. Journal of Paleontology, 66, 228-255.

Westrop, S. R. 1996. Temporal persistence and stability of Cambrian biofacies: Sunwaptan (Upper Cambrian) trilobite faunas of North America. Palaeogeography, Palaeoclimatology, Palaeoecology, 127:33–46.

Westrop, S. R., R. Ludvigsen, and C. H. Kindle. 1996. Marjuman (Cambrian) trilobites of the Cow Head Group, western Newfoundland. Journal of Paleontology, 70:804–829.

Westrop, S. R., R. Ludvigsen, 2000. The late Cambrian (Marjuman) trilobite genus *Hysteropleura R*aymond from the Cow Head Group, western Newfoundland. Journal of Paleontology, 74:1020–1030.

Westrop S. R., Eoff J. D., Ng T-W., Dengler A. A., Adrain J. M. 2008. Classification of the Late Cambrian (Steptoean) trilobite genera *Cheilocephalus* Berkey, 1898 and *Oligometopus* Resser, 1936 from Laurentia. Canadian Journal of Earth Science, 45:725–744.

Westrop S. R. and Eoff J. D. 2012. Late Cambrian (Furongian; Paibian, Steptoean) Agnostoid Arthropods from the Cow Head Group, Western Newfoundland. Journal of Paleontology, 86:201–237.

Whitehouse, F.W. 1936. The Cambrian faunas of north-eastern Australia, parts I and 2. Memoirs of the Queensland Museum, Il: 59–112.

Whitfield, R. P., 1878, Preliminary descriptions of new species of fossils from the lower geological formations of Wisconsin: Ann. Rept. Geol. Survey Wisconsin, pp. 50–89.

Whitfield, R. P.,1882, Species from the Potsdam sandstone: Geology of Wisconsin, paleontology, 4:169-193.

Whittington, H.B. 1988. Hypostomes and ventral cephalic sutures in Cambrian trilobites. Palaeontology, 31:577–609.

Wilson, J. L., 1948, Two Upper Cambrian *Elvinia* zone trilobite genera: Journal of Paleontology, 22:31–34.

Wilson, J.L. 1949. The trilobite fauna of the *Elvinia* Zone in the basal Wilberns Limestone of Texas. Journal of Paleontology, 23:25–44.

Wilson, J.L. 1951. Franconian trilobites of the central Appalachians. Journal of Paleontology, 25:617–654.

Yuan, J.-L. and G.-Z. Yin. 1998. New polymerid trilobites from the Chefu Formation in early Late Cambrian of eastern Guizhou. Acta Palaeontologica Sinica, 37:138–172.

CHAPTER 4

SUMMARY

The Abrigo Formation is a middle to late Cambrian mixed carbonate–siliciclastic unit that crops out in southeastern Arizona. It records deposition in the inner detrital belt during the Sauk transgression. In contrast to previous sedimentological studies which suggested a peritidal environment for deposition of the Abrigo Formation, i.e. in shallow subtidal lagoons and on intertidal to supratidal flats, integration of sedimentological, paleontological and ichnological data reveals that the Abrigo Formation was deposited under open-marine conditions. Accordingly, the unit was formed solely in a relatively shallow-marine setting dominated by storms alternating with tranquil conditions, with no evidence of patch-reef development, strong tidal activity, or restricted conditions of elevated salinity, for example on tidal flats. In addition to the clay, silt and sand derived from the adjacent land surface, the carbonate constituents include lime mud, bioclasts, ooids, oncoids, and intraclasts, all allochems typical of Cambrian–Ordovician limestones. The Abrigo Formation consists of fifteen sedimentary facies, which comprise eight facies associations representing lower offshore, upper offshore, offshore transition, lower/middle shoreface, and upper shoreface. With this thesis, the Abrigo Formation is now fully and authoritatively documented in detail, not just to the current level of sedimentological understanding, but beyond by proposing innovative and differing interpretations of particular lithofacies that others have encountered elsewhere. Recognition of waves and storms as a major processes involved in the development of this system is important for the understanding of the distribution, geometry and architecture of the sedimentary facies

developed in a mixed carbonate-siliciclastic system in general. Some differences between the Abrigo Formation and other Cambrian inner detrital belt examples lie in relative dominance of carbonate versus siliciclastic sediment in the offshore transition setting. This reflects periods when clastic, especially clay, input decreased, such that carbonate production was promoted in shallow areas just below fair-weather wave base.

The sequence-stratigraphic scheme proposed for this system has permitted construction of a much more complete characterization of depositional environments and sea level changes in this region during the time of the Abrigo Formation deposition. The unit can be divided into six distinct phases that are interpreted to reflect changing rates of relative sea-level rise and fall and the corresponding influence on the carbonate factory. The newly constructed trilobite biostratigraphy, based on detailed collections and exhaustive preparation, is key to understanding the lateral and vertical evolution of the sedimentary system. The succession starts in *Bolaspidella* Biozone time with transgression and deposition of a fine-grained offshore facies over the shallow-marine Bolsa Quartzite. This overall deepening and retrogradational trend comprises a transgressive systems tract, and during the maximum flooding phase lime mud sedimentation dominated. Second phase comprises a highstand systems tract and is characterized by and aggradation and subsequent progradation of a number of coarsening- and thickening-upwards intervals reflecting deposition in the lower offshore followed by gradual shoaling to the upper offshore and offshore transition setting. A sea-level fall that left no lowstand deposits in the area. A sequence boundary is placed above the shallow-water bioclastic and oolitic–oncolitic grainstones and packstones around the base of the *Cedaria* Biozone. In addition, this surface represents a flooding surface at the base of the succeeding transgressive systems tract that represents the third phase. Maximum transgression in early *Cedaria* Biozone time is interpreted

to coincide with the thick units of nodular lime mudstone, reflecting low-energy, suspension fall-out. Subsequently, the stacking pattern becomes aggradational. This transition, with a few asymmetric coarsening-upward intervals, marks a change from a transgressive to a highstand systems tract, that comprises the fourths stage. Sedimentation during the latter *Cedaria* Biozone and *Crepicephalus* Biozone time interval was dominated by carbonate deposition in an offshore transition setting and progradation of sand that accumulated in the lower to upper shoreface. The fifth stage, which is a falling stage systems tract, recorded in *Aphelaspis* Biozone time is recorded by a progradaton of erosive-based shoreface sands. The presence of *Elvinia* Biozone trilobites near the base of the highest sandstone unit suggests that delivery and deposition of the these sands took place during the lowstand that characterizes the last sixth stage of the succession. These shoreface sandstone in the uppermost Abrigo Formation provides a record of the Sauk II–Sauk III hiatus which broadly correlates with the peak of the Steptoean Positive Carbon Isotope Excursion (SPICE) event recognized globally. Sequence straticrapic models for the Abrigo Formation and other inner detrital belt examples across Laurentia are compared in this study. The only sequence-stratigraphic elements that may correlate over a large portion of Laurentia are possibly one sequence boundary in the *Bolaspidella* Biozone and the Sauk II–Sauk III hiatus. The stratigraphic architecture in different coeval regions is governed by other phenomena in addition to sea-level, including variation in crustal flexure, sedimentation rate, and paleoclimate, such that distinguishing continental-scale events is mostly elusive. This is a new interpretation that will provoke further testing in other regions.

My study of this mixed carbonate-siliciclastic system allowed me to characterize in a more theoretical way the interplay between siliciclastic sediment input and carbonate productivity. This reveals that siliciclastic sediment input and dispersal were not only restricted

to the falls in sea level, but appear to have dominated the transgressive systems tract and late phase of the highstand. Thus, carbonate sedimentation does not dominate the entire highstand systems tract but, rather, only during the late phase of the transgressive and early highstand phase. It remains to be tested whether or not this paradigm applies to mixed carbonate–siliciclastic systems elsewhere and of different ages. Varying proportions of carbonate versus siliciclastic deposits in the Abrigo Formation indicate a variable influx of terrigenous material over a period of changing accommodation space, which had a significant impact on carbonate production. Admixed quartz sand in grainstone suggests that minor amounts of coarse siliciclastic sediment are not especially deleterious. However, during the highstand of the lower part of the Abrigo Formation, fine-grained siliciclastic sediment supply dominated and suppressed carbonate productivity.

The Abrigo Formation suggests a departure from the traditional view of the tropical carbonate factory, whereby carbonate sediments were generated by a single carbonate factory in inshore areas with lime mud preferentially transported offshore (e.g., Aurell et al. 1988). The Cambrian inner detrital belt here appears to have consisted of two carbonate factories, the distal offshore one dominated by pelagic lime mud production, and the nearshore one in which a variety of carbonate particle types was generated on the sea floor, including lime mud, ooids, oncoids, and bioclasts. These areas were separated by a proximal offshore zone of siliciclastic sedimentation of muds and fine sands. Paleogeographically, the offshore carbonate factory of the Abrigo Formation eventually graded seaward into the middle carbonate belt.

The second part of this study provides a full taxonomic account and documents the distribution of the trilobite fauna in the Marjuman and Steptoean interval. One hundred eighty-two collections, yielding 940 trilobite remains have been recovered. They represent 69 species

belonging to 42 genera. Eight new species are identified: *Blairella* n. sp., *Camaraspis* n. sp., *Modocia* n. sp., *Crepicephalus* n. sp., *Coosia* n. sp., *Bolaspidella* n. sp., *Paracedaria* n. sp., *Llanoaspis* n. sp. Trilobites are assigned to five biostratigraphic zones: *Bolaspidella*, *Cedaria*, *Crepicephalus*, *Aphelaspis*, and *Elvinia* Zones. In addition, two subzones are recognized, the *Cedaria eurycheilos* Subzone defined in the upper part of the *Cedaria* Zone and the *Coosella helena* Subzone recognized in the upper part of the *Crepicephalus* Zone.

A biostratigraphic zonal scheme is erected that is applicable to the inner detrital belt of Laurentia. These zones are integrated with the pattern of trilobite biofacies characterized for the shallow-marine storm-dominated environment, and combined with a detailed lithofacies analysis of the Abrigo Formation, aid in the evaluation of the overall ecologic controls on faunal distribution. Eight trilobite biofacies are defined from the generic relative abundance data: *Ehmaniella, Olenoides–Bolaspidella, Blairella, Eldoradia, Modocia–Paracedaria, Cedaria, Coosella–Coosina,* and *Camaraspis*. These associations represent environmentally and temporally controlled trilobite communities. These add to the biofacies mosaic being assembled for Laurentia through the Cambrian from nearshore to marginal slope settings. A comparison of biofacies with other regions shows that trilobite community development was at times comparable in similar environments elsewhere, but at other times there prove to be intriguing differences. The differences show that there is still much to be learned about trilobite paleobiology and paleoecology during this time interval.